

# **International Journal of Computational and Engineering**

MARCH 2016 VOLUME1 NUMBER1

**Publisher: ACADEMIC PUBLISHING HOUSE**  
**Address: Quastisky Building, Road Town, Tortola, British Virgin Islands**  
**UK Postal Code: VG1110**

**E-mail: [editorial@ij-ce.com](mailto:editorial@ij-ce.com)**  
**[www.ij-ce.com](http://www.ij-ce.com)**



**ACADEMIC PUBLISHING HOUSE**



# CONTENTS

|   |     |
|---|-----|
| THE RESEARCH ON HUMANIZED DESIGN FOR CHILDREN'S MUSEUM .....  | 1   |
| STUDY ON NONLINEAR INPUT-OUTPUT ANALYSIS OF THE REAL ESTATE INDUSTRY WITH PERSISTENT DISTURBANCES.....                                  | 8   |
| A SPLINE SMOOTHING NEWTON METHOD FOR L FITTING ELLIPSOIDS.....  | 14  |
| THE KERNEL FUNCTION PRINCIPAL COMPONENT ANALYSIS MODEL FOR DISPOSING INFORMATION OF STUDENTS' EVALUATION OF TEACHING.....               | 18  |
| A IMPROVED ROUTING ALGORITHM OF WIRELESS SENSOR NETWORK .....   | 23  |
| AN XML QUERY AGGREGATION BASED ON MEAN SQUARE RESIDUAL.....   | 26  |
| A ROUTING ALGORITHM OF WIRELESS SENSOR NETWORK BASED ON ROBUST MEASURE.....   | 32  |
| EVALUATION AND OPTIMIZATION ON APPLICABILITY OF BIG DATA TECHNOLOGIES IN SMART GRID .....   | 35  |
| NEW URBANIZATION UNDER THE BACKGROUND OF STUDY ON RURAL SPORTS PUBLIC SERVICE INNOVATION SUPPLY .....                                   | 41  |
| TAIJIQUAN GAME THEORY ANALYSIS AND RESEARCH OF CULTURAL INHERITANCE SYSTEM .....  | 44  |
| THE BEST OFFENSIVE AND DEFENSIVE FOOTBALL PENALTY MODEL BASED ON BIOMECHANICS .....   | 47  |
| WEIGHTED HARDY-LITTLEWOOD INTEGRAL INEQUALITY FOR THE RESULT OF P-HARMONIC TYPE EQUATION.....   | 50  |
| THE RESEARCH ON TRAFFIC CIRCLE SIGNAL CONTROL .....   | 53  |
| A STUDY OF THE BATH HEAT PRESERVATION METHOD BASED ON THE THREE DIMENSIONAL STEADY HEAT CONDUCTION EQUATION .....                       | 57  |
| THE DESIGN OF TEMPERATURE CONTROL AND WATER-SAVING BATHTUB BASED ON GAME ANALYSIS.....  | 60  |
| TRACKING AND ANTI-TRACKING OF THE MANEUVERING TARGET THE ALGORITHM BASED ON THE MINIMUM DISTANCE ALGORITHM AND THE TRACK CURVATURE..... | 63  |
| ANALYSIS OF FACTORS INFLUENCING H-R FORTE COMPLEX POST——BASED ON THE CONTROL VARIABLE METHOD .....                                      | 67  |
| CPU UTILIZATION-BASED ENERGY CONSUMPTION MODEL IN CLOUD COMPUTING.....  | 72  |
| STUDY ON HEATING SUPPLY LOAD FORECASTING BASED ON SPARSE KERNEL PARTIAL LEAST SQUARES .....   | 74  |
| CURRENT SITUATION REVIEW OF THE MICROPILE.....  | 81  |
| RISK ANALYSIS OF PUBLIC HOSPITALS MEDICAL TECHNOLOGY INNOVATION .....   | 87  |
| STUDY ON THE VIRUS RESISTANCE OF CHIFN-A TRANSGENIC TOBACCO.....  | 93  |
| THE 3D CUBE16 BASED ON ARM.....   | 96  |
| THE PREDICTION OF PHOTOVOLTAIC POWER OUTPUT BASED ON THE EXTREME LEARNING MACHINE ALGORITHM OF PARTICLE SWARM OPTIMIZATION .....        | 100 |

|  |     |
|--|-----|
| THE RESEARCH ON AUTOMATIC ASSEMBLY DEVICE DESIGN METHOD OF THREADED CONNECTIONS BATH PRODUCT BASED ON TRIZ.....      | 103 |
| ANALYSIS ON SINGLE ARCH RIB ULTIMATE BEARING CAPACITY AND STABILITY OF CONCRETE-FILLED STEEL TUBES ARCH BRIDGE ..... | 107 |
| AN INDEX PAGE REPLACEMENT POLICY FOR KNN ALGORITHM.....  | 112 |
| THE KEY RESEARCH ON RECOGNITION OF THE PARTS ORIENTATION BASED ON TEMPLATE MATCHING.....                             | 116 |
| RESEARCH OF WIRELESS RELAY MONITORING NETWORKS STATUS.....   | 119 |
| A CERTAINTY-BASED ACTIVE LEARNING FRAMEWORK OF MEETING SPEECH SUMMARIZATION.....                                     | 125 |
| ALGORITHM FOR THREE ASSOCIATED CONTINUED FRACTIONS NEWTON BLENDING RATIONAL INTERPOLANT.....                         | 130 |
| RESEARCH OF CONSTANT TEMPERATURE AND ENERGY SAVING BATH CYCLE OF BATHTUB .....                                       | 135 |
| BASED ON THE FINITE ELEMENT ANALYSIS OF STEEL STRUCTURE FIRE RESISTANCE RESEARCH.....                                | 138 |
| ENERGY-SAVING THERMOSTAT BATH TUB MODEL BASED ON HEAT CONDUCTION PRINCIPLE .....                                     | 143 |
| RESEARCH OF CONSTANT TEMPERATURE AND ENERGY CONSERVATION BATH ON THE BASIS OF DYNAMIC PROGRAMMING MODE.....          | 147 |
| TERAHERTZ'S DEVELOPMENT AND UTILIZATION PROSPECT .....   | 151 |
| RESEARCH ON APPLICATION OF ACTIVE HEAD RESTRAINT OF AUTOMOBILE SEAT .....  | 154 |
| RESEARCH ON AERIAL SPARE PARTS JOINT SUPPORT METHODS .....   | 156 |

# The Research on Humanized Design for Children's Museum

Yingmei Wang<sup>1,\*</sup>, Aihua Cao<sup>1</sup>, Junli Zhang<sup>2</sup>, Chunli Wang<sup>2</sup>

<sup>1</sup>Nanjing University of Information Science and Technology, Nanjing, 210044, China

<sup>2</sup>Institute of Information Technology of Guilin University of Electronic Technology, Guilin 541004, China

**Abstract:** The humanized design is vital for the development of the Children's Museum. Initially, the height of the booth should conform to the children's body, and the safety of exhibits as well as devices should also be guaranteed. With the computer technology, the museum could set up automatic inductive and interactive devices, which creates virtual reality environment combined with the sound, light and electricity. Secondly, the mouse with silica gel shell can protect the joints of the children's hands; the concise and vivid images of the cartoons on the screen can capture the interests of children. While, the light reflection rate and the contrast should not be too sharp, and the words on the computer should be simple with a few strokes. Meanwhile, the layout and proportion of the text on the screen should be appropriate. In addition to the lightness, the museum can also creatively use the space by making dining area, recreation area, souvenir area, special room for mothers and babies. Last, it is necessary to perfect the evaluation system and allow the children to visit museums with questions whose answers could be found in the system.

**Keywords:** Human engineering, Virtual reality, Interactive device, Evaluation system

## 1. INTRODUCTION

On February 8, 2013, Guangming Daily of China issued a shocking news on page nine: six state-level museums might be downgraded. According to the regulations, the museum assessed as the "minimally qualified" or "unqualified" for successively two times would be denied the title of "National Museum" [1]. Museum, as a collection of cultural heritage, primarily aims to collect and study. In addition, museum also bears the responsibility of lifelong education through the way of communication and display. As early as 1880, the British museum scholar, Lukin, published the paper *the Function of the Museum*, emphasizing that the museum should be the education scene for the general public. Two monographs *the Museum of the Future* and *the Principle of Administrative Management of the Museum* by American scholar Di Gu, further emphasized on committing to innovation education and carrying out positive activities. Thus the museums will become not only the scene for the research works where experts and scholars engaged in, but also the facilities to complement for education

institutions and off-campus teaching garden [2]. The display design of contemporary museums is generally composed by the performance of the theme, the division of space, the equilibrium of scale, the modelling of the props, the combination of the exhibits, the use of color and light. During the concrete implementation, a variety of constituent elements and high-tech auxiliary means should be used, such as adopting an integrated approach by comparing the actual and virtual, and by the combination of dynamic and static, making the ideological level, scientificity, artistic quality, interestingness of the main body to be fully displayed, so as to achieve a high degree of unity in content and form [3]. Our country's museum is stagnant, which has a lot to do with the factors below: the display technology is outdated and the form is mechanical, the pavilion is lacking in interaction, the commentary for the exhibits remains the same. For the vast majority of the audiences, they may not know a lot of histories, cultural relics or the background of the exhibits on display, they need the help of all-round exhibition way full of humanistic care. And more research indicates that in the exhibition, the visit will change from static state into dynamic state, the hands-on opportunities of the audiences is being increased in the future.

## 2. EXPERIMENTAL

The operation mechanism of the museum in our country has showed a variety of problems. Then, as one branch of the museums, the design of Children's Museum is a serious problem to be solved at present. For a long time, most of the museums in our country used to target adult visitors who are equipped with certain knowledge, ignoring the special group of children. Fortunately, in recent years, all kinds of the preparation of the museums have taken children into account and set up "Children's Museum" specifically for children. Compared with the Children's Museum, the traditional museum pays more attention to collection, preservation of historical relics, exhibition and research. But the exhibits in the Children's Museum are mainly dynamic and interactive, and the research is principally for the development and manufacture of the interactive exhibits. In the nature of the museum, the Children's Museum primarily provides children with places to accept all kinds of knowledge outside school education. Furthermore, the purpose of collection and

study all points to the education function. Therefore, the Children's Museum basically has the following functions such as education, entertainment, interaction, exploration, and so on [4].

In order to realize the dream “giving the most precious things to children” of Qingling Song, the Children's Museum supported by many institutions was firstly built in Shanghai in 1996. For the purpose of giving full play to the education function of the museum, the museum had provided educational places and contents suitable for children. At present, the Children's Museum in Shanghai is opened to the public for free, and this has catered to the comment of government work report: “the public museum, memorial museum and the demonstration base for national patriotism education will be opened to the society for free this year or next” from premier Jiabao Wen in 2008. In addition, other museums such as “Children's Museum” and “Women's and Children's Museum” of Beijing in China have gradually grown up. Compared to China, foreign Children's Museums are quite mature. The courses of the science of museum at the University of Iowa defined the Children's Museum as an institution specifically for children, and all the contents were made in accordance with the children's mental capacity. The arrangement is often unified by educational experts, with the classroom for interest activities and self-expression activities, where children can be free to exchange views pleasantly. It is an education facilities of extending the sensory experience and stimulating imagination. As the birthplace of the Children's Museum in the world, the United States has established nearly three hundreds of different sizes of children's museums. In 1899, the United States established the first Children's Museum called the Brooklyn Museum in the world, whose education philosophy was centered on children, and it emphasized on attaching great importance to the exploration and contacting with the material directly [5]. Another museum named “Children's Museum in Boston” has also won the praise of children with its fairy tale educational contents. In other countries and regions, such as Europe, Canada, South Korea, Japan, China Taiwan, a batch of Children's Museums have also been built. In today's quality-oriented education, the effect of the Children's Museum has gained wide recognition in the society.

Someone said: “the traditional Children's Museum merely consider the interior design and architectural design, paying attention to the application of the theory to space art and environment, and exploring into the design of light environment, color and ecological architecture solely. But with the development of high-end technology, the technology of virtual reality will be applied to the field of interior design, that will point out a new direction for the development of modern Children's Museum” [6]. Thus it can be seen that no matter how the design

trend changes, the idea needs to follow certain practical principles. Children's physical and mental characteristics are different from adults', so the design concept of the Children's Museum should be in accordance with the characteristics of children's body engineering and be able to meet children's strong desire to explore as a benchmark. In a word, the humanized design will be the vitality of the development in Children's Museum.



Figure 1.a magic pavilion conforms to the ergonomics of children



Figure 2. Harry Potter in the window

2.1 The height of the booth needs to conform to the children's ergonomics. The perspective is different between children and adults in viewing things. A lot of public facilities were built on the basis of human body engineering of adult for standard. As people are enjoying various kinds of items on the booth, children can often see adults' legs moving back and forth, so when you go shopping with your child, they were often found to be restless. Consequently, in Children's Museum, the design concept must give the child full respect in details such as thinking about the children's ergonomics. According to statistics, children between the ages of 3 and 8, have the height between 98.7 cm and 138.7 cm. On the one hand, compared with adults, the proportion of children's head is relatively larger than the rest of his body, the ratio of the body and head is approximately 5:1, the ratio of the width between shoulder and head is almost 2:1, and the ratio of the width between hand and head is probably 1:2. On the other hand, like adults, the wingspan is approximately equal to the height. So the settings of display technology should be operable and visible for children. The height of the exhibits should be on the basis of the child's eye level in order to let the children touch the outline of the exhibits with the hand (figure 1). And then the security of exhibits and devices should also be paid

enough attention to. For instance, a square table angle should be converted into round angle and all sharp edges and corners need to be smooth, exhibits such as sword should all be placed in the window. The safety of windows should also be considered. Is glass installations firm or not? Will they hurt the child when they are broken? If it is glass, toughened glass is preferred.

2.2 At present, the development of computer and network technology have provided important and wide range of technical support to modernization construction of Children's Museum, including personnel management, archives management, virtual environment, image processing of the display design, the interactional device, man-machine dialogue system and exhibition of digital museum, etc. The above techniques make the effect remarkable. As is known to all, the traditional exhibition content is restricted by geography, physical carrier, time and space, children are at the bottom of the propaganda chain, and they accept information passively and indiscriminately, so the children can easily form resistance to the museum. At present, the collision between traditional means and new media means has opened up a new train of thought for the exhibition display. Among them, display modes by various types of technologies and the application of interactive devices are very attractive technologies. A virtual environment has been made by the reasonable and moderate application of sound, light and electricity [7]. At the same time dynamic picture has emerged realistically by making the animals or plants move. During this, the child will stay in the application space of high-tech and enjoy the game all the time. In conclusion, the technology above is very popular with children because it has aroused great interest in them.

A. People all know that magic has a magical attraction to children. Can it improve the child's imagination as the breakthrough point? New Walk Museum in Leicester, Britain has set up a special magic pavilion for the children. At the door, you can't help watching, because the voice of magic would attract you as a tour guide. After entering the door, you will find the person model of Harry Potter was displayed in the glass window (figure 2). The book of Harry Potter was placed aside. Also in the corner of the magician pavilion, the posters on the wall according with the nature of magic are beyond common sense. And on the TV nearby, shows some segments of magician's performance accompanied by humorous laughter occasionally. Looking around, various kinds of distorting mirrors on the wall were designed in the shape of butterflies, aircrafts and others. When you pass by, your image will be changed in the mirror. Even if you don't understand magic, you will also be infected by the mysterious atmosphere deeply. In the exhibition center, there is a transparent glass window, the model inside was a

magician's props, which looks dignified and mysterious. The glass's transparency and reflectance are very high, if you take photos, your image will be reflected even more clearly than the magician's image. It's very funny, but that kind of effect is surprising, which might be the magician's idea.

B. Automatic induction function has been set up properly in the venues. When the audience stand before the gallery of virtual reality environment, the use of computers with sounds and pictures will generate a simulated environment, which makes you feel as if you were in a real situation. For example, when you are in the unmanned cloth store in the middle ages, you will never feel lonely and cheerless. In front of the counter, the voice of weaving and chatting will appear. When you're gone, the sound will stop automatically. This reflects the pursuit of humanized design. At the same time New Walk Museum follows the idea of 'low cost competition is one of the most important competition strategy, controlling the cost effectively is the key of the project management.' It is worth noticing that the application of a variety of technologies cannot be overflowed. When many galleries are using the technology of sound, the painting exhibition should try to reduce or cancel the sound, to give the audience full of space to think. In addition, part of the animal specimens are static, and some are even shaded in the dim light and look fierce, which is easy to make the child feel anxiety and illusion, not to mention the help of sound. So, simulating realistic situation selectively is necessary, and the environment that may cause fear should be avoided. We should also pay attention to the adjustment of the colors and light in the gallery. A research result from forint, a famous lighting expert, shows that the illumination can produce a series of effects on people's space perception [8]. In Children's Museum, maintaining adequate light is very helpful to children's mental health.

2.3 The museum should provide suitable interactive device, which makes the child get the corresponding information feedbacks by touching and controlling, and to acquire knowledge in the interaction. Servicing for children indeed, the standard of programming of the museum should be based on the characteristics of children's physical and mental development [9]. Children's psychological and physiological characteristics determine their short attention span, but the desire to explore and the manipulative ability of the child are better than adults. Due to large gap between different children's mental and physical abilities, prescribing a limit to the age of the child gives the exhibition more difficulty. Experts analyze: 3 to 9 years old is the critical period for the development of children's self-consciousness[10]. Children like to play games in droves between 3 to 6 years old, during which they learn to handle interpersonal relationships in the interaction, and



personality will be formed; children between 6 to 8 years old will be attracted by the activities of physical skills. They like to test their physical alertness through some activities unquestionably. Therefore, the Children's Museum should set interactive contents in accordance with the children aged 3 to 9 years old. Moreover, for strange things, a psychology study result shows that the acceptance rate is 15% just by hearing; the acceptance rate is 25% only by sight; the acceptance rate can reach 65% by the combination of all three (visual, auditory, and kinesthetic). In addition, for the temporary storage time of the message, the sense of touch is 20 times longer than visual sense and 10 times longer than sense of hearing [11].



Figure 3. brochure with excellent pictures



Figure 4. big screen simulate



Figure 5. a manual device



Figure 6. small architect



Figure 7. the photos will be amplified and become three-dimensional



Figure 8. coin can make it move

A. In New Walk Museum, TV set, computer and other interactive devices are all installed in each exhibition area. Normally, the TV is highly hung in the exhibition area, while the computers and interactive devices are limited to the positions for children to operate. For example, the height of the computer in the gallery of birds is limited to one meter, so as to let the child touch the screen with the hand. There is a beautiful forest environment on the screen and the birds are placed in every corner of the forest respectively, as long as the children like, they can press the mouse to choose any kind of bird. Then, all kinds of information such as the foods and migration of the birds will be listed in a subdirectory. At the same time brochure recording details of each bird is placed on the window sill. Reading paper books by traditional method can also help your child find the answers if he does not like to use computer (Fig.3). Besides, the area for fossils of ancient fish shows the prehistoric giant fishes swimming in the water on the huge slide show (Fig.4). One by one, the fishes appear and stay for a period of time for you to understand. How to understand it? If you watch carefully, you will find that there is a manual device below the slide show, there are two control handles below the screen of the device, one handle can show different angles of the fish, and then the details could also be enlarged; the other handle is used to control the speed and direction of the swimming fish(Fig.5).



And for another example, the children can choose a suitable shape of stone to fill the gap of the Parthenon on the computer after visiting the ancient Greek architecture (Fig.6). Moreover, magnifying glasses in the exhibition are not uncommon. In general, a group of black and white photos can be shifted below a magnifying glass which is fixed on the shelf. During this process, the photo will be amplified and become three-dimensional (Fig.7). As long as the children like to manipulate, they could see more beautiful things in this way. There also placed a special microscope on some tiny animal specimens, you will be able to observe the texture and structure of the specimen further through the microscope. It is worth noting that designers don't like to waste any space, so at the corner of the hall, where children often pass by, designers designed a unique small window, where a group of ancient biological models (Fig.8) were put in. A mother inserted a coin for her child, the animals begin to move vividly, roc hovering over the temple begins to scream in the air, dinosaurs are stretching their necks and screaming to the roc, the atmosphere is very real. The children are quite happy and could not bear to leave.

In a word, the coordination ability of brain, eyes and hands are enhanced during the process of manipulating. If possible, more control buttons should be installed on the interactive devices, which are more suitable for children aged 2 to 4 years old than a computer mouse.

B. Older children can use mouse properly during watching and exploration process. But the design of the mouse should meet the needs of the growth of the children's hand. As far as a child is concerned, the mouse needs not only to meet the functional requirements, but also to be safe, comfortable, convenient and beautiful. School-age children are in a particular stage of growth, wrist, finger and vertebra are still immature with less calcium in the bone tissue. The process of ossification has not yet completed and the elasticity of the bone is very strong, so the bone is easy to be bended. Consequently, school-age children would suffer carpal tunnel syndrome if they touch the mouse too often or use the computer for a long time. Accordingly, stylist must attach importance to the characteristics of children's hand during the process of designing, to give full consideration to the demands on the structure, the size, hardness and softness of the children's hand. The mouse shell is built by size 7 plastic polycarbonate in the past, but this material is relatively hard for young children's fingers, children's fingers are susceptible to the mouse, and thus the development of the fingers are affected by the mouse inevitably. Then, what materials can suit children's hand and promote the growth of them? The answer is soft and flexible material. Many people give top priority to silica gel, which is very helpful to protect the child's hands and joints with its soft, comfortable, safe non-toxic, high

fracture resistance and high temperature resistant material. Also, the size of mouse for Children should be smaller than that for adults.

2.4 In the webpage design, the size of the font should be larger than ever. In addition, children are unlikely to have much interest in literacy, and the understanding of the text is not mature, so the space and the proportion of the text should be as little as possible. Common words with few strokes are welcome because too much ornament is likely to cause visual fatigue, which makes the child feel bored easily. According to research, the increase of the number of strokes is a major cause of visibility reduction [12]. With the development of children's vision, the number of strokes can be appropriately increased. We also know that eyesight drops easily if adults stare at a screen for too long, let alone the children. Therefore, the designer needs to try to minimize the stimulation from computer screen. The reflective rate and the color contrast of the computer screen should not be too sharp. Also, pictures should be in harmony, concise, lively and not be too complicated. For example, pictures with vivid cartoon or comic forms have to be given priority. In the galleries of the duck, it is a good design to set Donald Duck's image on the screen as background images. When the children see Donald Duck on the screen, friendly feeling will be aroused. Consequently they might compare Donald Duck with the duck in actual life and then the thought of creation will be sparked and the children's artistic view will be improved by looking at life with art gradually.



Figure 9. The imagination is developed by making use of the trees full



Figure10. restaurant next to the bookstore



Figure 11. recreation area for children

2.5 Refusing boring exhibits in Children's Museum. Developing the child's imagination and using the exhibition space opportunely are necessary. In the overall environment, especially vivid images and color settings will no doubt make children feel everything is new and fresh. So their imagination will be improved rapidly. Imagination is one of the ways of promoting children to become more intelligent. For instance, in the animal pavilion, there are some tall trees reaching the roof, and you will discover the mystery hiding in the trunk (figure 9). As long as you open a piece of bark by hand, you'll find small animal specimens inside, such as birds, insects, etc. All those little animals are placed in delicate glass windows and lighted up. The imagination of the child is developed by making full use of the trees as a prop.

2.6 Museum is a place where designers and artists look for inspiration. It should also alleviate social pressure and help get rid of the fatigue [13]. As is known to all, a dining area is the most popular place in Children's Museum (figure 10). In the meantime, baby stroller, baby chairs and maternal special room are compulsory too, because the children can enjoy some drinks and snacks when they are tired of visiting. Moreover, souvenir area was found beside the dining area, where large numbers of arts and crafts closely around the exhibits are sold. This souvenir area is special for children, for the child can hardly forget the exhibits after visiting, then they can get compensation in the souvenir, and choose their favorite exhibits models and buy them, which enable them to continue to ponder or share with friends. Playing is the nature of children, so recreation area is essential too, because the children can have a good time if they feel bored in Children's Museum (figure 11). New Walk Museum has provided omni-directional services for the audience by this concept. It has become a favorable place for family entertainment, entertaining friends, study and communication.

### 3. CONCLUSIONS

Estimating the quality of the exhibitions by evaluation system. What about the effects of the humanized museum? Perhaps only children can give the right remark. In order to get accurate feedbacks, the children can enter the evaluation system on the computer voluntarily before visiting, then press the buttons at the bottom of the screen and select the questions they like, such as: "how humans evolved?" "how birds take things?" Then the computer will

automatically print out the questionnaire. Taking the questionnaire, the child begins to visit the museum. Normally, small audiences can all think about the questions carefully and submit the answers after visiting. Careful children will find that there is a miniature computer at the exit of the pavilion, which stores lots of information closely related to the exhibitions, 24 terminal devices in it can answer any question [14]. If you want to check your answers, search the answers then. The child can also take the questions away, and then give feedbacks to the museum [15] via the Internet after careful consideration.

The children not only have contact with the static objects, but also the dynamic simulation by strolling in the exhibition hall. They have a profound impression on the exhibits in no time and will be educated vividly gradually by viewing, operating, conversation, etc. In short, with children as the center, the exhibition ways supported by various technological means has aroused the children's curiosity and desire to seek knowledge. During this, the cooperation ability between eyes, hands and brain is improved by participation, observing, listening and practical operation. All in all, humanized design idea and practices are the vitality and direction for the development of the Children's Museum. As a kind of knowledge industry, the Children's Museum will grow strong and promising.

### REFERENCES

- [1] Y. Li, The Museum can not be Made as Exhibition Hall - Interview Chairman Xinchao Song of the Association of Chinese Museum, Guangming Daily, Beijing, China, February 8, 2013.
- [2] J. L. Wang, The Present Situation in Function Development and Research of the problems in Virtual Museum of China, Master's Degree Thesis of Beijing second Foreign Languages Institute, Beijing, China, 2008.
- [3] H. Li, Introduction to the Display Design of Art Museum, Information of Science and Technology, 2008, 12(21): 529-530.
- [4] L. Hu, Trying to Talk About the Characteristics of the Children's Museum and the Requirements of the Exhibition Design, The Journal of Chinese Women's College, 2013, 15(8):110-112.
- [5] X. Ge, X. Song and W. H. Wu, The Development and Evolution of the Education Function of American Children's Museum, Master's Degree Thesis of the Development of Foreign Education of Primary and Secondary Schools, 2011.
- [6] X. Liu and J. G. Qiao, Research on Chinese Museum Design based on Virtual Reality, International Workshop on Modelling, Simulation and Optimization, Hong Kong, China, 2008: 372-373.
- [7] S. T. Xu, The Dynamic Display and Art Education of Children's Museum, Teacher's Principle,

Teaching and Research, 2011, 6 (5):23-25.

[8] Y. Yang, Space, Light, Color, Texture, Four Elements of Modern Indoor Environment Design, Annual meeting of the design education of Chinese environmental art, Beijing, China, 2007:114-116.

[9] Q. X. Teng, The Education Mode and Management Research of Children's Museum, Shanghai, China, 2005:7-8.

[10] Zh. Y. Lu and J. Zh. Du, Memory Psychology, People's Education Press, Beijing, China, 2005.

[11] H. Ch. Chen, Factors that affect the characteristics of children's social development and its measurement, the psychological development and education, Beijing, China, 1994.

[12] Y. X. Liu, The architectural design of Children's Library and the Research of Human Engineering,

Journal of Jin Finger, Taiyuan, China, 2009, 4 (3):57-58.

[13] S. Ton, O. Jun, K. Jun, and E. Makoto, Study of the Creation Processes-Based System for Exhibiting Artistic Works, Electronic intelligence communication technology study, Japan, 2005, 105(13):683-684.

[14] Zh. H. Wang, Visiting the Children's Museum in the United States, the Enlightenment (3 to 7 years old), Tianjin, China, 2011, p:27-30.

[15] L. N. Andreas, D. D. Betsy, K. Hub, J. Schmuck, and R. Ian, 12<sup>th</sup> Enriching the Children's Experiences during and after a Museum Visit, IEEE International Conference on Advanced Learning Technologies, Rome, 2012:290-293.

# Study on Nonlinear Input-Output Analysis of the Real Estate Industry with Persistent Disturbances

Jin Li<sup>1</sup>

<sup>1</sup>Department of Building Material Engineering, Chongqing College of Electronic Engineering, Chongqing, 401331, China

## ABSTRACT

A new successive approximation approach (SAA) is introduced to obtain a new decision-making law for a class of nonlinear input-output analysis of the real estate industry with persistent disturbances. By applying the SAA, the original optimal tracking control problem is transformed into a sequence of nonhomogeneous linear two-point boundary value (TPBV) problems. The solution sequence of the inhomogeneous linear TPBV problem uniformly converges to the solution of the original optimal tracking control problem. A feedforward and feedback optimal tracking control (FFOTC) law is derived, which consists of analytic linear feedforward and feedback terms and a nonlinear compensatory term. We give the existence and uniqueness conditions of the FFOTC law. In practical application, by taking the finite-step iteration of nonlinear compensatory term, we may obtain an approximate FFOTC law. In order to obtain a physically realizable feedforward control, a reference input observer and a disturbance observer are introduced. At last, an FFOTC algorithm of solving the approximate FFOTC law is presented, and simulation results demonstrate the validity of this design algorithm.

Keywords: real estate industry; nonlinear input-output analysis; computerized method; persistent disturbances; optimal tracking control; successive approximation approach

## 1. INTRODUCTION

Economic analysis is one of the main purposes of input-output analysis. Input-output table simultaneously reflects the distribution direction and value composition of products or services, completely reflects the technical and economic links among the various departments in the process of social reproduction.

The real estate industry as basic industry of the national economy is closely linked to other industries. And input-output analysis of the real estate industry is inherently nonlinear (Banks & Mhana, 1992; Aganovic & Gajic, 2004; Ian, 2011). Being an important category of nonlinear systems, the bilinear system has been widely used to design real physical systems for enhancing the

performance in purposeful ways.

Optimal control problems for the nonlinear systems are widely studied by many researchers, and some important results are obtained. For example, Becerra (1996) studied the dynamic integrated system optimization for discrete-time optimal control of nonlinear systems, and the equation for estimating the parameter was given. Alt (1990) analyzed the stability of nonlinear optimal control system with constraint. Because the analytical solution of optimal control problems is not existed generally, it is interested to find the approximate approaches for solving the optimal control problem for nonlinear systems. One of the approximation approaches is called as power series approximation (PSA). This approach is by using a power series, or by introducing a temporary variable and expanding around it (Nishikawa et al, 1971; Tang et al, 2002), or by using so-called Adomian's decomposition (Chanane, 1998) to separate the nonlinear terms and approximate the solution of the HJB equation. Another approach is the successive Galerkin approximation (SGA), where an iterative process is used to find a sequence of approximations approaching the solution of the HJB equation. This is done through solving a sequence of the generalized HJB equation (Mracek & Cloutier, 1998; Liu, 2008; Liu, 2010; Jih, 2011). Other approaches include the works of Ghazali *et al.*, (2011), Qian, Ma, Dai, & Fang, (2012), and so on.

In this thesis, we will consider to develop an approximation method to research bilinear input-output analysis of the real estate industry. The rest of the paper is organized as follows. Section 2 we present a model of bilinear input-output systems. Section 3 discusses the detailed design scheme and algorithm of the decision-making law for bilinear input-output analysis of the real estate industry. Conclusions are presented in Section 4.

## 2. PROBLEM STATEMENT

Consider an input-output nonlinear analysis of the real estate industry with persistent disturbances



described by

$$\begin{aligned}\dot{x}(t) &= Ax(t) + Bu(t) + f(x) + Dv(t), \quad t > 0 \\ x(0) &= x_0 \\ y(t) &= Cx(t)\end{aligned}\quad (1)$$

where  $x \in R^n$ ,  $u \in R^p$ ,  $v \in R^p$ , and  $y \in R^m$  are the state vector, the control vector, the external disturbance vector, and output vector, respectively.  $f(x)$  is the nonlinear vector.  $A, B, C$ , and  $D$  are real constant matrices of appropriate dimensions.

**Assumption 1.** The nonlinear vector  $f(x)$  satisfies  $f(0) = 0$  and Lipschitz condition on  $R^n$

$$\|f(x) - f(\hat{x})\| \leq \alpha \|x - \hat{x}\|, \quad \forall x, \hat{x} \in R^n \quad (2)$$

where  $\alpha$  is some constant.

**Assumption 2.** The desired output (reference input)  $\tilde{y}$  which is tracked by  $y$  in system (1) can be given by the following exosystem

$$\begin{aligned}\dot{z}(t) &= Fz(t) \\ \tilde{y}(t) &= Hz(t)\end{aligned}\quad (3)$$

where  $z \in R^q$ ,  $\tilde{y} \in R^m$ ,  $F$  and  $H$  are constant matrices of appropriate dimensions, and the pair  $(F, H)$  is observable completely.

**Assumption 3.** The dynamic characteristics of external disturbance vector  $v(t)$  can be expressed as the following exosystem.

$$\begin{aligned}\dot{w}(t) &= Gw(t) \\ v(t) &= Mw(t)\end{aligned}\quad (4)$$

where  $w \in R^r$ ,  $G$  and  $M$  are constant matrices of appropriate dimensions. All eigenvalues of  $G$  satisfy

$$\operatorname{Re}(\lambda_i(G)) \leq 0, \quad i = 1, 2, \dots, r \quad (5)$$

Besides, eigenvalues with the zero real part are simple roots of minimum polynomial of  $G$  in order to guarantee that exosystem (4) is stable or asymptotically stable. The pair  $(G, M)$  is observable completely.

If the exosystem (4) is asymptotically stable, we select the following quadratic performance index;

$$J = \int_0^\infty [e^T(t)Qe(t) + u^T(t)Ru(t)]dt \quad (6)$$

If the exosystem (4) is stable but not asymptotically stable, the disturbance vector  $v(t)$  will not tend to zero so that the state vector  $x(t)$  and the control vector  $u(t)$  are impossible to tend to zero contemporaneously. Therefore, the quadratic performance index (6) cannot be

convergent. In this case, we can choose the quadratic average performance index

$$J = \lim_{T \rightarrow \infty} \frac{1}{T} \int_0^T [e^T(t)Qe(t) + u^T(t)Ru(t)]dt \quad (7)$$

where  $Q$  and  $R$  are positive definite matrices of appropriate dimensions, and  $e(t)$  is the output error

$$e(t) = \tilde{y}(t) - y(t) \quad (8)$$

The optimal tracking control problem is to search a control law  $u^*(t)$ , which makes the value of quadratic performance index (6) or (7) minimum. It is well known that the designing processes of the FFOTC laws are the same for quadratic performance indexes (6) and (7).

Applying the maximum principle to the problem (1) and (6), the optimal control law can be written as

$$u(t) = -R^{-1}B^T\lambda(t) \quad (9)$$

where  $\lambda(t)$  is the solution to the following nonlinear TPBV problem

$$\begin{aligned}-\dot{\lambda}(t) &= C^TQCx(t) - C^TQHx(t) + A^T\lambda(t) + f_x^T(x)\lambda(t) \\ \dot{x}(t) &= Ax(t) - S\lambda(t) + f(x) + Dv(t) \\ \lambda(\infty) &= 0, \quad x(0) = x_0\end{aligned}\quad (10)$$

where  $S = BR^{-1}B^T$  and  $f_x^T(x) = \partial f^T(x)/\partial x$ .

Unfortunately, the analytical solution of nonlinear TPBV problems (16) is very difficult to be solved generally. Therefore, we will propose a new SAA in this paper.

### 3. DESIGN OF THE FFOTC LAW FOR NONLINEAR INPUT-OUTPUT ANALYSIS OF THE REAL ESTATE INDUSTRY

In this section, we will discuss the design of the FFOTC law of the system (1) with the quadratic performance index (6) or (7), the FFOTC law will be presented in theorem 1.

**Theorem 1:** Consider the optimal tracking control problem to minimize the quadratic performance index (6) or (7) subject to system (1). Assume that:

(i) The pair  $(A, B)$  is completely controllable and the pair  $(A, C)$  is completely observable, where  $C$  is a full rank matrix, which is defined by  $Q = C^TC$ .

(ii) Assumptions (1), (2) and (3) all hold.

Then the FFOTC law  $u^*(t)$  is existent and unique, and its form as follows:

$$u^*(t) = -R^{-1}B^T[P\dot{x}(t) + Pz(t) + \bar{P}w(t) + g^{(\infty)}(t)] \quad (11)$$

where  $P$  is the unique positive definite solution

of the *Riccati* matrix equation

$$A^T P + PA - PSP + C^T QC = 0 \quad (12)$$

$P_1$  is the unique solution of the matrix equation

$$(A - SP)^T P_1 + P_1 F = C^T QH \quad (13)$$

$\bar{P}$  is the unique solution of the matrix equation

$$(A - SP)^T \bar{P} + \bar{P} G = -PDM \quad (14)$$

The adjoint vector  $g^{(k)}(t)$  is the solution of the following TPBV sequences

$$\begin{aligned} g^{(0)}(t) &\equiv 0 \\ -\dot{g}^{(k)}(t) &= (A^T - PS)g^{(k)}(t) + Pf(x^{(k-1)}) \\ &\quad + Y^{(k-1)}[Px^{(k-1)}(t) + P_1 z(t) + \bar{P}w(t) + g^{(k-1)}(t)] \\ g^{(k)}(\infty) &= 0, \quad k=1, 2, \dots \end{aligned} \quad (15)$$

where  $x^{(j)}(t)$  satisfies

$$\begin{aligned} x^{(0)}(t) &\equiv 0 \\ \dot{x}^{(k)}(t) &= (A - SP)x^{(k)}(t) + (DM - \bar{S}\bar{P})w(t) - SP_1 z(t) \\ &\quad - Sg^{(k)}(t) + f(x^{(k-1)}) \\ x^{(k)}(0) &= x_0, \quad k=1, 2, \dots \end{aligned} \quad (16)$$

and  $Y^{(k)} = \partial f^T(x^{(k)}) / \partial x^{(k)}$ .

**Proof:** Let

$$\lambda(t) = Px(t) + P_1 z(t) + P_2 v(t) + g(t) \quad (17)$$

In addition, define  $\bar{P} = P_2 M$  in view of the disturbance  $v(t)$  with the form (3). So we get

$$\begin{aligned} \dot{\lambda}(t) &= P\dot{x}(t) + P_1 \dot{z}(t) + P_2 \dot{v}(t) + \dot{g}(t) \\ &= P\dot{x}(t) + P_1 Fz(t) + \bar{P}Gw(t) + \dot{g}(t) \\ &= (PA - PSP)x(t) + (P_1 F - PSP_1)z(t) + \\ &\quad (\bar{P}G - PSP\bar{P} + PDM)w(t) + \dot{g}(t) - PSg(t) + Pf(x) \end{aligned} \quad (18)$$

By substituting the derivative of  $\lambda$  in (18) for the left side of the first equation in (10), we obtain the *Riccati* matrix equation (12), the matrix equations (13) and (14), and the adjoint vector equation

$$\begin{aligned} -\dot{g}(t) &= (A^T - PS)g(t) + Pf(x) \\ &\quad + f_x^T(x)[Px(t) + P_1 z(t) + \bar{P}w(t) + g(t)] \\ g(\infty) &= 0 \end{aligned} \quad (19)$$

It is well known that  $P$  is the unique positive-definite solution of *Riccati* matrix equation (12). Substituting  $P$  in equation (13) and (14), we can solve  $P_1$  and  $\bar{P}$  uniquely (Ref. 10). When  $P$ ,  $P_1$  and  $\bar{P}$  are got uniquely, therefore, we have the FFOTC law

$$u^*(t) = -R^{-1}B^T[Px(t) + P_1 z(t) + \bar{P}w(t) + g(t)] \quad (20)$$

Substituting  $u^*(t)$  in the first equation of (10), the state equation is obtained

$$\begin{aligned} \dot{x}(t) &= (A - SP)x(t) + (DM - \bar{S}\bar{P})w(t) \\ &\quad - SP_1 z(t) - Sg(t) + f(x) \end{aligned} \quad (21)$$

$$x(0) = x_0$$

Because equations (19) and (21) is coupling, it is difficult for  $g(t)$  in the FFOTC law to be solved, so we need to realize equations (19) and (21) decoupling.

Now, according to equations (19), (21) and (20), we construct the TPBV sequences (15) and (16), as well as the corresponding control sequence  $u^{(k)}(t) = -R^{-1}B^T[Px^{(k)}(t) + P_1 z(t) + \bar{P}w(t) + g^{(k)}(t)]$  (22)

Under the assumption of  $x^{(0)}(t) \equiv 0$  and  $g^{(0)}(t) \equiv 0$ ,  $g^{(k)}(t)$  and  $x^{(k)}(t)$  in (15) and (16) for  $k \geq 1$  can be obtained from solving the linear inhomogeneous vector differential equations (15) and (16) together with known initial and terminal conditions because  $P$ ,  $P_1$ ,  $P_2$ ,  $x^{(k-1)}(t)$ ,  $f(x^{(k-1)})$ , and  $Y^{(k-1)}$  in (15) and (16) have been obtained from the previous iteration. So the approximation of  $g^{(k)}(t)$  and  $x^{(k)}(t)$  can be calculated successively. By Lemma 1 in Ref. 11, the solution sequences  $\{g^{(k)}(t)\}$  and  $\{x^{(k)}(t)\}$  of (15) and (16), respectively are uniformly convergent. It is clear that the control sequence  $\{u^{(k)}(t)\}$  in (22) is only related to  $\{g^{(k)}(t)\}$  and  $\{x^{(k)}(t)\}$ , so  $\{u^{(k)}(t)\}$  is uniformly convergent.

When  $k \rightarrow \infty$ , the limits of  $\{x^{(k)}(t)\}$  and  $\{u^{(k)}(t)\}$  become the optimal state trajectory  $x^*(t)$  and the optimal control law  $u^*(t)$  of systems (1), respectively. Define  $\lim_{k \rightarrow \infty} g^{(k)}(t) = g^{(\infty)}(t)$ , then the FFOTC is rewritten as the expression (11). The proof is complete.

It is usually impossible to obtain the exact adjoint vector  $g^{(\infty)}(t)$  when designing a FFOTC law in practice. In many cases, it may be better to choose an  $g^{(N)}(t)$  as the approximation of  $g^{(\infty)}(t)$  where  $N$  depends on a concrete error criterion. For instance, we give a small enough number  $\sigma > 0$  in this paper. Then every time when  $g^{(k)}$  is obtained from (13) we got a control law as follows



$$u_k(t) = -R^{-1}B^T[Px(t) + P_1z(t) + \bar{P}w(t) + g^{(k)}(t)] \quad (23)$$

**Remark 1.** The state vector  $x(t)$  in (23) is an accurate solution of system (16) in case of  $N \rightarrow \infty$ , only  $g^{(k)}(t)$  is an approximation by substituting finite-step iteration for  $g^{(\infty)}(t)$ . So the feedforward and feedback suboptimal tracking control law  $u_k(t)$  in (23) is closer to the optimal tracking control law than that in (22).

A successive approximation algorithm to obtain the feedforward and feedback suboptimal tracking control law (23) is proposed as follows.

**Algorithm 1.**

Step 1. Obtain the desired output  $\tilde{y}(t)$  from (5); solve  $P$  from the Riccati matrix equation (12),  $P_1$  and  $\bar{P}$  from the matrix equations (13) and (14). Let  $k=1$ ;  $x^{(0)} = g^{(0)} = 0$ ;  $\sigma > 0$ .

Step 2. Solve  $g^{(k)}(t)$  and  $x^{(k)}(t)$  from (15) and (16); calculate  $u^{(k)}(t)$  from (22), and substituting  $u^{(k)}(t)$  in system (1), obtain the closed-loop system; then get  $e_k(t)$  from (6); At last calculate  $J_k$  according to

$$J_k = \int_0^\infty [e^T(t)Qe(t) + u_k^T(t)Ru_k(t)]dt \quad (24)$$

or

$$J_k = \lim_{T \rightarrow \infty} \frac{1}{T} \int_0^T [e^T(t)Qe(t) + u_k^T(t)Ru_k(t)]dt \quad (25)$$

Step 3. If  $|(J_k - J_{k-1})/J_k| \leq \sigma$ , stop and output  $u_k(t)$ .

Step 4. Let  $k = k + 1$  and go to step 2.

**4. PHYSICALLY REALIZABLE PROBLEM OF THE FFOTC LAW**

In fact, because  $z(t)$  and  $w(t)$  in (11) are the state vectors of exosystems (3) and (4) respectively, the FFOTC law is physically unrealizable in the practical engineering. In this section, we will introduce a reduced-order reference input observer and a reduced-order disturbance observer to make it realizable.

It is well known that for the full rank matrix  $H$  in (3) and  $M$  in (4), it must exist some constant matrices  $L \in R^{(q-m) \times q}$  and  $N \in R^{(r-p) \times p}$  so that the matrix  $[H^T \ L^T] \in R^{q \times q}$  and  $[M^T \ N^T] \in R^{r \times r}$  are nonsingular. Let

$$T = \begin{bmatrix} H \\ L \end{bmatrix}^{-1} = \begin{bmatrix} T_1 & T_2 \end{bmatrix}, \quad T^{-1}FT = \begin{bmatrix} F_1 & F_{12} \\ F_{21} & F_2 \end{bmatrix} \quad (26)$$

$$O = \begin{bmatrix} M \\ N \end{bmatrix}^{-1} = \begin{bmatrix} O_1 & O_2 \end{bmatrix}, \quad O^{-1}GO = \begin{bmatrix} G_1 & G_{12} \\ G_{21} & G_2 \end{bmatrix} \quad (27)$$

where  $T_1 \in R^{q \times m}$ ,  $T_2 \in R^{q \times (q-m)}$ ,  $F_1 \in R^{m \times m}$ ,  $F_{12} \in R^{m \times (q-m)}$ ,  $F_{21} \in R^{(q-m) \times m}$  and  $F_2 \in R^{(q-m) \times (q-m)}$ ;  $O_1 \in R^{r \times p}$ ,  $O_2 \in R^{r \times (r-p)}$ ,  $G_1 \in R^{p \times p}$ ,  $G_{12} \in R^{p \times (r-p)}$ ,  $G_{21} \in R^{(r-p) \times p}$  and  $G_2 \in R^{(r-p) \times (r-p)}$ .

In order to construct two observers, we make the equivalent linear transformation  $z = T\bar{z}$  and  $w = O\bar{w}$ . Denote that  $\bar{z}^T = [\bar{z}_1^T \ \bar{z}_2^T]$  and  $\bar{w}^T = [\bar{w}_1^T \ \bar{w}_2^T]$ , where  $\bar{z}_1 \in R^m$ ,  $\bar{z}_2 \in R^{(q-m)}$ ,  $\bar{w}_1 \in R^p$ , and  $\bar{w}_2 \in R^{(r-p)}$ . So the equivalent systems of exosystem (3) and exosystem (4) are obtained as follows

$$\begin{aligned} \dot{\bar{z}}_1(t) &= F_1\bar{z}_1(t) + F_{12}\bar{z}_2(t) \\ \dot{\bar{z}}_2(t) &= F_{21}\bar{z}_1(t) + F_2\bar{z}_2(t) \end{aligned} \quad (28)$$

$$\begin{aligned} \tilde{y}(t) &= \bar{z}_1(t) \\ \dot{\bar{w}}_1(t) &= G_1\bar{w}_1(t) + G_{12}\bar{w}_2(t) \\ \dot{\bar{w}}_2(t) &= G_{21}\bar{w}_1(t) + G_2\bar{w}_2(t) \\ v(t) &= \bar{w}_1(t) \end{aligned} \quad (29)$$

In (28) and (29),  $\bar{z}_1$  is just the reference input of  $\tilde{y}$ ,  $\bar{w}_1$  is just the reference input of  $v$ . We only need construct a reduced-order observer with respect to  $\bar{z}_2$  and  $\bar{w}_2$ .

Noting that  $HT = [I_m \ 0]$ ,  $MO = [I_p \ 0]$ ,  $(F, H)$  and  $(G, M)$  are completely observable. Therefore, obviously  $(F_2, F_{21})$  and  $(G_2, G_{21})$  are also completely observable. Construct the reduced-order reference input observer and the reduced-order disturbance observer as follows

$$\dot{m}(t) = \hat{F}m(t) + \hat{H}\tilde{y}(t) \quad (30)$$

$$\hat{z}_2(t) = m(t) + K_1\tilde{y}(t)$$

$$\dot{n}(t) = \hat{G}n(t) + \hat{M}v(t) \quad (31)$$

$$\hat{w}_2(t) = n(t) + K_2v(t)$$

where  $m \in R^{(q-m)}$  and  $n \in R^{(r-p)}$  are the constructed variables;  $\hat{z}_2$  and  $\hat{w}_2$  are the observing values of  $\bar{z}_2$  and  $\bar{w}_2$ ;

$\hat{F} = F_2 - K_1 F_{12}$  ,  
 $\hat{H} = F_2 K_1 - K_1 F_{12} K_1 + F_{12} - K_1 F_1$  ,  
 $\hat{G} = G_2 - K_2 G_{12}$  ,  
 $\hat{G} = G_2 K_2 - K_2 G_{12} K_2 + G_{12} - K_2 G_1$  ;  $K_1$  and  $K_2$  are some undetermined coefficient matrices.  
 In order to guarantee the speediness and nicety of observers in (30) and (31), we can select matrix  $K_1$  and  $K_2$  such that all the eigenvalues of matrices  $F_2 - K_1 F_{12}$  and  $G_2 - K_2 G_{12}$  are assigned to appointed places. From (3), (4), (30) and (31), we can get the observing values of  $z(t)$  and  $w(t)$  as follows

$$\hat{z}(t) = T_2 m(t) + (T_1 + T_2 K_1) \tilde{y}(t) \quad (32)$$

$$\hat{w}(t) = O_2 n(t) + (O_1 + O_2 K_2) v(t) \quad (33)$$

By above reconstruction of  $z(t)$  and  $w(t)$ , finally, a dynamic physically realizable FFOTC law is obtained in the form

$$\begin{aligned}
 \dot{m}(t) &= \hat{F}m(t) + \hat{H}\tilde{y}(t) \\
 \dot{n}(t) &= \hat{G}n(t) + \hat{M}v(t) \\
 u^*(t) &= -R^{-1}B^T [Px(t) + P_1 T_2 m(t) + P_1 (T_1 + T_2 K_1) \tilde{y}(t) \\
 &\quad + \bar{P} O_2 n(t) + \bar{P} (O_1 + O_2 K_2) v(t) + g^{(\infty)}(t)]
 \end{aligned} \quad (34)$$

## 5. SIMULATION AND DISCUSSION

Consider an input-output nonlinear analysis of the real estate industry with persistent disturbances, system parameters as follows

$$A = \begin{bmatrix} 0 & 1 \\ -1 & 0.2 \end{bmatrix}, \quad B = \begin{bmatrix} 0 \\ 1 \end{bmatrix}, \quad C = \begin{bmatrix} 1 \\ 0 \end{bmatrix}, \quad D = \begin{bmatrix} 1 & 0 \\ 0 & 1 \end{bmatrix}, \quad (35)$$

$$f(x) = \begin{bmatrix} x_1 x_2 \\ x_1^2 - x_2^2 \end{bmatrix}, \quad \begin{bmatrix} x_1(0) \\ x_2(0) \end{bmatrix} = \begin{bmatrix} 0.5 \\ 0 \end{bmatrix}$$

The parameters of the desired output  $\tilde{y}$  as follows:

$$F = \begin{bmatrix} -0.1 & 1 \\ -1 & -0.2 \end{bmatrix}, \quad H = \begin{bmatrix} 0.5 & 0 \end{bmatrix}, \quad \begin{bmatrix} z_1(0) \\ z_2(0) \end{bmatrix} = \begin{bmatrix} 0.5 \\ 0 \end{bmatrix} \quad (36)$$

And the parameters of the disturbances,

$$M = \begin{bmatrix} 0.5 & 0 \\ 0 & 0.5 \end{bmatrix}, \quad \begin{bmatrix} w_1(0) \\ w_2(0) \end{bmatrix} = \begin{bmatrix} 1 \\ 0 \end{bmatrix} \quad (37)$$

(1) Supposing  $G = \begin{bmatrix} -0.1 & 1 \\ -1 & -0.1 \end{bmatrix}$ , the exosystem

(4) is stable asymptotically because of eigenvalues  $\lambda_{1,2} = -2 \pm i$ . So we select the quadratic performance index (6), and the parameters are  $Q=1$ ,  $R=1$ . Then selecting  $\sigma = 0.001$ , if  $|(J_k - J_{k-1})/J_k| \leq \sigma$ , we consider that the FFOTC law satisfies the control precision. The

simulation curves of  $u(t)$  as follows

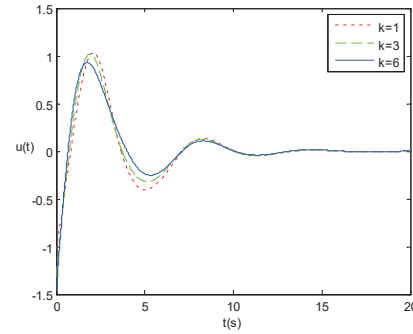


Fig. 1 The simulation curves of  $u(t)$

Table 1. Performance index values and errors

| $k$                     | 1        | 2        | 3       | 4       | 5       | 6       |
|-------------------------|----------|----------|---------|---------|---------|---------|
| $J_k$                   | 114.3450 | 107.4541 | 97.5106 | 96.4088 | 95.7056 | 95.6889 |
| $ (J_k - J_{k-1})/J_k $ | /        | 0.0603   | 0.0925  | 0.0115  | 0.0073  | 0.0002  |

From Table 1, it is shown that the value of cost functional diminishes as  $k$  increases and tends to an optimal value  $J^*$ . At the same time the error decreases to zero. When  $k=6$ ,  $J_6$  satisfies the error, Therefore,  $u_6(t)$  can be considered as the optimal control  $u^*(t)$ .

(2) Supposing  $G = \begin{bmatrix} 0 & 2 \\ -2 & 0 \end{bmatrix}$ , the exosystem (4)

is stable but not asymptotically stable because of eigenvalues  $\lambda_{1,2} = \pm 2i$ . So we select the quadratic average performance index (7), and the parameters are  $Q=1$ ,  $R=10$ . Then selecting  $\sigma = 0.01$ , if  $|(J_k - J_{k-1})/J_k| < \sigma$ , we consider that the FFOTC law satisfies the control precision. And the simulation curves of  $u(t)$  as follows

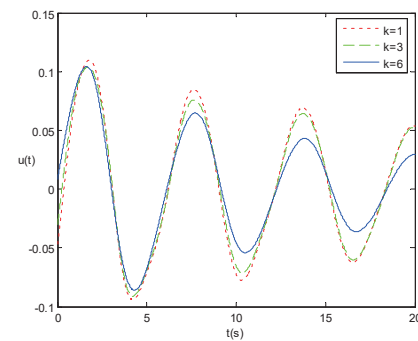


Fig. 2 The simulation curves of  $u(t)$

Table 2. Performance index values and errors

| $k$ | 1 | 2 | 3 | 4 | 5 | 6 |
|-----|---|---|---|---|---|---|
|-----|---|---|---|---|---|---|

|                   |             |             |             |             |             |             |
|-------------------|-------------|-------------|-------------|-------------|-------------|-------------|
| $J_k$             | 17.4<br>969 | 16.5<br>479 | 16.0<br>548 | 15.7<br>536 | 15.4<br>917 | 15.4<br>414 |
| $ J_k - J_{k-1} $ | /           | 0.05<br>42  | 0.02<br>98  | 0.01<br>88  | 0.01<br>66  | 0.00<br>33  |

From Table 2, it is shown that the value of cost functional diminishes as  $k$  increases and tends to an optimal value  $J^*$ . At the same time the error decreases to zero. When  $k = 6$ ,  $J_6$  satisfies the error, Therefore,  $u_6(t)$  can be considered as the optimal control  $u^*(t)$ .

## 5. CONCLUSION

In this paper, we have presented a design scheme of the FFOTC law for nonlinear input-output analysis of the real estate industry with persistent disturbances and given a proof for the uniform convergence of the successive approximation algorithm. This approach only requires solving a sequence of linear vector differential equations, instead of a sequence of HJB equations as the SGA approach or the state-dependent *Riccati* equation as the SAA approach. The successive approximation approach reduces the computational time and avoids the trouble of direct solving the nonlinear TPBV problem or the HJB equation. Finally, simulation results show that the FFOTC law is high in efficiency, easy to implement. Future effort should be directed towards proving more general nonlinear systems.

## ACKNOWLEDGEMENT

This work is supported by the science and technology research project of Chongqing City Board of Education (KJ132206); the "twelfth five-year" project of Chongqing municipal education science (2014-GX-055).

## REFERENCES

- [1]Aganovic, Z., & Gajic, Z. (2004). The Successive Approximation Procedure For Finite-Time Optimal Control of Bilinear Systems. *IEEE Transactions on Automatic Control*, 39 (9), 1932-1935.
- [2]Alt, W. (1990). Stability of solutions to control constrained nonlinear optimal control problems. *Applied Mathematics and Optimization*, 21, 53-68.
- [3]Banks, S. P., & Mhana, K. J. (1992). Optimal Control and Stabilization For Nonlinear Systems.

IMA Journal of Mathematical Control and Information, 9(4), 179-196.

- [4]Becerra, V. M., & Roberts, P. D. (1996). Dynamic integrated systems optimization and parameter estimation for discrete time optimal control of nonlinear systems. *International Journal of Control*, 63, 257-281.
- [5]Chanane, B. (1998). Optimal control of nonlinear systems: a recursive approach. *Computers & Mathematics with Applications*, 35, 29-33.
- [6]Ghazali, R., Sam, Y. M., Rahmat, M. F., Zulfatman, & Hashim, A. W. I. M. (2011). Perfect Tracking Control with Discrete-time LQR for a Non-minimum Phase Electro-hydraulic Actuator System. *International Journal on Smart Sensing and Intelligent Systems*, 4(3), 424-439.
- [8]Ian, A. W., (2011). The Evolution of the Massively Parallel Processing Database in Support of Visual Analytics. *Information Resources Management Journal*, 24(4), 1-26.
- [9]Jih, W.J. (2011). Impact of e-CRM on Website Loyalty of a Public Organization's Customers *Journal of Computational Information Systems*, 24(2), 46-60.
- [10]Liu, P. (2008). An Approximate Discrete Controller for Networked Control Systems with Time Delay. *Journal of Computational Information Systems*, 4(5), 1955-1959.
- [11]Liu, P. (2010). A New Approximation Congestion Controller for Multiplayer Networked Control Systems with Time Delay. *Journal of Computational Information Systems*, 6(5), 3725-3730.
- Mracek, C. P., & Cloutier, J. R. (1998). Control Designs for the Nonlinear Bench-mark Problem Via the State-dependent Riccati Equation Method. *International Journal of Robust and Nonlinear Control*, 8(3), 401-433.
- [13]Nishikawa, Y., Sannomiya, N., & Itakura, H. (1971). A method for suboptimal design of nonlinear feedback systems. *Automatica*, 7, 703-712.
- [14]Qian, K., Ma, X.D., Dai, X. Z., & Fang, F. (2012). Spatial-temporal Collaborative Sequential Monte Carlo for Mobile Robot Localization in Distributed Intelligent Environments. *International Journal on Smart Sensing and Intelligent Systems*, 5(2), 487-503.
- [15]Tang, G. Y., Qu, H. P., & Gao, Y. M. (2002). Sensitivity approach of suboptimal control for a class of nonlinear systems. *Journal of Ocean University of Qingdao*, 32, 615-620

# A Spline Smoothing Newton Method for $l_\infty$ Fitting Ellipsoids

Li Dong<sup>1\*</sup>, Meili Zhang<sup>2</sup>

<sup>1</sup> College of Science, Dalian Minzu University, Dalian, Liaoning, 116600, China

<sup>2</sup> Department of Basic, Dalian Naval Academy, Dalian, Liaoning, 116018, China

**Abstract:** We consider the ellipsoids fitting problem in this paper. Generally, when the measured data are accurate and they are not orthogonal distance, it is appropriate to use  $l_\infty$  norm instead of  $l_2$  norm.  $l_\infty$  fitting ellipsoids need to minimize the maximum function of some nonsmooth functions. We often need to fit large amount of ellipsoids repeatedly in some practical application, moreover, when a large number of measured data are to be fitted to one ellipsoid, the number of components in the maximum function is very large. So we develop an efficient solution method for such optimization problem. Firstly, using spline smoothing technique to maximum function and the absolute value function, a uniform smooth approximation to the objective function is constructed. Then, we give a spline smoothing Newton algorithm for  $l_\infty$  fitting ellipsoids. At any fixed point, only a few of components of maximum function are concerned, so it acts as an active set technique. From the numerical tests, we can see the new method is very efficient for  $l_\infty$  fitting ellipsoids.

**Keywords:** Fitting ellipsoids; Spline function; Newton method

## 1. INTRODUCTION

For the parametric representation of an ellipsoid, we consider measured data points  $(\phi_k, \varphi_k, \omega_k)$  in space as well as associated measured angles  $(u_k, v_k)$   $k=1, \dots, n > 8$ . The center and the radius or the three half axes, respectively, and two other parameters will be fitted.

We assume an ellipsoid given by

$$\begin{aligned}\phi(u, v) &= a + p \cos(\alpha + u) \sin(\beta + v), \\ \varphi(u, v) &= b + q \sin(\alpha + u) \sin(\beta + v), \\ \omega(u, v) &= c + r \cos(\beta + v),\end{aligned}\quad (1)$$

where  $(p, q, r)$  are the half axes,  $(a, b, c)$  is the center,  $0 \leq u \leq 2\pi$ ,  $-\pi/2 \leq v \leq \pi/2$  unknown angles  $\alpha$  and  $\beta$ .

Given  $(\phi_k, \varphi_k, \omega_k)$  and  $(u_k, v_k)$ ,  $k=1, \dots, n$ .

Let  $x = (a, b, c, p, q, r, \alpha, \beta)$ , then the  $l_\infty$  fitting ellipsoids problem can be stated as

$$\min_x g(x) = \max_{1 \leq j \leq 3n} |\hat{g}_j(x)| \quad (2)$$

where

$$\hat{g}_j(x) = \begin{cases} \phi_j - \phi(u_j, v_j) & j=1, \dots, n, \\ \varphi_{j-n} - \varphi(u_{j-n}, v_{j-n}) & j=n+1, \dots, 2n, \\ \omega_{j-2n} - \omega(u_{j-2n}, v_{j-2n}) & j=2n+1, \dots, 3n. \end{cases}$$

Due to  $|\hat{g}_j(x)| = \max\{-\hat{g}_j(x), \hat{g}_j(x)\}$ , then (2)

is equivalent

$$\min_x g(x) = \max_{1 \leq j \leq 6n} g_j(x) \quad (3)$$

$$\text{where } g_j(x) = \begin{cases} \hat{g}_j(x) & j=1, \dots, 3n, \\ -\hat{g}_j(x) & j=3n+1, \dots, 6n. \end{cases}$$

In this paper, we use the smooth spline introduced in [1] to approximation  $g(x)$  uniformly.

Firstly, We recall the formulation of multivariate spline. A function  $s(z)$ , expressed for short as  $s(z) \in S_k^r(D, \Delta)$ , defined on  $D$  is called a  $k$ -spline function with  $r$ -th order smoothness, if  $s(z) \in C^r(D)$  and  $s(z)|_{\Delta_i} = p_i \in P_k$ ,

where  $D$  is a polyhedral domain of  $R^n$  which is partitioned with irreducible algebraic surfaces into cells  $\Delta = \{\Delta_i | i=1, \dots, N\}$ ,  $P_k$  is the set of all polynomial of degree  $k$  or less in  $n$  variables.

Similar to the smooth spline in [1], we can give the smooth spline  $s_3^2(z, \varepsilon) \in S_3^2(R^n, \Delta_{MS}^2)$  to approximate uniformly  $\max\{z_1, z_2, \dots, z_n\}$  (as  $\varepsilon \rightarrow +0$ ), as follows

$$s_3^2(z_1, z_2, \dots, z_n; \varepsilon) = z_{i_1} + \sum_{l=1}^{r-1} c_l (l z_{i_{l+1}} - \sum_{j=1}^l z_{i_j} + \varepsilon)^3$$

for  $z \in \Delta_{i_1, \dots, i_r}(\varepsilon)$ ,

where  $c_1 = 1/(6\varepsilon^2)$ ,  $c_r/c_{r+1} = (r+2)/r$ ,  $1 \leq r \leq n$  and the cell  $\Delta_{i_1, \dots, i_r}(\varepsilon)$  is

$$\begin{cases} z_{i_l} - z_{i_{l+1}} \geq 0, & \text{when } 1 \leq l \leq r, \\ (r-1)z_{i_r} - \sum_{j=1}^{r-1} z_{i_j} + \varepsilon \geq 0, \\ rz_{i_r} - \sum_{j=1}^r z_{i_j} + \varepsilon \leq 0, & \text{when } r+1 \leq l \leq n. \end{cases}$$

The composite function  $g_t(x)$  approximates uniformly  $g(x)$  as  $t \rightarrow +0$ , where

$$g_t(x) = s_3^2(g_1(x), g_2(x), \dots, g_{6n}(x); t), \text{ for } x \text{ such that } (g_1(x), g_2(x), \dots, g_{6n}(x)) \in \Delta_{i_1, \dots, i_r}(t) \\ g(x) \leq g_t(x) \leq g(x) + (t(1-1/r))/3 \quad (4)$$

Using the Proposition 3.1 of [2], we can obtain

hence  $g_t(x) \rightarrow g(x)$ , as  $t \rightarrow 0$ .

**Assumption 1.1** We assume that the functions  $g_j(\cdot)$ ,  $j \in \{1, 2, \dots, 6n\}$  are twice continuously differentiable.

**Remark 1.1** Under Assumption 1.1,  $g_t(x)$  is twice continuously differentiable for arbitrary  $t > 0$ .

**Theorem 1.1** (Theorem 4.2.8, [3]) Suppose that the functions  $g_j(\cdot)$ ,  $j \in \{1, 2, \dots, 6n\}$  are continuously differentiable. If  $\hat{x} \in R^n$  is a local minimizer for (2), then  $0 \in \partial g(\hat{x}) \triangleq \text{conv}_{j \in \{1, 2, \dots, 6n\}} \{\nabla g_j(\hat{x})\}$ ,

where  $\hat{Q}(\hat{x}) \triangleq \{j \in \{1, 2, \dots, 6n\} | g_j(\hat{x}) = g(\hat{x})\}$  and  $\text{conv}\{A\}$  denotes the convex hull of  $A$ .

## 2. SPLINE SMOOTHING NEWTON METHOD

Like the Algorithm 6 in [4], we combine Newton algorithm with a cubic spline, the spline smoothing Newton algorithm for solving (2) is given. To stabilize the Newton method, the Hessian  $\nabla^2 g_t(x)$  of the smoothing spline function  $g_t(x)$  can be modified by adding a multiple of the identity introduced in [5-7] i.e.,

$$B_t(x) = \theta(x)I + \nabla^2 g_t(x) \quad (5)$$

where  $\theta(x) = \max\{\delta - e(x), 0\}$  with  $e(x)$  denoting the minimum eigenvalue of  $\nabla^2 g_t(x)$  and  $\delta > 0$ .

**Algorithm 2.1**

**step 0:** Choose  $x^0 \in R^n$ ,  $t^0 > 0$ ,  $\hat{t} \gg 1$ ,  $\alpha, \beta, \kappa_1 \in (0, 1)$ ,  $\kappa_2 \gg 1$ ,  $0 < \kappa_3 \ll 1$ ,  $\delta > 0$ ; functions  $\varepsilon_p(t)$ ,  $\varepsilon_q(t)$ ,  $\tau(t) : (0, \infty) \rightarrow (0, \infty)$  satisfying  $\varepsilon_q(t) \geq \varepsilon_p(t) > \tau(t)$  for all  $t > 0$ .

Set  $i = 0, r = 0, s = 1, x^{r,i} = x^0$ .

**step 1:** Let

$$\bar{I} = \{j | \max\{g_1(x^{r,i}), \dots, g_{6n}(x^{r,i})\} - g_j(x^{r,i}) < t_r\}$$

,  $\bar{r}$  be the cardinality of  $\bar{I}$ , and  $\bar{I} = \{i_1, i_2, \dots, i_{\bar{r}}\}$ .

Range  $\{g_{i_j}(x^{r,i})\}_{j=1}^{\bar{r}}$  according

to  $g_{i_1}(x^{r,i}) \geq g_{i_2}(x^{r,i}) \geq \dots \geq g_{i_{\bar{r}}}(x^{r,i})$ .

If  $\bar{r} = 1$ , the cell is  $\Delta_{i_1}(t_r)$ .

Else if  $(\bar{r}-1)g^{i_{\bar{r}}}(x^{r,i}) - \sum_{j=1}^{\bar{r}-1} g_{i_j}(x^{r,i}) + t_r \geq 0$  for every  $\bar{r} \in \{\bar{r}, \bar{r}-1, \dots, 2\}$ , we have

$$\bar{r} \in I = \{\bar{r}, \bar{r}-1, \dots, 2\}.$$

Let  $\hat{r}$  be the maximum element of  $I$ , then the cell is  $\Delta_{i_1, \dots, i_{\hat{r}}}(t_r)$ .

**step 2:** Compute  $\nabla g_{t_r}(x^{r,i})$ . If  $\|\nabla g_{t_r}(x^{r,i})\|^2 > \tau(t_r)$ , go to step 3. Else go to step 8.

**step 3:** Compute  $B_{t_r}(x^{r,i})$  according to (5), then compute Cholesky factor  $R$  such that  $B_{t_r}(x^{r,i}) = RR^T$  and the reciprocal condition number  $c(R)$  of  $R$ .

If  $c(R) \geq \kappa_1$  and  $t_k \geq \kappa_3$ , go to step 4.

Else if  $c(R) \geq \kappa_1$  and the largest eigenvalue  $\sigma_{t_r, \max}(x^{r,i})$  of

$B_{t_r}(x^{r,i})$  satisfies  $\sigma_{t_r, \max}(x^{r,i}) \leq \kappa_2$ , go to step 4.

Else go to step 5.

**step 4:** Compute the search direction

$$h_{r,i} = -B_{t_r}(x^{r,i})^{-1} \nabla g_{t_r}(x^{r,i}) \quad (6)$$

go to step 6.

**step 5:** Compute the search direction

$$h_{r,i} = -\nabla g_{t_r}(x^{r,i}) \quad (7)$$

**step 6:** Compute the step length  $\lambda_{r,i} = \beta^l$ , where  $l \geq 0$  is the smallest integer satisfying

$$g_{t_r}(x^{r,i} + \beta^l h_{r,i}) - g_{t_r}(x^{r,i}) \leq \alpha \beta^l < \nabla g_{t_r}(x^{r,i}), h_{r,i} >$$

**step 7:** Set  $x^{r,i+1} = x^{r,i} + \lambda_{r,i} h_{r,i}$ ,  $i = i + 1$ . Go to step 1.

**step 8:** If  $s = 1$ , compute  $t^*$  such that  $\varepsilon_p(t_r) \leq \|\nabla g_{t^*}(x^{r,i})\|^2 \leq \varepsilon_q(t_r)$ , go to step 9.

Else set  $t_{r+1} = 1/(s(r+2))$ ,  $r = r + 1$ ,  $i = 0$ , go to step 1.

**step 9:** If  $t^* > \hat{t}$ , set  $t_{r+1} = \min\{t^*, t_r/(t_r + 1)\}$ ,  $r = r + 1$ ,  $i = 0$ , go to step 1.



Else set  $s = \max \{2, (1/\hat{t} + 2)/(r + 1)\}$ ,

$t_{r+1} = 1/(s(r + 2))$ ,  $r = r + 1$ ,  $i = 0$ , go to step 1.

Similar to the proof of Theorem 2 of Dong et al. [8], we can prove the following theorem. Theorem 2.1

Suppose that Assumption 1.1 holds and  $\{x^{r,i_r}\}_{r=0}^{\infty}$  is a bounded sequence generated by Algorithm 2.1. Then, there exists an infinite subset  $K \subset N$  and a point  $\hat{x} \in R^n$  such that  $x^{r,i_r} \rightarrow^K \hat{x}$  and  $0 \in \partial f(\hat{x})$ ; i.e.  $\hat{x}$  is a stationary point for (2).

### 3. NUMERICAL EXPERIMENT

We have implemented the Algorithm 2.1 using the MATLAB. In order to show the efficiency of the algorithm, we also have implemented a sequential quadratic programming (abbreviated by SQP) algorithm that is implemented by calling matlab function fminimax directly.

The default parameters are chosen as follows:

$\alpha = 0.5$ ,  $\beta = 0.7$ ,  $\hat{t} = 10^5 \ln(6n)$ ,  $\kappa_1 = 10^{-7}$ ,  $\kappa_2 = 10^{30}$ ,  $\kappa_3 = 1000\hat{t}$ ,  $\tau(t) = 10^{-3}$ ,  $t_0 = 1$ ,  $(\varepsilon_a, \varepsilon_b) = (0.01, 0.2)$ ,  $\delta = 0.1$ .

In [9], the algorithm was stopped when  $\|g_{t_r}(x^{r,i}) - g(\hat{x})\| \leq p$ , where  $g(\hat{x})$  is the known optimum value. We also take this stopping criterion in Algorithm 2.1.

To test Algorithm 2.1, we also generated test data sets as that in [10]. Starting with  $(p, q, r) = (3, 5, 8)$  and  $(a, b, c) = (0, 1, 2)$ , we randomly generated values  $(u_k, v_k)$ ,  $k = 1, 2, \dots, n$  with  $0 \leq u_k \leq 2\pi$ ,  $-\pi/2 \leq v_k \leq \pi/2$ . Then according to the formula (1), we calculated the corresponding values  $(\phi_k, \varphi_k, \omega_k)$ ,  $k = 1, 2, \dots, n$  were disturbed by multiplying them with  $1 + h/100$  where  $h$  was randomly chosen from the interval  $[-g, g]$  for  $g = 2, 5$  in turn and the results were rounded in each case to two decimals after the floating point. For the starting value  $(\alpha, \beta) = (0, 0)$ . In the following tables, we list the results, where  $x^*$  denotes the final approximate solution point,  $g(x^*)$  is the value of the objective function at  $x^*$ . Time is the CPU time in seconds.

TABLE 1. TEST RESULTS FOR  $N=1000$   $P=10^{-3}$

| g          | 2                 |        | 5                 |        |
|------------|-------------------|--------|-------------------|--------|
| Metho<br>d | Algorith<br>m 2.1 | SQP    | Algorith<br>m 2.1 | SQP    |
| Time       | 0.90779           | 1.9530 | 1.3735            | 2.1140 |

|          |         |         |         |         |
|----------|---------|---------|---------|---------|
| $f(x^*)$ | 0.2905  | 0.2891  | 0.1776  | 0.1773  |
| a        | 0.0000  | 0.0000  | 0.0000  | 0.0000  |
| b        | 1.0149  | 1.0165  | 1.0109  | 1.0180  |
| c        | 2.0237  | 2.0010  | 2.0207  | 1.9999  |
| p        | 3.0000  | 3.0000  | 3.0000  | 3.0000  |
| q        | 5.0927  | 4.9968  | 5.0411  | 5.1978  |
| r        | 8.0075  | 7.9999  | 7.9959  | 7.9983  |
| $\alpha$ | -0.0580 | -0.0582 | -0.0357 | -0.0365 |
| $\beta$  | 0.0027  | -0.0013 | -0.0005 | -0.0013 |

TABLE 2. TEST RESULTS FOR  $N=10000$ ,  $P=10^{-3}$ .

| g          | 2                 |         | 5                 |             |
|------------|-------------------|---------|-------------------|-------------|
| Metho<br>d | Algorith<br>m 2.1 | SQP     | Algorith<br>m 2.1 | SQP         |
| Time       | 3.6534            | 10.4863 | 17.0345           | 22.157<br>5 |
| $f(x^*)$   | 0.2777            | 0.2759  | 0.3474            | 0.3061<br>3 |
| a          | 0.0000            | -0.0000 | 0.0000            | 0.0000      |
| b          | 1.0177            | 1.0175  | 0.9791            | 0.9786      |
| c          | 2.0033            | 2.0005  | 1.9932            | 1.9935      |
| p          | 3.0000            | 3.0000  | 3.0000            | 3.0000      |
| q          | 5.0430            | 4.9912  | 5.0861            | 4.6385      |
| r          | 8.0037            | 7.9999  | 8.0083            | 8.0113      |
| $\alpha$   | -0.0553           | -0.0552 | 0.0669            | 0.0666      |
| $\beta$    | -0.0010           | -0.0025 | -0.0037           | -0.0000     |

TABLE 3. TEST RESULTS FOR  $N=100000$ ,  $P=10^{-3}$ .

| g          | 2                 |             | 5                 |              |
|------------|-------------------|-------------|-------------------|--------------|
| Metho<br>d | Algorith<br>m 2.1 | SQP         | Algorith<br>m 2.1 | SQP          |
| Time       | 46.7215           | 91.057<br>2 | 59.7760           | 244.375<br>2 |
| $f(x^*)$   | 0.3045            | 0.3013      | 0.2771            | 0.2558       |
| a          | 0.0000            | -0.0000     | 0.0000            | 0.0263       |
| b          | 1.0192            | 1.0192      | 0.9826            | 0.9826       |
| c          | 2.0015            | 2.0015      | 2.0000            | 1.9506       |
| p          | 3.0000            | 3.0000      | 3.0000            | 3.0000       |
| q          | 4.9904            | 5.0571      | 5.0461            | 4.7034       |
| r          | 8.0000            | 8.0020      | 8.0077            | 8.0521       |
| $\alpha$   | -0.0603           | -0.0602     | 0.0544            | 0.0545       |
| $\beta$    | -0.0014           | 0.0032      | 0.0019            | 0.0026       |

### 5. CONCLUSION

In the past, algorithm to fit ellipsoids had been given in some least squares sense. When the measured data



are generally accurate and they are not orthogonal distance, it is appropriate to use  $l_\infty$  norm instead of  $l_2$  norm. Fitting ellipsoids is a problem that arises in many application areas. In case a large number of measured data are to be fitted to one ellipsoid, it is very large for the number of components in the maximum function. Hence it is necessary to develop an efficient solution method to solve such optimization problem. In this paper, firstly, combining spline smoothing technique to the maximum function and the absolute value function, a uniform smooth approximation to the objective function is constructed. Then, according to the method in [8], we give a spline smoothing Newton method for  $l_\infty$  fitting ellipsoids. From the numerical tests, we know that the new method is very efficient.

#### CONFLICT OF INTEREST

The authors confirm that this article content has no conflicts of interest.

#### ACKNOWLEDGMENT

This work is supported by the Fundamental Research Funds for the Central Universities (No. DC201502050408, DC20150209), the Doctoral Starting up Foundation of Dalian Nationalities University, China (No.0701110100), the National Natural Science Foundation of China (No.71373035), Research Funds of Department of Education of Liaoning Province in China (No. L2015125).

#### REFERENCES

[1] G.H. Zhao, Z.R. Wang and H. N. Mou, Uniform Approximation of Min/Max Functions by Smooth

Splines. *Journal of Computational and Applied Mathematics*, 2011, 236 :699–703.

[2] L. Dong, B. Yu and G. H. Zhao, A smoothing spline homotopy method for nonconvex nonlinear programming, *Optimization*, 2015, online.

[3] E. Polak, *Optimization: Algorithms and Consistent Approximations*, Springer Verlag, New York NY, 1997.

[4] L. Dong and B. Yu, A Spline Smoothing Newton Method for  $L_\infty$  Distance Regression with Bound Constraints, *ISRN Operations Research*, 2013, 2013:1–7.

[5] J. Nocedal and S. J. Wright, *Numerical Optimization in: Peter Glynn, Stephen M. Robinson*, Springer Series in Operations Research, Springer-Verlag New York, 1999.

[6] Y. Xiao, B. Yu and D. L. Wang, Truncated Smoothing Newton Method for  $l_\infty$  Fitting Rotated Cones, *Journal of Mathematical Research & Exposition*, 2010, 30(1):159–166.

[7] Y. Xiao and B. Yu, A truncated aggregate smoothing Newton method for minimax problems, *Applied Mathematics and Computation*, 2010, 216(6):1868–1879.

[8] L. Dong and B. Yu, A spline smoothing Newton method for finite minimax problems, *Journal of engineering mathematics*. 2015, 93(1):145–158.

[9] E. Polak, J. O. Royset and R. S. Womersley, Algorithms with adaptive smoothing for finite minimax problems, *J Optim Theory Appl*, 2003, 119: 459–484.

[10] H. Späth, Least squares fitting of spheres and ellipsoids using not orthogonal distances, *Mathematical Communications*, 2001, 6:89–96.

# The Kernel Function Principal Component Analysis model for disposing information of Students' Evaluation of teaching

Zhou Lihui Wan Xinghuo Song Ruiqi

School of Science, North China University of Science and Technology Tangshan 063009, P.R.China

**Abstract:** How to use the information of students' evaluation of teaching in reason, how to describe, analysis and explain the result of the evaluation decide the effect of Students' Evaluation of teaching in a certain sense. This article disposes the information of students' evaluation of teaching by the Kernel Function Principal Component Analysis (KPCA) and compare with the result disposed by PAC, so that we can try to discuss from methodology, and improve the scientificness, validity and objectivity of letting the students' evaluation of teaching as the method of evaluating the teaching quality in class.

**Key words:** Kernel Function Principal Component Analysis ; Students' Evaluation of teaching ; Comprehensive Evaluation

## 1. INTRODUCTION

Teaching is the core work of the school, and it is the basic way to realize the goal of training at all levels. Every individual participating in the teaching process does the value judgment of teaching process and its effect, and then comes into being the teaching information. As an important means of teaching quality evaluation, students' evaluation of teaching has been widely carried out in colleges and universities in recent years. In a certain sense, the evaluation of students can better reflect the real situation of teachers teaching, but teaching quality assessment is a very complex process. How to use the information of "students' evaluation of teaching" reasonably; how to express, analysis, explain and use the result of teaching evaluation, related to the ability to mobilize the enthusiasm of those teachers and students, and whether they can pay attention to and participate in teaching evaluation, making the evaluation to play a greater role. Student evaluation has a lot of features, such as being involved widely, large information, participating object dynamic changes year by year etc. the features of teaching phenomenon can be reflected from the large amount of information. So it is very important for the statistical information dealing with students' evaluation of teaching information to choose appropriate statistical analysis methods. In order to reflect the characteristics of the teaching phenomenon and avoid missing information, it is necessary to select more indicators to form the evaluation index

system of the students. Usually use principal component analysis (PCA) to deal with the students' evaluation of teaching information [3]. As one of linear dimension reduction methods, PCA provides a very good method to solve the comprehensive evaluation of multi indexes. But in reality, the relationship between indicators is often nonlinear. In addition, when the correlation between the indexes is smaller, it may appear this kind of situation where each of the index contribution rate is too scattered, at this time if we take more principal components, different combinations will lead to the inconsistency of the results of the evaluation so as to affect the evaluation results. Thus, we need to synthesize those variables in little correlation. It's improper to apply the linear principal component analysis. In this paper, we use the kernel principal component analysis (KPCA) to deal with the student's evaluation of teaching information. The aim of the paper is to improve the science, effectiveness and objectivity of the "students' evaluation of teaching" by means of the methodology of methodology.

## 2. Kernel principal component analysis (KPCA)

### 1 kernel function

Kernel function plays an important role in Support Vector Machine (SVM), it is the key to solve the nonlinear problem and overcome the curse of dimensionality. The idea of SVM is to map the linear non separable sample set to the high dimension feature space by using the feature map, which makes them linear in the high dimensional feature space. In order to avoid the problem of computational cost calculating in the feature space directly, the inner product of the sample space will be replaced by the kernel function, that is to say, the operation is carried out in the sample space actually. Above is the idea of the nuclear method.

According to the statistical learning theory, as long as the function  $K(x, x_i)$  satisfies mercer [1], it can be used as a kernel function. Different kernel function will form different algorithms in SVM. At present, the commonly used kernel functions are polynomial kernel function, Gauss radial kernel function, multi-layer perceptron kernel function and dynamic kernel function. The specific forms are as follows:

### (1) Polynomial kernel function

$$K(x, x_i) = [c(x \cdot x_i) + m]^\beta$$

(2) Gauss radial kernel function

$$K(x, x_i) = \exp\left(-\frac{|x - x_i|^2}{\sigma^2}\right)$$

(3) Multi-layer perceptron kernel function

$$K(x, x_i) = \tanh[v(x \cdot x_i) + c]$$

In this paper, we use the polynomial kernel function mainly

2 Kernel based principal component analysis

Set data  $x = (x_1, x_2, \dots, x_l)$ ,  $x_k \in R^N$ ,  $\sum_{k=1}^l x_k = 0$ , the

sample covariance matrix is:

$$C = \frac{1}{l} \sum_{j=1}^l x_j x_j^T \quad (1)$$

The general principal component analysis is to find the characteristic vector and the corresponding eigenvalue of the matrix, and then to extract the principal component of the data according to the linear combination of the characteristic value.

Kernel based principal component analysis is a nonlinear feature extraction method. It maps the data from the input space to the feature space through a nonlinear mapping, then the usual principal component analysis is performed in the feature space, the inner product is replaced by a kernel function. Set the nonlinear map is:

$$\phi(x) \rightarrow F$$

Thus,  $F$  is generated by  $\phi(x_1), \phi(x_2), \dots, \phi(x_l)$ .

Hypothesis mapping has been central, that is

$$\sum_{k=1}^l \phi(x_k) = 0 \quad (2)$$

The covariance matrix in the feature space is

$$\bar{C} = \frac{1}{l} \sum_{j=1}^l \phi(x_j) \phi(x_j)^T \quad (3)$$

Thus, PCA in the feature space is the characteristic value and the characteristic vector  $v \in F \setminus \{0\}$  of the equation

$$\lambda v = \bar{C} v \quad (4)$$

Because  $v$  belongs to the generation space of  $\phi(x_1), \phi(x_2), \dots, \phi(x_l)$ ,

$$\lambda \{\phi(x_k) \cdot v\} = \{\phi(x_k) \cdot \bar{C} v\}, \quad k = 1, 2, \dots, l \quad (5)$$

And there are parameters  $\alpha_i (i = 1, 2, \dots, l)$ , so that  $v$  can be produced by the  $\phi(x_k), k = 1, 2, \dots, l$  linear list. That is

$$v = \sum_{i=1}^l \alpha_i \phi(x_i) \quad (6)$$

Merge (5) and (6), and define a matrix  $K$ , among

$$K_{ij} = (\phi(x_i) \cdot \phi(x_j)) \quad (7)$$

The equivalent form of (4) is

$$l \lambda \alpha = K \alpha \quad (8)$$

Among,  $\alpha = (\alpha_1, \alpha_2, \dots, \alpha_l)^T$

Since a constant coefficient has no effect on the eigenvector, we can obtain the result of (4) only from the characteristic value and the characteristic vector of  $K$ .

Set  $K$ 's characteristic value is  $\lambda_1 \leq \lambda_2 \leq \dots \leq \lambda_l$ , corresponding feature vector is  $\alpha^1, \alpha^2, \dots, \alpha^l$ , set  $\lambda_p$  is a characteristic value that is not zero. Because the feature vector of  $F$  needs to be normalized, that is

$$(v^k \cdot v^k) = I, \quad k = p, \dots, l \quad (9)$$

According to (6) and (7), obtain

$$\begin{aligned} I &= \sum_{i,j=1}^l \alpha_i^k \alpha_j^k (\phi(x_i) \cdot \phi(x_j)), \quad k = p, \dots, l \\ &= \sum_{i,j=1}^l \alpha_i^k \alpha_j^k K_{ij} = (\alpha^k \cdot K \alpha^k) = \lambda_k (\alpha^k \cdot \alpha^k) \end{aligned} \quad (10)$$

The purpose of the principal component extraction is to compute the map on the feature vector  $v_k (k = 1, 2, \dots, l)$ . Let  $x$  be a test sample point, the map in  $F$  is  $\phi(x)$ , then

$$(v^k \cdot \phi(x)) = \sum_i \alpha_i^k (\phi(x_i) \cdot \phi(x)) = \sum_i \alpha_i^k K(x_i, x) \quad (11)$$

As we all know, the number of the principal components extracted from the general  $N$  is up to the dimension of the input vector PCA. But in KPCA, when the number of samples is more than the dimension, the number of principal components extracted can be more than the input dimension.

Supposing (2) is not setting up, it is necessary to adjust the mapping. Set

$$\tilde{\phi}(x_i) = \phi(x_i) - \frac{1}{l} \sum_{j=1}^l \phi(x_j) \quad i = 1, 2, \dots, l \quad (12)$$

After transformation, assuming (2) is established clearly, define matrix  $\tilde{K}$ ,

$$\tilde{K}_{ij} = (\tilde{\phi}(x_i) \cdot \tilde{\phi}(x_j)) = K_{ij} - \frac{1}{l} \sum_{p=1}^l K_{ip} - \frac{1}{l} \sum_{q=1}^l K_{qj} + \frac{1}{l^2} \sum_{p,q=1}^l K_{pq} \quad (13)$$

And then

$$\tilde{K} = K - I_l K - K I_l + I_l K I_l \quad (14)$$

Among,  $I_l$  is a matrix  $(l \times l)$ ,

$$(I_l)_{ij} = \frac{1}{l} \quad (15)$$

Calculate the characteristic value and characteristic vector of  $\tilde{K} / l$ , and find out  $m$  characteristic values and characteristic vectors, then calculate the contribution rate of the principal component.

From the theoretical knowledge above, we give the specific evaluation steps of KPCA method:

(1) Initialize input sample  $x$  applying the methods of standardization management, then obtain the matrix  $K$  by mapping the kernel function.

(2) Solve the matrix  $\tilde{K}$ ,  $\tilde{K} = K - I_l K - K I_l + I_l K I_l$ ,

$$(I_l)_{ij} = \frac{1}{l}.$$

(3) Calculate the characteristic values  $\lambda_r$  and the feature vectors  $v_i (i=1,2,3,\dots,l)$  of the matrix  $\tilde{K}/l$ .

(4) Find out  $m$  characteristic values  $\lambda_r$  and characteristic vectors  $v_r (r=1,2,3,\dots,m)$ .

(5) Calculate the contribution rate and cumulative contribution rate of characteristic values.

### 3. Statistical Methods of Teaching Information Processing

Teaching evaluation from others includes generally: leadership assessment, peer evaluation and student evaluation. Different perspectives, the evaluation index system is also different. Students are in the position of the educator who can't recognize the problem from the educational goal and the height of the educational law. Thus to the teacher's teaching style, teaching attitude, teaching methods of ethics aspects, they don't have the most direct feeling. So the index system of student evaluation of teaching is microscopic and specific. The following 10 indicators are selected to form the student evaluation index system:

X<sub>1</sub>- Teachers work with a strong sense of responsibility, carefully prepared for the teaching

content and method, explain clearly, suitable for students.

X<sub>2</sub>- Teachers can master the teaching content skillfully, the lectures is vivid and Infectious.

X<sub>3</sub>- Teachers can list some of the new information and results, and have a unique view with wide range of knowledge.

X<sub>4</sub>- Teacher's explanation is enlightening, they can encourage students to ask questions or participate in classroom discussions actively.

X<sub>5</sub>- Teachers often give guidance of learning methods to students to lead students to study independently and think independently.

X<sub>6</sub>- Teacher's teaching makes the students interested in learning, and students' ability has also been improved.

X<sub>7</sub>- Teachers adopt modern and creative teaching methods reasonably with good effects.

X<sub>8</sub>- Teachers correct the homework in time and guide the students in all aspects of practice carefully.

X<sub>9</sub>-Teachers treat every student objectively, communicate with students sincerely. They not only impart knowledge, but also teach students to be a man.

X<sub>10</sub>- The teacher who is elegant, graceful, honest, self-discipline, loving the post and working as a teacher. Collect information by questionnaire survey, and use the fuzzy qualitative language to describe students' evaluation of various indicators. Take five evaluation levels (very consistent, consistent, common, reluctant to correspond, ineligible)

Collected 40 college teachers' teaching evaluation information, and the principal component analysis and kernel principal component analysis were carried out for the statistical data.

Table 1 statistical data of students' evaluation of teaching

| teachers | X <sub>1</sub> | X <sub>2</sub> | X <sub>3</sub> | X <sub>4</sub> | X <sub>5</sub> | X <sub>6</sub> | X <sub>7</sub> | X <sub>8</sub> | X <sub>9</sub> | X <sub>10</sub> |
|----------|----------------|----------------|----------------|----------------|----------------|----------------|----------------|----------------|----------------|-----------------|
| 1        | 3.23           | 3.53           | 2.74           | 3.82           | 4.04           | 3.76           | 4.04           | 3.55           | 4.03           | 3.73            |
| 2        | 4.03           | 4.12           | 3.25           | 3.93           | 4.13           | 4.04           | 3.52           | 4.25           | 3.89           | 3.92            |
| 3        | 4.52           | 4.22           | 4.12           | 4.05           | 4.01           | 4.62           | 3.41           | 4.69           | 4.12           | 4.68            |
| 4        | 4.00           | 4.40           | 4.37           | 4.52           | 4.37           | 4.58           | 4.73           | 4.16           | 3.57           | 4.03            |
| 5        | 3.76           | 3.34           | 4.23           | 4.03           | 3.94           | 3.45           | 4.04           | 3.61           | 3.76           | 3.86            |
| 6        | 4.12           | 4.23           | 4.27           | 4.11           | 4.13           | 4.54           | 3.65           | 4.22           | 4.02           | 4.35            |
| 7        | 4.24           | 3.74           | 2.73           | 3.87           | 3.74           | 3.75           | 3.62           | 4.49           | 4.12           | 4.32            |
| 8        | 4.03           | 4.18           | 4.24           | 4.32           | 4.12           | 4.31           | 4.15           | 3.46           | 3.80           | 4.02            |
| 9        | 3.88           | 3.52           | 2.89           | 4.58           | 3.26           | 3.05           | 4.10           | 3.98           | 2.78           | 4.01            |
| 10       | 4.20           | 2.89           | 2.98           | 4.13           | 3.64           | 3.52           | 3.61           | 4.08           | 2.68           | 3.15            |
| 11       | 2.36           | 3.46           | 3.86           | 3.57           | 4.52           | 4.13           | 4.26           | 3.52           | 3.41           | 2.35            |
| 12       | 2.86           | 2.98           | 3.10           | 3.09           | 4.03           | 4.52           | 3.59           | 3.17           | 3.24           | 3.33            |
| 13       | 4.44           | 2.35           | 3.65           | 3.43           | 4.31           | 3.89           | 3.71           | 3.61           | 3.52           | 4.05            |
| 14       | 4.04           | 3.15           | 3.06           | 4.19           | 3.61           | 2.98           | 3.65           | 3.32           | 3.22           | 3.58            |
| 15       | 3.24           | 3.26           | 3.28           | 3.49           | 3.56           | 3.81           | 3.57           | 4.06           | 4.18           | 2.98            |
| 16       | 3.58           | 3.65           | 4.28           | 4.03           | 3.15           | 2.98           | 2.56           | 4.22           | 4.12           | 4.05            |
| 17       | 3.26           | 3.05           | 4.10           | 3.98           | 2.78           | 2.98           | 4.13           | 3.64           | 3.52           | 3.62            |
| 18       | 2.89           | 4.58           | 3.26           | 3.05           | 4.10           | 3.98           | 2.78           | 4.01           | 3.57           | 4.12            |
| 19       | 4.31           | 3.89           | 3.71           | 3.61           | 3.52           | 4.05           | 2.53           | 2.64           | 3.46           | 3.58            |
| 20       | 2.98           | 3.10           | 3.09           | 4.03           | 4.52           | 3.59           | 3.17           | 3.53           | 4.32           | 3.76            |

|    |      |      |      |      |      |      |      |      |      |      |
|----|------|------|------|------|------|------|------|------|------|------|
| 21 | 4.03 | 4.52 | 3.59 | 3.17 | 3.24 | 3.76 | 4.04 | 3.55 | 4.03 | 3.51 |
| 22 | 3.82 | 4.04 | 3.76 | 4.04 | 3.55 | 4.03 | 3.51 | 3.92 | 4.52 | 3.12 |
| 23 | 3.25 | 3.93 | 4.13 | 4.04 | 3.52 | 4.10 | 3.98 | 2.78 | 4.10 | 3.98 |
| 24 | 2.98 | 3.28 | 3.49 | 3.56 | 3.81 | 3.57 | 4.06 | 4.54 | 3.65 | 4.22 |
| 25 | 3.93 | 4.13 | 4.04 | 3.52 | 4.25 | 3.89 | 3.92 | 2.35 | 3.15 | 2.98 |
| 26 | 3.55 | 4.03 | 2.98 | 4.13 | 3.64 | 3.52 | 3.61 | 4.10 | 3.98 | 3.59 |
| 27 | 3.15 | 3.06 | 4.19 | 3.61 | 2.98 | 3.15 | 2.98 | 4.10 | 3.98 | 2.78 |
| 28 | 3.53 | 4.32 | 3.76 | 4.58 | 3.26 | 3.05 | 4.10 | 3.98 | 3.53 | 2.74 |
| 29 | 2.98 | 4.32 | 4.12 | 2.35 | 3.65 | 3.43 | 4.31 | 3.89 | 3.71 | 3.61 |
| 30 | 4.32 | 4.12 | 2.98 | 3.15 | 3.76 | 4.04 | 3.55 | 4.03 | 3.51 | 3.94 |
| 31 | 4.10 | 3.98 | 3.15 | 2.98 | 4.20 | 2.89 | 2.98 | 4.13 | 3.64 | 3.52 |
| 32 | 3.26 | 3.28 | 3.49 | 3.56 | 3.81 | 3.57 | 4.32 | 4.12 | 3.15 | 2.98 |
| 33 | 3.65 | 4.28 | 4.03 | 3.15 | 2.98 | 2.56 | 2.35 | 4.10 | 3.98 | 2.78 |
| 34 | 4.32 | 4.12 | 3.26 | 3.28 | 3.49 | 3.56 | 3.81 | 3.57 | 4.06 | 3.59 |
| 35 | 4.54 | 3.65 | 4.22 | 3.86 | 3.57 | 4.52 | 4.13 | 4.26 | 3.52 | 4.20 |
| 36 | 4.58 | 3.26 | 3.05 | 4.10 | 3.98 | 2.78 | 4.01 | 3.94 | 4.10 | 3.98 |
| 37 | 3.46 | 3.86 | 3.57 | 4.52 | 4.13 | 4.26 | 3.52 | 3.53 | 2.74 | 2.35 |
| 38 | 4.54 | 3.65 | 4.22 | 4.22 | 4.12 | 4.05 | 4.01 | 4.62 | 3.41 | 4.69 |
| 39 | 4.19 | 3.61 | 2.98 | 3.65 | 3.32 | 3.22 | 3.58 | 3.59 | 3.53 | 2.74 |
| 40 | 4.13 | 3.64 | 3.52 | 3.61 | 4.08 | 2.68 | 3.15 | 4.10 | 3.98 | 3.94 |

Firstly, the statistical software SPSS15.0 is used to carry out the standardization of the data, and then do the principal component analysis using the data matrix standardized. Since the first 3 characteristic values of the principal component score matrix (omitting the output results) are 2.058, 1.733, 1.392, 1.147, and the total contribution is 20.580, 37.906, 63.299, dimensionality reduction effect is not ideal.

Do kernel principal component analysis of raw data by the program of Matlab. The polynomial kernel function is chosen as the kernel function of this test.

That is  $K(x, x_i) = [(x \cdot x_i) + m]^\beta$ .

Set  $c = 1.5, m = 1.5, \beta = 60$ . From the data above, we obtain the characteristic value and its cumulative probability, and the first kernel principal component contribution rate reached 87.991%.

$$F_1 = -0.1123x_1 - 0.1035x_2 - 0.1035x_3 - 0.1035x_4 - 0.1035x_5 - 0.1116x_6 - 0.1037x_7 - 0.1035x_8 - 0.1035x_9 + 0.9486x_{10}$$

According to the score of the first kernel principal component, the ranking of the 40 teachers are: 38, 24, 18, 7, 3, 9, 16, 13, 40, 36, 23, 30, 6, 20, 35, 17, 14, 1, 5, 19, 2, 29, 31, 8, 12, 34, 26, 21, 4, 10, 15, 32, 33, 27, 25, 39, 22, 28, 11, 37.

Table 2 statistical data of students' evaluation of teaching Comparison between PCA and KPCA

|    | Total | % of Variance | Cumulative % | Eigenvalue number | Eigenvalue          | Contribution rate/% | Cumulative contribution rate /% |
|----|-------|---------------|--------------|-------------------|---------------------|---------------------|---------------------------------|
| 1  | 2.058 | 20.580        | 20.580       | 1                 | 1.0e+092<br>*3.0406 | 87.991              | 87.991                          |
| 2  | 1.733 | 17.327        | 37.906       | 2                 | 1.0e+092<br>*0.2303 | 6.664               | 94.655                          |
| 3  | 1.392 | 13.922        | 51.828       | 3                 | 1.0e+092<br>*0.1768 | 5.116               | 99.771                          |
| 4  | 1.147 | 11.471        | 63.299       | 4                 | 1.0e+092<br>*0.0055 | 0.159               | 99.930                          |
| 5  | 0.906 | 9.056         | 72.356       | 5                 | 1.0e+092<br>*0.0012 | 0.035               | 99.965                          |
| 6  | 0.735 | 7.351         | 79.706       | 6                 | 1.0e+092<br>*0.0008 | 0.023               | 99.988                          |
| 7  | 0.651 | 6.510         | 86.216       | 7                 | 1.0e+092<br>*0.0003 | 0.009               | 99.997                          |
| 8  | 0.617 | 6.173         | 92.389       | 8                 | 1.0e+092<br>*0.0001 | 0.003               | 100.000                         |
| 9  | 0.405 | 4.054         | 96.443       | 9                 | 1.0e+092<br>*0.0000 | 0.000               | 100.000                         |
| 10 | 0.356 | 3.557         | 100.000      | 10                | 1.0e+092<br>*0.0000 | 0.000               | 100.000                         |



From the comparison above, we can see that the principal component analysis method and the kernel principal component analysis method are not the same as the results obtained from the same group of data. Obviously, the index affecting the teaching evaluation is more accurate by the kernel principal component analysis. The first kernel principal component contribution rate reached 87.991%, it shows that we can sort the teachers according to the scores of principal component based on the teaching information, and compared with other information in to grasp the teaching situation of teachers better. But in the principal component analysis method, we need to consider these 3 principal component that the cumulative probability is less than 80%. And for the comprehensive evaluation function sorting the teachers, it's not only little accurate, but also a waste of time and energy. Besides, there are another difference between these two methods:

1. The general principal component analysis is to find the characteristic vector and the corresponding eigenvalues of the sample covariance matrix, and to extract the principal components of the data according to the linear combination of the feature vectors; the kernel principal component analysis (PCA) is a nonlinear feature extraction methods, it maps the data from the input space to the feature space by a nonlinear mapping, and then do the general principal component analysis in feature space, the inner product uses a kernel function to replace.

2. The general principal component analysis is a method dealing with high dimensional data which is produced under the idea of dimension reduction. It is used in engineering practice widely, but it can't get good results when it comes to deal with nonlinear problems. The kernel principal component analysis is a method dealing with nonlinear data which is produced under the idea of rising dimension. Firstly, the nonlinear problem is transformed into a linear problem in high dimensional feature space, and then uses a kernel function to replace the inner product in the feature space, which solves the complex computing problems, and overcome the curse of dimensionality and local minimum problem effectively.

3. The general principal component analysis requires two to three principal components in to make the contribution rate up to 80%; for the kernel principal component analysis, the contribution rate of the first principal component can be more than 85% in the selection of appropriate kernel function and parameter.

#### 4. Conclusion

In recent years, the number of college students expands sharply because of the college enrollment expansion, however the university teachers and other teaching resources have failed to get a synchronous growth. In this case, the quality of personnel training

in colleges and universities has become concern of the whole society. There is no doubt that how to improve the quality of personnel training has become the center of the work of the university. Using quality control method is a good way to improve the quality of personnel training. As an important means of classroom teaching quality evaluation, in a certain sense, "students' evaluation of teaching" can reflect the true teaching situation of the teachers, which plays a very important role in improving the teaching of teachers and promoting the development of teachers. Some experts pointed that the results of the discussion may be the most important step in the evaluation process. As an important part of the teaching quality assurance system in colleges and universities, it's also one of the effective resources of teaching quality management in colleges and universities. It not only provide feedback information for teachers to help them adjust and improve their teaching behavior, and optimize the teaching process, but help to seek effective methods, and provide a reliable basis for monitoring the quality of teaching for teaching management of colleges and universities. For the teaching management work, "students' evaluation of teaching" contains information and advice from the classroom. Making full use of the resources of "students' evaluation of teaching" is beneficial to the adjustment and improvement of the teaching management work.

#### Acknowledgment

This paper is supported by the following items, the first is Research and practice of education and teaching reform of North China University of science and technology (Item number: J1509-09; Z1514-05), and the second is Project funding for the reform program of graduate education in North China Institute of science and technology (Item number: K1503).

#### Reference

- [1] Cortes C, Vapnik V. Support vector net works [J]. Machine Learning, 1995, 20(3)
- [2] Vapnik V. The Nature of Statistical Learning Theory [M]. New York: Springer, 2001.
- [3] Zhang Youzheng et al. Application of multivariate statistics in teaching evaluation system [J]. Journal of Ningbo Institute of education, 2006 (1).
- [4] Liang Shouzhuan, conscientiously implement the "teaching evaluation" to improve the teaching quality of [J]. Journal of Zhongshan University journal, 2006, 26 (2)
- [5] Wang Fangliang, the teaching and management of errors and regulation in the course of teaching evaluation of teaching and learning, 2005 (4).
- [6] Chen Yukun, Beijing: People's education press [M], 1999.



# A improved routing algorithm of wireless sensor network

Fan Jingjing, Zhao Jianguang, Chen Sujun

Hebei University of Architecture, Department of Computer Science

**Abstract:** Short life for sensor network nodes, limited energy characteristics, based on the existing robust measure algorithm, an improved algorithm to optimize the robustness threshold, improved route discovery process. Through simulation experiments, by improving the threshold, effectively improve the utility node number of rounds, so the minimum residual energy has a more substantial increase; the discovery process through improved routing, reducing the network overhead, reducing the total network traffic while shortening the route discovery period. By the above means, effectively improve the energy efficiency of a single node, extending the life of the node.

**Keywords:** wireless sensor networks; routing discovery; energy

## 1. INTRODUCTION

The application of wireless sensor network is very extensive. Based on the characteristics of the wireless sensor networks (such as battery-powered energy is limited; limited computing power and data processing capabilities of the sensor nodes; huge number of sensor nodes; form a network node self-organization; dynamic node, may at any time enter or leave the network; node does not have a unique IP, data-centric; communication need intermediate node routing, multi-hop routing), the pros and cons of wireless sensor network algorithms directly affects the performance and life of the entire network.

## 2. RELAXED WORK

Wireless sensor networks, each sensor node is the smallest unit of the network of information collection, forwarding and routing are completed by a single node, so it is necessary to understand and grasp the health of each node in the network decision-making and support for further routing algorithm. In this paper, the concept of a robust measure used to measure the health of a wireless sensor network node. A node of good health should have plenty of battery power, excellent location, good connections. In this paper, design a node robust measure, defined as follows:

Set a measure of value:

$$H = \frac{E \times n}{n_o \sqrt{(D_x - O_x)^2 + (D_y - O_y)^2}}$$

Where:  $E$  is the current node energy level values;  $D_x, D_y$  is plane coordinates of the current node;  $O_x, O_y$  is coordinate regional centers;  $n$  is the node hop

up to the maximum number of nodes within the communication range is up to,  $n_o$  for the current node to reach the center the number of hops of nodes.

The determination of the central node is determined by Euclidean distance

$$d = \sqrt{(D_x - O_x)^2 + (D_y - O_y)^2}, \text{ wherein the}$$

nodes of minimum value  $d$  of the node to the central node. The energy level using four binary bits ( $2^4-1$ ) energy level, i.e., (15) energy level, the energy levels reflected the battery energy level of the node, the node with the higher energy level higher battery

energy.

$n_o \sqrt{(D_x - O_x)^2 + (D_y - O_y)^2}$  reflects the location of the node, the more the number of hops of the distance to the central node, the farther away from the central region, the worse the geographical location of the node.  $n$  for node hop can reach within the communication range is up to a maximum number of nodes, reflects the degree of contact and connections of the node and other nodes, the node  $n$  values greater the more extensive network of contacts.  $n$  value can be determined by the following formula, so that the number of

$$\text{nodes } \sqrt{(D_x - D_{xi})^2 + (D_y - D_{yi})^2} \geq d + d_i$$

established, both the size of  $n$ , where  $D_x, D_y$  is the nodal coordinates to be investigated,  $D_{xi}, D_{yi}$  is the coordinates of all nodes in the maximum communication range of the node of the network coverage to be investigated can be achieved,  $d$  for neighboring nodes of the communication range,  $d_i$  for the communication range by the influence of the energy level, the higher the energy level, the greater the communication range.

Assuming that follows the rectangular area, with the following topology wireless sensor network, as shown in Fig.1.  $O$  points for the regional center point coordinates ( $O_x, O_y$ ). Plane coordinates of the respective nodes ( $x_i, y_i$ ), the energy level assumes the highest energy level (i.e.  $E_i = E$ ),  $n_i$  can reach the maximum number of nodes for each node hop, wherein ( $i = 1, 2, 3, 4, 5, 6, 7, 8$ ).

Assuming that each node is equal to the energy level are  $E$ , so each node of the communication area of the same, are based on the node as central circular area of

radius  $d$ , shown in dashed lines in Fig.2 the circular region. Maximum number of nodes, each node hop up according to the formula  $\sqrt{(D_X - D_{Xi})^2 + (D_Y - D_{Yi})^2} \geq d + d_i$  can be calculated, easy to get  $n_1 = 2$ ,  $n_2 = 3$ ,  $n_3 = 3$ ,  $n_4 = 0$ ,  $n_5 = 3$ ,  $n_6 = 5$ ,  $n_7 = 3$ ,  $n_8 = 3$ , visible personal connections of node 6 is the best, followed by the node 2,3,5,7,8 and then node 1. For the same as the value of  $n$  nodes, such as node 2,3,5,7,8, considering the location, energy level, etc. to determine the degree of robust nodes should be in the routing. Node 4 this situation occurs in the practical application should be avoided.

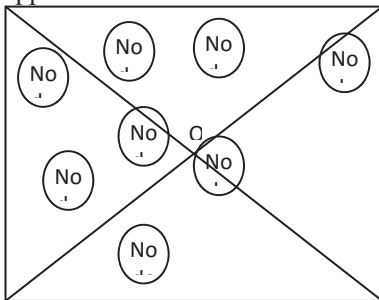


Figure 1 sensor network node maps example

### 3. ALGORITHM DYNAMIC DESCRIPTION

Shown in Fig.1, the distribution of nodes shown in Fig.2 under the premise of communication range of each node, it is assumed that node 1 has the information to be transmitted to the node 7, as shown in the routing policy may be shown in Fig.3, up to the path:

1->2->6->7, 1->2->3->7, 1->2->3->6->7, 1->5->6->7, 1->5->8->7, and so on. Specific routing using what path the RM value according to each node to determine the because each node RM values

change over time, the solid for the same source node and the sink node between the transmission of the same data may be using a different routing path.

At time  $T_1$ , the routing path 1->2->6->7, in the next time  $T_2$  ( $T_2 > T_1$ ), the routing path may be 1->2->3->7, it may be the other may be up the path.

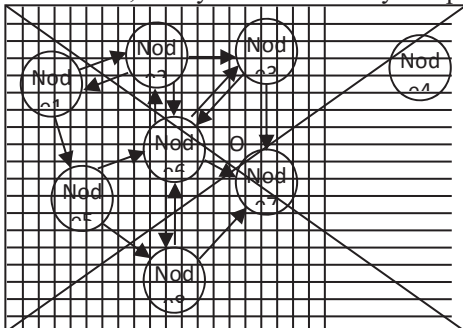


Figure 2 Node 1 to Node 7 reachable path

### 4. RESULTS AND DISCUSSION

When transmit the same amount of information in Fig.3, the total energy consumed by the three algorithms similar. In the total energy consumption of

similar circumstances, the life of the network, we are more concerned about the problem. Due to excessive use of a node so that it runs out of energy die prematurely, will inevitably affect the entire network topology,

$\sqrt{(D_{X1} - D_{X2})^2 + (D_{Y1} - D_{Y2})^2} < d_1 + d_2$ , the of the intermediate routing nodes communication range can not cross, the entire network will die. Assuming the information to arrive according to a Poisson distribution, for the above-described example, the lifetime of the network shown in Fig.3.

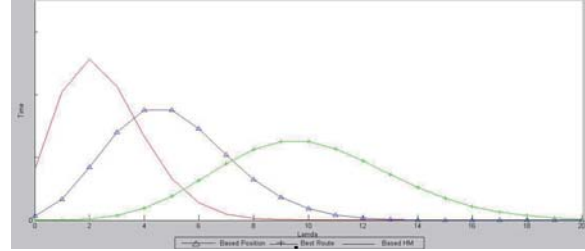


Figure 3 network lifetime mapsAs can be seen from Fig.3, RM-based wireless sensor network lifetime longer than the other two network lifetime. An area surrounded by three curves and the horizontal axis is equal to the, i.e. three algorithms consumption is equal to the total energy.

### 5. CONCLUSION

In this paper, Short life for sensor network nodes, limited energy characteristics, based on the existing robust measure algorithm, an improved algorithm to optimize the robustness threshold, improved route discovery process. Through simulation experiments, by improving the threshold, effectively improve the utility node number of rounds, effectively improve the energy efficiency of a single node, extending the life of the node.

### ACKNOWLEDGEMENTS

This work was financially supported by the Education Department of Hebei Province youth fund project, project number: QN20131148. Hebei Institute of Architectural Engineering School Fund, NO: QN201414, Project Name: Based on the ski slopes of wireless sensor network security key technology research. Hebei Institute of Architectural Engineering School Fund, NO: ZD201407, Project Name: Campus Card intelligent consumer terminal Key Technology Research. Hebei provincial science and technology plan special work projects, NO: 16236004D-8, Project Name: Tian Road Zhangbei grassland surrounding mountains outdoor tourism micro backpack sites and intelligent search field development.

### REFERENCES

- [1]Shanta Mandal , Rituparna Chaki. "A SECURE ENCRYPTION LOGIC FOR COMMUNICATION IN WIRELESS SENSOR NETWORKS", IJCIS,2012,Vol.2,No.3,pp107-116.
- [2]Jain-Skiing Liu, Lin C-HP. Power-efficiency

- clustering method with power-limit for sensor networks[C] Eric Johnson. Performance, Computing, and Communications Conference 2003, Arizona, USA: [S. n.], 2003: 129-136.
- [3]Wang liang, Zhong xianxin, Shi jun feng. Wireless sensor network energy consumption balance strategy[J]. Sensor World, 2007(3):32-37.
- [4]Li J, Mohapatra P. An analytical model for the energy hole problem in many to one sensor networks[C] Bob Shapiro. IEEE 62nd Semiannual Vehicular Technology Conference, Dallas, USA: [S.n.], 2005:2721-2725.
- [5] Hein Zelman W. Application-Specific protocol architectures for wireless networks [D]. Boston: Massachusetts Institute of Technology, 2000.
- [6]Gupta I, Riordan D, Sampalli S. Cluster-Head election using fuzzy logic for wireless sensor networks[C] Jacek Ilow. Proc. of the 3rd Annual Communication Networks and Services Research Conference, Halifax: [S.n.], 2005:255-260.
- [7]Lindsey S, Raghavendra C. Pegasus: Power-Efficient gathering in sensor information systems[C] Proc. of the IEEE Aerospace Conf, New York:[S.n.], 2002:9-16.
- [8]Heinzelman W, Chandrakasan A, Balakrishnan H. Energy-efficient communication protocol for wireless micro sensor networks[C] Hawaii International Conference on System Sciences, Hawaii:[S.n.], 2000:1-10.
- [9]Li Hao, Qianping Wang, Yu e Su. A CUT-based Routing Protocol for Wireless Sensor Networks in Coal Mine[C] Third International Conference CPCA 2008, 851-856.
- [10]M. Li and Y. Liu. Underground Structure Monitoring with Wireless Sensor Networks [C]. In Proceedings of the 6th International Conference on Information Processing in Sensor Networks 2007:69-78.

# An XML Query Aggregation Based on Mean Square Residual

HUANG Shao-bin, LI Yan-mei\*, LI Ya, XU Li

College of Computer Science and Technology, Harbin Engineering University, Harbin 150001, China

**Abstract:** At present, the availability of large numbers of heterogeneous data raises the enthusiastic to research how to represent and manage semi-structured data. In order to manage and present enormous scale of semi-structured document data with effectively and efficiently retrieval, we present a high-order hierarchical joint clustering algorithm (MSR-HHCC) based on minimum mean square residual of XML to optimize the retrieval of XML document. We use the bottom-up aggregation approach to divide the query set into initial subset, then combine the two minimum mean square residual subset to upper level clustering. The query division and hierarchical clustering can be obtained based on the tree built by clustering. MSR-HHCC has been proved that its performance is better than four classical homogeneous hierarchical clustering algorithms.

**Keyword:** XML; joint clustering; mean square residual

## 1. INTRODUCTION

XML provides a new model for web data management as a self-description semi-structure data, and becomes to a standard of both information representation and data communication of Internet. With the development of the Internet application, XML documents compose a large scale of knowledge resource database so that how to retrieval become to a challenge. It usually can affect the retrieval in scale repository to apply clustering into retrieval before inquiry. First, clustering can do effective classification and organized inquiry, or narrow the retrieval into a small XML document space to efficient retrieval. Second, we often need to process numerous isomerism XML document data from different sources, and users sometimes want the information which is related to the inquiry rather than accurate match information. XML inquiry language will not be suitable in this situation, so a new method to take both clustering and information retrieval into consideration is needed.

Classical clustering algorithms or information retrieval methods are rarely considering the characteristic of XML inquiry and the structure nesting of document, and the characteristic of the element which is always isomerism, high-end and multi-dimensional of structure flame. It is difficult for classical clustering method to reflect the high-level isomerism element and the structure nesting of

retrieval query. CAS inquiry based on XPath(`//author[about[name,wang]]//article[about[title,xml]][about[journal,ACM]]`) include structure inquiry and keyword inquiry.

Based on the above analysis we find out that compared with the classical single query, the retrieval of XML documents include multiple interrelated data objects with structure nesting[2]. For the purpose of optimizing the XML clustering performance by taking full advantage of interrelated information between XML documents and queries [2-4], we need to explore the clustering nesting structure based on XML documents and queries. In this paper, we using the joint clustering with high-level isomerism to combine multiple characteristic space information [3,6,9]. Based on the information of retrieval structure, we present a high-order hierarchical joint clustering algorithm based on the minimum mean squared residual (MSR-HHCC). Mean squared residual is a norm to measure the consistency of feature of clustering internal objects. Internal objects from the same cluster often exhibit similar properties and companied with a higher consistency [17,18].

## 2. HIERARCHICAL CLUSTERING ALGORITHM

The main methods of clustering contains: k-graph learning [1,13]; norm statistics based on Goodman Kruskal [2]; minimum cutting division based on graph [3,5-8]; method based on information theory [9-12]; method based on matrix factorization [4,16]; Jiawei Han [14,15] provide a clustering based on ranking. All these algorithms are flat clustering with single hierarchical division of objects and features. Meanwhile, hierarchical clustering algorithm of homogeneous data has been widely studied and many hierarchical clustering algorithm were presented such as BIRCH [19], CURE [20], ROCK [21] and Chameleon [22].

Firstly, we expressed XML documents inquiry unit as high-order multidimensional vector to quantify the entire query sets into a set of vectors. It can combine the analysis of semi-structured text structure and text content. Then each space feature divided into sub cluster according to XML query vectors, combine the two sub cluster with minimum mean squared residual into a high level cluster. XML query set can be finally organized as a query cluster tree by repeating these procedures.

Set XML inquiry unit set  $X = \{x_1, \dots, x_m\}$   
and its feature space



$$Y^1 = \{y_1^1, \dots, y_{n(1)}^1\}, \dots,$$

$$Y^N = \{y_1^N, \dots, y_{n(N)}^N\}, \text{ which } y_j^v \text{ represent}$$

the  $j$ th feature of the  $v$ th feature space. The feature

matrix of  $X$  in the  $Y^v$  feature space is

$$A^{(v)} = (a_{ij}^{(v)})_{m \times n(v)}, \text{ which } a_{ij}^{(v)}$$

represents the eigenvalues of  $x_i$  of  $y_j^v$ , and

$$v \in \{1, \dots, N\}$$

Turn feature vector  $y_j^v$  and inquiry unit  $x_i$  to

graph nodes to form unit nodes and feature nodes,

then set the eigenvalues  $a_{ij}^{(v)}$  as the weight

between the inquiry unit nodes and the feature nodes. Fig.1(a) shows a XML inquiry unit set which is

composed with three objects,  $X$ ,  $Y^1$ ,  $Y^2$ . The

thick solid line means the weight is 1, thin solid line means the weight is 0.5, and the rest of them means the weight is 0. We think the weight as the frequency of this feature appears or inquiries weight.

MSR-HHCC using the bottom-up clustering method. There are two sections. First, divide those unit nodes and feature nodes which have large weight into sub-clustering as is shown in Fig.1. The Fig.1 (b) displays the result of division of Fig.1. Second, combine the two sub clusters with minimum mean squared residual into a high level cluster. Fig.1 (c) shows the result of the combination of Fig.1. After these procedures, we can find out the inner hierarchical clustering structure.

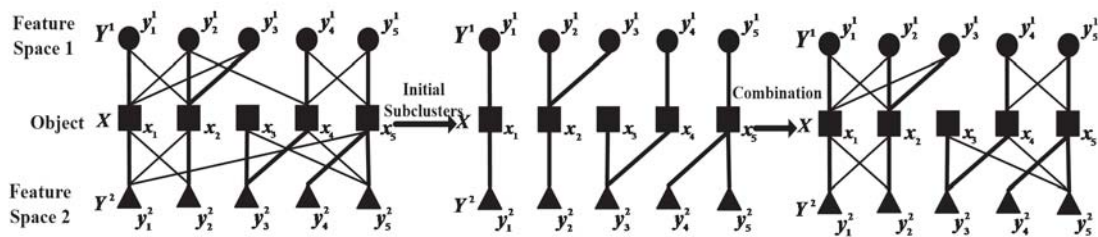


Fig 1 Hierarchical Clustering Process

### 2.1 Initial Sub Cluster

The minimum mean square measure of the consistency of clustering makes sense only if every cluster has at least one object and a vector, so the division before clustering is necessary.

For insurance the combination of object node with high weight and feature node, MSR-HHCC do this

$$\begin{aligned} & \left\{ (x_p, y_q^v) \mid q = \arg \max_{1 \leq j \leq n(v)} a_{pj}^{(v)} \right\} \cup \\ & \left\{ (x_p, y_q^v) \mid p = \arg \max_{1 \leq j \leq m} a_{iq}^{(v)} \right\} \end{aligned}$$

combination. We combine  $x_p$  with  $y_q^v$  into a sub

cluster  $O$  if they meet the after rules: which means

the weight of the link between  $x_p$  and  $y_q^v$  is the

largest in feature space  $Y^v$  or the weight of the link

between  $x_p$  and  $y_q^v$  is the largest weight in object

$X$ . In the case of the dataset in Fig.2(a),  $x_1$  is the

largest weight that connected with  $y_1^1$  in  $Y^1$

feature space, and the weight between  $x_1$  and  $y_1^1$

or  $y_1^2$  are the largest of object  $X$ , so  $y_1^1$  and  $y_1^2$

are divided into an initial sub cluster. The result of Fig 1(a) to initial sub cluster is shown in Fig1(b).

### 2.2 Mean Squared Residual

The main procedure of MSR-HHCC is how to select the sub cluster. We select two sub cluster of current level to do combination to form a high level cluster.

Set  $O_p$  is a high level joint cluster which is composed by sub object set  $I$  and feature sub set

$J^{(v)}$  of every space.  $h_{ij}^{(v)}$  is the residual of

eigenvalues  $y_j^v$ , it is a statistical indicator of the consistency of eigenvalues between feature sub set  $y_j^v$  and object in sub cluster  $o_p$  [17,18]. The residual  $h_{ij}^{(v)}$  of eigenvalues  $a_{ij}^{(v)}$  are defined as follows:

$$h_{ij}^{(v)} = a_{ij}^{(v)} - a_{Ij}^{(v)} \quad (2a)$$

$$h_{ij}^{(v)} = a_{ij}^{(v)} - a_{ij}^{(v)} - a_{Ij}^{(v)} + a_{IJ}^{(v)} \quad (2b)$$

While  $|I|$  means the number of object in sub set ,

$|J^{(v)}|$  means the number of feature in  $J^{(v)}$ .

$$a_{IJ}^{(v)} = \frac{\sum_{i \in I, j \in J} a_{ij}^{(v)}}{|I| \cdot |J^{(v)}|} \quad \text{present the mean}$$

eigenvalues that all objects of cluster  $o_p$  present

$$\text{with the feature sub set } J^{(v)} . a_{IJ}^{(v)} = \frac{\sum_{i \in I} a_{ij}^{(v)}}{|I|}$$

means the mean eigenvalues of all object in cluster  $o_p$  upon feature  $y_j^{(v)}$ .

Set  $H = [h_{ij}^{(v)}]_{m \times n^{(v)}}$  as the residual matrix, the value of element is defined by (2a) and (2b), then the mean square residual of cluster  $o_p$  in feature

space  $Y^{(v)}$  is defined as follows:

$$\|H_p^{(v)}\|^2 = \frac{\sum_{i \in I, j \in J^{(v)}} (h_{ij}^{(v)})^2}{|I| \cdot |J^{(v)}|} \quad (3)$$

Mean square residual is to measure the consistency of eigenvalues of all objects in sub cluster  $o_p$  with

feature sub set  $J^{(v)}$ . The lower the mean square residual is, the higher the consistency is. High level joint cluster divide feature sub set  $J^{(v)}$  and the

object sub set  $I$  with high consistency into cluster

$o_p$ . In an ideal division, the consistency of

eigenvalues objects in sub set  $I$  is high which means they are equal or similar. The mean square

residual of sub cluster  $o_p$  is the norm to measure

the consistency of clusters. Using mean square residual can value the quality of high level joint cluster, the low the mean square residual is, the high quality the cluster is. The turning of high level joint cluster of XML inquiry problem to optimal division of feature of every space or objects make the mean square residual of each cluster become to the minimum. XML inquiry unit object reference to multiple feature spaces. The weight of mean square residual for each feature space is defined as follows:

$$SR(o_p) = \sum_{v=1}^N \beta^{(v)} \|H_p^{(v)}\|^2 \quad (4)$$

Where  $\beta^{(v)}$  is the weight of feature space  $Y^{(v)}$ . If

$o_t$  is the combination of cluster  $o_p$  and  $o_q$ , then

the incremental of mean square residual is defined as follows:

$$MergeSR(o_p, o_q) = SR(o_t) - SR(o_p) - SR(o_q) \quad (5)$$

In order to get a efficiency of cluster to make the mean square residual of combination cluster is low, MSR-HHCC combine two sub cluster which has

minimum mean square residual. Set level  $l$ th has

$K^{(l)}$  number of clusters, then the combination rules is defined as follows:

$$o = \left\{ (o_p, o_q) \mid (p, q) = \arg \min_{1 \leq p \leq q \leq K^{(l)}} (MergeSR(o_p, o_q)) \right\} \quad (6)$$

### 3 MSR-HHCC Algorithm

MSR-HHCC using the bottom-up hierarchical clustering method. We firstly divide the objects and features into initial sub clusters according to (1). Then select the two sub clusters to do a combination which has a minimum increase of the mean square residual. Finally, we get a tree hierarchical clustering structure..

(1)Divide objects and feature into initial sub clusters based on formula (1) to form the first level of the cluster tree.



(2) Calculate the each increase of mean square residual of the combination causes based on the formula (6).

(3) Repeat these two processes until all sub clusters combination to a cluster or the level number of cluster tree is enough.

**Input:**  $A^{(v)}$  which represent the related matrix of  $X$  and  $Y^{(v)}$ ,  $1 \leq v \leq N$ , the number of cluster level is  $L$ .

**Output:** The cluster tree.

Create an empty hierarchy  $H$ ;

**for**  $y = 1$  to  $N$  **do**

$$o \leftarrow \left\{ \left\{ (x_p, y_q^v) \mid q = \arg \max_{1 \leq j \leq n^{(v)}} a_{pj}^{(v)} \right\} \right\} \\ \cup \left\{ \left\{ (x_p, y_q^v) \mid p = \arg \max_{1 \leq j \leq m} a_{pj}^{(v)} \right\} \right\}$$

/\*the first level initial sub cluster\*/

**end for**

SubclusterList  $\leftarrow$  subclusters  $o_1, \dots, o_{K^{(1)}}$

**for**  $l = 1$  to  $L$  **do**

$$o \leftarrow \left\{ (o_p, o_q) \mid (p, q) = \arg \min_{1 \leq p \leq q \leq K^{(l)}} (M$$

/\*sub cluster combination\*/

Remove  $o_p, o_q$  from SubclusterList;

Add  $o$  to SubclusterList;

Add SubclusterList to  $H$  at a higher layer;

**end for**

**Time complexity analysis:** When the MSR-HHCC form initial sub clusters, we only need to search the max of line column and row column of the feature

matrix  $A^{(v)}$  ( $1 \leq v \leq N$ ). The time

complexity analysis is  $O(m \sum_{v=1}^N n^{(v)})$ . The

time complexity analysis to calculate the residual

matrix  $H^{(v)}$  ( $1 \leq v \leq N$ ) is

$O(m \sum_{v=1}^N n^{(v)})$ . The time complexity analysis

of residual matrix  $H^{(v)}$  ( $1 \leq v \leq N$ ) to calculate the increase of each pair of sub clusters is

lower then  $O(m \sum_{v=1}^N n^{(v)})$ . The time

complexity analysis to select a pair of sub clusters with minimum increase based on the combination of

two sub clusters of  $l$ th layer, totally  $\frac{K^l(K^l-1)}{2}$

pairs of sub clusters, is

$O(m(K^{(l)})^2 \sum_{v=1}^N n^{(v)})$ . The time

complexity analysis to form the  $L$  layer of cluster

tree is  $O(m \sum_{i=1}^L (K^{(i)})^2 \sum_{v=1}^N n^{(v)})$ . The

number of sub clusters in first layer is  $K^{(1)}$ , then

the number of sub clusters in  $l$ th layer is

$K^{(l)} = K^{(1)} - l$ . The time complexity analysis

to form a  $L$  layers cluster tree is

$$O(m \sum_{i=1}^L (K^{(i)} - l)^2 \sum_{v=1}^N n^{(v)})$$

which is equal with

$$O(m(K^{(l)})^3 \sum_{v=1}^N n^{(v)})$$

. For the worst

situation, which means the  $K^{(l)}$  is the minimum of

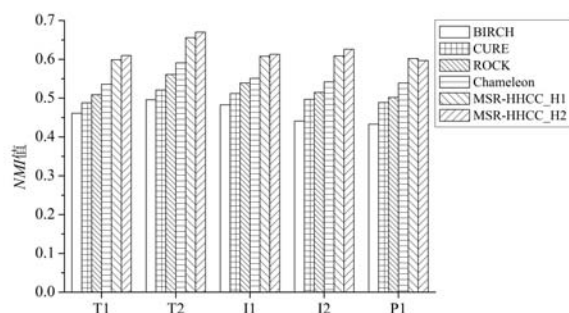
objects  $n$  and the number of features  $n^{(v)}$ ,

$$K^{(1)} = \min(m, \min n^{(v)}).$$

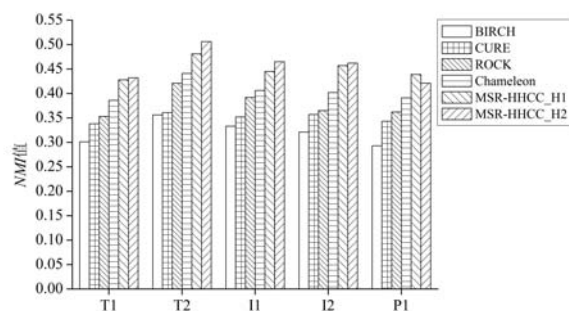
#### 4. EXPERIMENTAL ANALYSIS

BIRCH[19], CURE[20], ROCK[21] and Chameleon[22] are widely used in hierarchical division methods. In this section, we compared MSR-HHCC\_H1 and MSR-HHCC\_H2 with BIRCH, CURE, ROCK and Chameleon. Considering that the algorithm used in the experiments has a certain

randomness, each algorithm executed 20 times, and its average as the final statistical results. The evaluation of the first layer of clustering results is shown in Fig.2(a) and the result of the second layer is shown in Fig.2(b). The result shows that MSR-HHCC is obviously higher than BIRCH, CUBE, ROCK and Chameleon. The weight of NMI is 10 percentage points higher. This reasons are as follows. First, the dimension of dataset is high in this experiment. Such as T1, T2 and P1 has thousands words. BIRCH, CURE, ROCK and Chameleon using all features that dataset contains, some particular features information were flooding in useless features and causes adversely effects. MSR-HHCC using multiple type of data to do clustering to insurance every type of data were formed to clustering. By taking advantage of the relationship of different types of data to do the division to decrease the adversely effect of useless features. Second, the clustering process can be influenced by the type of data object. For example, an author may take participate conferences in a field and published papers in a same field, or conferences in the same field published papers in a same field. Keywords are always the same for papers in a same field. BIRCH, CUBE, ROCK and Chameleon using feature vector to represent data features to clustering data with same type without taking the influence of the relationship between objects into consideration. The result shows that MSR-HHCC algorithm can effectively use a variety of relationships between types of data information to improve the accuracy of clustering compared with the traditional hierarchical clustering.



(a)NMI of first layer of clustering



(b)NMI Of Second Layer Of Clustering

Figure 2. NMI of BIRCH、CURE、ROCK、Chameleon、MSR-HHCC\_H1 and MSR-HHCC\_H2

## 5. CONCLUSION

In this paper, we present a clustering algorithm, MSR-HHCC, of XML documents inquiry based on minimum mean square residual. The result of experiment shows that MSR-HHCC can effective explore the hidden data clustering structure hierarchy. The next step is to consider how to introduce a priori information in a hierarchical clustering process to improve the clustering effect.

## REFERENCE

- [1].Long B, Wu Xiaoyun, Zhang Zhongfei, Yu P S. Unsupervised Learning on K-Partite Graphs[C]//12th ACM SIGKDD International Conference on Knowledge Discovery and Data Mining, Philadelphia, 2006: 317-326
- [2].Dino I, Robardet C, et al. Parameter-less Co-clustering for Star-structured Heterogeneous Data[J]. Data Mining Knowledge Discovery, 2012, 26: 217-254
- [3].Wang Hua, Nie Feiping, Huang Heng, Ding C. Nonnegative Matrix Tri-Factorization Based High-Order Co-Clustering and Its Fast Implementation // 11th IEEE International Conference on Data Mining, Arlington, 2011: 174-183
- [4].Gao Bin, Liu Tieyan, Feng Guang, et al. Hierarchical Taxonomy Preparation for Text Categorization using Consistent Bipartite Spectral Graph Co-partitioning[J]. IEEE Transactions on Knowledge and Data Engineering, 2005, 17(9): 1263-1273
- [5].Gao Bin, Liu Tieyan, et al. Consistent Bipartite Graph Co-Partitioning for Star-Structured High-Order Heterogeneous Data Co-Clustering[C]//11th ACM SIGKDD International Conference on Knowledge Discovery in Data Mining, Chicago, 2005: 41-50
- [6].Gao Bin, Liu Tieyan, et al. Web Image Clustering by Consistent Utilization of Visual Features and Surrounding Texts[C]// 13th annual ACM International Conference on Multimedia, Singapore, 2005: 112-121
- [7].Rege M, Dong Ming, Hua Jing. Graph Theoretical Framework for Simultaneously Integrating Visual and Textual Features for Efficient Web Image Clustering[C]//17th International Conference on World Wide Web, Beijing, 2008: 317-326
- [8].Liu Tieyan, Ma Weiyang. Star-Structured High-Order Heterogeneous Data Co-Clustering Based on Consistent Information Theory[C]// 6th IEEE International Conference on Data Mining, Hong Kong, 2006: 880-884
- [9].Antonio D C, Greco G, Guzzo A, Pontieri L. An

- Information-Theoretic Framework for High-Order Co-clustering of Heterogeneous Objects[C]//17th European Conference on Machine Learning, Berlin, 2006: 598–605
- [10].Greco G , Guzzo A . Coclustering Multiple Heterogeneous Heterogeneous Domains : Linear Combinations and Agreements[J]. IEEE Transactions on Knowledge and Data Engineering, 2010, 22( 12 ): 1649-1663
- [11].Jing Liping , Yun Jiali , Yu Jian , Huang Joshua . High-Order Co-clustering Text Data on Semantics-Based Representation Model[C] //15th Pacific-Asia Conference on Advance in Knowledge Discovery and Data Mining , Shenzhen , 2011 : 171–182
- [12].Shao Jian , Yin Wentao , Ma Shuai , Zhuang Yueting . Topic Discovery of Web Video Using Star-structured K-partite Graph[C]//International Conference on Multimedia, Firenze, 2010: 915-918
- [13].Sun Yizhou , Yu Yintao , Han Jiawei . Ranking-Based Clustering of Heterogeneous Information Networks with Star Network Schema// 15th ACM SIGKDD International Conference on Knowledge Discovery and Data Mining, Paris, 2009: 797-805
- [14].Sun Yizhou , Han Jiawei , et al. RankClus: Integrating Clustering with Ranking for Heterogeneous Information Network Analysis[C]//12th International Conference on Extending Database Technology : Advances in Database Technology , Saint Petersburg , 2009 : 565-576
- [15].Wang Lijun , Dong Ming. Non-Negative Matrix Factorization for Semisupervised Heterogeneous Data Coclustering[J] . IEEE Transactions on Knowledge and Data Engineering, 2010, 22(10): 1459-1474.
- [16].Hartigan J A , Direct Clustering of a Data Matrix[J]. Journal American Statistical Association, 1972, 67 (337): 123-129.
- [17].Cheng Yizong , Church G M. Biclustering of Expression Data[C]//8th International Conference of Intelligent Systems for Molecular Biology , 2000: 93-103
- [18].Zhang Tian , Ramakrishnan R , Livny M. BIRCH: An Efficient Data Clustering Method for Very Large Database[C]//1996 ACM SIGMOD international conference on Management of data , Montreal, 1996: 103-114
- [19].Guha S, Rastogi R, Shim K. CURE: An Efficient Clustering Algorithm for Large Databases[C]//1998 ACM SIGMOD international conference on Management of data, Seattle, 1998: 73-84
- [20].Guha S, Rastogi R, Shim K. ROCK: A Robust Clustering Algorithm for Categorical Attributes[J]. Information, 2000, 25(5): 345-366
- [21].Karypis G , Han E H , Kumar V . CHAMELEON : A Hierarchical Clustering Algorithm using Dynamic Modeling[J] . IEEE Computer, 1999, 32(8) : 68-75
- [22].Strehl A , Ghosh J . Cluster Ensembles-A Knowledge Reuse Framework for Combining Multiple Partitions[J]. Journal of Machine Learning Research, 2002, VOL.3: 583-617

# A Routing Algorithm of Wireless Sensor Network based on Robust Measure

Zhao Jianguang, Fan Jingjing, Feng Yingwei  
Hebei University of Architecture, Department of Computer Science

**Abstract:** For the problem of wireless sensor network routing algorithm load imbalance, proposed the concept of wireless sensor network node robust measure, and elaborated a robust measure calculation methods. On the basis of the concept of robust measure the routing algorithm based on node robust measure was proposed, an effective solution to the problem of load imbalance and to avoid the network nodes overuse died prematurely, and extend the network lifetime. Computational simulation, routing algorithm based on node robust measure than the shortest path routing algorithm, location-based routing algorithm in the energy consumption of the same conditions, can effectively prolong the network lifetime.

**Keywords:** wireless sensor networks; robust; routing; load balancing

## 1. INTRODUCTION

The application of wireless sensor network is very extensive. Based on the characteristics of the wireless sensor networks (such as battery-powered energy is limited; limited computing power and data processing capabilities of the sensor nodes; huge number of sensor nodes; form a network node self-organization; dynamic node, may at any time enter or leave the network ; node does not have a unique IP, data-centric; communication need intermediate node routing, multi-hop routing), the pros and cons of wireless sensor network algorithms directly affects the performance and life of the entire network.

Currently, in order to meet different application needs, the researchers have developed a large number of routing protocols. These routing protocols are mainly based on the following focus:

### 1.1 Reduce energy consumption.

The energy consumption of wireless sensor networks is mainly generated by wireless communication, data transmission one bit energy required for rapid growth, with increasing communication distance [2] pointed out that the relationship between energy consumption and communication distance can be approximated as:  $E = kd^2$  when after more than a certain critical value, the relationship between energy consumption and the communication distance can be approximated as:  $E = kd^4$ . Visible, the pros and cons of wireless routing algorithm is very large impact on the energy consumption, superior performance and design of wireless routing algorithm is essential. Literature [3,4] proposed in the uniform distribution of fixed transmit

power of the network, the node load only concerned with the location and number of node hops, and a base station, regardless of the distribution of density in the area, the base station should be at the center of a network location. Many researchers have proposed LEACH and its improved algorithm, cluster heads choose to become a research focus in the algorithm[5,8].

### 1.1.1 Data Fusion

Have great relevance to the data collected by each sensor node wireless sensor network consists of a large number of sensor nodes, how to reduce the transmission of redundant data in the network is a key technology to improve the efficiency and life cycle of the sensor network. Therefore required sensor nodes before transferring data for data fusion, such as the DD (directed diffusion) GITDC (the greedy the incremental tree data centric protocol), GEAR (geographic and energy aware routing), adopted a data fusion algorithm to improve network performance. Efficient data compression algorithm, became wireless sensor network another research focus[10].

### 1.1.2 Sleep-wake mechanism

Wireless sensor networks used to monitor the specific area of data, some applications is not necessary for continuous detecting Area, only unusual event occurs only need to transmit data at the same time very dense distribution of sensor nodes, monitoring of regional overlapping, and therefore do not need all sensor nodes all the time in the wake state. No task node goes to sleep and wake node has a mission. The typical algorithms: Grid-based coverage positioning sensor configuration algorithm, Node Self-Scheduling algorithm, the worst coverage, circumference coverage etc[7,9].

### 1.2 Security

The characteristics of the wireless sensor network to determine the security of the wireless sensor network routing is more fragile than the traditional networks, by the types of attacks more resistance to attack weaker, existing routing algorithms have begun to add security mechanisms, such as has been proposed added to the routing protocol based on link-layer encryption and authentication, multi-path routing, authentication mechanisms such as authentication and authenticated broadcast, two-way connection is still very grim, but the wireless sensor network security issues, from the practical application and the formation of a universally accepted standard very



far[10].

## 2. LOAD BALANCING

Wireless sensor networks through multi-hop routing to reduce the energy consumption of communication, sensor node is a terminal routing, large number of nodes the data collected by the multi-hop flow of very small quantities of the base station, which makes near the base station node than the remote node to be sent more data packets, so the vicinity of the base station node energy consumption quickly. Order to maximize the life cycle of the nodes in the vicinity of the base station, it is necessary to avoid this from happening, a large number of researchers have proposed a variety of algorithms, [7] proposed PEGASIS formed based on the node location between an adjacent node the shortest distance from the chain, and a communication only between the adjacent nodes, each time only to select a random node to communicate with a base station. Literature [8] proposed LEACH, adopted to avoid the use of fixed node or low energy nodes act as cluster head, to some extent solve the problem of load imbalance.

Throughout the wireless sensor network algorithm, the starting point and focus of the same advantages and disadvantages. There is currently no measure of the node health of the amount to quantitative description of the robustness of the node. This paper presents the concept of wireless sensor network node robust measure, and gives the mathematical expression from the number on the quantitative analysis of the robustness of a node, the number of the basis and guarantee for wireless sensor network algorithm. On the basis of this concept node robust measure-based routing algorithm, the algorithm considering the energy consumption, geographic location, load balancing, can effectively balance the load, and prolong the network lifetime.

## 3 The algorithm

### 3.1 Algorithm Description

With the above node robust measure value, a quantitative calculation of the degree of health of each node, and lay the foundation for the routing algorithm based on robust measure. Node robust measure-based routing algorithm can be described as follows:

Step1 Source node detects communication radius of all reachable nodes.

Step2. Detection up to the nodes the robust measure value (referred to as the RM value).

Step3. Select the next hop node based on robust measure.

Step4. Arrival of the junctions, end reaches the junctions, otherwise continue.

Step5. Nodes Step3 selected as the source node to return to perform Step1.

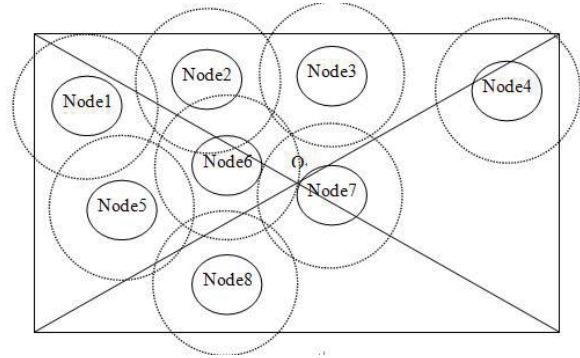


Figure 1 each node communication area

The algorithm program flow chart shown in Fig.2,

### 3.2 algorithm dynamic description

Shown in Fig.1, the distribution of nodes shown in Fig.2 under the premise of communication range of each node, it is assumed that node 1 has the information to be transmitted to the node 7, as shown in the routing policy may be shown in Fig.4, up to the path:

1->2->6->7, 1->2->3->7, 1->2->3->6->7, 1->5->6->7, 1->5->8->7, and so on. Specific routing using what path the RM value according to each node to determine the because each node RM values

change over time, the solid for the same source node and the sink node between the transmission of the same data may be using a different routing path.

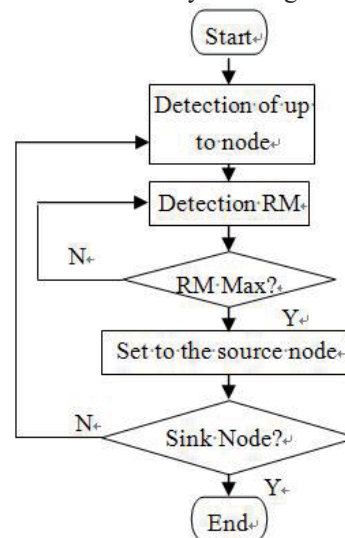


Figure 2 algorithm flowchart

## 4 Results and discussion

RM value calculated for each node, the part of the routing algorithm based on robust measure, the shortest path routing algorithm, throughout the lifetime of the network location-based routing algorithm simulation. Node hardware platform of TI's CC2431 and wireless sensor networks operating system TinyOS platform. Assuming that the number of nodes  $n=7$ , the network topology shown in Fig.4, the data transmission from node 1 to node 7 bits of the transmission unit 1 order of magnitude of the energy consumption, each node is full energy level is assumed to be 15000, the transmission information



the amount is 1024,2048,4096,8192,16384 robust measure of the value of each node as shown in Fig.3.

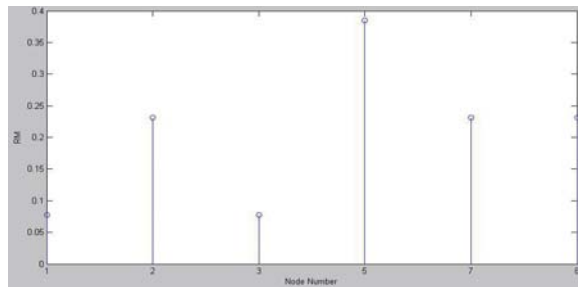


Fig.3 node RM value results Assuming the information to arrive according to a Poisson distribution, for the above-described example, the lifetime of the network shown in Fig.4.

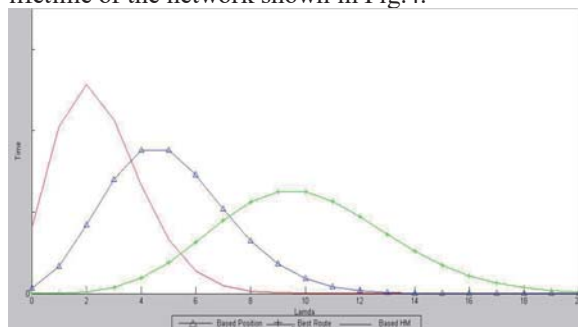


Fig.4 network lifetime maps As can be seen from Fig.4, RM-based wireless sensor network lifetime longer than the other two network lifetime. An area surrounded by three curves and the horizontal axis is equal to the, i.e. three algorithms consumption is equal to the total energy.

## 5. CONCLUSION

In this paper, the wireless sensor network load imbalance, robust measure of the degree measure of the wireless sensor node, robust measure to measure the node robust the robust measure conceptual basis, based on robust measures of wireless sensor network routing algorithm. Computational simulation, under the same conditions in the network total energy consumption wireless routing algorithm based on robust measure can effectively balance the load, to extend the network lifetime.

## ACKNOWLEDGEMENTS

This work was financially supported by the Education Department of Hebei Province youth fund project, project number: QN20131148. Hebei Institute of Architectural Engineering School Fund, NO: QN201414, Project Name: Based on the ski slopes of wireless sensor network security key technology research. Hebei Institute of Architectural Engineering School Fund, NO: ZD201407, Project

Name: Campus Card intelligent consumer terminal Key Technology Research. Hebei provincial science and technology plan special work projects, NO: 16236004D-8, Project Name: Tian Road Zhangbei grassland surrounding mountains outdoor tourism micro backpack sites and intelligent search field development.

## REFERENCES

- [1]Shanta Mandal , Rituparna Chaki. "A SECURE ENCRYPTION LOGIC FOR COMMUNICATION IN WIRELESS SENSOR NETWORKS",IJCIS,2012,Vol.2,No.3,pp107-116.
- [2]Jain-Skiing Liu, Lin C-HP. Power-efficiency clustering method with power-limit for sensor networks[C] Eric Johnson. Performance, Computing, and Communications Conference 2003, Arizona, USA: [S. n.], 2003: 129-136.
- [3]Wang liang, Zhong xianxin, Shi jun feng. Wireless sensor network energy consumption balance strategy[J]. Sensor World, 2007(3):32-37.
- [4]Li J, Mohapatra P. An analytical model for the energy hole problem in many to one sensor networks[C] Bob Shapiro. IEEE 62nd Semiannual Vehicular Technology Conference, Dallas, USA: [S. n.], 2005:2721-2725.
- [5]Hein Zelman W. Application-Specific protocol architectures for wireless networks [D]. Boston: Massachusetts Institute of Technology, 2000.
- [6]Gupta I, Riordan D, Sampalli S. Cluster-Head election using fuzzy logic for wireless sensor networks[C] Jacek Ilow. Proc. of the 3rd Annual Communication Networks and Services Research Conference, Halifax: [S. n.], 2005:255-260.
- [7]Lindsey S, Raghavendra C. Pegasus: Power-Efficient gathering in sensor information systems[C] Proc. of the IEEE Aerospace Conf, New York:[S. n.], 2002:9-16.
- [8]Heinzelman W, Chandrakasan A, Balakrishnan H. Energy-efficient communication protocol for wireless micro sensor networks[C] Hawaii International Conference on System Sciences, Hawaii:[S. n.], 2000:1-10.
- [9]Li Hao, Qianping Wang, Yu e Su. A CUT-based Routing Protocol for Wireless Sensor Networks in Coal Mine[C] Third International Conference CPCA 2008, 851-856.
- [10]M. Li and Y. Liu. Underground Structure Monitoring with Wireless Sensor Networks [C]. In Proceedings of the 6th International Conference on Information Processing in Sensor Networks 2007:69-78.

# Evaluation and Optimization on Applicability of Big Data Technologies in Smart Grid

Chenjun Sun<sup>1</sup>, Jing Zhou<sup>2,\*</sup>

<sup>1</sup>State Grid Hebei Electric Power Corporation, Shijiazhuang 050021, China

<sup>2</sup>School of Control and Computer Engineering, North China Electric Power University, Beijing 102206, China

**Abstract:** As a newly emerging solution to electricity problems in China, smart grid is also the development tendency of electric power industry worldwide in the future. In smart grid, huge data of electricity production involve multi-type big data technologies. Selecting suitable ones from these technologies, which will be used to analyze, compute and manage big data, is a vital to find out the potential value, law and pattern of smart grid. Therefore, this paper proposes evaluation criterion and approach based on data encapsulation analysis and characteristics of big data technologies in smart grid, and finally explores the applicability of various big data technologies in smart grid.

**Keywords:** Big data, data mining algorithm, Daily electricity load

## 1. INTRODUCTION

Smart grid is a new type of power grid integrating multiple modern scientific technologies (such as modern sensing measurement technology, communication technology, control technology and so on). The development of smart grid should not only meet customers' demand for electric power but also ensure smart grid could operate safely and reliably at a low cost. The electricity production in smart grid includes processes of power generation, transmission, transformation, power distribution, utilization and scheduling. For each process, there are a lot of sensor networks used to collect, transfer and analyze data, and then calculate. Only by analyzing huge volume of available data, the effective, implicit and valuable law and pattern for smart grid operation could be found out, and customers' electricity consumption behavior could be understood, and the system of electric power demand response & short-term load prediction could be designed reasonably. Therefore, we will adopt data mining technology to figure out certain law and pattern from huge outer and inner data of and find an optimal solution to existing problems in smart grid so to meet customers' demand for electricity power.[1,2]

At present, a lot of data mining algorithms prevail, to name a few: there are models of DT (decision tree) C4.5, SVM, KNN, CART, Naive Bayes etc. However, all of them have defects themselves and only some of them could be used in smart grid. To effectively use data, to extend the application scope of big data technologies, and to meet customers' demand while

lowering the operation cost in smart grid, we selected 5 typical data mining algorithms to analyze in a certain field of smart grid in this paper, then we evaluated the applicability for each algorithm according to the analysis results whereby evaluation system, and finally had selected the most optimal solution.

## 2.SOURCES, CHARACTERISTICS, AND KEY TECHNOLOGIES OF BIG DATA IN SMART GRID

### 2.1. sources of big data

The sources of big data in smart grid come from 3 aspects below,[3]

- Data of operation, detection and surveillance in power grid
- Marketing data of electric power enterprises
- Management data of electric power enterprises

Power grid operation, detection and surveillance data are big data mainly from power generation side and transmission & transformation side. For instance, there are more than 100,000 various sensors equipped on various devices to monitor and control their operation in power grid, which means total data will geometrically grow. Besides, other data, including isolation discharging information, environment radiation and interference information etc., often become huge due to being collected frequently. Mass data above help to ensure the safety of operation on both power generation side and transmission & transformation side. Marketing data and management data of electric enterprises mainly source from electricity utilization side, for example, a lot of data from the smart meters, sensors on large power equipments etc., which help electric enterprises to analyze the electricity utilization habit and pattern of users, and consequently to design and control charging-discharging time reasonably.

### 2.2. characteristics of big data in smart grid

In smart grid, big data are characterized by the typical features of "4V" and "3E". "4V" is short for *Volume*, *Variety*, *Value* and *Velocity*. "3E" is short for *Energy*, *Exchange*, and *Empathy*. [4]

#### ●Volume

With rapid information construction and development in smart power system, the growth of data is beyond electric enterprises' expectation. So far, the magnitude of data in smart grid has jumped from TB to PB. For example, automation of power generation requires more precise, more frequent and more

accurate values of pressure, flow, and temperature, which results in data size going up tremendously.

#### ●Variety

The sources of data are extensive in all processes of smart grid. The types of data are various (structured, semi-structured or non-structured), such as Text data, History data, Time series data and so on. Video and audio are non-structured data and their percentage is creasing gradually. Meanwhile, the demand for analyzing other industries' data brings more data types into power grid.

#### ●Value

There is a lot of irrelevant information. Most data are not available so that finding out the law and pattern in smart grid is hard, which means the low value density of data in smart grid.

#### ●Velocity

Data processing rate is high enough to support real-time or quasi real-time analysis and decision-making. The requirement on time limit to handle a business is harsh with the target to real-timely process electric power big data within 1 second.

#### ●Energy

Electric power big data are durable, non-consumable, pollution-free and easy-to-transfer. The value of data could be refined and appreciated while being used. The process of applying electric power big data (i.e. the process of releasing energy of electric power big data), aims at the target to save energy by analyzing electric power big data to some extent.

#### ●Exchange

Electric power big data are not only valuable within electric power industry but also for the whole national economy, social improvement, and innovation & development of various industries. The value of electric power data will be greatly appreciated whereby interaction and integration with data from other industries. Then the value could be mined, analyzed and illustrated further.

#### ●Empathy

The vital aim for an enterprise is to develop customers and create demand. Smart grid big data are in a transition period from electricity generation-oriented to customer-oriented involving all links from demand of customers to power production. The ultimate aim is to care electricity power users, that is, electric enterprises should develop emotional connection with users and supply them more quality, safer, and more reliable services by mining and meeting their demands.

### 2.3. key technologies of big data in smart grid

The applications of big data are in three aspects: integration management of big data, data analysis and data processing. [5]

#### ●Integration management of big data

Big data management involves technologies of relational & non-relational database, data fusion & integration, data extraction, data cleaning & filtering

etc. To specifically speaking, big data management refers to technologies of power data' ETL (Extract, Transfer, and Load), and of common model of power data unification, etc. In other words, it is a course to transfer data into power application system by extracting, filtering and cleaning data, after integrating data from multi-sensor networks. Integration management of big data aims at solving the problems of data redundancy and information islands among various systems in smart grid.

#### ●Data analysis

Big data analysis technology involves data mining, machine learning, etc. It specifically refers to power grid safety on-line analysis, estimation on electricity generation of intermittent power source, and running state analysis of facilities & transmission lines, etc. It is a course to find out the law and pattern of mass data from multi-dimensions by analyzing and refining the data collected from sensors. The key technology of electric power big data analysis derives from Statistics, and then combines with computer technology to conduct correlation analysis, machine learning, data mining and pattern recognition.

#### ●Data processing

Big data processing technology involves technologies of visualization, history flow display, spatial information flow display etc. It specifically refers to technologies of power grid running state real-time monitoring, interactive screen & map, 3D display & virtual reality of transformer substation, etc. These technologies mainly make use of the large-scale computing technology of modern computer to boost the speed of processing data. The large-scale computing technology could subdivide into technologies of distributional parallel computing, memory computing, flow processing, etc.

### 3.EVALUATION MODEL

After analyzing sources, characteristics and key technologies of big data in smart grid, we consider to establish an evaluation criterion system to analyze which one of these various technologies is applicable in smart grid under different circumstance, so that we could select the most applicable one.

Merits and defects obviously exist for all algorithms, which may be taken as positive features and negative features respectively here. To ensure the algorithm is with the impartiality of evaluation criterion, we could not only consider the positives features (e.g. precision) but also the negative ones (e.g. memory space, run time, training & testing time, etc.). Traditional algorithms always adopt interestingness as evaluation criterion, which includes algorithm's positive features like novelty, effectiveness, and understandability, etc., and most of them cannot be measured objectively. Therefore, Charnes et al. proposed the method of data encapsulation analysis in 1987, which considers all positive and negative features of data mining algorithm at the stage of definition so to objectively and impartially evaluate an algorithm.[6]

It is assumed that we will evaluate  $a$  algorithms of data mining with regard to  $m$  positive features and  $n$  negative ones. Then vectors of positive and negative features are expressed as,

$$X_j = (u_{1j}, u_{2j}, \dots, u_{mj})^T, \quad (1)$$

and  $Y_j = (y_{1j}, y_{2j}, \dots, y_{nj})^T$  respectively,

herein  $j = 1, 2, \dots, a$ . The vectors of corresponding

weights are expressed as,  $U = (u_1, u_2, \dots, u_x)^T$ , and

$$V = (v_1, v_2, \dots, v_x)^T \text{ respectively. As for the}$$

algorithm  $k$ , let  $x_{ik}$  = the value of positive feature,

$y_{rk}$  = the value of negative feature, and

$x_{ik}, y_{rk} > 0$ ; Meanwhile let  $u_i$  = the value of

positive feature,  $v_r$  = the value of negative feature,

and  $u_i, v_r \geq 0$ . If  $E_k$  represents the efficiency of the algorithm, then it could be calculated as below.

$$E_k = \frac{\sum_{i=1}^m u_i x_{ik}}{\sum_{r=1}^n v_r y_{rk}} \quad (1)$$

By selecting suitable weigh vectors  $U$  and  $V$ , make  $E_k \leq 100\%$  true for any algorithm  $k$ . When

evaluating the algorithm  $k_0$ , set its efficiency index as the target and set the efficiency of all algorithm which will be evaluated as the constrain, then the general optimized model is expressed as below.

$$\begin{aligned} MAX &= \frac{U^T P_0}{V^T N_0} \\ \begin{cases} \frac{U^T P_0}{V^T N_0} = E_k, k = 1, 2, \dots, a \\ V \geq 0, U \geq 0 \end{cases} \end{aligned} \quad (2)$$

Planning application transform will be conducted in formula 2 to make it a linear planning model. By solving this model to find the optimal solution, the relative effectiveness of  $E_{k_0}$  will be determined. The model is shown as following.

$$\begin{cases} \max E_{k_0} = \mu^T x_0 \\ s.t. \omega^T x_j - \mu^T y_j \geq 0, j = 1, 2, \dots, a \\ \omega^T x_0 = 1 \\ \omega \geq 0, \mu \geq 0 \end{cases} \quad (3)$$

In this paper, we select positive feature of testing accuracy and negative features of training error rate, training time, testing time and the applicability of comprehensive evaluation algorithm. There is a certain correlation between positive and negative features so that the method to determine weights by

simply increasing or decreasing of positive and negative features could not meet the requirement of evaluation. To describe the impact of multi-features on evaluation result, we will determine the weights of these features according to their entropy, [7] that is, the weight of an feature is the ratio of its entropy difference coefficient to sum of all entropy difference coefficient. Entropy weight can help to deeply diminish the blindness of objective weight, to judge the discrete degree of certain index feature, and to analyze the contribution of different features, consequently make evaluation more objective. The steps in detail are below.

●Data offset

Let  $y_{ij} = y_{ij} + 1$ , herein  $i = 1, 2, \dots, m; j = 1, 2, \dots, n$ .

While calculating the weight from entropy, data offset can help to avoid meaningless logarithmic calculation.

●The weight  $i$  of index  $j$  is calculated

$$\text{as } p_{ij} = y_{ij} / \sum_{i=1}^m y_{ij}, \quad \text{herein } i = 1, 2, \dots, m; j = 1, 2, \dots, n.$$

●The entropy of index  $j$  is calculated as

$$e_i = -k \sum_{i=1}^m p_{ij} \ln p_{ij}, \quad \text{herein } k > 0, k = 1/\ln(n), e_j \geq 0.$$

●Calculate the difference coefficient of index  $j$ . For index  $j$ , if the value  $Y_{ij}$  is bigger, the impact of  $Y_{ij}$  on the evaluation result is more significant, and the entropy is smaller. Difference coefficient is defined as

$$g_j = 1 - e_j / \sum_{j=1}^n (1 - e_j) = 1 - e_j / n - E_e, \quad \text{herein } E = \sum_{j=1}^n e_j, 0 \leq g_j \leq 1, \sum_{j=1}^n g_j = 1.$$

●Calculate weights as  $\omega_j = g_j / \sum_{j=1}^n g_j$ , herein  $j = 1, 2, \dots, n$ ,

#### 4.CASE STUDY

##### 4.1sources of data

In order to study the applicability of various data mining technologies in smart grid, taking short-term load prediction in power grid as an example in this paper, we collected 1000 sets of historical meteorological data and daily load data of electric power sector within 3 years in a certain area. Meteorological data source from local meteorological station, and load data come from local power grid. Meteorological elements including temperature, rainfall, humidity, air pressure and wind force were selected as the input attributes of prediction model.



By using data mining technology, the relevant knowledge rules between meteorological elements and features of short-term daily load, and their time series pattern had been mined. In this paper, we adopted 5 algorithms of data mining (Decision tree C4.5, CART, Naïve Bayes model, KNN, and SVM) to build the short-term daily load prediction model. [8,9,10] We had also established different prediction models after studying on fluctuation of daily load. Before data are input into the prediction model, missing data should be repaired and all data should be normalized to ensure that data would be input into each model with the same quality. Weighted mean of normal data at the time after and before when data are missed is used to repair missing data as calculated as below.

$$x(d, t) = \omega_1 x(d_1, t) + \omega_2 x(d_2, t) \quad (4)$$

Herein,  $x(d, t)$  refers to the load at the time  $t$  on the day,  $x(d_1, t)$  and  $x(d_2, t)$  refer to the loads at the time  $t$  on the day before or after the day  $d$  respectively.  $\omega$  is the weight of weighted mean. In this paper, let  $\omega_{1,2} = 0.5$ .

Data normalization will make data unified, that is, data with different magnitude will be transformed into the same numerical interval  $[0, 1]$ . Data could be unified via the formula below.

$$L = \frac{L - L_{\min}}{1.2L_{\max} - L_{\min}} \quad (5)$$

Where  $L_{\min}$  and  $L_{\max}$  are the minimum value and the maximum value in the training set.

#### 4.2. case study

According to 5 prediction models and the prediction results, we picked out 1 positive feature of testing accurate rate and 3 negative features of training error rate, training time, and testing time to input into evaluation models, and the output will be the all-around rating. Using the established DEA( Data Encapsulation Analysis) evaluation model, prediction results from 5 algorithms had been analyzed, we visually observed the impact of different algorithms on short-term load of power grid, and evaluated various algorithms.

We divided 1000 sets of data into 2 groups, that is, one includes 950 training sets and the other one includes 50 testing sets. Data size and the numbers of attributes of data will greatly impact on positive and negative features (for instance, big data size will make training time increasing), therefore, we selected training sets in 3 different contexts, trained them and observed the results. 3 contexts are training sets with all data, training sets with random half data, and training sets with 2 input attributes taken out. We compared prediction models built in above 3 contexts, and used them to analyze and evaluate applications of 5. ALGORITHMS IN SMART GRID

Table 1. Evaluation results on positive and negative

features of 5 algorithms in a context of training sets with all data

| Name of algorithm            |               | Train ing time (s) | Testi ng time (s) | Train ing error rate (%) | Testin g accur acy (%) | Rati ng |
|------------------------------|---------------|--------------------|-------------------|--------------------------|------------------------|---------|
| Train ing sets with all data | C4.5          | 125.59             | 30.22             | 5.9                      | 92.82                  | 1       |
|                              | CA RT         | 140.66             | 27.087            | 6.1                      | 92.74                  | 2       |
|                              | Naï ve Bay es | 170.54             | 50.13             | 9.5                      | 90.17                  | 5       |
|                              | SV M          | 278.72             | 50.48             | 5.7                      | 93.66                  | 3       |
|                              | KN N          | 350.6              | 70.21             | 4.9                      | 92.65                  | 4       |

Table 2. Evaluation results on positive and negative features of 5 algorithms in a context of training sets with random half data

| Name of algorithm                    |               | Train ing time (s) | Testi ng time (s) | Train ing error rate (%) | Testin g accur acy (%) | Rati ng |
|--------------------------------------|---------------|--------------------|-------------------|--------------------------|------------------------|---------|
| Train ing sets with random half data | C4.5          | 100.02             | 21.58             | 8.2                      | 89.62                  | 3       |
|                                      | CA RT         | 97.35              | 18.47             | 5.8                      | 92.05                  | 1       |
|                                      | Naï ve Bay es | 132.49             | 37.62             | 8.7                      | 89.97                  | 5       |
|                                      | SV M          | 198.23             | 42.61             | 4.4                      | 93.28                  | 2       |
|                                      | KN N          | 200.78             | 53.27             | 6.1                      | 91.37                  | 4       |

Table 3. Evaluation results on positive and negative features of 5 algorithms in a context of training sets with 2 attributes taken out

| Name of algorithm                       |               | Train ing time (s) | Testi ng time (s) | Train ing error rate (%) | Testin g accur acy (%) | Rati ng |
|---|---------------|--------------------|-------------------|--------------------------|------------------------|---------|
| Train ing sets with 2 attrib utes taken | C4.5          | 89.37              | 17.89             | 9.6                      | 88.33                  | 3       |
|   | CA RT         | 94.025             | 15.23             | 8.2                      | 90.95                  | 2       |
|   | Naï ve Bay es | 110.21             | 24.28             | 8.33                     | 90.5                   | 4       |



|     |         |            |           |     |       |   |
|-----|---------|------------|-----------|-----|-------|---|
| out | SV<br>M | 189.4<br>2 | 39.8<br>4 | 4.8 | 93.18 | 1 |
|     | KN<br>N | 230.9<br>2 | 60.7<br>7 | 8.7 | 90.15 | 5 |

#### 4.3. results and discussion

The result shows that the difference of positive and negative features among 5 algorithms is not significant in Tab. 1, 2, and 3 respectively. The accuracy of prediction for all algorithms is high with an average value at 90% around. The training error rate is low varying from 4% to 9%. To sum up, it is shown that these 5 algorithms could meet the requirement to predict daily load of power grid. In this paper, each set of test only were done in the same context each time. The results show that decreasing both data size and the numbers of attributes would impact on algorithms' features as shown below.

##### ●All data, all attributes

In this context, C4.5 has the highest all-around rating compared with other algorithms. The training error rate is low, testing accuracy is high, and training time and testing time are short. Meanwhile, in the same context, the training time and testing time of SVM and KNN are twice of those of other algorithms, so to seriously impact on the evaluation results of these two algorithms. Computation of these 2 algorithms is mass so that its efficiency is low. Besides, the rating of Naïve Bayes is lowest due to its worst features.

##### ●Data size

In comparison with Tab. 1 and Tab. 2, while input attributes are constant and data size decreases down to half randomly, training time and testing time both shorten, training error rate increases and testing accuracy decreases accordingly for all 5 algorithms. Rather than other algorithms, C4.5 varied most significantly: the rating of its evaluation result decreases the most, its training error rate almost doubles, and its testing accuracy decreases the most. C4.5 is the most sensitive algorithm to the decrease of data size. Algorithm CART and SVM are more stable to the changes of data size, all features change very slightly, their testing accuracy decreases a little, their prediction accuracy is high, and their rating of evaluation result goes up. The prediction accuracy of KNN is higher than the one of C4.5, but its training time and testing time are the longest ones among 5 algorithms so to low its rating of evaluation result.

##### ●Numbers of attributes

Comparing Tab.1 with Tab.3, positive and negative features of 5 algorithms decrease significantly while data size is constant and 2 input attributes are randomly cut out. Comparing Tab.1 with Tab.2, training time and testing time changes slightly but testing accuracy decrease a lot and training error rate goes up a lot. Among all algorithms, SVM has longer training time and testing time but this algorithm is relatively stable, that is, its testing accuracy and testing error rate almost keep constant, and the rating of evaluation result is the highest. For algorithm

Naïve Bayes, its testing accuracy increases greatly in spite of other features are not ideal. However, Naïve Bayes algorithm can perform better when sample attributes are few. Algorithms of C4.5, CART and KNN are greatly influenced by changes of input attributes, their testing accuracy all decrease at a different degree. Among them, the testing error rate of CART changes most significantly and its testing accuracy decrease the most.

●While data size is mass and attributes are intact, C4.5 can predict daily load with a higher accuracy. This algorithm is more applicable to analyze data with a bigger size. When sample data size and sample attributes change, CART and SVM are robust and vary slightly with a relatively stable testing accuracy, and SVM's accuracy is higher than the CART's. However, testing time and training time of SVM are very long resulting in a low efficiency of computation, SVM should be selected only when there are no requirements on computation efficiency, and CART should be selected when there are requirements of real-time prediction. Naïve Bayes would be used to improve features when attributes of samples are few, and the numbers of attributes input will directly impact on the classification efficiency of Naïve Bayes.

●Models' prediction efficiency has an inter connection with data size and the numbers of input attributes. Big size of data could decrease error rate of prediction model but would increase prediction time so to possibly lower model's efficiency. Increasing the numbers of input attributes could increase the comprehensive efficiency of an algorithm, but would make algorithm itself more complex and consequently running slowly or even looping endlessly.

#### 5. CONCLUSION

Via the analysis above, it is obviously that selecting appropriate data mining algorithm to use in a right field of smart grid is the way to improve the algorithm's applicability and make most of the algorithm to serve smart grid. In this paper, we verified application effectiveness of 5 algorithms in smart grid, analyzed and evaluated the practical effectiveness in different contexts, and demonstrated the application of 5 algorithms to some extent. In the field of smart grid, although there are a lot of algorithms available, evaluation methods and algorithms still need extending, application range needs enlarging, the connection between big data technologies and smart grid needs enhancing.

#### ACKNOWLEDGMENT

This work was supported by the State Grid Corporation headquarters projects(KJGW2015-020)

#### REFERENCE

[1]Xi Fang, Satyajayant Misra, Guoliang Xue, et al. Smart Grid, the new and improved power grid:

- a survey[J]. IEEE Communications Surveys and Tutorials (COMST), 2012, 14(4): 944-980.
- [2]ZHANG Wen-liang, TANG Guang-fu, ZHA Kun-peng, HE Zhi-yuan. Application of advanced power electronics in smart grid[J]. Proceedings of the CSEE, 2010, 30(4): 1-7.
- [3]SONG Yaqi, ZHOU Guoliang, Zhu Yongli. Present status and challenges of big data processing in smart grid[J]. Power system technology, 2013, 37(4): 927-935.
- [4]DUN Jun-hong, ZHANG Nai-dan, ZHAO Bo, YAN Xiao-bin. Research on basic system architecture and application of electric power big data[J]. Electric Power ICT, 2015, 13(2): 92-95.
- [5]Wang Hong-yan, Guo Yun-feng. Research on application of big data technology in AI [J].Technology and Application of Digital, 2015,(12):109-110.
- [6]HA Jin-cai. Evaluation criterion and method of DM algorithm[J]. Microelectronic & Computer, 2006, 23(12):195-196.
- [7]Li Yulin, Gao Zhigang, Han Yanling. The Determination of weight value and the choice of composite operators in fuzzy comprehensive evaluation[J]. Computer Engineering and Applications, 2006, 42(23):38-42, 197.
- [8]HAN Qiyun. A mobile communication enterprise customer churn prediction model based on CART algorithm[J]. Bulletin of Science and Technology, 2012, 28(2):120-122.
- [9]ZHU Liuzhang. Short-term electric load forecasting with combined data mining algorithm[J]. Automation of Electric Power System, 2006, 30(14):82-86.
- [10]LI Xiang, ZHOU Bo. A performance prediction method based on Naïve Bayes classification[J]. Computer application and software, 2011,28(1):231-234,290.

# New Urbanization under the Background of Study on Rural Sports Public Service Innovation Supply

Lu Liu<sup>1,\*</sup>, Libin Yu<sup>1</sup>, Bo Ling<sup>1</sup>, Ting Zhou<sup>2</sup>, Honghai Wu<sup>3</sup>

<sup>1</sup>Institute of Physical Education, Huanggang Normal University, Huangzhou 438000, Hubei, China

<sup>2</sup>Qichun Xiangqiao Eementary School, Hubei, China

<sup>3</sup>Qichun Tongzi Elementary School, Hubei, China

**Abstract:** As led the country to the city, to work with farmers, reciprocity of workers and peasants, urban and rural integration policy, a new type of rural urbanization is hot; the construction of sports public services has been in the innovation. This article through to the supply of public sports service to consider policy management, profit, brand effect and influence factors such as the social cohesion, it is concluded that new rural sports public service supply mode in the public sector, private sector and their respective proportion of social organization. As a result, the rural sports public service supply of new style should be in the public sector and private sector cooperation to supply, and the public sector to the right amount of selective acquisitions of social organizations of public service.

**Key words:** Sports public services; Urbanization; Rural sports

## 1. INTRODUCTION

Since new China has been founded, China's comprehensive strength has started to promoting, after opening-up and reformation, Chinese economy has been rapidly developed, national demands increase, therefore public service has become Chinese government reform concept important contents, government reformation on public service should involve in multiple aspects of society [1]. Therefore, public services have many contents, represented forms are various, from which it can divide into lowest basic public service, economic aspect service, social welfare service and public security and safety so on. And sports public service is an important reflection of national physical quality [2]; it reflects a country and a society people health extent, which is also reflection of the country vital force. And China is gradually going ahead with socialist harmonious society construction, puts emphasis on driving rural development that is new pattern urbanization [3]. Therefore, supply that confronts to new situation rural sports public services should also make reformation, the paper makes research and analysis on new pattern urbanized China's rural sports public services, and finds out the supply way that is more suitable to China's rural status.

## 2. MODEL ESTABLISHMENTS

### 2.1 Establish hierarchical structure

In order to find out more suitable supply way for China's rural status, firstly it should find out supply's most influential unit, with new rural policies releasing, no matter society, enterprises or nation, all focus on rural construction. Therefore, the paper firstly based on analytic hierarchy process to make quantization on rural sports public service. Establish target layer, criterion layer and scheme layer relations.

### 2.2 Consistency test

Use consistency test formula as:  $CI = \frac{\lambda_{\max} - n}{n - 1}$ .

Among them,  $\lambda_{\max}$  is maximum feature root value of comparison matrix,  $n$  is comparison matrix order. It is clear that judgment matrix and  $CI$  value are in inverse proportion.

Judgment matrix is

$$C_1 = \begin{Bmatrix} 1 & 1 & 1/3 \\ 1 & 1 & 1/3 \\ 3 & 3 & 1 \end{Bmatrix}, C_2 = \begin{Bmatrix} 1 & 5 & 5 \\ 1/5 & 1 & 5 \\ 1/5 & 1/5 & 1 \end{Bmatrix}, C_3 = \begin{Bmatrix} 1 & 5 & 8 \\ 1/5 & 1 & 5 \\ 1/8 & 1/5 & 1 \end{Bmatrix}, C_4 = \begin{Bmatrix} 1 & 5 & 8 \\ 1/5 & 1 & 5 \\ 1/8 & 1/5 & 1 \end{Bmatrix}$$

Corresponding maximum feature value and feature vector are in order as:

$$\lambda_{\max}^{(1)} = 3.62, y_{(1)}^{(1)} = \begin{Bmatrix} 0.244 \\ 0.244 \\ 0.512 \end{Bmatrix}, \lambda_{\max}^{(2)} = 3.29, y_{(2)}^{(1)} = \begin{Bmatrix} 0.656 \\ 0.255 \\ 0.087 \end{Bmatrix}$$

$$\lambda_{\max}^{(3)} = 3.31, y_{(3)}^{(1)} = \begin{Bmatrix} 0.650 \\ 0.212 \\ 0.137 \end{Bmatrix}, \lambda_{\max}^{(4)} = 3.12, y_{(4)}^{(1)} = \begin{Bmatrix} 0.604 \\ 0.248 \\ 0.148 \end{Bmatrix}$$

For judgment matrix  $C$ ,  $\lambda_{\max}^{(0)} = 5.063, RI = 1.12$

$$RI = \frac{5.063 - 4}{4 - 1} = 0.039$$

$$CR = \frac{CI}{RI} = \frac{0.039}{1.12} = 0.035 < 0.1$$

It represents  $C$  inconsistency extent is within permissible range, now it can use  $C$  feature vector to replace weight vector.

Similarly, to judgment matrix  $C_1, C_2, C_3, C_4$ , utilize above principle, all pass consistency test. Calculation structure is as following:

$$y^{(1)} = (y_1^{(1)}, y_2^{(1)}, y_3^{(1)}, y_4^{(1)}) = \begin{Bmatrix} 0.624 & 0.185 & 0.252 & 0.575 \\ 0.234 & 0.240 & 0.089 & 0.286 \\ 0.136 & 0.575 & 0.66 & 0.139 \end{Bmatrix}$$

;

$$y = y^{(1)} y^{(0)} = \begin{Bmatrix} 0.252 & 0.575 & 0.624 & 0.185 \\ 0.089 & 0.286 & 0.240 & 0.240 \\ 0.66 & 0.139 & 0.136 & 0.575 \end{Bmatrix} \begin{Bmatrix} 0.577 \\ 0.066 \\ 0.124 \\ 0.253 \end{Bmatrix} = \begin{Bmatrix} 0.423 \\ 0.385 \\ 0.192 \end{Bmatrix}$$

#### 2.4 New rural sports public service supply way game analysis

By above analytic hierarchy process, it is clear that in new rural sports public service aspect, leading component is changing from previous government and the third department to enterprises that rapidly develops into rural sports public service supply main party. According to game analysis, it can roughly regard government and enterprise as main parts, their implemented strategies are both two kinds that are supply and don't supply. Set in case government supplies sports public service and enterprise doesn't supply, government payoff is  $P_1$ , enterprise payoff is 0; on the contrary in case enterprise supplies while government doesn't supply, enterprise payoff  $P_1'$ , government payoff is  $p_2$ , cause is though government doesn't supply, enterprise supplies and meanwhile adheres to government system, is beneficial to socialist harmonious society construction. When both government and enterprise simultaneously supply sports public service, government payoff is  $P$ , enterprise payoff is  $P'$ ; If both government and enterprise don't supply, then both two payoff is 0.

Among them,  $P > P_1 > P_2$ , but size of  $P', P_1'$  cannot define, therefore the paper will adopt evolution game analysis to analyze government and enterprise sports public service supply practices, and make respectively strategies adjustment.

#### 2.5 New rural sports public service supply evolution game analysis

Due to government and enterprise strategies selection in sports public service supply and don't supply independent and random and can carry on repeated games. Therefore, set government supply probability to be  $U$ , probability that don't supply is  $1-U$ ; enterprise supply probability is  $R$ , probability that don't supply is  $1-R$ . According to Malthusian theorem, it is clear that government strategies support times selection growth rate  $\dot{U}/U$  should be

differences between fitness  $E_w T\{f, 1-R\}^T$  and average fitness  $\{U, 1-U\} T\{R, 1-R\}^T \cdot E_w = [1, 0]$ , when government supply probability is 1, its payoff matrix

$$\text{is } T = \begin{bmatrix} P & P_1 \\ P_2 & 0 \end{bmatrix}$$

Simplify  $\dot{U} = U(1-U)\{1, -1\} Q\{R, 1-R\}^T$  and

$$\text{get } \dot{U} = U(1-U)[(P - P_1 - P_2)R + P_1]$$

Similarly, enterprises strategies supply times growth rate should be differences between  $\dot{R}/R$  fitness

$$E_J H\{R, 1-R\}^T \text{ and average}$$

fitness  $\{R, 1-R\} H\{U, 1-U\}^T \cdot E_J = [0, 1]$ , When

enterprise probability is 1, its payoff matrix is  $H = \begin{bmatrix} P' & 0 \\ P_1' & 0 \end{bmatrix}$

Simplify  $\dot{R} = R(1-R)\{-1, 1\} H\{U, 1-U\}^T$  and

$$\text{get } \dot{R} = R(1-R)[P_1' + (P' - P_1')U]$$

Therefore when  $\dot{U} = 0, \dot{R} = 0$ ,  $(0, 0)$ ,  $(0, 1)$ ,  $(1, 0)$ ,  $(1, 1)$  are public cultural service supply balance points. According to matrix stability, analyze these balance points partial stability, solve partial

derivatives of  $\dot{U}$  to  $U$ , and partial derivatives of

$\dot{R}$  to  $R$ , Tab.1 is balance point partial stability.

Table 1. Balance point partial stability

| Balan<br>ce<br>point<br>(U, R) | det W                  |   | tr W             |             | Stabil<br>ity         |
|--------------------------------|------------------------|---|------------------|-------------|-----------------------|
| (0,0)                          | $P_1 \bullet P_1'$     | + | $P_1 + P_1'$     | +           | unsta<br>ble<br>point |
| (0,1)                          | $-(P - P_2) \bullet$   | - | $P - P_2 - P_1'$ | Unkno<br>wn | Saddl<br>e<br>point   |
| (1,0)                          | $-P_1 \bullet P'$      | - | $P' - P_1$       | Unkno<br>wn | Saddl<br>e<br>point   |
| (1,1)                          | $(P - P_2) \bullet P'$ | + | $-(P - P_2 + P'$ | -           | Stabl<br>e<br>point   |

By above table, it is clear  $(0, 0)$  point is unstable point,  $(0, 1)$  and  $(1, 0)$  are saddle points, evolution stable point is  $(1, 1)$ . Fig.1 is strategy evolution graph.

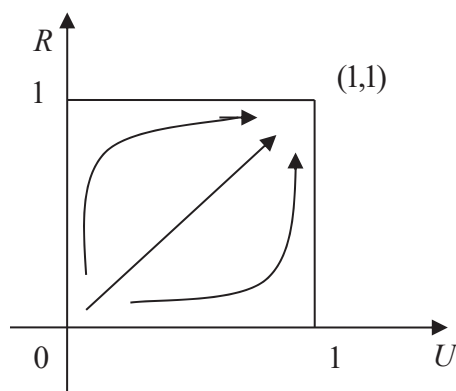


Figure 1. Strategy evolution graph

Therefore, it is clear that government and enterprise optimal supply strategy to sports public service should be government collaborating with enterprise to supply sports public services.

### 3. CONCLUSION

Firstly by establishing analytic hierarchy process model, considering policy support, yield returns, the brand effect and authority and social cohesion and other influence factors when supply sports public service, the paper solved rural new pattern sports public service supply way's government, enterprise and third department respectively occupied proportions are respectively. It gets that government and enterprise supply in rural sports public service new pattern supply way are the main parts. Then according to game analysis and evolution game analysis, it solves government and enterprise

supplying public cultural service strategies should be government collaborating with enterprise to supply sports public service, so rural sports public service new pattern supply way should be government and enterprise collaborative supply on it, and government should properly carry out selective acquisition on the third department public service, adopt strategies of stimulating foreign companies by competition to promote new rural area sports public service construction.

### ACKNOWLEDGMENT

2014 Hubei province project in humanities and social science: in the construction of urbanization path of the development of rural school sports research (14G383). 2015 Huanggang normal university research projects, rural school sports development path, based on the perspective of government purchasing public sports services (2015017003).

### REFERENCES

- [1] Chen Yu-Zhong, Social transformation and sports public service management system reformation, *Journal of sport culture Tribune*, 2008, 44(3):33-36.
- [2] Hua Ai., Roshan citizen's club houses: Hard choices in new and old systems' conflict, *Journal of communities*, 2006, 23(4S):8-10.
- [3] Zhang Wen-Li, Wu Guang-Yun. Theory of service-oriented government and the effective supply of public services, *Journal of Lanzhou university: social science edition*, 2007, 35(3):96-102.



# Taijiquan Game Theory Analysis and Research of Cultural Inheritance System

Libin Yu<sup>1,\*</sup>, Qiaohui Wang<sup>2</sup>, Kunling Qin<sup>3</sup>, Qiongqiong Hu<sup>4</sup>, Qian Yang<sup>1</sup>

<sup>1</sup>Institute of Physical Education, Huanggang Normal University, Huangzhou 438000, Hubei, China

<sup>2</sup>Macaomiao Primary School, Tuanfeng, Hubei, China

<sup>3</sup>Yidu Gaobazhou Middle School, Yidu 443300, Hubei, China

<sup>4</sup>Fangxian Mengu Middle School, Shiyan 442108, Hubei, China

**Abstract:** Taijiquan contains the essence of the Chinese in five thousand, contains great Confucian, Taoist thought, it is a precious cultural heritage in our country, so it is necessary to establish inheritance of Taijiquan sport culture system. Is analyzed in this paper, by establishing the first model, the Taijiquan movement culture to consider cultural heritage protection, social influence, thought and the factors influencing the profit and so on the Taijiquan movement under the cultural inheritance of folk, the school pavilion and their respective proportion of modern mass media, and obtained the Taijiquan sport cultural history, the modern mass media company to obtain more profits for the purpose, so need outside intervention from the government. Then according to game theory and evolutionary game analysis obtained the government problems in the Taijiquan movement of modern mass media culture inheritance and the best strategy for the modern mass media inheritance Taijiquan culture contribute to the company to deal with, and the government should actively support and supervise the modern mass media company of Taijiquan sport culture heritage.

**Key words:** Hierarchical analysis, game theory, cultural inheritance, Taijiquan exercise

## 1. INTRODUCTION

Taijiquan was originated above 3000 years ago, King Wen of Zhou Dynasty created "The Book of Changes" wrote that I had Tai Chi, and then had two ways. From which word "Tai" meant maximum, "Chi" meant furthest. Tai Chi represents a kind of philosophical thought; our ancient people thought that Tai Chi was the source of all things generation, and starting point of changes. And Taijiquan as legacy left by China's ancestors, it always adheres to principles of regulating of body, heart and breathing, and highlights practice's should harmonize Yin and Yang, subdue activity with serenity, alternate activity with serenity, simultaneous train body and heart, make integration of body and spirit [1]. Since new China was founded, Taijiquan was enrolled in gymnastics event, and listed into heritage application lists since 2008. Taijiquan not only is a kind of event of national people body building, but also contains lots of great thoughts, it extracts Confucian and Taoist thoughts, and thinks that individual not only

should keep physical health, but also should cultivate character, and highlights that people should treat each other sincerely and live in harmony [2, 3]. So inherit Taijiquan type event culture is very necessary to Chinese construction of a socialist harmonious society, and then the paper makes analysis and studies on Taijiquan type movement cultural inheritance issues.

## 2. MODEL ESTABLISHMENTS

### 2.1 Hierarchical structure establishment

In order to analyze China's Taijiquan movement cultural inheritance pattern, firstly it should find out Taijiquan movement cultural inheritance main paths, and look for most influential unit, therefore the paper firstly makes quantization on Taijiquan movement cultural inheritance based on analytic hierarchy process. Establish target layer, criterion layer and scheme layer relations.

Target layer: Inheritance of Taijiquan culture.

Criterion layer: scheme influence factors,  $E_1$  is cultural protection,  $E_2$  is social influence,  $E_3$  is thinking of the inheritance,  $E_4$  is yield returns.

### 2.2 Consistency test

Use consistency test formula as:  $CI = \frac{\lambda_{\max} - n}{n - 1}$ .

Among them,  $\lambda_{\max}$  is maximum feature root value of comparison matrix,  $n$  is comparison matrix order. It is clear that judgment matrix and  $CI$  value are in inverse proportion.

$$CY^{(0)} = \begin{Bmatrix} 1 & 1/5 & 4 & 3 \\ 5 & 1 & 6 & 6 \\ 1/4 & 1/6 & 1 & 1 \\ 1/3 & 1/6 & 1 & 1 \end{Bmatrix} \begin{Bmatrix} 0.5322 \\ 0.1003 \\ 0.3145 \\ 0.0530 \end{Bmatrix} = \begin{Bmatrix} 3.634 \\ 0.456 \\ 2.768 \\ 0.343 \end{Bmatrix}$$

$$\lambda_{\max}^{(0)} = \frac{1}{4} \left( \frac{3.634}{0.5322} + \frac{0.456}{0.1003} + \frac{2.768}{0.3145} + \frac{0.343}{0.0530} \right) = 4.12$$

$$; u^{(0)} = \begin{Bmatrix} 0.413 \\ 0.103 \\ 0.332 \\ 0.152 \end{Bmatrix}$$

Judgment  
is

matrix

$$C_1 = \begin{Bmatrix} 1 & 1 & 1/3 \\ 1 & 1 & 1/3 \\ 3 & 3 & 1 \end{Bmatrix}, C_2 = \begin{Bmatrix} 1 & 5 & 5 \\ 1/5 & 1 & 5 \\ 1/5 & 1/5 & 1 \end{Bmatrix}, C_3 = \begin{Bmatrix} 1 & 5 & 8 \\ 1/5 & 1 & 5 \\ 1/8 & 1/5 & 1 \end{Bmatrix} \quad \lambda_{\max}^{(3)} = 3.31, y_{(1)}^{(3)} = \begin{Bmatrix} 0.650 \\ 0.212 \\ 0.137 \end{Bmatrix}$$

Corresponding maximum feature value and feature vector are in order as:

$$\lambda_{\max}^{(1)} = 3.56, y_{(1)}^{(1)} = \begin{Bmatrix} 0.244 \\ 0.244 \\ 0.512 \end{Bmatrix};$$

$$\lambda_{\max}^{(2)} = 3.29, y_{(1)}^{(2)} = \begin{Bmatrix} 0.656 \\ 0.255 \\ 0.087 \end{Bmatrix}$$

$$\lambda_{\max}^{(4)} = 3.12, y_{(1)}^{(4)} = \begin{Bmatrix} 0.604 \\ 0.248 \\ 0.148 \end{Bmatrix}$$

According to  $CI = \frac{\lambda_{\max} - n}{n-1}$ , it gets  $RI$  value that can refer to Tab. 1.

Table 1. RI value

| n  | 1 | 2 | 3    | 4    | 5    | 6    | 7    | 8    | 9    | 10   | 11   |
|----|---|---|------|------|------|------|------|------|------|------|------|
| RI | 0 | 0 | 0.58 | 0.90 | 1.12 | 1.24 | 1.32 | 1.41 | 1.45 | 1.49 | 1.51 |

For judgment matrix  $C$ ,  $\lambda_{\max}^{(0)} = 5.120, RI = 1.12$

$$RI = \frac{5.120 - 4}{4 - 1} = 0.038; CR = \frac{CI}{RI} = \frac{0.038}{1.12} = 0.034 < 0.1$$

It represents  $C$  inconsistency extent is within permissible range, now it can use  $C$  feature vector to replace weight vector. Similarly, to judgment matrix  $C_1, C_2, C_3, C_4$ , utilize above principle, all pass consistency test. Calculation structure is as following:

$$y^{(1)} = (y_1^{(1)}, y_2^{(1)}, y_3^{(1)}, y_4^{(1)}) = \begin{Bmatrix} 0.624 & 0.185 & 0.252 & 0.575 \\ 0.234 & 0.240 & 0.089 & 0.286 \\ 0.136 & 0.575 & 0.66 & 0.139 \end{Bmatrix}$$

$$y = y^{(1)} y^{(0)} = \begin{Bmatrix} 0.252 & 0.575 & 0.624 & 0.185 \\ 0.089 & 0.286 & 0.240 & 0.240 \\ 0.66 & 0.139 & 0.136 & 0.575 \end{Bmatrix} \begin{Bmatrix} 0.577 \\ 0.066 \\ 0.124 \\ 0.253 \end{Bmatrix} = \begin{Bmatrix} 0.432 \\ 0.366 \\ 0.202 \end{Bmatrix}$$

## 2.4 Taijiquan movement cultural inheritance system game analysis

By above analytic hierarchy process, it is clear that in the aspect of Taijiquan movement cultural inheritance, it should take folk heritage and the school gym inheritance as subjects. And modern mass media transmission is mostly with purposes of profit-making. So in order to improve such kind of inheritance system, it needs government support and monitoring to play external force roles. In the following, according to game analysis, it can roughly regard government and mass media as game main parts, its implemented strategies are two types, government strategy is support and nonsupport. Set that in case government supports inheritance and mass media do not inherit, government profit is  $U_1$ ,

media profit is 0; on the contrary media makes transmission while government don't play supporting roles, enterprises profit is  $U_1'$ , government profit is  $U_2$ , causes is though government don't play supporting role, mass media transmission is beneficial to harmonious socialist society construction. When both government and mass media are with positive attitudes, government earnings is  $U$ , mass media is  $U'$ ; Tab.2 is government and modern mass media transmission earnings matrix.

| classification |             | Modern mass media |               |
|----------------|-------------|-------------------|---------------|
|                |             | Inherit           | Don't inherit |
| Government     | Support     | $U, U'$           | $U_1, 0$      |
|                | Non-support | $U_2, U_1'$       | 0,0           |

Among them,  $U > U_1 > U_2$ , but size of  $U', U_1'$  cannot define, therefore the paper will adopt evolution game analysis to analyze government and modern mass media practical status of Taijiquan movement cultural inheritance, and make respectively strategies adjustment.

## 2.5 Taijiquan movement cultural inheritance evolution game analysis

Due to government and modern mass media strategies positive and non-positive selection in Taijiquan movement cultural inheritance is independent and random, and can carry on repeated games. Therefore, set government supporting mass media transmission probability as  $p$ , non-support probability as  $1-p$ ; mass media inheritance probability is  $q$ , probability that don't inherit is  $1-q$ . According to Malthusian theorem, it is clear

that government strategies support times selection growth rate should be differences between  $\frac{\dot{p}}{p}$

fitness  $E_w H\{f, 1-q\}^T$  and average

fitness  $\{p, 1-p\} H\{q, 1-q\}^T \cdot E_w = [1, 0]$ , when

government supporting probability is 1, its earnings matrix is  $H = \begin{bmatrix} U & U_1 \\ U_2 & 0 \end{bmatrix}$

Simplify  $\dot{p} = p(1-p)\{1, -1\} H\{q, 1-q\}^T$  and

get  $\dot{p} = p(1-p)[(U - U_1 - U_2)q + U_1]$

Similarly, mass media strategies inheritance times' selection growth rate should be differences between

$\frac{\dot{q}}{q}$  fitness  $E_J H\{q, 1-q\}^T$  and average

fitness  $\{q, 1-q\} M\{p, 1-p\}^T \cdot E_J = [0, 1]$ , When mass

media inheritance probability is 1, its earnings matrix is  $M = \begin{bmatrix} U' & 0 \\ U_1' & 0 \end{bmatrix}$

Simplify  $\dot{q} = q(1-q)\{-1, 1\} M\{t, 1-q\}^T$  and

get  $\dot{q} = q(1-q)[U_1' + (U' - U_1')p]$

Therefore when  $\dot{p} = 0, \dot{q} = 0$ ,  $(0, 0)$ ,  $(0, 1)$ ,  $(1, 0)$ ,  $(1, 1)$  are balance points of Taijiquan movement cultural inheritance. According to matrix stability, analyze these balance points partial stability.

By above figure, it is clear that government and modern mass media to Taijiquan movement cultural inheritance optimal strategy is modern mass media

companies should make contributions to inherit Taijiquan movement culture, and government should positive support and monitor modern mass media companies to inherit Taijiquan movement cultural.

### 3. CONCLUSION

By firstly establishing analytic hierarchy process model, the paper solves Taijiquan movement cultural inheritance folk, when inherit Taijiquan movement culture in case considering cultural protection, social influence, thinking of inheritance and yield returns as well as other influence factors, and gets that in Taijiquan movement cultural inheritance aspect, modern mass media companies are mostly with purposes of getting profits, therefore it needs government external force interference. After that, according to game analysis and evolution game analysis, it solves that in government and modern mass media Taijiquan movement cultural inheritance problems, the best strategy is that modern mass media companies should make contributions to inherit Taijiquan movement culture, and government should positive support and monitor modern mass media companies inheritance on Taijiquan movement culture.

### REFERENCES

- [1]Chen Xue-Bin, Game learning theory[M], Shanghai: shanghai University of finance and economics press, 1999:65-76.
- [2]Xiao Tiao-Jun, Game theory and its application [M], Shanghai Sanlian bookstore, 2004:457-460.
- [3]Sun Qing-Wen, Lu Liu, Yan Guang-Le, Che Hong-An, Evolution game equilibrium stable analysis under incomplete information condition, Journal of systems engineering theory and practice, 2003,23(7):11-16.

# The Best Offensive and Defensive Football Penalty Model based on Biomechanics

Renzhuo Zhang\*

Department of Physical Education, School of Science, Jiangxi University of Science and Technology, Ganzhou 341000, Jiangxi, China

**Abstract:** In football, maximize the goal and catching efficiency is the goal of the teams in technology. In this paper, the geometric model, the human body physiology such as knowledge, from two aspects of kick and the goalkeeper. After research found a penalty shootout model is mainly a function of time and space of the research. Shooting athlete should take what initial speed and Angle, makes football scored a goal in a relatively short time and the goalkeeper can not pick up. And use the Matlab tool to simulate, as far as possible so that the model is reasonable.

**Key words:** P human physiology, geometric model, probability model

## 1. INTRODUCTION

Brazil World Cup in 2014 will soon be held, though presently Chinese football sports level is barely satisfactory, as first world sports, football still attracts attentions of hundreds million football fans. And penalty kick in game is even the exciting and breathtaking moment. Goalkeeper can save by left and right shifting, opening arms, diving and other motions in the goal line, whether penalty kick can be saved or not is related to goalkeeper technical level, height and reaction speed so on [1-3].

In case without considering psychological warfare and other human factors influences and on the premise of adhering to game rules, the paper established mathematical model to illustrate how to

effective save penalty kicks and shoot into penalty kick respectively from the perspectives of goalkeepers and penalty kickers [4].

## 2. Goalkeeper catching model

To make reaction and catch ball in short time, then goalkeeper must study in some special regions. It finds as Figure 1 shows, football incidence of A(C) and E(R) regions are relative special that need to be focus on researching [5].

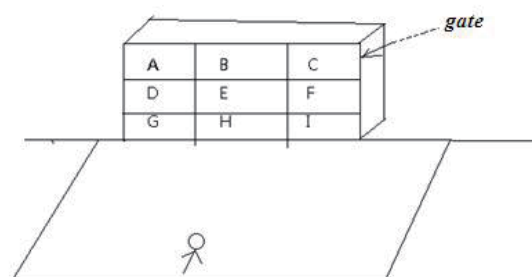


Figure 1: Shooting schematic diagram

By above analysis, make weighted average number of nine regions. By analysis of goalkeeper jumping time and minimum initial speed, it gets following numerical values as Table 1.

Set jumping time difficulty coefficient proportion is 50%, and jumping initial speed difficulty coefficient proportion is 50%.

Table 1: Identification table of goalkeeper defense difficulty coefficient in each region

| Region | Jumping time | Jumping time<br>$t(i)*10*50\%$ | Takeoff<br>minimum<br>speed | Jumping<br>minimum<br>initial speed<br>$v(i)*50\%$ | Defense<br>difficulty<br>coefficient |
|--------|--------------|--------------------------------|-----------------------------|--|--------------------------------------|
| A      | 0.306        | 1.53                           | 3.93                        | 1.965  | 3.495                                |
| B      | 0.167        | 0.835                          | 1.67                        | 0.835  | 1.67                                 |
| C      | 0.306        | 1.53                           | 3.93                        | 1.965  | 3.495                                |
| D      | 0            | 0                              | 0                           | 0  | 0                                    |
| E      | 0            | 0                              | 0                           | 0  | 0                                    |
| F      | 0            | 0                              | 0                           | 0  | 0                                    |
| G      | 0.79         | 3.95                           | 3.6992                      | 1.8496   | 5.7996                               |
| H      | 0            | 0                              | 0                           | 0  | 0                                    |
| I      | 0.79         | 3.95                           | 3.6992                      | 1.8496   | 5.7996                               |

By above data analysis, it gets that goalkeeper has larger defense difficulties in G, I regions, so ,

shooters only need to attack G,I regions then relative goal odds will increase.

### 3. ATHLETE SHOOTING MODEL

By above analysis of goalkeeper, it is known that shooters get into football into the goal in the shortest time, the problem changes into what initial speed and initial angle that football are needed so can get into the goal. We similarly use above regional analysis method to analyze and summarize on each region this time. But it cannot make equivalent of left and right regions as above statement this time, because according to human shooting habits analysis, it is known that frequency that football flies into left side(A,D,G region)is larger than frequency it flies into (C,F,I region). The football left region goal speed is larger than right regional goal speed. Due to suffer air resistance influence and gravity accelerated speed influence.

Known that air resistance formula is:  $f = \frac{1}{2} C \rho S V^2$  (c

is air resistance coefficient;  $\rho$  is air density;  $s$  is object windward area ;  $v$  is object and air relative motion speed ). By physical analysis hypothesis and Newton's second law:  $F = ma$  then it can roughly calculate football reduced speed due to resistance in every second is nearly:  $\therefore \Delta a = \frac{\Delta v}{\Delta t} = \frac{\Delta f}{\Delta t}$

$\Delta f = \frac{1}{2} c \rho s \Delta v^2$  , While:  $\therefore \frac{dv(t)}{dt} = \frac{c \rho s v^2(t)}{2m}$  , By

differential equation, it solves:  $v(t) = \frac{v_{2i}}{1 - ktv_{2i}}$  , In

above formula, time  $t$  shouldn't surpass  $t \leq \frac{1}{kv_{2i}}$  .

(1) Football shot into A and C region model

①As Figure 2 shows, height that football shot into A region is nearly:

$$H_A = a - \frac{d}{2} = 2.34m$$

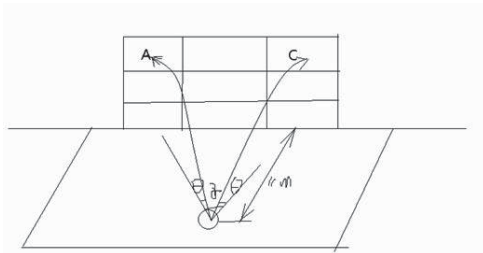


Figure 2: Football shot into A and C region schematic diagram

When football shot into A region at minimum initial speed  $v_{0a \min}$  ,

Then it can define that arrive at A region is the high point that vertical ending speed is 0:

$$H_A = \int_0^t \frac{V_0}{1 - ktv_0} dt + \int_0^t g t dt$$

It gets vertical initial speed  $V_0$  and time  $t$  relations:

$$H_A = \frac{1}{k} \ln(1 - kv_0^2) + \frac{1}{2} g t^2$$

And because that horizontal direction horizontal initial speed and time  $t$  relation

$$\text{is: } v(t) = \frac{v_{21a}}{1 - ktv_{21a}}$$

Then football flying initial speed  $v$  is:  $v^2 = v_{0a}^2 + v_{21a}^2$

Horizontal displacement that football arrives at A

$$\text{region is: } L = \frac{b}{2} - \frac{d}{2}$$

Then football horizontal displacement trajectory  $(x, y)$  and time  $t$  as well as horizontal speed  $v$  functional relationship:  $F(x, y, t, v)$

Then trajectory equation that football arrives at A region is:  $S(Z_0 = HA, F)$  ,  $S(x, y, z, t, v)$

However, shooters should send ball into A region before goalkeeper arriving at A region, then time is limited in  $t_{1 \max} = 0.306s$  , therefore it can solve above formula initial speed  $v_{0a} : V_{0a} \approx 38.378m/s$

Then angle  $\theta = 11.487^\circ$  ,  $\theta_{1a} = 12.5, \theta_{2a} = 18.4$

② When football shot into C region, due to human self conditions factors, assume his service initial speed is 1.1 times A region so that to be A region service speed, difficulty coefficient is one more than A region.

(2) Football shot into G and I region model

As Figure 3 shows, distance that football shot into

$$\text{G region is } L_1 : L_1^2 = \left( \frac{b}{2} - \frac{d}{2} \right)^2 + 11^2$$

$$L_1 \approx 11.56m$$

Similarly, when goalkeeper arrives at G region, time  $t_{20} = 0.79s$

Now football minimum initial speed  $v_{0g}$  is

$$dL = v(t) dt$$

nearly:

$$L = \int_0^{t_{20}} v(t) dt = \int_0^{t_{20}} \frac{V_0}{1 - ktv_0} dt = L_1$$

$$v_{0g} \approx 14.7m/s$$

$$\theta_{1a} = 0, \theta_{2a} = 18.4^\circ$$



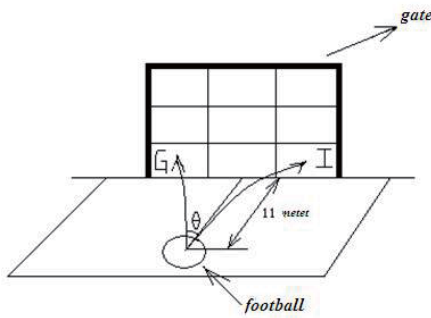


Figure 3: Football shot into G and I region schematic diagram

③ When football shot into I region, shooter difficulty coefficient is 1.01 times G region.

Horizontal direction area horizontal speed

$$v_{\text{Horizontal } B}(t) = \frac{v_{\text{Horizontal initial } B}}{1 - kt v_{\text{Horizontal initial } B}}$$

$$v_{\text{Horizontal}} : \frac{ds}{dt} = v_{\text{Horizontal } B}(t)$$

$$s = \int_0^{t_{33}} \frac{v_{\text{Horizontal initial } B}}{1 - kt v_{\text{Horizontal initial } B}} dt = l = 11$$

It solves  $v_{\text{Horizontal initial } B} = 65.89 \text{ m/s}$

Then football shot into B region required initial speed

$$v_{OB} \text{ is: } v_{oB} = \sqrt{v_{\text{Horizontal initial } B}^2 + V_{\text{vertical}}^2} \approx 67.67 \text{ m/s}$$

Initial angle  $\theta_{1a} = 12.5, \theta_{2a} = 0$ .

To sum up, shooters have lowest attacking difficulties in G, I regions, while have highest difficulty coefficient in H, E regions that is up to goalkeeper defense ability.

#### 4. CONCLUSION

The paper uses models tables as well as data to analyze defense and attack problems, therefore gets following conclusions: Make comprehensive analysis, region G and I are fear regions of goalkeeper. Because the two regions are of weakest defense while relative powerful attacking. Therefore, shooters should major in attacking in G and I regions; For region D E F H these regions that are goalkeeper strongest defense ability regions, in theoretical cases, shooters should try to avoid attacking these regions. For region A and B, both are regions that goalkeeper and shooters are well-matched in strength, it compares individual technological advantages and self agility.

#### REFERENCES

- [1]ZHANG Qiu-fen,SU Jing.Analysis on Medal Distribution and Medallist's Playing Type of Table Tennis in the Olympic Games. China Sport Science and Technology,2005,41(5):90-92.
- [2]YANG Hua,GUAN Zhi-ming.Simulation of Ping-pong Trajectory Based on ODE. Computer Simulation,2011,28(9),230-233.
- [3]SUN Zai,YU Guang-xin,GUO Mei,ZHU Li-li,YANG Jun,HE Zheng-bing.Aerodynamic Principles of Table Tennis Loop and Numerical Analysis of Its Flying Route. China Sport Science,2008,28(4):69-71.
- [4]GAO Ying.The Study of Loop Track under Dynamic Mathematical Model. Journal of Hebei Institute of Physical Education,2013(4):79-82.
- [5]ZHONG Yu-jing,WANG Da-zhong,WANG Juan.Philosophy in Table Tennis Development. Journal of Beijing Sport University,2008,31(4):456-459.

# Weighted *Hardy–Littlewood* Integral Inequality for the Result of $p$ -Harmonic Type Equation

Xiaoli Liu<sup>1</sup>\*, Xiujuan Xu<sup>2</sup>

<sup>1</sup> Jitang college of North China University of science and technology, Hebei Tangshan ,06300, China

<sup>2</sup> college science of North China University of science and technology, Hebei Tangshan ,06300, China

**Abstract:** The article proves a weighted *Hardy–Littlewood* integral estimates for conjugate  $P$ -harmonic type tensors by using the generalized *Hölder* inequality and the properties of the weight. Using the result of  $A$ -harmonic equation.  
**Keywords:**  $p$ -harmonic type equation; the generalized *Hölder* inequality; reverse *Hölder* integral inequality; *Hardy–Littlewood* integral inequality;  $A_r$ -weighted

## 1. INTRODUCTION

The article consider the following  $p$ -harmonic type system, we say the Hodge system  $A(x, a + du) = b + d^*v$

where  $a \in L^p(\Omega, \wedge^l)$ ,  $b \in L^q(\Omega, \wedge^l)$ , is a  $p$ -harmonic type system, if  $A$  is a mapping from  $\Omega \times \wedge^l$  to  $\wedge^l$  satisfying

(1)  $x \rightarrow A(x, \xi)$  is measurable in  $\Omega$ , for every  $\xi \in \wedge^l$ ;

(2)  $x \rightarrow A(x, \xi)$  is continuous in  $\wedge^l$ , for almost every  $x \in \Omega$ ;

(3)  $A(x, t\xi) = t^{p-1}A(x, \xi)$  for every  $t \geq 0$ ;

(4)  $K \langle A(x, \xi) - A(x, \varsigma), \xi - \varsigma \rangle \geq |\xi - \varsigma|^2 (|\xi| + |\varsigma|)^{p-2}$ ;

(5)  $|A(x, \xi) - A(x, \varsigma)| \leq K |\xi - \varsigma| (|\xi| + |\varsigma|)^{p-2}$

for almost every  $x \in \Omega$ , and all  $\xi, \varsigma \in \wedge^l$ , where  $K \geq 1$  is a constant. It should be noted that  $A(*, x): \Omega \times \wedge^l \rightarrow \wedge^l$  is invertible and its inverse denoted by  $A^{-1}$ , satisfies similar conditions as  $A$  but with *Hölder* conjugate exponent  $q$  in place of  $p$ .

If the equation (2.1) is a  $p$ -harmonic type system, then we say the equation

$$d^*A(x, a + du) = d^*b \quad (1)$$

is a  $p$ -harmonic type equation.

If we let  $a = 0, b = 0$ , then (1.1) becomes

$$d^*A(x, du) = 0 \quad (2)$$

It is the conjugate  $A$ -harmonic equation.

Recently, amount of work about the  $A$ -harmonic equation for the differential forms has been done. In 1999, C.A. Noldé [1, 2] proved *Hardy–Littlewood* integral inequality for  $A$ -harmonic type tensors in [2]. In [3], S. Ding proved local result weighted *Hardy–Littlewood* integral inequality and global weighted *Hardy–Littlewood* integral inequality in  $\delta$ -John domains. In 2010, Bao Genjun proved *Hardy–Littlewood* integral inequality for  $p$ -harmonic type tensors. In 2012, Xu Xiujuan proved *Hardy–Littlewood* integral inequality for  $p$ -harmonic type tensors in  $\delta$ -John domains. In this paper, we will prove local result weighted *Hardy–Littlewood* integral inequality for  $p$ -harmonic type tensors and global weighted *Hardy–Littlewood* integral inequality in  $\delta$ -John domains.

## 2. EXPERIMENTAL LEMMA AND PRELIMINARY KNOWLEDGE

**Definition 2.1** [2] We call  $\Omega$ , a proper subdomain of  $R^n$ , a  $\delta$ -John domain,  $\delta > 0$ , if there exists a point  $x_0 \in \Omega$  which can be joined with any other point  $x \in \Omega$  by a continuous curve  $\gamma \subset \Omega$ , so that

$$d(\xi, \partial\Omega) \geq \delta |x - \xi|$$

for each  $\xi \in \gamma$ . Here  $d(\xi, \partial\Omega)$  is the Euclidean distance between  $\xi$  and  $\partial\Omega$ .

**Definition 2.2** [3-5] A weight  $\omega(x) > 0$  satisfies the  $A_r(\Omega)$  condition in a subset  $\Omega \subset R^n$ , where  $r > 1$ , and write  $\omega \in A_r(\Omega)$ , when

$$\sup_{B \subset \Omega} \left( \frac{1}{|B|} \int_B \omega dx \right) \left( \frac{1}{|B|} \int_B \left( \frac{1}{\omega} \right)^{1/(r-1)} dx \right)^{r-1} < \infty$$

where the supreme is over all balls  $B \subset R^n$ .

**Lemma 2.1** [6] If  $\omega \in A_r$ ,  $r > 1$ , then there exist constants  $\beta > 1$  and  $C$  independent of  $\omega$ , such that

$$\|\omega\|_{\beta, Q} \leq C |Q|^{(1-\beta)/\beta} \|\omega\|_{1, Q}$$

for all cubes  $Q \subset R^n$ .

**Lemma 2.2** [3] (the generalized *Hölder* inequality)

Let  $0 < \alpha, \beta < \infty$  and  $s^{-1} = \alpha^{-1} + \beta^{-1}$ . If  $f$  and  $g$  are measurable functions on  $R^n$ , for  $\Omega \subset R^n$ , then

$$\|fg\|_{s,\Omega} \leq \|f\|_{\alpha,\Omega} \cdot \|g\|_{\beta,\Omega}$$

**Lemma 2.3**[5,6] Let  $(u, v)$  be a pair of a solution to the  $p$ -harmonic type tensors with  $(a, b) \in L^p(\Omega, \wedge^l) \times L^q(\Omega, \wedge^l)$  and  $q$  be the conjugate exponent of  $p$ . if  $\sigma > 1$  and  $0 < s, t < \infty$ , then there exists a constant  $C$ , independent of  $a, b, u, v$  and  $Q$

$$\|u - u_Q\|_{s,Q} \leq C|Q|^\alpha \left( \|v - c\|_{t,\sigma Q}^{q/p} + \|a\|_{p,\sigma Q} + \|b\|_{q,\sigma Q}^{q/p} + \|b\|_{t,\sigma Q}^{q/p} \right) \quad (2.1)$$

for cubes with  $Q \subset \sigma Q \subset \Omega$ , where  $c$  is any co-closed form,

$$\alpha = \max \left( \frac{1}{s} - \frac{1}{p} + \frac{1}{n}, \frac{1}{s} + \frac{1}{n} - \frac{q}{tp} - \frac{q}{np} \right) \text{ for } |Q| \geq 1$$

$$\alpha = \min \left( \frac{1}{s} - \frac{1}{p} + \frac{1}{n}, \frac{1}{s} + \frac{1}{n} - \frac{q}{tp} - \frac{q}{np} \right) \text{ for the others.}$$

**Lemma 2.4**[4] If  $v$  is a collection of cubes in  $R^n$  and  $C_Q$  are non-negative numbers associated with the cubes  $Q \in v$  and  $\omega \in A_r$ ,  $d\mu(x) = \omega(x) dx$ , then  $1 \leq p < \infty$  and  $N \geq 1$ , we have

$$\left( \int_{R^n} \left( \sum_{Q \in v} C_Q \cdot \chi_{NQ} \right)^p d\mu(x) \right)^{1/p} \leq B_p \left( \int_{R^n} \left( \sum_{Q \in v} C_Q \cdot \chi_Q \right)^p d\mu(x) \right)^{1/p}$$

where  $B_p$  is independent of the collection  $v$  and the numbers  $C_Q$ .

### 3. THEOREM AND ITS PROOF

**Theorem 3.1** Let  $(u, v)$  be a pair of a solution to the  $p$ -harmonic type system with  $(a, b) \in L^p(\Omega, \wedge^l) \times L^q(\Omega, \wedge^l)$  and  $q$  be the conjugate exponent of  $p$ . if  $\sigma > 1$  and  $0 < s, t < \infty$ , then there exists a constant  $C$ , independent of  $a, b, u, v$  and  $Q$

$$\|u - u_Q\|_{s,Q,\omega} \leq C|Q|^\beta \left( \|v - c\|_{\frac{qt}{p},\sigma Q,\omega^{\frac{t}{s}}}^{q/p} + \|a\|_{t,\sigma Q,\omega^{\frac{t}{s}}} + \|b\|_{\frac{qt}{p},\sigma Q,\omega^{\frac{t}{s}}}^{q/p} \right)$$

for cubes with  $Q \subset \sigma Q \subset \Omega$ , where  $c$  is any co-closed form,  $s > p(r-1)$ ,  $t = \frac{sp}{s-p(r-1)}$ ,

$$\beta = \frac{r}{s} - \frac{1}{p} + \frac{1}{n},$$

for  $|Q| \geq 1$ ;  $\beta = \frac{r}{s} - \frac{1}{p} - \frac{q}{np} + \frac{1}{n}$  for the others.

Proof. Since  $\omega \in A_r$  for some  $r > 1$ , from Lemma 2.2, there exists a constant

$$\|\omega\|_{\alpha,\sigma Q} \leq C_1|Q|^{(1-\alpha)/\alpha} \|\omega\|_{1,\sigma Q} \quad (3.1)$$

for all cubes  $Q \subset R^n$ .

Since  $\frac{1}{s} = \frac{1}{\alpha s} + \frac{\alpha-1}{\alpha s}$ , by Lemma 2.2, then

$$\|u - u_Q\|_{s,Q,\omega} \leq \|\omega\|_{\alpha,Q}^{1/s} \cdot \|u - u_Q\|_{\alpha s/(\alpha-1),Q} \quad (3.2)$$

by Lemma 2.3, then there exists a constant  $C_2$ , independent of  $a, b, u, v$  and  $Q$ , for any  $0 < s, t' < \infty$ , we have

$$\|u - u_Q\|_{\alpha s/(\alpha-1),Q} \leq C_2|Q|^{\alpha'} \left( \|v - c\|_{t',\sigma Q}^{q/p} + \|a\|_{p,\sigma Q} + \|b\|_{q,\sigma Q}^{q/p} + \|b\|_{t',\sigma Q}^{q/p} \right) \quad (3.3)$$

where

$$\alpha' = \max \left( \frac{\alpha-1}{\alpha s} - \frac{1}{p} + \frac{1}{n}, \frac{\alpha-1}{\alpha s} + \frac{1}{n} - \frac{q}{t'p} - \frac{q}{np} \right) \text{ for } |Q| \geq 1$$

$$\alpha' = \min \left( \frac{\alpha-1}{\alpha s} - \frac{1}{p} + \frac{1}{n}, \frac{\alpha-1}{\alpha s} + \frac{1}{n} - \frac{q}{t'p} - \frac{q}{np} \right)$$

for the others.

Combing (3.2) and (3.3), we obtains

$$\|u - u_Q\|_{s,Q,\omega} \leq C_2|Q|^{\alpha'} \|\omega\|_{\alpha,Q}^{1/s} \left( \|v - c\|_{t',\sigma Q}^{q/p} + \|a\|_{p,\sigma Q} + \|b\|_{q,\sigma Q}^{q/p} + \|b\|_{t',\sigma Q}^{q/p} \right) \quad (3.4)$$

Now, we choose  $t = \frac{sp}{s-p(r-1)}$ , since

$$\frac{1}{p} = \frac{1}{t} + \frac{r-1}{s}, \text{ by Lemma 2.2, then}$$

$$\begin{aligned} \|a\|_{p,\sigma Q} &= \left( \int_{\sigma Q} |a|^p dx \right)^{1/p} = \left( \int_{\sigma Q} \left( |a| \omega^{\frac{1}{s}} \left( \frac{1}{\omega} \right)^{\frac{1}{s}} \right)^p dx \right)^{1/p} \\ &\leq \left( \int_{\sigma Q} \left( |a| \omega^{\frac{1}{s}} \right)^t dx \right)^{1/t} \left( \int_{\sigma Q} \left( \frac{1}{\omega} \right)^{\frac{1}{s} \frac{s}{r-1}} dx \right)^{\frac{r-1}{s}} \\ &\leq \|a\|_{t,\sigma Q,\omega^{\frac{t}{s}}} \left( \int_{\sigma Q} \left( \frac{1}{\omega} \right)^{\frac{1}{r-1}} dx \right)^{\frac{r-1}{s}} \end{aligned} \quad (3)$$

since  $\frac{1}{q} = \frac{s-p(r-1)}{sq} + \frac{p(r-1)}{sq}$ , by lemma 2.2,

then

$$\begin{aligned} \|b\|_{q,\sigma Q}^{q/p} &= \left( \int_{\sigma Q} |b|^q dx \right)^{\frac{1}{q} \frac{q}{p}} = \left( \int_{\sigma Q} \left( |b| \omega^{\frac{p}{sq}} \left( \frac{1}{\omega} \right)^{\frac{p}{sq}} \right)^q dx \right)^{\frac{1}{q} \frac{q}{p}} \\ &\leq \left( \int_{\sigma Q} \left( |b| \omega^{\frac{p}{sq}} \right)^{\frac{sq}{s-p(r-1)}} dx \right)^{\frac{sq}{s-p(r-1)} \frac{q}{p}} \left( \int_{\sigma Q} \left( \frac{1}{\omega} \right)^{\frac{1}{r-1}} dx \right)^{\frac{r-1}{s}} \\ &\leq \|b\|_{\frac{sq}{s-p(r-1)},\sigma Q,\omega^{\frac{t}{s}}}^{\frac{q}{p}} \left( \int_{\sigma Q} \left( \frac{1}{\omega} \right)^{\frac{1}{r-1}} dx \right)^{\frac{r-1}{s}} \end{aligned} \quad (6)$$

we choose  $t' = \frac{sq t}{sp + pt(r-1)}$ , since

$\frac{1}{t'} = \frac{p}{qt} + \frac{p(r-1)}{sq}$ , then

$$\|b\|_{t',\sigma Q}^{q/p} \leq \|b\|_{\frac{qt}{p},\sigma Q,\omega^{\frac{t}{s}}}^{\frac{q}{p}} \left( \int_{\sigma Q} \left( \frac{1}{\omega} \right)^{\frac{1}{r-1}} dx \right)^{\frac{r-1}{s}} \quad (7)$$

$$\|v-c\|_{t',\sigma Q}^{q/p} \leq \|v-c\|_{\frac{qt}{p},\sigma Q,\omega^{\frac{t}{s}}}^{\frac{q}{p}} \left( \int_{\sigma Q} \left( \frac{1}{\omega} \right)^{\frac{1}{r-1}} dx \right)^{\frac{r-1}{s}} \quad (8)$$

Combing (3.1),(3.4)~(3.8),we have

$$\begin{aligned} \|u-u_Q\|_{s,Q,\omega} &\leq C_2 |\mathcal{Q}|^{\alpha} \|\omega\|_{s,Q}^{\frac{1}{s}} \left( \int_{\sigma Q} \left( \frac{1}{\omega} \right)^{\frac{1}{r-1}} dx \right)^{\frac{r-1}{s}} \left( \|v-c\|_{\frac{qt}{p},\sigma Q,\omega^{\frac{t}{s}}}^{\frac{q}{p}} + \|a\|_{t,\sigma Q,\omega^{\frac{t}{s}}} + \|b\|_{\frac{qt}{p},\sigma Q,\omega^{\frac{t}{s}}}^{\frac{q}{p}} \right) \\ &\leq C_3 |\mathcal{Q}|^{\frac{1-\alpha}{s}} |\mathcal{Q}|^{\alpha} \|\omega\|_{s,Q}^{\frac{1}{s}} \\ &\quad \left( \int_{\sigma Q} \left( \frac{1}{\omega} \right)^{\frac{1}{r-1}} dx \right)^{\frac{r-1}{s}} \left( \|v-c\|_{\frac{qt}{p},\sigma Q,\omega^{\frac{t}{s}}}^{\frac{q}{p}} + \|a\|_{t,\sigma Q,\omega^{\frac{t}{s}}} + \|b\|_{\frac{qt}{p},\sigma Q,\omega^{\frac{t}{s}}}^{\frac{q}{p}} \right) \end{aligned} \quad (9)$$

since  $\omega \in A_r(\Omega)$ , so that

$$\begin{aligned} \left( \int_Q \omega dx \right)^{\frac{1}{s}} \left( \int_{\sigma Q} \left( \frac{1}{\omega} \right)^{\frac{1}{r-1}} dx \right)^{\frac{r-1}{s}} &\leq \\ |\sigma Q|^{\frac{r}{s}} \left( \frac{1}{|\sigma Q|} \int_{\sigma Q} \left( \frac{1}{\omega} \right)^{\frac{1}{r-1}} dx \right)^{\frac{r-1}{s}} &\leq C_4 |\sigma Q|^{\frac{r}{s}} = C_5 |\mathcal{Q}|^{\frac{r}{s}} \end{aligned} \quad (10)$$

combing(3.9),(3.10)we can obtain

$$\begin{aligned} \|u-u_Q\|_{s,Q,\omega} &\leq C |\mathcal{Q}|^{\alpha' + \frac{r-1-\alpha}{s}} \left( \|v-c\|_{\frac{qt}{p},\sigma Q,\omega^{\frac{t}{s}}}^{\frac{q}{p}} + \|a\|_{t,\sigma Q,\omega^{\frac{t}{s}}} + \|b\|_{\frac{qt}{p},\sigma Q,\omega^{\frac{t}{s}}}^{\frac{q}{p}} \right) \\ &\leq C |\mathcal{Q}|^{\beta} \left( \|v-c\|_{\frac{qt}{p},\sigma Q,\omega^{\frac{t}{s}}}^{\frac{q}{p}} + \|a\|_{t,\sigma Q,\omega^{\frac{t}{s}}} + \|b\|_{\frac{qt}{p},\sigma Q,\omega^{\frac{t}{s}}}^{\frac{q}{p}} \right) \end{aligned}$$

where  $\alpha' = \max \left( \frac{\alpha-1}{\alpha s} - \frac{1}{p} + \frac{1}{n}, \frac{\alpha-1}{\alpha s} + \frac{1}{n} - \frac{q}{t'p} - \frac{q}{np} \right)$ ,

$$= \frac{\alpha-1}{\alpha s} - \frac{1}{p} + \frac{1}{n}$$

$\beta = \alpha' + \frac{r}{s} + \frac{1-\alpha}{\alpha s} = \frac{r}{s} - \frac{1}{p} + \frac{1}{n}$ , for  $|\mathcal{Q}| \geq 1$

$\alpha' = \min \left( \frac{\alpha-1}{\alpha s} - \frac{1}{p} + \frac{1}{n}, \frac{\alpha-1}{\alpha s} + \frac{1}{n} - \frac{q}{t'p} - \frac{q}{np} \right)$ ,

$$= \frac{\alpha-1}{\alpha s} + \frac{1}{n} - \frac{q}{t'p} - \frac{q}{np}$$

$\beta = \alpha' + \frac{r}{s} + \frac{1-\alpha}{\alpha s} = \frac{r}{s} - \frac{1}{p} - \frac{q}{np} + \frac{1}{n}$  for the others.

## REFERENCES

- [1] L.D'Onofrio, T.Iwaniec. The  $P$ -harmonic transform beyond its natural domains of Definition, Indiana Univ.math.2004, 53(3):683-718.
- [2] C.A.Nolder. Hardy-Littlewood Theorems for A-harmonic Tensors, Illinois J.Math.1999, 4(43):613-632
- [3] S.Ding. Weighted Hardy-Littlewood Inequality for A-harmonic Tensors. Proc.Amer. Math. Soc.1997, 125(6):1727-1735.
- [4] T.Iwaniec, C.A.Nolder. Hardy-Littlewood Inequality for Quasiregular Map-pings in Certain Domains in  $R^n$ . Ann.Acad.Sci.Fenn.Ser.A I Math.1985,(10):267-282.
- [5] Z.Cao, G.Bao and R.Li. The Hardy-Littlewood Inequality for the Solution to P-harmonic Type System. Tamsui Oxford Journal of Mathematical Sciences, 2010, 26(2) 149-159.
- [6] J.B.Garnett Bounded Analytic Functions. Academic Press, 1970.

# The Research on Traffic Circle Signal Control

Tianlong Li <sup>1,\*</sup>, Yang Han <sup>2</sup>, Di Zhang <sup>3</sup>, Shanshan Li <sup>2</sup>

<sup>1</sup> Yisheng College, North China University of Science and Technology, Tangshan, 063000, China

<sup>2</sup> College of Science, North China University of Science and Technology, Tangshan, 063000, China

<sup>3</sup> Mining Engineering, North China University of Science and Technology, Tangshan, 063000, China

**Abstract:** This paper builds up and solves a flow balance model whose target is to increase the traffic capacity of the traffic circle. Firstly, only when the flowing out vehicles are more than the flowing in vehicles, can the flow amount in the loop decreases and the traffic capacity increases. So the model firstly solves the maximum amount of the vehicles in the loop when the amount increases, and then makes the amount of the flowing out vehicles reach the maximum by the signals control the flowing in vehicles. We confirm the signal period from the saturation which is the ratio of the actual value and the theoretical value of the traffic capacity. The model finally numerically simulates the peak time of the traffic circle, the signal period which is about 130 seconds, and the lasting time between every two signals which is 80s to 90s. Compared with the situation under which there is no signal, this model can make the traffic capacity of 5-lane traffic circle increases. By using simulation software VISSIM 3.70, any obvious delayed time and traffic jam don't happen.

**Keywords:** traffic circle, the delayed time, traffic capacity, signal control

## 1. INTRODUCTION

In order to control the traffic flow in, around and out during the peak time, this model chooses the delayed time as the evaluation standard. The aim of the model is to shorten the delayed time when the vehicle flow reaches the maximum, so in order to solve the problem this essay shows the minimum random delayed time model.

The delayed time includes random delayed time and passing time in the circle. Because the normal delayed time is comparatively fixed, we only study on how to shorten the random delayed time. Firstly we take the characters which result in the delayed time into consideration. The delayed time includes time spent in the crossing and the time spent in the circle. When vehicles running within the traffic circle, the delayed time spent in the loop is regarded as the normal delayed time. So this essay only analyzes how to shorten the random delayed time spent in the crossing.

The vehicles arrive in the crossing randomly. The total average saturation is less than 1, but during some special period of time, the saturation will be more than 1 temporarily caused by fluctuation of the arrival rate of the vehicles. In order to give sufficient estimate to the temporary supersaturation, this essay

provides minimum random delayed time model based on the steady state theory raised by F.Webster[1].

Solving process of the model is shown as follows:

- 1) To calculate the average delayed time before the vehicles entering the loop;
- 2) To calculate the additional delayed time caused by the different arrival rate of different time period, which

includes the additional delayed time caused by temporary supersaturation;

- 3) To overlap the above two parts and obtain the total random delayed time of the vehicles. The aim of the model is

to shorten the total delayed time and we study on the signal control of the entrance of the loop.

## 2. EXPERIMENTAL

### 2.1 STUDY AREA

The goal of this problem is to use a model to determine how best to control traffic flow in, around, and out of a circle. The traffic conditions of a ring island are supposed as the following:

- 1) The people's walking and the traffic of non-motor vehicles are not taking into account, and the two may be conducted in an underpass or an overhead bridge;
- 2) Any sudden traffic accident is not taken into account;
- 3) Suppose the flows at all the coming roads' entrances are even at the same time;
- 4) When a bigger flow at the traffic circle is considered, design a signal to ease the traffic pressure, with no second control signal considered.

Here the quota system is the supervising standard, which is used to show that designing signals improves traffic. So here two traffic control models are created:

- 1) The traffic ability of the ring island under the conditions of both with and without signs and the comparison. When the traffic flow is bigger, the weaving section and the crossings in the circle are biggest difficulties. So the biggest number of the vehicles flowing out is the target of the model, which shows the smooth of the traffic. Accordingly, the sign at the incoming road is decided. And designing the sign at the incoming road also can ensure the vehicles in the circle to flow out firstly and make both the flowing in and out balanced.

- 2) The vehicles' waiting time under the two conditions of both with and without signs. When the traffic flow is bigger, traffic crossing and violent traffic without signs will make the traffic disordered, which may have some vehicles wait there for too



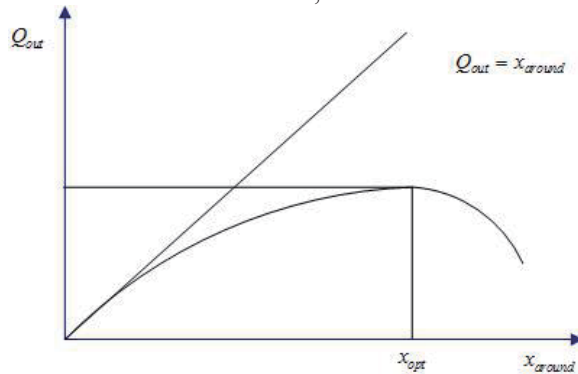
long time. So the model aims at reducing the vehicles' waiting time and the time's length is regarded as the standard to judge the model.

## 2.2 METHOD

In order to increase the passing capacity of the traffic circle in the peak time and stabilize the amount of vehicles flow-in and flow-out.

In order to consider how to design the symbol sign of the entrance, we should find out the amount of the vehicles in the loop when the flowing out vehicles amount reaches the maximum. So we can confirm the amount of the flowing in vehicles and make the signal at the entrance meet the need of the mentioned above, so that the loop can get the maximum passing capacity.

Firstly, supposing there are  $n$  crossings of the traffic circles, which are bidirectional lanes,  $x_{around}$  is the total amount of the vehicles in the loop. The probability of the vehicles arriving at each crossing is  $k_i (i = 1, 2, 3 \dots)$ ; the flowing out amount of the  $i^{th}$  crossing is  $Q_i = k_i Q_{out}$ ; and the flowing out amount of the crossing in certain period of time is  $Q_i$ . Supposing the correlation between flowing out amount of each crossing and total amount of the vehicles in the loop is  $Q_{out} = f(x_{around})$ , we fit  $f(x_{around})$  based on the survey and the function curve fit is shown as follows,



**Fig.1:** amount of the vehicles firstly increases

As shown in Fig. 1, the flowing out amount of the vehicles firstly increases and then decreases with the increase of the total amount  $x_{around}$  of the vehicles

Table 2: simulated example

| $x_{around}$ | $Q_{out}$ | $x_{around}$ | $Q_{out}$ | $x_{around}$ | $Q_{out}$ |
|--------------|-----------|--------------|-----------|--------------|-----------|
| 3            | 1         | 5            | 0         | 8            | 2         |
| 5            | 1         | 4            | 0         | 6            | 2         |
| 6            | 2         | 2            | 3         | 7            | 3         |
| 2            | 1         | 5            | 0         | 11           | 3         |
| 3            | 1         | 5            | 1         | 7            | 3         |
| 4            | 1         | 8            | 1         | 10           | 5         |
| 1            | 0         | 5            | 1         | 11           | 5         |

Fitting results is got in the table 3.

in the loop, which shows that flow amount can not increase infinitely in the loop, that is, there is a extreme value point  $(x_{opt}, \max\{Q_{out}\})$ . When

there is a  $\max\{Q_{out}\}$ , there is a maximum flow capacity, which is the target we want to get.

The aim of setting traffic lights is to confirm the permitted passing time and signal period of the lights when the flowing out amount reaches the maximum. The condition for designing symbol sign is that the flowing in amount equals to the flowing out amount in one signal period, that is,  $\sum Q_{in} = \sum Q_{out}$ . So

we firstly numerically simulate  $Q_{out} = f(x_{around})$ , and get an extreme point  $(x_{opt}, \max\{Q_{out}\})$ .

Tab.1 The statistic table of flow amount of the vehicles in the traffic circle and flowing out amount.

Table 1: firstly numerically simulate

| $Q_{out}$ | $x_{around}$ | $x_{around}^2$ | $x_{around}^3$ |
|-----------|--------------|----------------|----------------|
| a         | $x_{11}$     | $x_{21}$       | $x_{31}$       |
| b         | $x_{12}$     | $x_{22}$       | $x_{32}$       |
| c         | $x_{13}$     | $x_{23}$       | $x_{33}$       |
| d         | $x_{14}$     | $x_{24}$       | $x_{34}$       |

Note: a, b, c, d and  $x_{ij} (i = 1, 2, 3; j = 1, 2, 3, 4)$  are all statistical data.

Based on least square method fitting the above data by cubic polynomials, we get the approximate solution which is as follows,

$$Q_{out} = p_0 + p_1 x_{around} + p_2 x_{around}^2 + p_3 x_{around}^3$$

The coefficients can be obtained from the following

$$\text{equations, } \begin{pmatrix} 1 & x_{11} & x_{21} & x_{31} \\ 1 & x_{12} & x_{22} & x_{32} \\ 1 & x_{13} & x_{23} & x_{33} \\ 1 & x_{14} & x_{24} & x_{34} \end{pmatrix} \begin{pmatrix} p_0 \\ p_1 \\ p_2 \\ p_3 \end{pmatrix} = \begin{pmatrix} a \\ b \\ c \\ d \end{pmatrix}$$

When the coefficient matrix is singular, the unique solution  $p_i (i = 0, 1, 2, 3)$  is obtained.

Now let us look at a simulated example. According to the data in the table 2.

Table 3: correlation between flow amount

| coefficient       | $p_0$          | $p_1$            | $p_2$               | $p_3$                 |
|-------------------|----------------|------------------|---------------------|-----------------------|
| coefficient value | 0.8437         | 0.07398          | 0.02454             | -0.000647             |
| error range       | (-0.459,2.147) | (-0.2809,0.4288) | (0.0008404,0.04824) | (-0.00108,-0.0002138) |
| SSE               | 96.04          | R-square         | 0.7398              |                       |
| Adjusted R-square | 0.7263         | RMSE             | 1.287               |                       |

So the correlation between flow amount  $x_{around}$  and flowing out amount  $Q_{out}$  in the loop can be got as follows,

$$Q_{out} = f(x_{around}) = 0.8437 + 0.0739x_{around} + 0.02454x_i$$

The following function relation graph is obtained from the data fitting.

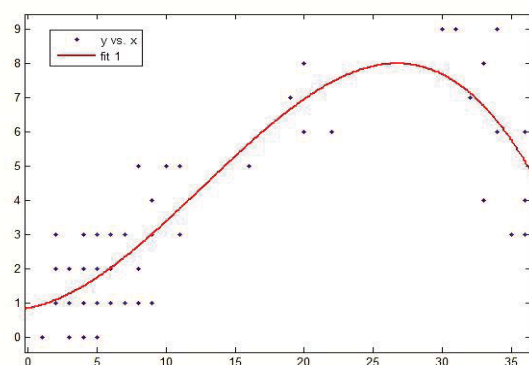


Fig. 2: flowing out increases

The unique stationary point is  $x_{opt} = 28.11$ , then

$$\max\{Q_{out}\} = f(x_{opt}) = 8.23.$$

After analyzing Fig. 2, when there is no control in traffic circle, the flowing out increases with the increases of the vehicles amount. And the increase of vehicles will result the traffic jam which is why a traffic light be needed. Thus, we can obtain that the goal of traffic control is to control the saturation remain at point  $x_{opt}$ , then the flowing out be maximum. By controlling the saturation in circle to control the practical outflow, and keep the max balance of flowing into and outflow vehicles.

To solve the saturation of traffic flow in circle, the max traffic capacity of the circle should be solved first.

### 3. RESULTS AND DISCUSSION

Suppose the flow reaches the maximum in the case of no signal control, introduce the signal, We established the optimal control model on the balance of the

Table 4: the outflow comparison of signal and no signal control

| Name of each incoming road | Outflow in signal control | Outflow in no signal control |
|----------------------------|---------------------------|------------------------------|
| A                          | 442                       | 350                          |

inflow an out flow base on the multiple linear regression. Simulate on the outflow from the fork and the length of the signal's periods, and then make the comparison with the no signal control.

As the fig. 3, when

$$c_n = 3600 \frac{qe^{-\lambda(t_c-t_m)}}{1-e^{-\lambda t_f}} (1 - \frac{2q_1q_2}{q_1+q_2} t_m) + 3600 \frac{\alpha_2 q_2 e^{-\lambda_2(t_c-t_m)}}{1-e^{-\lambda_2 t_f}}$$

. In environment of VISSIM 3.70, we made the simulation of the inflow an out flow use this model to calculate the traffic circle in a city. And made the comparison with the outflow of no signal(Table 4, Fig.3), we obtained the length of the signal periods, the green light (Table 5) and the pictures of the inflow each entrance, for the fig.4.

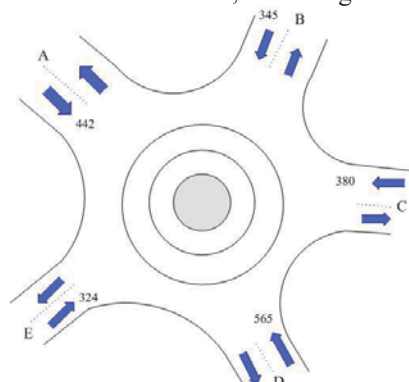


Fig.3 (a) the picture of 5-traffic circle Without Signal control

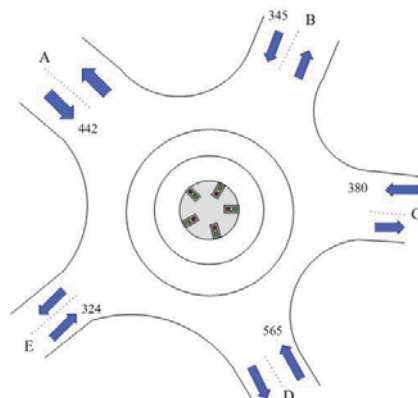


Fig.4 (b) the picture of 5-traffic circle with signal control

|   |     |     |
|---|-----|-----|
| B | 345 | 300 |
| C | 380 | 300 |
| D | 565 | 400 |
| E | 324 | 300 |

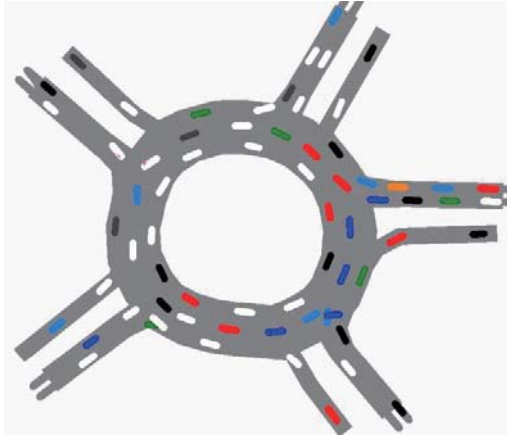


Fig.5 (a) 5-lane traffic circle simulation graph

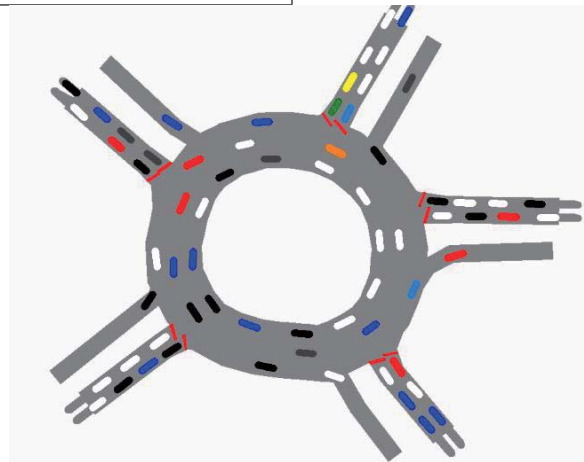


Fig. 6 (b) 5-lane traffic circle simulation graph

Table 5: the length of signal period and green light

| Name of the incoming road                       | A   | B   | C   | D   | E   |
|---|-----|-----|-----|-----|-----|
| The length of green light of each incoming road | 59  | 87  | 79  | 90  | 83  |
| Length of signal period (s)                     | 130 | 130 | 130 | 130 | 130 |

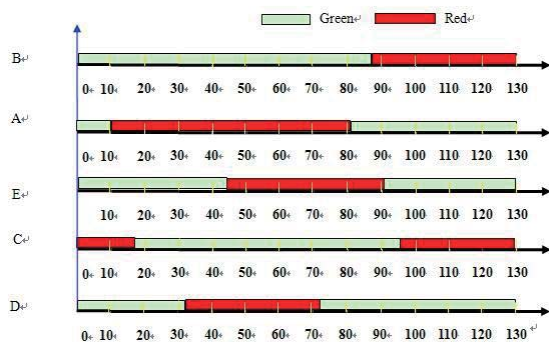


Fig.7: the picture of each signal lamp at the incoming

road

#### 4. CONCLUSIONS

In order to control the traffic flow in, around, and out of a circle much better, we presented a model for shortening the delayed time and increasing the capacity of traffic circle, and we obtain the desired effect in the numerical simulation.

#### 5. ACKNOWLEDGMENT

The authors wish to thank **Aimin Yang**. This work was supported in part by a grant from **College of Science of North China University of Science and Technology**

#### REFERENCES

- [1] <http://www.mathchina.com/cgi-bin/leobbs.cgi>

# A study of the Bath Heat Preservation Method based on the Three Dimensional Steady Heat Conduction Equation

Xu Yanghuan, Tang Yu, Wen xiaocan, Li Yan\*

North China University of Science And Technology, Mechanical Engineering Academy, Hebei Tangshan, 063000, China

**Abstract:** The paper studies on how to model a bathtub maintaining constant temperature and also analyzes the main affecting factors and the extent of the effect. thermal energy loss model of the cylinder wall is built according to three-dimensional stable heat conduction equation and the energy loss of the cylinder wall is 2.09J/s.

**Keywords:** Three-dimensional stable heat conduction; latent heat of evaporation; constant temperature; Bath heat dissipation

## 1. INTRODUCTION

With the rapid development of our country's economy, the continuous improvement of people's living standard, the concept of people for bath has developed from the initial bath to the humanized demand. Taking a hot bath to relax body and mind after returning home from a busy day has gradually become the choice of most people. Moreover, in the medical treatment[1], hot bath can be used to treat chronic arthritis, bone healing, and other chronic diseases. While, in the process of bathing, the bath water is gradually cool which makes people uncomfortable because most common bathtub does not have a secondary heating system and circulating jets device[2-10]. We are concerned about the method to slow down the cooling speed, and maintain a relatively stable temperature.

## 2. THE ENERGY LOSS MODEL OF THE CYLINDER WALL HEAT TRANSFER

This paper regarded the water in the bathtub as still with no large fluctuation and no relative flowing, and it's approximately regarded as solid. Here the loss of temperature mainly results from the heat conduction with the cylinder wall. So the bath heat dissipation of the three-dimensional heat conduction model is set under the condition of the three-dimensional temperature field.

### 2.1 Fourier law of heat conduction

According to the Fourier law of heat conduction, the heat transferred through a unit cross-sectional area in the unit time is direct proportion to the temperature gradient in vertical direction on the cross section.

$$\phi = -\lambda A \frac{\partial T}{\partial x} \quad (1)$$

In formula (1), the minus means that the direction of

heat transfer points to the direction where temperature decreases, which is necessary to meet the first law of thermodynamics. Fourier law of heat conduction is expressed as in heat conduction the heat of per unit time through a given cross section is direct proportion to the temperature gradient perpendicular to the cross section and sectional area, but the direction of heat transfer is opposite to the direction of temperature rise.

The Fourier law can be expressed as the following form in heat flux density:

$$q = -\lambda \frac{\partial T}{\partial x} \quad (2)$$

In the formula:  $\frac{\partial T}{\partial x}$  — the change rate of object temperature along the  $x$  direction.

$q$  — the transfer rate of heat flow along the  $x$  direction.

Strictly speaking, the heat flux is vector, so  $q$  should be the component of the heat flux vector in the  $x$  direction. When the temperature of the object is a function of three coordinates, the product of the unit vector on the three coordinate directions and the heat flow density component of this direction compound a heat flux vector[11], written as  $\vec{q}$ . The mathematical expression of the Fourier law is generally written by heat flux density vector as:

$$\vec{q} = -\lambda \text{grad}T = -\lambda \frac{\partial T}{\partial n} \vec{n} \quad (3)$$

In the formula:  $\text{grad}T$  —the temperature gradient of some point in space

$\vec{n}$  —the normal unit vector on the isotherm through this point  $\vec{q}$  — the heat density vector at the point

### 2.2 Differential equation of heat conduction

Randomly choose a micro-body parallelepiped from the heat-conducting objects to analyze its energy equilibrium. Supposing that there is an inner heat source in the object, the value is  $\Phi$ , which represents for the heat energy produced or consumed in unit volume per unit time, the unit is  $W/m^3$ . The thermal physical properties of conductive objects are assumed

as the function of temperature.

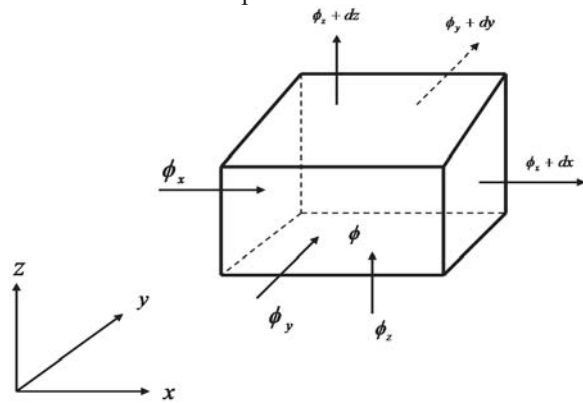


Figure 1: The micro-unit's thermal conductivity

As the heat flux density vector of any point in space can be decomposed into three coordinate directions' component, the heat flux of any direction can also be decomposed into heat flux along the x, y directions. It's shown as  $\phi_x, \phi_y, \phi_z$  in Figure 1. According to the Fourier law, the heat flux which is imported into the micro-unit through infinitesimal surfaces  $x = x, y = y, z = z$  can be written as:

$$\begin{cases} (\phi_x)_x = -\lambda \left( \frac{\partial t}{\partial x} \right)_x dydz \\ (\phi_y)_y = -\lambda \left( \frac{\partial t}{\partial y} \right)_y dxdz \\ (\phi_z)_z = -\lambda \left( \frac{\partial t}{\partial z} \right)_z dxdy \end{cases} \quad (4)$$

In the formula:  $(\phi_x)_x$  represents for the value of the heat flux's component  $\phi_x$  in the x direction at the point of x, the rest can be analogized.

$$\begin{cases} (\phi_x)_{x+dx} = (\phi_x)_x + \frac{\partial \phi_x}{\partial x} dx = (\phi_x)_x + \frac{\partial}{\partial x} [-\lambda \left( \frac{\partial t}{\partial x} \right)_x dydz] dx \\ (\phi_y)_{y+dy} = (\phi_y)_y + \frac{\partial \phi_y}{\partial y} dy = (\phi_y)_y + \frac{\partial}{\partial y} [-\lambda \left( \frac{\partial t}{\partial y} \right)_y dxdz] dy \\ (\phi_z)_{z+dz} = (\phi_z)_z + \frac{\partial \phi_z}{\partial z} dz = (\phi_z)_z + \frac{\partial}{\partial z} [-\lambda \left( \frac{\partial t}{\partial z} \right)_z dxdy] dz \end{cases}$$

As to the micro-body, the equilibrium relation can be reached at any time interval according to the conservation of energy. Total heat flux Imported micro-body + generated heat from the inner micro-body = total heat flux exported micro-body + increment of micro-body thermodynamic energy.

The type for the other two expressions:

Increment of micro-body thermodynamic energy

$$= pc \frac{\partial t}{\partial \tau} dxdydz$$

Generated heat from the inner micro-body

$$= \dot{\phi} dxdydz$$

In the formula:  $p, c, \dot{\phi}$  and  $\tau$  are respectively the micro-body's density, specific heat capacity, generated heat from heat source in unit time per unit volume, the formula can be systemized as:

$$pc \frac{\partial t}{\partial \tau} = \frac{\partial}{\partial x} \left( \lambda \frac{\partial t}{\partial x} \right) + \frac{\partial}{\partial y} \left( \lambda \frac{\partial t}{\partial y} \right) + \frac{\partial}{\partial z} \left( \lambda \frac{\partial t}{\partial z} \right) + \dot{\phi}$$

The formula is the general form in the three-dimensional unsteady heat conduction differential equation in Cartesian coordinate system, among

which  $p, c, \lambda$  and  $\dot{\phi}$  are variables.

In the whole heat dissipation process of continuous water, the temperature decreases, but not much. So it is assumed that the internal temperature of the bathtub is constant on the bathtub wall, that is to say, stable. In that state, the net heat of the inner surface wall transfers to the external surface through interior of the bathtub. Then it distributes around by convection and radiation. This part of the heat is the loss of heat dissipation. As shown in figure 2, heat transferred by heat flow,  $q \text{ kcal} / \text{m}^2 \cdot \text{h}$

$q_1 = q_2 = q_3$  So the tub wall heat loss can be calculated according to the inside surface temperature or outside surface temperature.

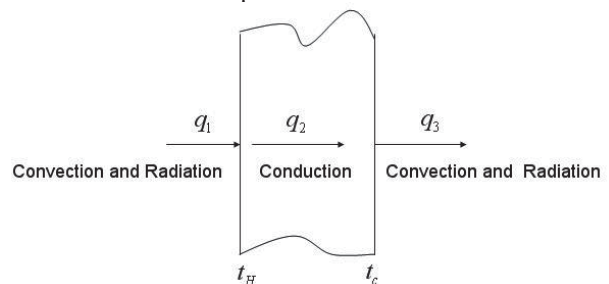


Figure 2: Diagram of bathtub wall's heat conduction

Heat dissipation loss of the bathtub wall

$$q = \frac{t_H - t_a}{\frac{s}{\lambda} + \frac{1}{\alpha}} \text{ kcal} / \text{m}^2 \cdot \text{h} \quad (5)$$

In the formula:  $t_H, t_a$  —respectively are bathtub surface's temperature and ambient temperature ( $^{\circ}\text{C}$ );

$s_1, s_2, \dots, s_n$  —bathtub wall's thickness of each layer is m;

$\lambda_1, \lambda_2, \dots, \lambda_n$  —the thermal conductivity Coefficient of materials in each layer;

$\alpha$  —total heat transfer coefficient of the outer surface to the surrounding air;

The formula (5) is the cylinder wall's heat loss per unit on surface area, the heat loss of the whole bathtub's surface is:



$$Q_A = \frac{t_H - t_a}{\frac{s}{\lambda} + \frac{1}{\alpha}} \times A \quad (6)$$

### 3. The result of model

According to the bathtub wall's temperature gradient from the inside-out that solved by the model, if the temperature of the inner wall is constant, the temperature outside the bathtub will be the lowest. Figure 3 is the bathtub wall's temperature variation diagram.

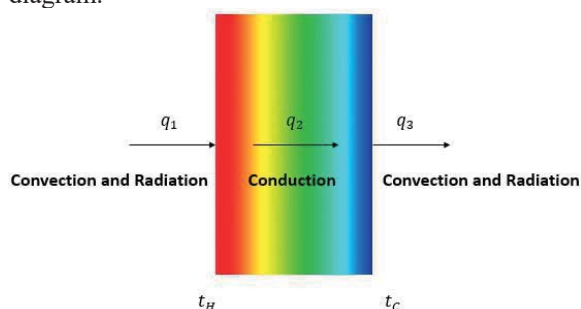


Figure 3: The bathtub wall's temperature variation diagram

The bathtub wall's temperature variation law can be clearly seen from figure 5. At the same time, according to the results of the model, the energy loss  $Q_A$  of the bathtub wall can be got. When the water temperature inside bathtub wall is consent 40 degrees. With the corresponding parameters, the heat loss of bathtub wall's conduction per unit time is  $Q_A = 2.09J/S$ . Figure 4 is distribution chart of the temperature field inside bathtub wall's simulated on MATLAB.

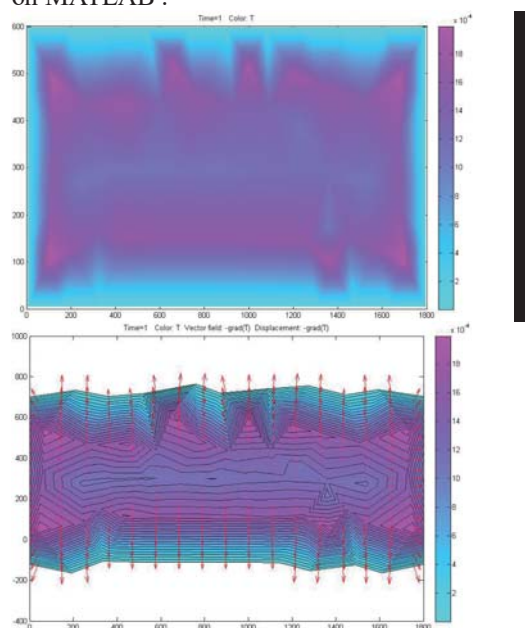


Figure 4: The distribution diagram of bathtub's energy filed

From figure 4 we can see that the energy diagram's color in the bathtub is deeper and the water's temperature is higher. The color outside the bathtub is deeper and the energy is lower, which accord with the fact.

### 4. CONCLUSION

According to the main heat dissipation model of bath crock, can get the major energy loss of bath crock, Can effectively control the hot water flow, always keep the showering people enjoy hot water bath.

### REFERENCES

- [1]Y. Zhang, X. Li, V. Sladek, J. Sladek, X. Gao, A new method for numerical evaluation of nearly singular integrals over high-order geometry elements in 3D BEM, J. Comput. Appl. Math. 277 (2015) 57–72.
- [2]Y.-M. Zhang, W.-Z. Qu, J.-T. Chen, BEM analysis of thin structures for thermoelastic problems, Eng. Anal. Boundary Elem. 37 (2) (2013) 441–452.
- [3]A. Karageorghis, D. Lesnic, The method of fundamental solutions for the inverse conductivity problem, Inverse Prob. Sci. Eng. 18 (4) (2010) 567–583.
- [4]Fei Wang, Yongxiang Pei. MATLAB programming of finite difference method [J]. Journal of xinjiang normal university (natural science edition), 2003,22(4):21-27.
- [5]A. Karageorghis, D. Lesnic, L. Marin, A survey of applications of the MFS to inverse problems, Inverse Prob. Sci. Eng. 19 (3) (2011) 309–336.
- [6]B.T. Johansson, D. Lesnic, T. Reeve, A method of fundamental solutions for the radially symmetric inverse heat conduction problem, Int. Commun. Heat Mass Transfer 39 (7) (2012) 887–895.
- [7]Y.M. Zhang, Z.Y. Liu, J.T. Chen, Y. Gu, A novel boundary element approach for solving the anisotropic potential problems, Eng. Anal. Boundary Elem. 35 (11) (2011) 1181–1189.
- [8]Y. Gu, W. Chen, B. Zhang, W. Qu, Two general algorithms for nearly singular integrals in two dimensional anisotropic boundary element method, Comput. Mech. 53 (6) (2014) 1223–1234.
- [9]Y. Liu, N. Nishimura, Z. Yao. A fast multipole accelerated method of fundamental solutions for potential problems, Eng. Anal. Boundary Elem. 29(11) (2005) 1016–1024.
- [10]Engl, H. Mathematics and its Applications: Regularization of Inverse Problems, Kluwer (2003).
- [11]Fauvel, J, Flood, R & Wilson, R (eds), Music and Mathematics, Oxford University Press (2003).

# The Design of Temperature Control and Water-Saving Bathtub based on Game Analysis

Yuhang Pan, Yanhong Kang, Yan Long, Guanchen Zhou\*  
North China University of Science and Technology,  
Tangshan, 060300, china

**Abstract:** There is contradiction between constant temperature and water resource saving, in order to make the bath water temperature reach the spa-style constant effect, at the same time avoid keeping the constant temperature process of water caused by the waste of water resources. Based on the trade-off problem of both, this paper carries on the game analysis, establishes the controlling-temperature and saving-water optimization model, and puts forward a optimal strategy which can not only effectively keep the bath water temperature constant, but also avoid the waste of water resources, and then effectively solve the contradiction between keeping the water temperature constant and saving water.

**Keywords:** constant temperature, game analysis, controlling-temperature, saving-water optimization model

## 1. INTRODUCTION

With the pursuit of continuous improvement of people's live, the warm and comfortable bathtub has become the focus of attention. [1]The ideal bathtub should like hot springs, can always keep a constant temperature. However, the bathtub is not a spa-style tub with a secondary heating system and circulating jets in this paper, but a water container need to inject hot water through a faucet. the bathtub as a open container. After a while, the bath gets noticeably cooler, at this time, in order to keep the temperature constant, we need to keep injecting hot water. When the water in the bathtub gets its own volume restriction, Water will overflow, resulting in wasting water. In the case of the study not to waste too much water, to maintain the constant temperature of the water bath, we establish the static water model from two angles of time and space.

## 2. CONSTRUCTION OF THE MODEL

Constant temperature analysis in bathtub: After analyzing on the input heat into bathtub water  $Q_{in}$  and the lost heat from the surface of bathtub water  $Q_{heat}$ , one static water temperature model is built based on the points of view from time and space; then using the control variate method, [2]the dependence degree of the static model on the shape and volume of bathtub is obtained. The results show that the degrees respectively depend on the size of the

water comprehensive surface  $h$  and the drainage rate  $V_{out}$ .

### 2.1 game analysis between constant temperature and water consumption

When people are in the bath process, they can take the following strategies:

- (1) In order to maintain a constant temperature, in the process of bathing, hot water was continuously injected.
- (2) In order not to waste more water, when the water gets cold, stop adding water.
- (3) Considering the heat loss at least, and with the least amount of water.

In the process of bathing, to keep the temperature constant, it needs to keep the water absorption of heat  $Q_{in}$  as much as possible is equal to the bath water

cooling  $Q_{heat}$  and heat discharge water away  $Q_{out}$ , because the heat cooling of the bath water is continuous, and the tap, as the only source of heat into the bath water, is needed to constantly inject hot water into the bathtub. When reaching the limit of the capacity of the bathtub, the water from the bathtub overflow caused a waste of water. Therefore, there are contradictions between maintaining a constant temperature and water saving, there exist two kinds of Nash equilibrium, one is the pure strategy Nash equilibrium, such as strategy (1) and (2); the other is a mixed strategy Nash equilibrium, such as strategy (3). Based on the game theory, the interaction between heat dissipation and water injection is studied, and the optimization strategy is studied by considering the relationship between heat dissipation and water consumption. Fig. 1 shows a simplified model of the bathtub water endothermic heat  $Q_{in}$  and bathtub water dissipate heat  $Q_{heat}$ .

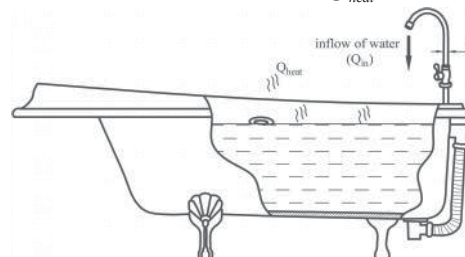


Figure. 1 The simplified model of the bathtub

## 2.2 model for bathtub of water temperature

### 2.2.1 water surface heat loss

The heat loss mainly in the form of surface heat dissipation,[3] the mode there are three: evaporative heat dissipation  $dQ_e$ , convective heat transfer  $dQ_c$  and radiant heat loss  $dQ_r$ .

The total amount of heat loss defined by  $dQ$ :

$$dQ = dQ_e + dQ_c + dQ_r = [\alpha(p_v'' - p_v) + \beta(k - \theta) + \varepsilon\sigma(k + 273)^4]S \quad (1)$$

After integration, we can yield:

$$Q_{heat} = [\alpha(p_v'' - p_v) + \beta(k - \theta) + \varepsilon\sigma(k + 273)^4]S \quad (2)$$

Where C is correction factor,

$$\alpha(p_v'' - p_v) + \beta(k - \theta) + \varepsilon\sigma(k + 273)^4 = h \quad (3)$$

And  $\alpha$  is evaporation coefficient,  $W/(m^2 \cdot hPa)$ ;

$p_v''$  is steam pressure of thin saturated surface of water,  $hPa$ ;

$p_v$  is vapor partial pressure in wet air,  $hPa$ ;

$S$  is water and air contact area,  $m^2$ ;

$\beta$  is heat release coefficient,  $W/m^2 \cdot ^\circ C$ ;

$\theta$  is dry bulb temperature of air,  $^\circ C$ ;

$S$  is water and air contact area,  $m^2$ ;

$\varepsilon$  is blackness, here  $\varepsilon = 0.97$ ;

$\sigma$  is a constant, here  $\sigma = 5.06 \times 10^{-8} W/(m^2 \cdot K^4)$ ;

$S$  is surface area of water,  $m^2$ ;

$h$  is comprehensive heat loss coefficient of surface of water of bathtub.

### 2.2.2 Total Heat Carried by Pouring Water

Since the heat of bathtub has been lost, in order to ensure a constant temperature, [4, 5] only keep injecting water to maintain the heat input. In the continuous process of adding water, the velocity of pouring water is not a fixed value, not a stable heat diffusion process, the heat carried by the injected water is considered to be full absorbed by the water bathtub. So that the heat of injected water can be expressed as following:

$$Q_{in} = cm(k_{in} - k_{mix}) \quad (4)$$

Where  $c$  is the specific heat capacity of water,  $J/(kg \cdot ^\circ C)$ ;  $m$  is the quality of injected water,  $kg$ .

Considering the quality of the injected water cannot be directly obtained, therefore, establishing a equation on velocity of flow based on unit time and mass as follows:

$$dm = \rho s v_{in} dt \quad (5)$$

Where  $\rho$  is density of injected water,  $kg/m^3$ ;  $s$  is section area of faucet outlet,  $m^2$ , can be calculated

by formula  $s = \frac{\pi d^2}{4}$ ;  $v_{in}$  is inlet velocity in

arbitrary occasion,  $m/s$ .

Combined with formula (4) and (5), we can get total heat expression:

$$Q_{in} = c(k_{in} - k_{mix}) \cdot \left( \int_0^t \rho s v_{in} dt \right) \quad (6)$$

Similarly get overflow water heat:

$$Q_{out} = c(k_{mix} - k_p) \left( \int_0^t \rho s v_{out} dt \right) \quad (7)$$

Where  $v_{out}$  is outlet velocity in arbitrary occasion,  $m/s$ .

### 2.2.3 Establish Static Water Temperature Model

Static water temperature model means no interference of factors, clearly, energy exchange only in the form of evaporation, convection, radiation and so on in this situation, since the bathtub has a limited capacity, when the volume of injected water volume exceeds the limit of bathtub, water overflow will take some heat, therefore, the static water temperature model need to divide into two situation according to the volume of injected water. To achieve constant temperature, it is necessary to reduce heat loss[3], as far as possible to keep the water temperature constant, namely, the difference between injection of heat and heat loss is equal to zero as possible. We can give the following relationship:

$$Q = \begin{cases} c(k_{in} - k_{mix}) \cdot \left( \int_0^t \rho s v_{in} dt \right) - hS \cdot t - C \\ V + \int_0^t s v_{in} dt < V_0 \\ c(k_{in} - k_{mix}) \cdot \left( \int_0^t \rho s v_{in} dt \right) - hS \cdot t - C - c(k_{mix} - k_p) \left( \int_0^t \rho s v_{out} dt \right) \\ V = V_0 \end{cases}$$

Where  $V$  is the volume of water remain in bathtub,  $m^3$ ;  $V_0$  is limit volume of bathtub,  $m^3$ .

## 3. CONCLUSIONS

Considering the fact that when the temperature of water is close to the temperature of people, it can meet the requirements, that is, when the range of water temperature is between  $35^\circ C$  and  $42^\circ C$ , it is considered that there is no need to add heat from outside. Compared with the constant temperature bath requirements, in the temperature range beyond the body feel comfortable to add water, but also play a role in reducing the waste of water.

## REFERENCES

[1]Zhengguo Zhao. Enthalpy difference formula for

calculating heat dissipation on water surface and its use [J]. *Journal of Hydraulic Engineering* , 2004, 2:34-38.

[2]Azad Jarrahiana, Hamid Reza Karamib, Ehsan Heidaryanc. On the isobaric specific heat capacity of natural gas[J].*Fluid Phase Equilibria*, 2014: 384: 16-24.

[3]R. Sangi, M. Baranski, J. Oltmanns, et al. Modeling and simulation of the heating circuit of a multi-functional building[J].*Energy and Buildings*,

2016,110:13-22.

[4]Assad H. Sayerab, Hazim Al-Hussainia, Alasdair N. Campbella.New theoretical modelling of heat transfer in solar ponds[J].*Solar Energy*, 2016, 125: 207-218.

[5]A. Degiovanniab, B. Remya. An alternative to heat transfer coefficient: A relevant model of heat transfer between a developed fluid flow and a non-isothermal wall in the transient regime[J].*International Journal of Thermal Sciences*, 2016, 102: 62-77.

# Tracking and Anti-Tracking of the Maneuvering Target the Algorithm based on the Minimum Distance Algorithm and the Track Curvature

Chun-feng Liu, Li-ting Wang\*, Yang Han and Hua Zhang

North China University of Science and Technology, College of Science, Tangshan, 063000, China

**Abstract:** The lectures is research on radar for maneuvering target tracking problem, combined with the minimum distance correlation rule and track radius of curvature method and presents a fast tracking radar target for algorithms and Matlab, solved the adjacent algorithm in multiple target tracking is prone to error and problems, at the same time the author put forward the strategy of the target escape and radar countermeasures, very good to keep the target tracking.

**Keywords:** Path tracking, Data correlation, Track curvature, Anti-tracking

## 1. INTRODUCTION

Tracking of the maneuvering target refers to the measurement object based on sensor information (such as radar, etc.) obtained, estimating the state of the target continuously and achieving the process that the main object to be concerned about the state of motion modeling, estimation and tracking. Its main task is to detect targets in a complex environment and estimate the motion parameters in real-time, then get the goal and intention of movement situation [1].

Tracking is a typical uncertainty. With the development of the surveillance and counter-surveillance techniques, especially because the military surveillance and destination mobility has undergone great changes so that the uncertainty of the target tracking problem is more serious. Tracking uncertainty is mainly from the target motion state of uncertainty, measurement (information) sources of uncertainty, more objective and intensive environment hybrid echo measurement data vague or uncertain. This requires more maneuvering target tracking system must adapt to changes in mobility and making the right decisions related. At the same time, target tracked in order to improve their ability to survive, will usually make evasion maneuver or release disturbances trying to get rid tracking when the radar is locked. The former mainly through the rapid changes in their own state of motion to lead to poor precision radar tracking device or even lost track targets, the latter cover itself by creating false targets, so introduce the problem when the target is maneuvering the radar how to track accurately [2-5].

With the rapid development of modern aviation,

navigation, space industry and modern warfare information, network development, the technology of maneuvering target tracking is attached more and more importance by the countries, now it has become a very active area of research. Target tracking is divided into a single target tracking and multi-target tracking, with the gradual deepening of target tracking, multiple target tracking has become the focus of research in this area. The early 1970s by the Y.Bar-Shalom and R.Singer pioneered in data association and Kalman filtering technology combine to sign multi-target tracking technology has made breakthrough progress. In the late 1970s and 1980s was a period of rapid development of multi-target tracking technology of, Y.Bar-Shalom, R.Singer as the representative of scientists put forward many classic algorithms, there are joint probabilistic data association, multi-hypothesis tracking, adaptive filtering algorithms and interactive multiple models algorithm. After 90 years, multidimensional allocation algorithm in data associated with the variable structure IMM, the probability of multiple hypothesis tracking, distributed fusion, random set theory and other aspects of the research activities have greatly enriched and developed the theory of multi-target tracking[1-5].

Essence of "nearest neighbor" algorithm proposed by Singer in 1971[6-7] is a "greedy" algorithm, we can not keep staying in the global sense and the mistaken with loss goals phenomenon often occurs, in order to prevent this phenomenon, we adopt a united algorithm which combines a minimum radius of curvature of the distance with trajectory and achieved a good effect.

## 2. TRACKING OF MULTIPLE TARGETS

The main application areas of multiple target tracking are: vehicle monitoring and highway traffic control, air defense, the ballistic missile defense, air attack, marine monitoring, battlefield surveillance and the air traffic control, etc. Data association is the core part of multiple target tracking. It is a process which compares the candidate echo data correlation with the target known trajectory and determine finally correct observation and trajectory matching process.

### 2.1 selection gates when path tracking

When radar track multiple targets simultaneously,



each cycle of antenna scan is likely to be admitted to many target tracking. After filtering algorithm was determined, priority is dealing with the track correlation processing (that is, the so-called rough related), with a predictive value as the center set up an area of track, when the observation data is in the area, will think some trace and track is related. This area is called relative wave gate.

The formation of the associated wave gate is the most important problem in multiple target tracking problems, the related wave gate is that take predict location of tracked target as the center, which is used to determine the possible target area of the range of value. The size of the area determined by the probability of receiving the echo rightly, which also means when the wave shape and size of the gate is determined, we should make the real measurements fall into the wave gate at high probability make a few of the related wave gate irrelevant point trace quantity at the same time .

Related wave gate is used to determine the decision threshold, the measured value which falls into the related echo called candidate echo wave gate, once the wave shape and size of the door is established, will determine the detection probability which is detected correctly and false targets' false-alarm probability which is detected by mistakes of the measurement of the real target. However the detection probability and false alarm probability are often contradictory, therefore , it is important to choose the appropriate relevant gate. If only one echo falls into the target related wave gate, then the echo will be directly used to track updates; if more than one echo falls into the related wave gate of tracked target, then it will be determined by certain rules and used to track update echo collection and through the data correlation technology more advanced to confirmed the target echo of track that is updated finally. Related waves that are widely used in the gate include the ellipse under the rectangular coordinate system (ball) wave, rectangular wave gate and the fan gate under polar coordinates.

## 2.2 data association

The key problem of the multiple target tracking is how to carry out effective data correlation. Because the sensor observation process and target tracking environment have many uncertain factors, especially when the target signals are submerged in a lot of noise signals and extraneous signals, it will lead to fuzzy cases of multi-sensor multi-target data association. Traditional data association methods such as nearest neighbor method, the probabilistic data association method, most of these use hard judgment method, and when the correlation is fuzzy the reliability will decline. With the increase of the number of goals, the traditional data correlation calculation will make computer saturated soon, limiting the engineering application of these methods. This article is based on the joint algorithm of the

minimum distance and trajectory curvature radius and achieved a good effect.

## 2.3 "NEAREST NEIGHBOR" ALGORITHM

Singer in 1971 put forward a kind of tracking filter which has fixed memory requirement and is able to work under the environment of multiple measurements. The filter takes prediction of tracked target location (tracking or associated wave gate center) recent measurement as a candidate for measurement only in statistical sense. The "recently" is often said statistical distance minimum or maximum residual error probability density, the statistical distance commonly use Euclidean distance:

$$d^2[z(k)] = [z(k) - \hat{z}(k|k-1)]^T \sum^{-1}(k) [z(k) - \hat{z}(k|k-1)]$$

The essence of this method is a kind of "greedy" algorithm, and it can't keep the optimal global sense, and this algorithm selects the nearest associated wave gate center measurement of target track to update, but the nearest center measurement is not necessarily the right target measurement. Therefore, the nearest neighbor method often happens with the phenomenon of missing targets.

## 3. NEAREST AND MINIMUM CURVATURE ALGORITHM

Because the nearest neighbor algorithm is a kind of greedy algorithm, it often takes place of mistakes at the intersection of tracks. To prevent such things happen, we combined algorithm of nearest with minimum curvature algorithm in the study and the effect is much better.

### 3.1 algorithm steps

**Step1.** Select the initial track. Because the starting points of these two tracks in this problem are same, so it needs a slight delay between the two parts. When the tracks become obvious, we can start tracking. In this algorithm, we selected several groups of adjacent data after 50s, and proceed simple clustering. The data of item No.49 and 50 which we get belongs to two different tracks. We set the raw data stored in the matrix A, the matrix B stored track 1 and the matrix C stored track 2. Given the same starting points of track 1 and 2, the initial value set as:  $B(1,:) = A(1,:)$ ;  $C(1,:) = A(1,:)$ ; the initial curvature of the tracks are  $b1 = A(1,:)$ ;  $c1 = A(1,:)$ ;  $b2 = A(49,:)$ ;  $c2 = A(50,:)$ ;  $b3 = b2$ ;  $c3 = c2$ ; then turn to the step two.

**Step2.** For the given data, we should compare the given data with newest data of track 1 and 2 firstly, finding out the difference; if  $d_1 < d_2 * 3$ , then the new waypoint belongs to track 1, otherwise it belongs to track 2 and turn to step 4.

**Step3.** If the track points of step 2 created by the track coincide of these two target aircraft, relevance of the new data will be misjudged. The curvature will be quite different when track coincide occurs, in this way we can correct new waypoints by calculating the curvature of the tracks. Thus, we can prevent the mistake when track coincide happens. Turn to step 4.

**Step4.** Each addition of 100 data points, we update a

time b2=B(j,:); b1=B(j-100,:); b3=B(j-50,:);  
 c2=C(k,:); c1=C(k-100,:); c3=C(k-50,:);  
 The Mat lab and data B, C of this algorithm attached  
 as affix, the details of execution as below:

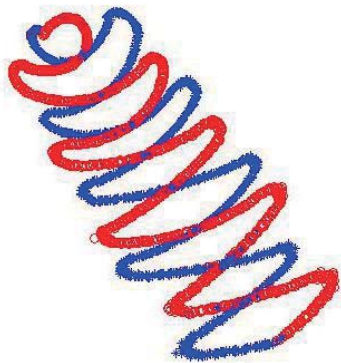


Figure 1. Data association schematic

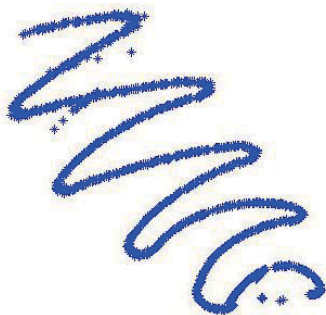


Figure 2. Track 1 schematic

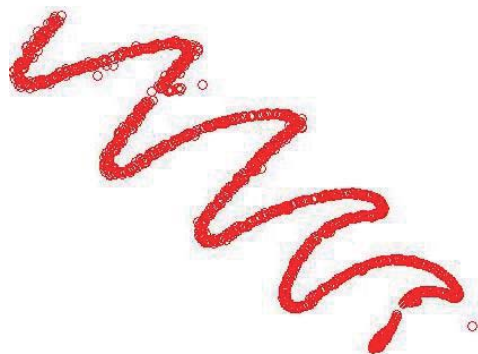


Figure 3. Track 2 schematic

### 3.2 ALGORITHM EVALUATION

We take the minimum distance as the associated principle in this algorithm, making the complexity of the algorithm much simple, it is convenient to the radar to proceed rapid tracking to multiple targets and we also solved the problem that the nearest algorithm is easy to take place mistake-tracking during the multiple targets tracking.

### 3.3 the treatment of track single echo point loss

By the algorithm we mentioned above, some data are lost occurred in track 2. By the analysis of algorithm, we can know that in this algorithm the main objects selected is track 1, it will lead to the data points of target overlap region back into track 1, which causes data loss of track 2. The solution is to separate the

data again for the raw and take the track 2 as the main object. In this way we can get the complete tracks. As shown below:

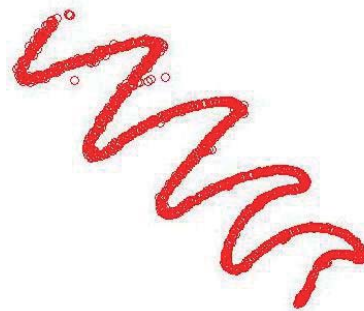


Figure 4. Track 2 after separation of the data  
 Comparing the Fig.3 with the Fig.4, we can conclude the integrity of the tracking diagram after the data is separated.

## 4. TRACKING AND ANTI-TRACKING OF THE TARGET

### 4.1 aircraft escape

Tracking radar is the radar which can track a target continuously and measure the target's coordinates of the radar. It can also provide the trajectory of the target. Tracking radar is mainly used for the control of arms and continuously providing the target indicator data for weapon system, also used to missile range measurement, etc. The first task for tracking radar is to capture the target. Tracking radar automatic tracking of target azimuth and elevation is the radar antenna to follow target motion and continuously change its direction, making the antenna electrical axis always point to the target.

When the two goals in the known data have been locked by radar tracking at the same time, assuming that the target in a timely manner to understand whether being tracked, and the measurement precision of known radar is the radar beam width which is  $3^\circ$ , namely when the radar is the cone roof and attachment for the shaft with the target radar, the goals within the cone whose half-apex angle is  $1.5^\circ$  can be detected; The minimum time interval between the two adjacent scanning is 0.5s.

From the analyzing of the given data, we can get the distance between the two goals and radar changes over time.

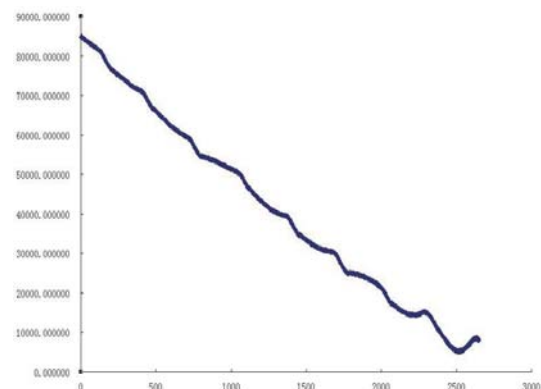


Figure 5. The distance between the target aircraft and

radar changes over time

As can be seen from Fig.5, the distance between the target and the radar is gradually reducing, and the maximum distance between the two target aircrafts is 30000m. Since the radar radiation cone angle is  $3^\circ$ , so the target aircraft can completely enter the radar blind area.

Set the distance between target and radar is  $d$ , then the detected diameter is:  $r = (2 \tan 1.5^\circ)d \approx 0.0524d$

Thus the radar detection diameter dropped from 4713.5m down to 500m. At the start, the target is unfavorable to escape because of its high detection range, but the radar need to track two goals, and the maximum distance between the goals is 30000m, so it cause the plane only takes 2s to escape radar tracking. Because of radar scanning interval is 0.5s, the plane just quickly deviate from the track with making three noise points, then it can escape the radar's tracking in 2s. When the target is relatively close to the radar, because the smallest detect diameter is only 500m, the aircraft just quickly turn a cycle of acceleration in radar escape radar.

Since the tracking radar to track the target needs to be rotated, so that it can lead to radar target appear on the edge of the radar when there has such sudden turn, and then make it easier for the goal to escape. Because the radar scan rate is 0.5s, turning along the direction of the radar scanning can increase the scanning interval, and provide the conditions for target from radar tracking.

Secondly, in order to improve its own survival ability, the tracked target which is locked by radar would circumvent the maneuver or release the interference to get rid of the track. The former mainly through rapid changes in its own motion state lead to poor precision radar tracking device and even lost tracking target, the latter by making false target to cover itself. Therefore the problem the radar how to track accurately when target is maneuvering is introduced.

- (1) The sudden change of movement state, such as the sudden increase movement speed can fly out of radar detection range;
- (2) Reduce the movement speed to adjust the flight direction, such as radar distance error is 100m, azimuth and elevation angle error is from 0.3 to 0.6 degrees, the flight distance of tracking target is less than 100m when target tracking radar scans two times or in the 0.5 seconds interval, at the same time it makes the radar scan twice to the azimuth and pitching angle difference within the error of radar, and then result in the loss of radar target;
- (3) To find reasonable shelters, such as mountains or flying low to avoid radar scan;
- (4) The two given goals detected by radar can keep flying at close range, and there is only one track

detected by the radar.

#### 4.2 countermeasures of radar

To keep track of the target, tracking strategy should make the following adjustments:

- (1) When the radar finds UFO, as soon as possible, it adjust the orientation of the radar making the object to keep on radar detection of the axis of the cone;
- (2) Enable secondary radar, using multiple radar combined operations to monitoring the same target aircraft at the same time;
- (3) Reduce the radar scanning time interval, and reduce the response time of the flying object;
- (4) Active radar is easily disturbed by enemy observation, combined with passive radar can better maintain the target track.

#### 5. CONCLUSION

When the radar monitors two targets at the same time, the points of different flight track will be mixed together, so we need through association rules to separation of waypoints, in this article, through combining the "nearest neighbor" algorithm with the radius of curvature of computational geometry, giving a new correlation algorithm.

When the target aircraft is monitored by the radar, it can accelerate quickly and avoid the range of the radar detection during two cycles of the radar scan, and radar aircraft should also focus on new target waypoints and track to avoid the target creating false targets to escape surveillance.

#### REFERENCES

- [1]QuanTaifan New theory and technology of target tracking[M], BeiJing: National Defense Industry Press, 2009.
- [2]PanQuan, LiangYan, YangFeng, etc. Modern target tracking and information fusion[M], BeiJing: National Defense Industry Press, 2009.
- [3]Chen, B, and Tugnait, J. K. Tracking of Multiple Maneuvering Targets in Clutter Using Multiple Sensors, IMM/JPDA Filtering and fixed-lag smoothing[J]. Automatica, 2001, 37(2):239-249.
- [4]A. Muir and D. P. Atherton. Adaptive Interacting Multiple Model Algorithm for Tracking a Maneuvering Targets [J]. IEEE Proceeding-Radar, Sonar Navigation,1995, 142(1):11-17.
- [5]Bar-Shalom Y, Tse E. Tracking in a cluttered environment with probabilistic data association[J]. Automatica, 1975, 11(9): 451-460.
- [6]Singer R.A, Stein J.J, An optimal tracking filter for processing sensor data of imprecisely determined origin in surveillance systems, Proceedings of the 1971 IEEE Conference on Decision and Control, Miami Beach: 1971,171-175.
- [7]Singer R.A, Sea R.G, A new filter for optimal tracking in dense multitarget environments, Proceedings of the ninth Allerton Conference Circuit and System Theory, Urbana: 1971, 201-211



# Analysis of Factors Influencing H-R Forte Complex Post - Based on the Control Variable Method

Wancheng Tao<sup>1,3</sup>, Xiaofei Li<sup>2,3,\*</sup>, Lihui Zhou<sup>2,3</sup>

<sup>1</sup>Surveying and mapping professional, Mining engineering institute, North China university of technology

<sup>2</sup>Applied statistics, Faculty of science, North China university of technology

<sup>3</sup>Hebei tangshan lunan district, 46 new huaxi road, north China university of science and the department

**Abstract:** There are a lot of whistles. It is widely used in earthquake, fire, flood, etc. It can achieve unexpected results in case of emergency. In order to more effectively convey information. So begin to study the world's loudest whistle.

Compared Hartmann whistle, reed whistle, whistle and rare composite vortex whistle of life prevalent and this passage analyzed the role of the principle and characteristic. This passage obtain the results that the complex whistle is more pertinence and practicality. Then with the control variable method is the same type of whistle which had the greatest influence factors of the whistle voice and the comparison between different types of whistle sound size. After analysis, this passage obtain the Hartmann whistle and spiral whistle compound as a representative compound whistle geometric model is set up. It is called H-R forte complex post.

**Keyword :** Simulation, geometric model, control variables method, complex post

## 1. ANALYSIS OF THE QUESTION

### 1.1 action principle of whistle

When the gas stream is blown whistle mouthpiece. After the air blow to the opposite edge of the mouthpiece. The split in two. Part of the flow to the whistle scattered outside. Part of the flow into the pipe and produce waves generated turbulence. This is called "edge of the sound" principle. The so-called "edge of the sound" that air flow through the solid edge sound. This is the most typical air vibration sound. Edge tone generally do not have a fixed base frequency. Effects shown in Fig.1.

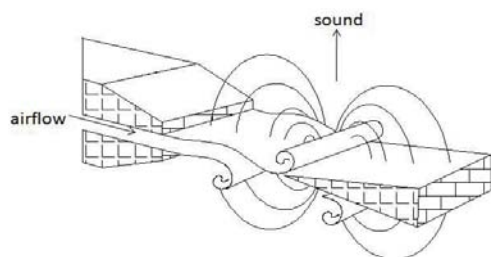


Figure1. An edge sound effect diagram

Generally, there is a small ball in the whistle. Whistle becomes a single frequency tone without it. It kept

the movement on the inside. It means changing the shape of the cavity resonance. It is changing pronunciation frequency. A bit like whistling when the role of the tongue. If this passage wants to sound reaches the maximum. Then start out to make a gas flow, and swirl out from the outlet of the air flow to reach resonance.

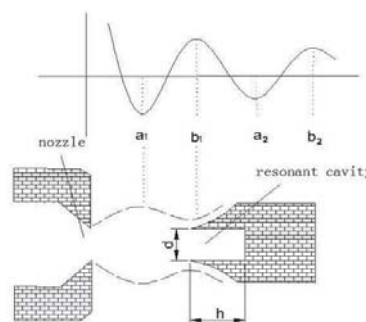
Whistles are hydrodynamic sounder which according to the type of fluid can be divided into three basic types, one is airflow, one is flow type, one is gas-liquid-type,

There are three types of power sources, although different, it can be applied to the whistle, and in addition to a combination of various types of composite sounder to whistle, whistle following selection Hartmann, vortex whistle, whistle and composite post this spring four types of posts were analyzed to compare the loudness, and then select the loudest whistle principle to make whistles.

## 2. ACTION PRINCIPLE

### 2.1 hartmann whistle action principle

Hartmann whistle works in the high-speed gas flow ejected from the supersonic nozzle, the partial pressure between the nozzle and the cavity resonator to generate a periodic fluctuation, as shown by the dashed lines. The experimental results obtained contractible nozzle better. Periodic pressure distribution is due to gas flow velocity that exceeds the speed of sound in the gas produced. In each of the pressure to the minimum between the next maximum pressure (in Figure 1,  $a_1b_1$  and  $a_2b_2$  so the pressure rising portion) is unstable region. Hartmann whistle mechanism shown in Fig.2



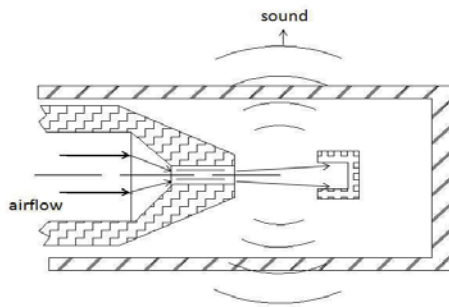


Figure2. Hartmann whistle effect  
Hartmann whistle resonant cavity resonance frequency empirical formula is:

$$f = \frac{c}{4(h + 0.3d)} \quad (1)$$

Where  $c$  in the speed of sound,  $h$  and  $d$  respectively the depth and diameter of the cavity resonator.

## 2.2 ACTION PRINCIPLE OF VORTEX WHISTLE

Vortex whistle sound power source may be either a gas or a liquid and may be relatively simple structure, composed mainly by a cylindrical cavity, high velocity jet tangentially into the cylindrical cavity, the cavity rapidly is rotated so vortex is formed, and finally from the cylindrical cavity the outlet port at the top of the body, there are sound waves. The structure shown in Fig.3 below

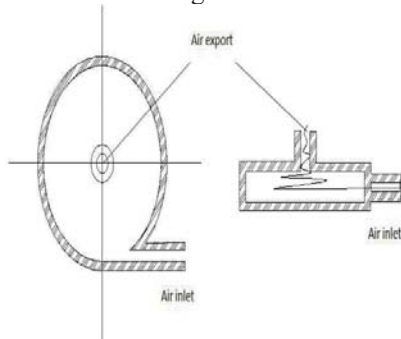


Figure3. Vortex whistle chart

As the frequency of the sound power supply for gas spiral whistle experience formula is:

$$f = \alpha \left( \frac{c}{\pi D} \right) \left( \frac{p_1 - p_2}{p_2} \right)^{\frac{1}{2}} \quad (2)$$

Which  $\alpha$  is constant and generally not more than one,  $c$  is the speed of sound,  $D$  is a cylindrical cavity diameter,  $p_1$  and  $p_2$  were imported pressure and outlet pressure.

## 2.3 action principle of the reed whistle[7]

Reed whistle on the principles of the sound source is liquid, but gas can also make it sound. Reed is divided into two, fulcrum style reed whistle and Cantilever reed whistle. Fulcrum style reed whistle from 5 support points support. Its natural frequency is

$$f = \frac{f_{\text{空}}}{\sqrt{1 + \beta}} \quad (3)$$

Cantilever spring whistle constituted mainly by a nozzle and a cantilever spring portfolio. The jet nozzle of the high-speed fluid jet sheet impact generated reed, so that the reed sound. Reed whistle cantilever structure as shown in Fig.4

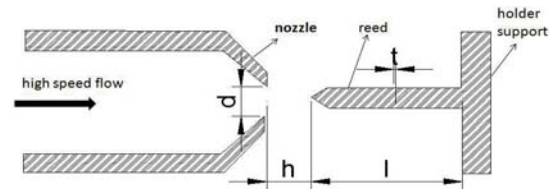


Figure4. Cantilever structure of reed whistle  
Natural frequency of the cantilever spring whistle for

$$f = \frac{f_{\text{空}}}{\sqrt{H - 0.34\rho_1 M / \rho t}} \quad (4)$$

Among them,  $f_{\text{空}} = 0.162 \frac{t}{l^2}$ ,  $M = 1.3\sqrt{hw}$ ,

$w$  is reed width.

## 2.4 composite action principle whistle[3][8]

There is a complex vortex whistle and Hartmann in series, export vortex whistle access Hartmann nozzle inlet air from the vortex whistle tangential inlet into the high-speed rotation of the cylindrical cavity in the cavity, then emitted from the outlet, directly into the gas stream exiting the nozzle inlet Hartmann whistle, and then emitted from the nozzle, a cavity resonator disposed downstream thereof, when the distance between the nozzle and the cavity resonator appropriate, there may be a sine wave.

Composite whistle in anti-interference and improve efficiency is better than hartmann whistle

## 2.5 basic theory of pneumatic acoustics

Pneumatic acoustics is the inter disciplinary aerodynamic and acoustic, in the early 1950s.They began to study. Wright hill ( *M.J.Lighthill* ) published the world famous pneumatic acoustic simulation equation (also called *Lighthill* equation)in 1952.That is:

$$\frac{\partial^2 \rho}{\partial t^2} - c_0^2 \nabla^2 \rho = \frac{\partial^2 \rho_0 v_i v_j}{\partial x_i \partial x_j} \quad (5)$$

## 3. MODELING AND SOLUTION

### 3.1 the geometric model of hartmann whistle

By designing four different sizes of tapered Hartmann whistles, this passage, under different pressure, measured spray chamber distance, frequencies, sound pressure levels and other indicators. The results are presented in the Tab.1 below, in which the four cone angles are respectively 30 degrees and that the nozzle diameter are equal to the resonance cavity diameter.



Table1. The Sizes of 4 Tapered Hartmann Whistles

| Serial number          | No.1 | No.2 | No.3 | No.4 |
|------------------------|------|------|------|------|
| Resonance Cavity Depth | 3.4  | 3.6  | 3.8  | 4.5  |
| Nozzle Diameter        | 2.4  | 2.0  | 1.6  | 1.2  |

Through many experiments, the final results are showed as Fig.5:

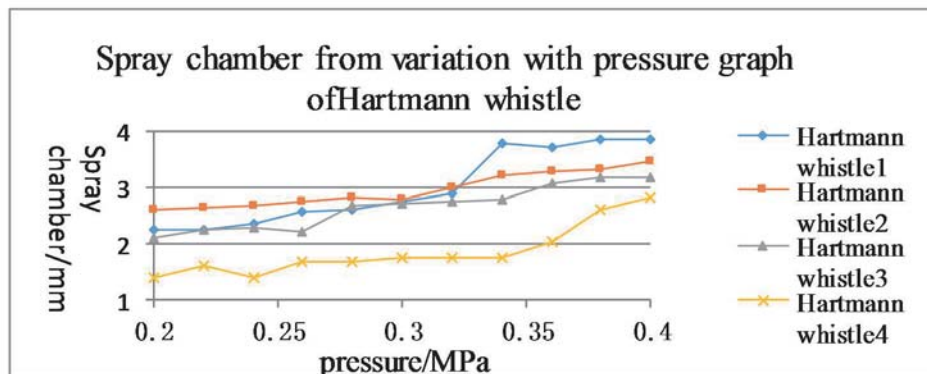


Figure5. The Line Chart Representing the Spray Chamber Distance of Each Hartmann Whistle Changing with Different Pressures

What can be seen from Fig.5 is that the spray chamber distance of Hartmann whistle increases with the pressure increasing. Moreover, the trend is substantially, in a certain proportion of the resonance cavity depth and the nozzle diameter as well as under the same pressure, that the more this ratio increases, the greater the spray chamber distance becomes.

Then the pressure rising, the levels are relatively

increasing and generally higher.

### 3.2 the geometric model of vortex whistle

Select seven vortex whistles with different diameters as in Tab.2. Furthermore, be sure of the inlet diameter of the vortex whistle 5mm, the exit diameter 10mm, the length the entry pipe and outlet pipe respectively 50mm and 15mm, and the height of the cylindrical cavity 12mm.

Table2. The Sizes of 7 Cylindrical Cavity Diameters of Vortex Whistles

| Serial number                      | No.1 | No.2 | No.3 | No.4 | No.5 | No.6 | No.7 |
|------------------------------------|------|------|------|------|------|------|------|
| Diameter of the cylindrical cavity | 40mm | 35   | 30   | 25   | 20   | 15   | 10   |

By giving different pressure to the vortex whistles, get the vibration frequency of each vortex whistle. As

shown in Fig.6:

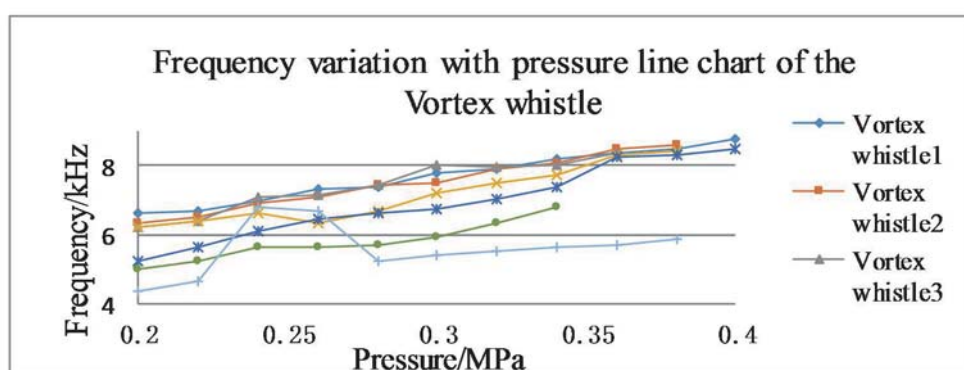


Figure6. Frequency variation with pressure line chart to the vortex whistles

As seen in Fig.6 as the inlet pressure increases, the frequency increases. From another point to analysis, under the same pressure, vortex whistle with decreasing frequency of occurrence of a cylindrical cavity diameter decreases.

Then within a certain range, different vortex whistle sound radiation can produce effective best inlet pressure, best parametric relationship needs further study.

### 3.3 the geometric model of reed whistle

Data obtained by looking up that the impact reed thickness of different sizes on the frequency of the reed whistle reed thickness of different sizes to learn frequency trend reed whistle. As shown in Tab.3:

Table 3. Frequency rectangular of the reed

| or<br>d<br>er | Frequency ( mm) |      |     |     |      |     |
|---------------|-----------------|------|-----|-----|------|-----|
|               | 47*             | 47*3 | 47* | 56* | 56*3 | 56* |
|               |                 |      |     |     |      | 65* |

|   |            |            |                 |            |           |            |            |
|---|------------|------------|-----------------|------------|-----------|------------|------------|
|   | 34*<br>1   | 4*1.<br>5  | 34*<br>2        | 34*<br>1   | 4*1.<br>5 | 34*<br>2   | 34*<br>1   |
| 1 | 746<br>.6  | 1056<br>.2 | 135<br>9.7      | 494<br>.8  | 695       | 893<br>.4  | 352<br>.1  |
| 2 | 298<br>6.4 | 4224<br>.8 | 543<br>8.8      | 197<br>9.2 | 2780      | 357<br>3.6 | 140<br>8   |
| 3 | 671<br>9.4 | 9505<br>.8 | 122<br>37.<br>7 | 445<br>3.2 | 6255      | 804<br>0.6 | 316<br>8.9 |

From the above analysis of the table available inside,

Table 4. The group of Composite whistles

|                      | Vortex<br>whistle1      | Vortex<br>whistle2      | Vortex<br>whistle3      | Vortex<br>whistle4      | Vortex<br>whistle5      | Vortex<br>whistle6      | Vortex<br>whistle7      |
|----------------------|-------------------------|-------------------------|-------------------------|-------------------------|-------------------------|-------------------------|-------------------------|
| Hartmann<br>whistle1 | Composite<br>whistle1-1 | Composite<br>whistle2-1 | Composite<br>whistle3-1 | Composite<br>whistle4-1 | Composite<br>whistle5-1 | Composite<br>whistle6-1 | Composite<br>whistle7-1 |
| Hartmann<br>whistle2 | Composite<br>whistle1-2 | Composite<br>whistle2-2 | Composite<br>whistle3-2 | Composite<br>whistle4-2 | Composite<br>whistle5-2 | Composite<br>whistle6-2 | Composite<br>whistle7-2 |
| Hartmann<br>whistle3 | Composite<br>whistle1-3 | Composite<br>whistle2-3 | Composite<br>whistle3-3 | Composite<br>whistle4-3 | Composite<br>whistle5-3 | Composite<br>whistle6-3 | Composite<br>whistle7-3 |
| Hartmann<br>whistle4 | Composite<br>whistle1-4 | Composite<br>whistle2-4 | Composite<br>whistle3-4 | Composite<br>whistle4-4 | Composite<br>whistle5-4 | Composite<br>whistle6-4 | Composite<br>whistle7-4 |

For each composite whistle through to pressure from 0.18 to 0.4, spray chamber to observe changes in their

within a certain range, and Other factors unchanged, The thicker the reed, the greater the frequency. Compare got tables, within a certain range, and Other factors unchanged, The shorter the length of the reed, the greater the frequency.

3.4 the composite post of hartmann whistle and whirlpool whistle

Will the exit of the spiral whistle with Hartmann whistle nozzle inlet connected on forming the composite whistle, get the combination types are shown in Tab.4 below:

distance, frequency and sound pressure level.

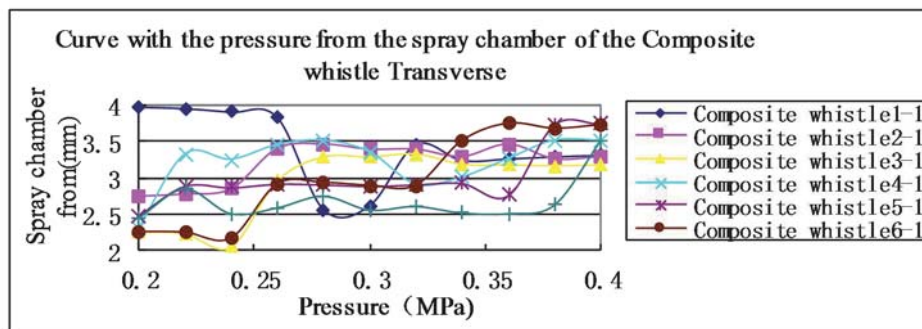


Figure7. Curve with the pressure from the spray chamber of the Composite whistle

Fig.7 is a composite whistle spray chamber with pressure from the curve, for each variable in the group for the transverse vortex whistle cylindrical cavity diameter, according to each line chart can be seen between pressure and the chamber spray distance roughly There was a positive correlation.

Under the same pressure, comparing the corresponding composite whistle variable is the ratio of the nozzle diameter and the diameter of cavity, the smaller the ratio, and the diameter of the spiral whistle, the greater the composite whistle, the best voice acoustic area location to the nozzle distance is relatively large, the opposite is smaller. Because of the existence of spiral whistle can adjust the air flow, make the compound of acoustic signal is stable, less vocal zone length, adjustable range larger, more helpful in practical application.

Composite whistle, the acoustic area the best location

of the acoustic radiation sound pressure level is lower than single Hartmann whistle, and the Hartmann whistle resonant cavity and the ratio of the nozzle diameter increase, separate Hartmann whistle sound pressure level is relatively reduced.

3.5 the composite post of hartmann whistle and reed whistle

the composite post of whirlpool whistle and reed whistle

The method of analysis by Hartmann and vortex whistle whistle to analyze complex and Reed Hartman whistle whistle composite vortex composite whistle whistle with reed. Hartmann whistle select a different reed whistle, vortex whistle, composed of a variety of composite post, provide a different pressure to give each group a composite whistle spray chamber distance, frequency and sound pressure level curve and analyzed.

3.6 reed hartman whistle composite structure of the new design --h-r forte complex post

Finally, a composite consisting of several single three whistle whistle and compare concluded loudest composite reed whistle whistle Hartmann composed, but Hartmann whistle with a composite vortex whistle whistle interference best, in addition, from the simple point of view, Hartmann whistle better, loudness is better. Ultimately, this passage devised a complex and reed whistle whistle Hartmann composition, the effect is shown below in Fig.8:

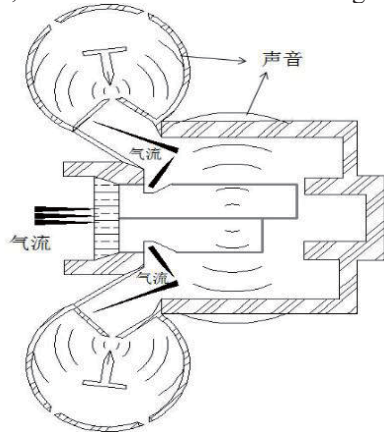


Figure8. Chart of Hartman and reed whistle whistle of a composite

Figure8 is the sectional view of a composite whistle ,whose middle part is Hartmann whistle(More than the average Hartmann whistle will sound) . next

spring around four holes to increase the loudness.

#### REFERENCES

- [1]R.F.Mcalevy , A.Pavlak.Tapered resonance tubes: some experiments[J]American Institute of Aeronautics and Astronautics, 1970,8 (2): 571-572
- [2]BinLu.Application of hydrodynamic Sounders in oil industry[J].Physics and high-tech, 2003,278 ~ 281.
- [3]XianYan Wang. Experimental study on the properties of the composite whistle[D].Shanxi Normal University, 2012.05.
- [4]Jiawei Liu.Simulation of chistle noise using computational fluid dynamics and acoustic finite element simulation. University of Kentucky.2012.
- [5]BinLu.Hartmann acoustic sounder acoustic propagation characteristics and applied research[J].Petroleum University (Natural Science), 2004,6 (10) :123~125.
- [6]Yangyang Li, Mingduo Zhang, Shuangwen Ma, JingYan.Vortex whistle internal flow field analysis [J] Shanxi Normal University (Natural Science Daily), 2014,42 (1): 46 ~ 51.
- [7]Xianyan Wang , Juan Li.HartmannReed whistle and whistle works and application status.Applied Optics, 2013,31 (12) :212~215
- [8]Yurong Lei.H-VStudy the acoustic properties of the composite fluid sounder[D].Shaanxi Normal University, 2010,5.

# CPU Utilization-based Energy Consumption Model in Cloud Computing

Zhang Gang, Dai Lu

School of computer, Dongguan university of technology, Dongguan, China, 523808

**ABSTRACT :** This paper aims to set a proper and reliable energy consumption model for the server of the Cloud Data Center based on the cloud infrastructure, as well as analyze the effects of different sample modes and mathematical methods on the energy consumption model. Firstly, this paper introduced the characteristics of the nonlinear energy model; then verifies the validity of the energy consumption model proposed by this paper based on the research achievements of this model in terms of the algorithms and experiments. This energy consumption model can also be applied to other researches on energy.

**KEYWORDS:** cloud computing; energy consumption model; nonlinear regression model

## 1. INTRODUCTION

Energy model is an important part for the cloud data center. It is necessary for the users and administrators to know how their behaviors are affecting the energy consumption of the computers in the ceaselessly operated Cloud Data Center, so as to take appropriate adjusting measures to optimize the energy efficiency. [1] Stiff increases in energy price and the environmental impact of carbon dioxide emissions associated with energy generation and transportation have forced the issue of reducing energy consumption to be extended to a broader range of system including High Performance Computing Systems (HPCS). In addition to power-aware battery-based systems, the issue of energy consumption has recently attracted a great amount of attention in high performance computing systems (HPCS). Energy consumption issue in such systems can be classified into three groups: (1) system-level resource allocation, (2) service-level energy-load distribution, and (3) task scheduling level. [2]

## 2. ENERGY CONSUMPTION DATA REGRESSION ANALYSIS METHOD

Regression analysis is a kind of effective processing variable correlation between tool, its aim is to forecast the change of the variable to estimate or predict based on known. According to the response variables to forecast a certain control, the energy consumption data of random regression analysis research should be the change of variables. In particular, Energy consumption of variable (y) and variable x (resource utilization), the relationship between them, for the determination of each of the x, y is one who has a certain distribution of random

variable, then (x) is called back to  $x = y \mu(x)$ , the fundamental problem of the regression analysis. The  $Ey = \mu(x)$  seeks the mean value of the function relationship between x and y expression, or for the return of the y to x.

### 2.1 The least square estimation of the multivariate linear model

The common methods of obtaining the estimation value of regression parameter  $\beta_0, \beta_1, \beta_2, \dots, \beta_p$  through sample data are Ordinary Least Square Estimation, OLSE and Maximum Likelihood Estimation, MLE. It is notable that the MLE is completed under the assuming of normal distribution of  $\varepsilon_i \sim N(0, \sigma^2 I_p)$ , while OLSE has no requirements on the distribution assuming. This paper mainly aims to study the improvement on the OLSE of the commonly used parameter estimation methods, thus the following contents only briefly introduced the OLSE. [19]

OLSE is adopted in the estimation of the regression model  $y = X\beta + \varepsilon$  expressed by the matrix form in the formula (3), and the estimation of the unknown parameter  $\beta_0, \beta_1, \beta_2, \dots, \beta_p$ , i.e. find the estimation value of parameter  $\beta_0, \beta_1, \beta_2, \dots, \beta_p$  to minimize the sum of squares of deviations. The  $\hat{\beta}_0, \hat{\beta}_1, \hat{\beta}_2, \dots, \hat{\beta}_p$  obtained from the above formula is the OLSE of the regression parameter  $\beta_0, \beta_1, \beta_2, \dots, \beta_p$ . The  $\hat{\beta}_0, \hat{\beta}_1, \hat{\beta}_2, \dots, \hat{\beta}_p$  obtained from the above formula is a problem of seeking the extreme value. According to the principle of seeking the extreme value in calculus,  $\beta_0, \beta_1, \beta_2, \dots, \beta_p$  should meet the following equation set:

$$Q(\beta_1, \beta_2, \dots, \beta_p) = \sum_{i=1}^n (y_i - \beta_0 - \beta_1 x_{i1} - \beta_2 x_{i2} - \dots - \beta_p x_{ip})^2 \quad (3)$$

$$\begin{aligned} Q(\hat{\beta}_1, \hat{\beta}_2, \dots, \hat{\beta}_p) &= \sum_{i=1}^n (y_i - \hat{\beta}_0 - \hat{\beta}_1 x_{i1} - \hat{\beta}_2 x_{i2} - \dots - \hat{\beta}_p x_{ip})^2 \\ &= \min_{\beta_1, \beta_2, \dots, \beta_p} \sum_{i=1}^n (y_i - \beta_0 - \beta_1 x_{i1} - \beta_2 x_{i2} - \dots - \beta_p x_{ip})^2 \end{aligned} \quad (4)$$



$$\begin{cases} \left. \frac{\partial Q}{\partial \beta_0} \right|_{\beta_0=\hat{\beta}_0} = -2 \sum_{i=1}^n (y_i - \hat{\beta}_0 - \hat{\beta}_1 x_{i1} - \hat{\beta}_2 x_{i2} - \dots - \hat{\beta}_p x_{ip}) = 0 \\ \left. \frac{\partial Q}{\partial \beta_1} \right|_{\beta_1=\hat{\beta}_1} = -2 \sum_{i=1}^n (y_i - \hat{\beta}_0 - \hat{\beta}_1 x_{i1} - \hat{\beta}_2 x_{i2} - \dots - \hat{\beta}_p x_{ip}) x_{i1} = 0 \\ \dots \dots \dots \\ \left. \frac{\partial Q}{\partial \beta_p} \right|_{\beta_p=\hat{\beta}_p} = -2 \sum_{i=1}^n (y_i - \hat{\beta}_0 - \hat{\beta}_1 x_{i1} - \hat{\beta}_2 x_{i2} - \dots - \hat{\beta}_p x_{ip}) x_{ip} = 0 \end{cases} \quad (5)$$

When  $(X'X)^{-1}$  exists, the OLSE of the regression parameter is

$$\hat{\beta} = (X'X)^{-1}X'y \quad (6)$$

and

$$\hat{y} = \hat{\beta}_0 + \hat{\beta}_1 x_1 + \hat{\beta}_2 x_2 + \dots + \hat{\beta}_p x_p \quad (7)$$

is called as experience regression equation.

### 3 THE EXPERSED ON THE SYATEM CONSUMPTION

Experimental parameters: cloud environment includes a data center, composing of N heterogeneous physical hosts, which is divided into two types according to the CPU processing capacity, and expressed by 1800MIPS and 2600MIPS. The two types of hosts (table 1) include two processing elements, i.e. CPU and memory RAM are 4G, band width is 1GB/S, storage space is 1 GB. The maximum energy consumption of the two hosts is 120W and 140W respectively.

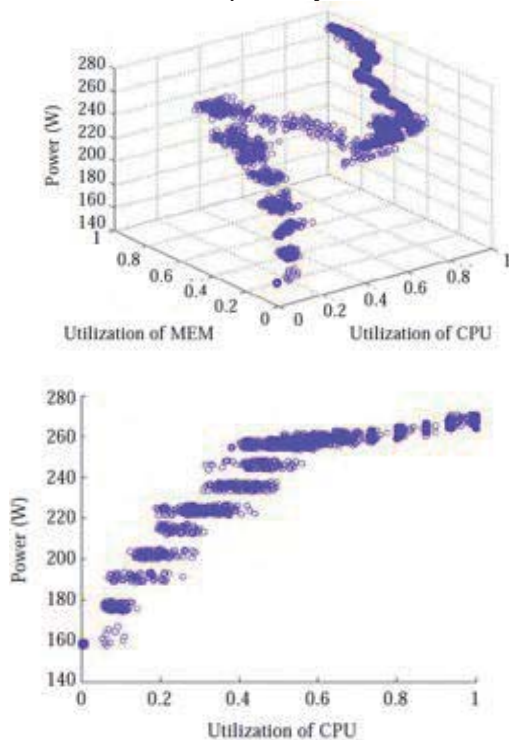


Figure.1 Relationship between system utilization and full-system power

### 4. CONCLUSION

Based on the system utilization, this paper combined with nonlinear Regression, including the least square regression and principal components regression, bridge regression, as well as analyzed and summarized the influence of different parameters and methods on server energy consumption modeling.

### ACKNOWLEDGEMENT

This paper was supported by the program of Popular science series into the campus Guangdong Province (NO.2014A070710018)

### REFERENCE

- [1]Moreno-Vozmediano R, Montero RS, Llorente IM. Key challenges in cloud computing: Enabling the future Internet of services. *Internet Computing*, IEEE, 2013,17(4):18–25. [doi: 10.1109/MIC.2012.69]
- [2]Barbulescu M, Grigoriu RO, Neculoiu G, Halcu I, Sandulescu VC, Niculescu-Faida O, Marinescu M, Marinescu V. Energy efficiency in cloud computing and distributed systems. In: *Proc. of the 2013 14th RoEduNet Int'l Conf. on Networking in Education and Research*. IEEE, 2013. 1–5. [doi: 10.1109/RoEduNet.2013.6714197].
- [3]Fan X, Weber WD, Barroso LA. *Power provisioning for a warehouse-sized computer*. *ACM SIGARCH Computer Architecture News*, 2007,35(2):13–23. [doi: 10.1145/1250662.1250665]
- [4]Hsu CH, Poole SW. Power signature analysis of the SPECpower\_ssj2008 Benchmark. In: *Proc. of the 2011 14th IEEE Int'l Symp.on Performance Analysis of Systems and Software (ISPASS)*. IEEE, 2011. 227–236. [doi: 10.1109/ISPASS.2011.5762739].
- [5]Lewis AW, Ghosh S, Tzeng NF. Run-Time energy consumption estimation based on workload in server systems. *HotPower*, 2008,8:17–21.
- [6]Kliazovich D, Bouvry P, Khan SU. GreenCloud: A packet-level simulator of energy-aware cloud computing data centers. *The Journal of Supercomputing*, 2012,62(3):1263–1283. [doi: 10.1007/s11227-010-0504-1]
- [7]Kliazovich D, Bouvry P, Khan SU. DENS: Data center energy-efficient network-aware scheduling. *Cluster Computing*, 2013,16(1): 65–75. [doi: 10.1007/s10586-011-0177-4].



# Study on Heating Supply Load Forecasting Based on Sparse Kernel Partial Least Squares

Yuanxiong Fu, Lijun Zhao and Chao Han

Beijing Jingneng Future Gas-fired Thermal Power Co., Ltd., Beijing, China

**Abstract:** Accurate heating load forecasting plays an important role in the regulation of heating system, and according to the predicted heat load heating control system, the control units of the system can be adjusted in a timely manner to achieve the maximum energy efficiency of heating system. A better method of sparse kernel partial least squares was proposed, the data amount is decreased in the training process by sparse in high dimension feature space, and the processing speed was improved. The simulation result shows that the algorithm has a better forecasting accuracy compared with the method of PLS.

**Keywords:** Heating load forecasting, sparse kernel partial least squares, forecasting accuracy

## 1. INTRODUCTION

The change of heating load of heating system is firstly analyzed in heating load forecasting, and then it achieves accurate prediction of heat load according to the factors which influence the load change. The factors includes user behavior, the outdoor temperature and meteorological parameters etc. Accurate heating load forecasting plays an important role in the regulation of heating system, and according to the predicted heat load heating control system, the control units of the system can be adjusted in a timely manner to achieve the maximum energy efficiency of heating system.[1-2]

Based on the past heating experience, heating load forecasting considers the climate, heating area and other factors, and it makes estimates or forecasts of calorific requirement of a certain period of time of the future through the historical data analysis. Heating load forecasting methods can be divided into four categories according to the prediction period difference of the prediction models: ultra short term load forecasting, short term load forecasting, medium-term load forecasting and long term load forecasting.[3]

With the increase of the forecast period, the error of the prediction method usually increases, but the error growth rate is not the same. Heating system has large hysteresis, scheduling valve switch and the unit dispatch will cause some loss of time to a certain extent and the response parameters also needs a certain time in the process of transformation of control strategy. Therefore, the ultra short term heating load forecasting in the actual operation can not be timely response and it has little study

significance. In contrast, medium and long term heating load forecasting has a very wide range of significance.

## 2. ANALYSIS of CLASSIFICATION and CHARACTERISTICS of HEATING LOAD.

The type of heat users can be divided into heating, ventilation, air conditioning, hot water and production technology etc. Heating, ventilation and air conditioning heating load belong to seasonal heating load. Seasonal heating load is closely related to the climatic conditions of outdoor temperature, humidity, wind speed, wind direction and sunshine etc, and among them outdoor temperature has the greatest effect. Therefore, seasonal heating load has great changes in a year, but has relatively small fluctuations in a day. Hot water and production technology heating load belong to annual heating load, the impact of climate conditions is small, that is it has little change in the whole year, but it has larger change in a day.[4]

Heating load is random. There is a certain fluctuation of heating load, so the load is random. Generally, the factors that affect the randomness of heating load generally are: political factors, traditional festivals and the weather etc. Heating load also has a periodic characteristic. Load changes in heating system is regular, it is mainly reflected in the periodicity of the load variation, and the periodicity includes daily, weekly and monthly periodicity.

## 3. KERNEL PARTIAL LEAST SQUARES

PLS can model a linear relationship between matrix  $\mathbf{X}(n \times N)$  and  $\mathbf{Y}(n \times M)$  which are both scaled and centered. The non-linear iterative partial least squares (NIPALS) algorithm is applied to the PLS regression in order to extract the latent vectors  $t, u$  and the weight vectors  $w, q$  from the matrices  $\mathbf{X}$  and  $\mathbf{Y}$  in decreasing order of their corresponding singular values. As a result, PLS decomposes  $\mathbf{X}$  and  $\mathbf{Y}$  into the form[5-6]

$$\begin{aligned} \mathbf{X} &= \mathbf{TP}^T + \mathbf{F} \\ \mathbf{Y} &= \mathbf{UQ}^T + \mathbf{G} \end{aligned} \quad (1)$$

where the  $\mathbf{T}$ ,  $\mathbf{U}$  are  $(n \times p)$  matrices of the extracted p score vectors (components, latent vectors), the  $(N \times p)$  matrix  $\mathbf{P}$  and the  $(M \times p)$  matrix  $\mathbf{Q}$  represent matrices of loadings and the  $(n \times N)$  matrix  $\mathbf{F}$  and the  $(n \times M)$  matrix  $\mathbf{G}$  are the matrices of residuals.

The PLS model can be also expressed with regression coefficient  $\mathbf{C}^{PLS}$  and the residual matrix  $\mathbf{G}$  as follow:

$$\mathbf{Y} = \mathbf{XC}^{PLS} + \mathbf{G} \quad (2)$$

where regression coefficient  $\mathbf{C}^{PLS}$  can be calculated as follow :

$$\mathbf{C}^{PLS} = \mathbf{W}(\mathbf{P}^T \mathbf{W})^{-1} \mathbf{BQ}^T \quad (3)$$

where the matrix  $\mathbf{W}$  consist the weight vectors  $w$  from the matrices  $\mathbf{X}$ ,  $\mathbf{B}$  is a diagonal matrix which represents the regression coefficient between  $\mathbf{T}$  and  $\mathbf{U}$ . Due to the fact that

$$\begin{aligned} \mathbf{p}_i^T \mathbf{w}_j &= 0 & i > j \\ \mathbf{p}_i^T \mathbf{w}_j &\neq 0 & i < j \end{aligned} \quad (4)$$

the matrix  $\mathbf{P}^T \mathbf{W}$  is upper triangular and invertible, moreover, using the fact that

$$\begin{aligned} \mathbf{t}_i^T \mathbf{t}_j &= 0 & i \neq j \\ \mathbf{t}_i^T \mathbf{u}_j &= 0 & i < j \end{aligned} \quad (5)$$

then the following equalities can be derived:

$$\begin{aligned} \mathbf{W} &= \mathbf{X}^T \mathbf{U} \\ \mathbf{P} &= \mathbf{X}^T \mathbf{T} (\mathbf{T}^T \mathbf{T})^{-1} \end{aligned} \quad (6)$$

$$\mathbf{BQ}^T = \mathbf{Y}^T \mathbf{T} (\mathbf{T}^T \mathbf{T})^{-1}$$

Substituting (3.6) into (3.3) and using the orthonormality of all columns of the matrix  $\mathbf{T}$ , the matrix  $\mathbf{C}^{PLS}$  can be written in the following form

$$\mathbf{C}^{PLS} = \mathbf{X}^T \mathbf{U} (\mathbf{T}^T \mathbf{X} \mathbf{X}^T \mathbf{U})^{-1} \mathbf{T} \mathbf{Y} \quad (7)$$

Rosipal and Trejo [7-9] have extended the linear PLS model into its nonlinear kernel form. The K-PLS method is based on mapping the original input data into a high-dimensional feature space  $F$ . K-PLS can efficiently compute regression coefficients in high-dimensional feature spaces using non-linear kernel functions, and it avoids nonlinear optimization by utilizing the kernel function corresponding to the inner product in the feature space.

The nonlinear mapping  $\Phi(\cdot)$  is expressed as

$$\mathbf{x}_i \in \mathbb{R}^N \rightarrow \Phi(\mathbf{x}_i) \in F \quad \text{where } i=1,2,3,\dots,n$$

Denote  $\Phi$  as the  $(n \times S)$  matrix of mapped  $X$ -space data  $\Phi(x)$  into an  $S$ -dimensional feature space  $F$ .

In the feature space, the kernel trick is used as follows

$$\Phi(x_i)^T \Phi(x_j) = \mathbf{K}(x_i, x_j)$$

Note that  $\Phi\Phi^T$  represents the  $(I \times I)$  kernel Gram matrix  $\mathbf{K}$  of the cross dot products between all mapped input data points  $\Phi(x_i)$ . Similar to linear PLS, a zero mean nonlinear kernel PLS model is assumed. To centralize the mapped data in a feature space  $F$ , the following procedure must be applied

$$\mathbf{K} \leftarrow (\mathbf{I}_n - \frac{1}{n} \mathbf{1}_n \mathbf{1}_n^T) \mathbf{K} (\mathbf{I}_n - \frac{1}{n} \mathbf{1}_n \mathbf{1}_n^T)$$

where  $\mathbf{I}_n$  is an  $n$ -dimensional identity matrix and  $\mathbf{1}_n$  represents a  $(n \times 1)$  vector with elements equal to one. The regression coefficient  $\mathbf{C}^{KPLS}$  in K-PLS algorithm has the form

Table 1 Telecom North heat exchange station modeling data and calculation results

| Date<br>(year/month/day) | Daily mean<br>temperature<br>°C | Heating<br>load<br>GJ/h | Fitted values<br>GJ/h | Deviation<br>GJ/h | Deviation<br>ratio<br>% |
|--------------------------|---------------------------------|-------------------------|-----------------------|-------------------|-------------------------|
|--------------------------|---------------------------------|-------------------------|-----------------------|-------------------|-------------------------|

$$\mathbf{C}^{KPLS} = \Phi^T \mathbf{U} (\mathbf{T}^T \mathbf{K} \mathbf{U})^{-1} \mathbf{T}^T \mathbf{Y} = \Phi^T \mathbf{G} \mathbf{Y} \quad (8)$$

where  $\mathbf{G} = \mathbf{U} (\mathbf{T}^T \mathbf{K} \mathbf{U})^{-1} \mathbf{T}^T$ .

And to make prediction on training data we can write

$$\hat{\mathbf{Y}} = \Phi \mathbf{C}^{KPLS} \mathbf{Y} = \mathbf{K} \mathbf{G} \mathbf{Y} \quad (9)$$

For predictions made on testing points  $\{\mathbf{x}_i\}_{i=1}^l$  the matrix of regression coefficients have to be expressed as follow

$$\hat{\mathbf{Y}}_t = \Phi_t \mathbf{C}^{KPLS} \mathbf{Y} = \mathbf{K}_t \mathbf{G} \mathbf{Y} \quad (10)$$

where  $\Phi_t$  is the matrix of the mapped testing points and consequently  $\Phi_t \Phi^T$  represents the  $(l \times n)$  kernel matrix  $\mathbf{K}_t$  of cross dot products between testing points and training points.

#### 4. DATA PROCESSING EXAMPLE of HEATING LOAD FORECASTING

Theoretically the relationship between the heating load and the outdoor temperature is approximately linear, no clear weather feedback is given to determine the indicators to carry out heating and staffs often rely on experience to carry out the control of each link, which makes the current data and theoretical data has a large deviation. Therefore, more standardized data of the heating conditions is selected as a sample to determine the parameters of the prediction model.

Ideally, the more sample points, the more accurate the prediction results are. And the time interval of sample points is smaller, the sample points is mall. Sample data acquisition takes ten minutes as the least sampling interval. However, due to the special nature of the heating, it is usually continue heating according to experience after the determination of the outdoor temperature and in the heat exchanger station when the heating level reaches experience value, the flow valve should be closed. Therefore, if the choice of the time interval of the prediction model is too short, the validity of the data will be lost and will result in the deviation of prediction, so the choice of a day as the time interval of the prediction model is more reasonable. so choosing a day as the time interval of the prediction model is more reasonable.

In an intelligent network management platform, choosing December and January, a total of 62 days of outdoor temperature and heat of pipe network transmission of a heat exchange station, and take least squares fitting for all data. Initial data and calculation results of that two months are shown in Tab 1, Fig.1 is the fitting results of raw data for heating load and outdoor temperature, the horizontal axis is the outdoor temperature and The vertical axis is heating load. The fitting result is shown in the formula (11),  $R^2=0.1572$ .

$$y = 0.0054x^2 - 0.1063x + 5.6276 \quad (11)$$

|            |       |      |      |       |        |
|------------|-------|------|------|-------|--------|
| 2015/12/1  | 3.41  | 5.53 | 5.20 | 0.33  | 6.3%   |
| 2015/12/2  | 0.16  | 3.85 | 5.61 | -1.76 | -31.3% |
| 2015/12/3  | 1.58  | 5.22 | 5.45 | -0.23 | -4.2%  |
| 2015/12/4  | 2.51  | 5.05 | 5.33 | -0.28 | -5.2%  |
| 2015/12/5  | 0.48  | 5.53 | 5.58 | -0.04 | -0.8%  |
| 2015/12/6  | 2.87  | 5.06 | 5.28 | -0.22 | -4.2%  |
| 2015/12/7  | 3.41  | 4.52 | 5.20 | -0.69 | -13.2% |
| 2015/12/8  | 0.45  | 4.60 | 5.58 | -0.98 | -17.5% |
| 2015/12/9  | 3.87  | 3.90 | 5.14 | -1.23 | -24.0% |
| 2015/12/10 | 3.06  | 4.18 | 5.25 | -1.08 | -20.5% |
| 2015/12/11 | 4.27  | 4.31 | 5.08 | -0.76 | -15.0% |
| 2015/12/12 | 5.58  | 4.53 | 4.87 | -0.34 | -6.9%  |
| 2015/12/13 | 2.94  | 4.86 | 5.27 | -0.41 | -7.7%  |
| 2015/12/14 | 2.71  | 5.13 | 5.30 | -0.17 | -3.3%  |
| 2015/12/15 | 2.12  | 8.38 | 5.38 | 3.00  | 55.8%  |
| 2015/12/16 | 3.72  | 9.83 | 5.16 | 4.67  | 90.5%  |
| 2015/12/17 | 1.48  | 9.83 | 5.46 | 4.37  | 80.1%  |
| 2015/12/18 | 1.50  | 7.81 | 5.46 | 2.35  | 43.1%  |
| 2015/12/19 | -0.33 | 7.41 | 5.66 | 1.75  | 30.9%  |
| 2015/12/20 | 1.80  | 4.88 | 5.42 | -0.54 | -10.0% |
| 2015/12/21 | 0.40  | 4.80 | 5.58 | -0.78 | -14.0% |
| 2015/12/22 | 1.40  | 4.75 | 5.47 | -0.72 | -13.1% |
| 2015/12/23 | 0.50  | 4.78 | 5.57 | -0.79 | -14.3% |
| 2015/12/24 | 1.97  | 4.96 | 5.40 | -0.44 | -8.1%  |
| 2015/12/25 | 1.32  | 5.09 | 5.48 | -0.39 | -7.2%  |
| 2015/12/26 | 2.70  | 4.98 | 5.30 | -0.32 | -6.0%  |
| 2015/12/27 | 1.15  | 5.04 | 5.50 | -0.46 | -8.3%  |
| 2015/12/28 | -1.81 | 5.22 | 5.80 | -0.59 | -10.1% |
| 2015/12/29 | -3.99 | 5.67 | 5.97 | -0.29 | -4.9%  |
| 2015/12/30 | -7.36 | 5.51 | 6.12 | -0.60 | -9.9%  |
| 2015/12/31 | 0.22  | 5.14 | 5.60 | -0.46 | -8.2%  |
| 2016/1/1   | 2.07  | 4.87 | 5.38 | -0.52 | -9.6%  |
| 2016/1/2   | 0.90  | 5.05 | 5.53 | -0.48 | -8.7%  |
| 2016/1/3   | 0.79  | 5.08 | 5.54 | -0.46 | -8.3%  |
| 2016/1/4   | 2.31  | 4.93 | 5.35 | -0.43 | -7.9%  |
| 2016/1/5   | 1.16  | 4.95 | 5.50 | -0.55 | -10.0% |
| 2016/1/6   | 0.02  | 5.44 | 5.63 | -0.19 | -3.3%  |
| 2016/1/7   | -1.26 | 5.54 | 5.75 | -0.21 | -3.7%  |
| 2016/1/8   | -0.91 | 5.51 | 5.72 | -0.21 | -3.7%  |
| 2016/1/9   | -1.94 | 5.79 | 5.81 | -0.02 | -0.4%  |
| 2016/1/10  | 0.93  | 5.59 | 5.52 | 0.06  | 1.1%   |
| 2016/1/11  | -0.80 | 5.35 | 5.71 | -0.36 | -6.3%  |

|           |        |      |      |       |        |
|-----------|--------|------|------|-------|--------|
| 2016/1/12 | -0.46  | 5.35 | 5.67 | -0.32 | -5.7%  |
| 2016/1/13 | -0.07  | 5.86 | 5.64 | 0.23  | 4.1%   |
| 2016/1/14 | -4.26  | 6.01 | 5.98 | 0.03  | 0.5%   |
| 2016/1/15 | -1.03  | 5.75 | 5.73 | 0.01  | 0.3%   |
| 2016/1/16 | -0.44  | 5.65 | 5.67 | -0.02 | -0.3%  |
| 2016/1/17 | -0.10  | 5.25 | 5.64 | -0.39 | -6.9%  |
| 2016/1/18 | -0.55  | 4.88 | 5.68 | -0.81 | -14.2% |
| 2016/1/19 | -5.05  | 4.98 | 6.03 | -1.05 | -17.4% |
| 2016/1/20 | -8.74  | 5.76 | 6.14 | -0.39 | -6.3%  |
| 2016/1/21 | -6.33  | 6.05 | 6.08 | -0.03 | -0.5%  |
| 2016/1/22 | -5.25  | 6.49 | 6.04 | 0.45  | 7.4%   |
| 2016/1/23 | -3.81  | 6.59 | 5.95 | 0.63  | 10.6%  |
| 2016/1/24 | -8.57  | 7.52 | 6.14 | 1.38  | 22.4%  |
| 2016/1/25 | -14.22 | 8.41 | 6.05 | 2.36  | 39.1%  |
| 2016/1/26 | -9.11  | 8.71 | 6.15 | 2.56  | 41.7%  |
| 2016/1/27 | -1.29  | 8.28 | 5.76 | 2.52  | 43.9%  |
| 2016/1/28 | -1.25  | 7.25 | 5.75 | 1.50  | 26.1%  |
| 2016/1/29 | -1.94  | 6.64 | 5.81 | 0.83  | 14.3%  |
| 2016/1/30 | -0.52  | 6.40 | 5.68 | 0.72  | 12.6%  |
| 2016/1/31 | -2.92  | 6.30 | 5.89 | 0.40  | 6.9%   |

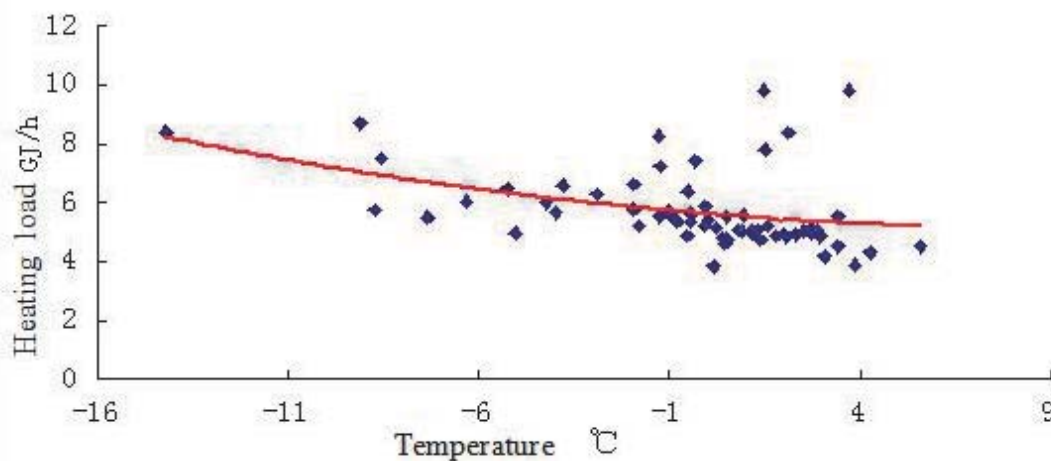


Figure 1 The fitting curve of Telecom North heat exchanger station heat load and outdoor temperature

It is can be seen through the fitting curve: the lower the outdoor temperature, the greater the heat supply. But there are some drift points will affect the results of the analysis. Sparse kernel partial least squares method proposed in this paper has been firstly used to sparse data in high dimension linear space, abnormal data has been eliminated and the fitting curve of heating load and outdoor temperature based on the

remaining sample points is shown in Fig. 2, data and calculation results after treatment of Telecom North heat exchange station is shown in Tab 2. Finally, the model expression of outdoor temperature and heat supply is obtained and it is shown in the formula(12),  $R^2=0.6424$ . Compared with the least square method, the method proposed in this paper is less error fitting.

$$y = 0.003x^2 - 0.1726x + 5.2672 \quad (12)$$

Table 2 Data and calculation results after treatment of Telecom North heat exchange station

| Date<br>(year/month/day) | Daily mean<br>temperature | Heating load<br>GJ/h | Fitted<br>values | Deviation<br>GJ/h | Deviation<br>ratio |
|--------------------------|---------------------------|----------------------|------------------|-------------------|--------------------|
|--------------------------|---------------------------|----------------------|------------------|-------------------|--------------------|

|            | °C    |      | GJ/h |       | %      |
|------------|-------|------|------|-------|--------|
| 2015/12/1  | 3.41  | 5.53 | 4.64 | 0.89  | 19.1%  |
| 2015/12/2  | 0.16  | 3.85 | 5.24 | -1.39 | -26.5% |
| 2015/12/3  | 1.58  | 5.22 | 4.99 | 0.23  | 4.6%   |
| 2015/12/4  | 2.51  | 5.05 | 4.82 | 0.23  | 4.9%   |
| 2015/12/5  | 0.48  | 5.53 | 5.18 | 0.35  | 6.7%   |
| 2015/12/6  | 2.87  | 5.06 | 4.75 | 0.31  | 6.5%   |
| 2015/12/7  | 3.41  | 4.52 | 4.64 | -0.13 | -2.7%  |
| 2015/12/8  | 0.45  | 4.60 | 5.19 | -0.59 | -11.3% |
| 2015/12/9  | 3.87  | 3.90 | 4.56 | -0.65 | -14.4% |
| 2015/12/10 | 3.06  | 4.18 | 4.71 | -0.53 | -11.3% |
| 2015/12/11 | 4.27  | 4.31 | 4.48 | -0.16 | -3.6%  |
| 2015/12/12 | 5.58  | 4.53 | 4.21 | 0.32  | 7.6%   |
| 2015/12/13 | 2.94  | 4.86 | 4.73 | 0.13  | 2.7%   |
| 2015/12/14 | 2.71  | 5.13 | 4.78 | 0.35  | 7.3%   |
| 2015/12/20 | 1.80  | 4.88 | 4.95 | -0.07 | -1.5%  |
| 2015/12/21 | 0.40  | 4.80 | 5.20 | -0.40 | -7.7%  |
| 2015/12/22 | 1.40  | 4.75 | 5.02 | -0.27 | -5.4%  |
| 2015/12/23 | 0.50  | 4.78 | 5.18 | -0.40 | -7.8%  |
| 2015/12/24 | 1.97  | 4.96 | 4.92 | 0.05  | 0.9%   |
| 2015/12/25 | 1.32  | 5.09 | 5.03 | 0.05  | 1.0%   |
| 2015/12/26 | 2.70  | 4.98 | 4.78 | 0.20  | 4.3%   |
| 2015/12/27 | 1.15  | 5.04 | 5.06 | -0.02 | -0.4%  |
| 2015/12/28 | -1.81 | 5.22 | 5.57 | -0.35 | -6.4%  |
| 2015/12/29 | -3.99 | 5.67 | 5.91 | -0.24 | -4.0%  |
| 2015/12/30 | -7.36 | 5.51 | 6.37 | -0.86 | -13.5% |
| 2015/12/31 | 0.22  | 5.14 | 5.23 | -0.09 | -1.6%  |
| 2016/1/1   | 2.07  | 4.87 | 4.90 | -0.03 | -0.6%  |
| 2016/1/2   | 0.90  | 5.05 | 5.11 | -0.06 | -1.2%  |
| 2016/1/3   | 0.79  | 5.08 | 5.13 | -0.05 | -0.9%  |
| 2016/1/4   | 2.31  | 4.93 | 4.85 | 0.08  | 1.6%   |
| 2016/1/5   | 1.16  | 4.95 | 5.06 | -0.12 | -2.3%  |
| 2016/1/6   | 0.02  | 5.44 | 5.26 | 0.17  | 3.3%   |
| 2016/1/7   | -1.26 | 5.54 | 5.48 | 0.06  | 1.1%   |
| 2016/1/8   | -0.91 | 5.51 | 5.42 | 0.09  | 1.6%   |
| 2016/1/9   | -1.94 | 5.79 | 5.59 | 0.20  | 3.6%   |
| 2016/1/10  | 0.93  | 5.59 | 5.10 | 0.48  | 9.4%   |
| 2016/1/11  | -0.80 | 5.35 | 5.40 | -0.05 | -0.9%  |
| 2016/1/12  | -0.46 | 5.35 | 5.35 | 0.01  | 0.1%   |
| 2016/1/13  | -0.07 | 5.86 | 5.28 | 0.58  | 11.1%  |
| 2016/1/14  | -4.26 | 6.01 | 5.95 | 0.06  | 1.1%   |
| 2016/1/15  | -1.03 | 5.75 | 5.44 | 0.30  | 5.6%   |



|           |        |      |      |       |        |
|-----------|--------|------|------|-------|--------|
| 2016/1/16 | -0.44  | 5.65 | 5.34 | 0.31  | 5.8%   |
| 2016/1/17 | -0.10  | 5.25 | 5.28 | -0.04 | -0.7%  |
| 2016/1/18 | -0.55  | 4.88 | 5.36 | -0.48 | -9.0%  |
| 2016/1/19 | -5.05  | 4.98 | 6.06 | -1.09 | -17.9% |
| 2016/1/20 | -8.74  | 5.76 | 6.55 | -0.79 | -12.1% |
| 2016/1/21 | -6.33  | 6.05 | 6.24 | -0.19 | -3.0%  |
| 2016/1/22 | -5.25  | 6.49 | 6.09 | 0.40  | 6.5%   |
| 2016/1/23 | -3.81  | 6.59 | 5.88 | 0.70  | 12.0%  |
| 2016/1/24 | -8.57  | 7.52 | 6.53 | 0.99  | 15.2%  |
| 2016/1/25 | -14.22 | 8.41 | 7.11 | 1.30  | 18.2%  |
| 2016/1/26 | -9.11  | 8.71 | 6.59 | 2.12  | 32.1%  |
| 2016/1/27 | -1.94  | 6.64 | 5.59 | 1.05  | 18.8%  |
| 2016/1/28 | -0.52  | 6.40 | 5.36 | 1.04  | 19.5%  |
| 2016/1/29 | -2.92  | 6.30 | 5.75 | 0.55  | 9.6%   |
| 2016/1/30 | -4.37  | 6.11 | 5.96 | 0.15  | 2.5%   |
| 2016/1/31 | -2.72  | 6.09 | 5.71 | 0.38  | 6.6%   |

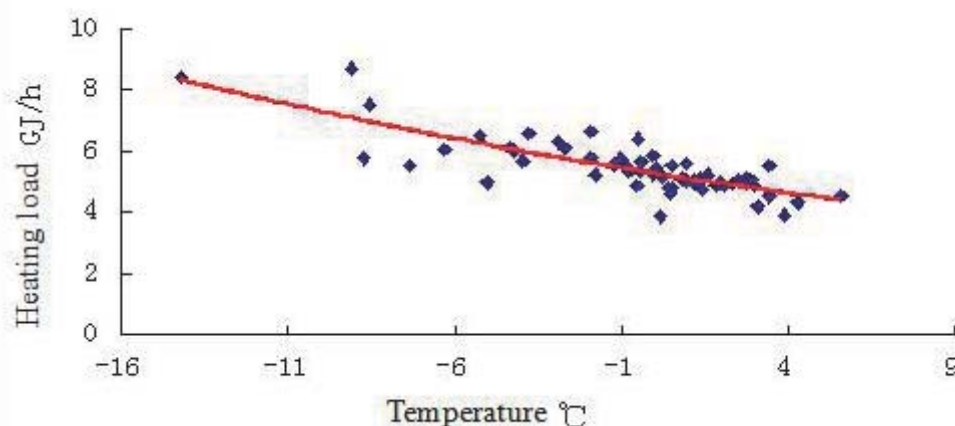


Figure 2 The fitting curve of Telecom North heat exchanger station heat load and outdoor temperature

#### 4.CONCLUSIONS

Heating load forecasting is a very complex work, the influence of many factors affect the change of the load. It is greatly affected by human factors, social events, meteorology etc., but these effects is often not accurate and quantitative description. Thus, the prediction is difficult. Sparse kernel partial least square method is used in this paper, firstly, Firstly, sparse in high dimensional linear space, and then the load is predicted by the partial least square method. Experimental results show that the proposed algorithm has higher prediction accuracy compared with the traditional method.

#### REFERENCE

[1] Jiayuan Dai, Lin wang, Youwei Zhang, Research and application of super short term heating load forecasting technology, Jiangsu Electrical

Engineering, 2013,32(5):74-76

[2] Pi Luo, JiChang Guo, and Keng Li, Discussion on Modeling Based on partial least squares regression, Journal of Tianjin University, 2002,35(6):783-786

[3] Bennett K P, Embrechts M J.An optimization perspective on kernel partial least squares, Proceedings of the NATO Advanced Study Institute on Learning Theory and Practice .2003:2 -21.

[4] Dingcheng Wang, Bin Jing, Research on online sparse least squares support vector machine regression, Control and Decision Making,2007,22(2):132-137

[5] Hipper H S, Pefreira C E, Souza R C, Neural network for short -term load fo recasting :A review and evaluation, IEEE Trans Power System .2001 , 16 (2):44-54

[6] Ziyang Liu, Li Feng, Application of information theory and data mining in power load forecasting,

Modern Machinery, 2003, (5):73-75

[7] Huiwen Wang, Partial least squares regression method and its application, Beijing:National Defence Industry Press,1999

[8] Engel Y, Mannor S, Meir R, Sparse online greedy

support vector regression , In 13th European Conference on Machine Learning, 2002

[9] Downs T, Gates K, Masters A, Exact simplification of support vector solutions, Journal of Machine Learning Research, 2001, (2):293 -297

# Current Situation Review of the Micropile

Dong Liu, Jiaming Zheng and Lang Liu

Civil Engineering, Chongqing University, Chongqing, China

**Abstract:** As a kind of supporting and blocking structure, micropiles are comprehensively studied and widely applied to foundation engineering and the regulation projects of landslides and slopes. The current domestic research on the utilization and development of the micro anti-slide piles is discussed in the paper, with the new combination of micropiles and other anti-slide facilities and its current situation, experimental and theoretical breakthrough included. Problems on the utilization and development of the micropiles, based on all these parts, are also pointed out.

**Keywords:** anti-slide micropile, engineering application, experimental research, design calculation

## 1. INTRODUCTION

The Micropile is defined as a 70-300mm wide bored pile [1] with enforcement bars injected. It is generally called root pile. A root pile has a small diameter, the ratio of length and width of it generally over 30. It is manufactured through bore, reinforcement, pressure grouting process or else. Strengthening elements, such as reinforcement bars, section steel and steel pipes, are added to the pile to meet the practical needs in engineering.

The major advantages [2] of a Micropile are as below:

- (1) Low settlement and high bearing capacity. The bearing capacity of a Micropile, made through second grouting, belling or other techniques, can be higher than a pile with identical size;
- (2) Small pore size. Hence the pile barely causes additional stress to the foundation and ground. Buildings can be normally used during the constructing of a Micropile;
- (3) Rapid and convenient constructing process. The construction site covers a small piece of ground. It takes a short duration. Vibration and noises are mild. Thereby, it is advantaged particularly in communities with strict restricts of environmental pollution;
- (4) Ability to be injected in diverse kinds of soil. It works well on moderately weathered rock, clay, sand soil, expansive soil, collapsible soil. A slightly modified pile is suitable for karst areas;
- (5) Ability to bear vibration and cyclic loading.

Benefit from the advantages above, Micropile is adopted originally in reconstruction of old buildings, reinforcement and rectification of old constructions, foundation underpinning and else. Later on, the study and utilization of micropiles has enlarged its domain over foundation engineering, landslide and slope regulation.

Currently, the systematic and deep understanding of the theory has not formed about the combined effect

of micropiles and surrounding rock mass, and the study about the new combination of micropiles and other anti-slide facilities is less than others. Thus, analysis and summary to the current theoretical calculation and experimental study have important significance for future depth research and application of engineering practice.

## 2. Current Engineering Application

Micropiles terminated its patent life in 1972, and so far had been widespread and applied [3] around the world. They have long been utilized and researched home and abroad mostly on axial loading bearing, while the transverse loading bearing has barely entered researchers' view.

Since 1990s, Local scholars have adopted micropiles to the regulation projects of moderate slopes and landslides [1], using experience of engineering home and abroad for reference. In the 21st century, many of the regulation projects of moderate slopes and landslides have successfully made great profit.

In 2010, Xiao Chunjin [4] adopted micropiles to the strengthening of landslide in Hongyan stream. The stream was located in Changyang county, Yichang, Hubei province. The landslide had been creeping for long. In this strengthening project, a 3-row 5-colum array of micropiles were placed at the upper middle part of the landslide. Piles of each one row were vertical to the ground and connected together by 120mm wide coupling beams on the top of them. The beams were A60mm seamless steel pipes grouted with C20 concrete under pressure. With such beams, piles of one row were integrated to become a pile frame. There were three pile frames, A, B, and C, each was set 1-meter away from the other. A was 25-meter-long, B 30-meter-long, C 20-meter-long. From an overview of them, the piles were placed in equilateral triangular shape so as to make a plum blossom shape.

Zhoulei and someone else set micropiles on the excavation spots of the cutting slope in K51+103—+205, Guangba (Guangyuan-Bazhong) highway. A 3-row 9-colum array of piles were placed at the lower middle part of the landslide. Each row was 0.6m away from the other, and each pile was 0.5m away from the other in one row. The middle row of piles were vertical while two other rows of piles were 15° inclined from the vertical line. Each pile was 12m long 130mm wide, and was equipped in its core with three 32HRB400 reinforcement bars, grouted with cement slurry under 0.2-0.3MPa pressure.

In 2013, landslide frequently occurred in Xiangong town, Chencang, Baoji province, due to rainfall and excavating on the foot of slopes. Zhang Dongdong [6] set a 3-row 6-colum array of micropiles at the middle

part of the landslide. Each row was 1m away from the other, and each pile was 1m away from the other in one row. Piles of one row were vertical and connected together by 200mm wide coupling beams on the top of them. The beams were A108mm seamless steel pipes grouted with slurry under 0.5-3MPa pressure.

In 2014, Gao Peng<sup>[7]</sup> used three rows of micropiles to protect some coal gangue hill against landslide. They were placed as an array, too. Each row was 1.5m away from the other, and each pile was 1.5m away from the other in one row. Piles of one row were vertical and connected together by 150mm wide coupling beams on the top of them. Each row was strapped by 6A22mm reinforcement bars, which were grouted with slurry under 0.4-0.7MPa pressure.

Concluding from domestic precedents of micro anti-slide pile projects, it is orthodox to set an array of many piles to prevent landslide. Each pile is set vertical or some degree inclined. There are generally coupling beams or top beams to unite piles.

The unity of piles can be made of completely vertical micropiles, or be made of completely inclined micropiles, or the combination of vertical and inclined ones<sup>[1]</sup>. It is commonly used in moderate shallow landslides and cutting slopes as a protection. When the previously built protective constructions on landslides and slopes are crashing, the micropiles can be an emergency treatment, or a temporary anti-slide measure to protect workers who are constructing. Micropiles are flexible to allocate. They can be set from the upper middle to the bottom of landslides as a major anti-slide construction, or be set on the top of landslides to prevent the enlargement of landslide so as to make time for regulation treatments.

The micro anti-slide piles for consolidating landslides are commonly 90mm wide to 200mm wide. Of them the 150mm wide piles are mostly used. The reinforcements inside piles are commonly reinforcement bars, steel pipes or joists. 2 rows to 6 rows of piles are common, mostly 3 rows. Piles are set either into an array or into a plum blossom shape. Gravity grouting and primary pressure grouting are adopted as general techniques of grouting, whereas some projects adopted second pressure grouting. The length is generally 8-20m, no longer than 25m.

As regulation projects with micropiles gradually come to practice, the new combinations of micropiles and other anti-slide measures has mushroomed. There are four major forms:

#### (1) Combination of micropiles and retaining walls<sup>[8]</sup>

This combination can be sorted out according to the logic of structure into two modes. One, construction mode. In this mode the micropiles are preset to enhance the bearing capacity of the foundation and the capability against deviation and stability of the retaining walls. First, set a group of vertical or inclined micropiles. When the retaining walls are constructing, anchor the micropiles to the foundation or body of the retaining walls. Two, consolidation

mode. Use micropiles to consolidate the retaining walls if they don't live up to the anti-slide need for somewhat. By directly drilling on the wall bodies or foundation and set micropiles there, the Micropile-retaining wall structure is established. It effectively diminishes the depth of foundation and enhances the capability against tumbling and slipping. It is a good solution for treatments of moderate landslides and consolidation projects of damaged retaining walls.

#### (2) Combination of micropiles and prestressed anchor<sup>[9]</sup>

When the top of the hill building requirements more sensitive to deformation slip surface or buried deeper landslide thrust is large, the added anchors on coupling beams or top beams of the Micropile unity can elongate the strength against slipping and reduce the pile top displacement. This combination draws anchor pile structural characteristics, effectively overcome the anti-slide pile top displacement miniature big disadvantage.

#### (3) Combination of micropiles and pressure grouting technique

It is easy to construct and the structure is advantageous to bear load. It is accomplished generally by setting several rows of holes, and stick steel floral tubes into pores. Grout the pores under pressure and consolidate the rock and soil around piles so as to make a consistent composite. It is suitable to be used in landslide and slope consolidation in a wet land.

#### (4) Combination of micropiles and normal anti-slide piles

This approach can ensure construction safety. It usually uses micropiles to consolidate the landslides, thus to play the role of a temporary retaining, and then set the normal anti-slide piles, or set micropiles at the bottom of the anti-slide piles, anchor the top of the micropiles to the anti-slide piles, thereby effectively increase the skid resistance of micropiles.

### 3. EXPERIMENTAL BREAKTHROUGH

There are commonly three methods of research on the properties of micro anti-slide piles: indoor small proportion geotechnical simulation, large proportion or real size field test, and computational simulation using numerical calculation software.

Wu wenping<sup>[11]</sup> designed a simulation test in 2009 based on some possible forms of micropiles in engineering. He proposed a simplified calculation model of Micropile unities and calculation samples for uniform loading. His model and samples were on the basis of the analysis of test data and under assumption where the impacts of soil off the landslide on the upper body of the hill to the piles were omitted. Results showed that the rigidity of Micropile unities was much lower than normal anti-slide piles. And the adhesive strength between soil and piles was much lower than anti-slide piles' case, where the reinforcement bars in the piles were stuck in the

concrete.

For the transverse loading bearing capability, there are currently scholars who has proved from transverse loading experiments that micropiles are good at bearing transverse loading. In particular, inclined micropiles can considerably diminish the displacement of piles caused by transverse loading. For the axial loading bearing capability, there are no estimation formula of bearing capacity in domestic standards at present. Exotic ways of estimating are generally two: one is to see how deep the pile can be stuck in the soil, another is to see what kinds of anchors it uses. To make experiments safe to do, the first is mostly used.

In 2010, Yan Jinkai <sup>[12]</sup> researched the features of micropiles in treatments of landslides with a combination of methods of indoor physical modeling experiment, large scale physical modeling experiment and finite element numerical simulation. From the analysis of these experiments he concluded the principles of displacement of pile body, bending moment and shear force distribution, and worked out the collapse forms of micropiles, including single pile, a row of piles and an array of piles which can be equipped with different kinds of reinforcement bars.

In 2015, Shi Yusong <sup>[13]</sup> made a model of soil nailing walls combined with micro steel piles. A series of indoor experiments were made on that model. He collected the strain of soil nails, the displacement of slopes, the strain of steel piles and other data. With method of finite element analysis, he converted and analyzed the data, more clearly, he used traditional foundation pit design software, finite element analytical software to analyze the engineering samples he got, comparing them with actually measured data. Results showed micro steel piles are much better at bearing soil pressure in clay pit than in sand pit.

For the reasons that most domestic experiments are designed to test the axial load bearing capability, and the scale of such experiments are small, the results are limited for the study of landslide treatments.

Meanwhile, due to late beginning of the domestic application of new anti-slide structure, its calculation methods are incomplete. Actual experience and statistics rules are mostly used. The design of micropiles is conservative, which fail to make the most of the advantages of micropiles, and even causes large economical waste. For example, according to Composite Soil Nailing Wall Pit Supporting Technical Specifications (GB 50739-2011), the calculation takes only the soil nails into account, omitting the impacts of steel piles. Except for the verification of the stability of pit, where the impact of steel piles is considered a reduction coefficient.

The theory of the new combination forms, including the four forms mentioned in the paper, is incomplete. The internal forces and deformation inside those composite structures are still under researches.

Therefore, it is of practical use to have large scale

physical modeling experiments on landslide treatments, to study on the deformation principles of micropiles in landslide treatments, to study on their interaction, the displacement and deformation of soil body and the forces. These work and conclusions from the work can be a good guide for actual engineering.

#### 4. THEORETICAL BREAKTHROUGH

In terms of the current situation of engineering application, the design and calculation of micropiles are commonly an imitation of the calculation methods for normal anti-slide piles. The calculation methods are modified though according to the real constructing situation in order to meet practical needs in engineering. Definitely, there are two: one for single Micropile calculation, the other for united Micropile calculation.

Yang Xucheng <sup>[14]</sup> proposed a theory on the design of micropiles at the slopes to consolidate the edge of railways. Based on a simple logarithmic spiral failure mode (it was shown in Fig.1 and Fig.2), limit analysis upper limit theory is used to get stability equations of subgrade slope, single pile reinforcement slope reinforcement and multi-pile reinforcement slope reinforcement respectively. Considering micropile reinforcement energy effects, analysis of reinforcement stability of subgrade slope micropile and optimized design parameters expressions are put with. On the basis of comprehensive analysis of literature research, theoretical calculation and numerical simulation results, combined with the supporting information from the project site, the construction technology of micropile reinforcement railway subgrade slope and quality control method are summed up.

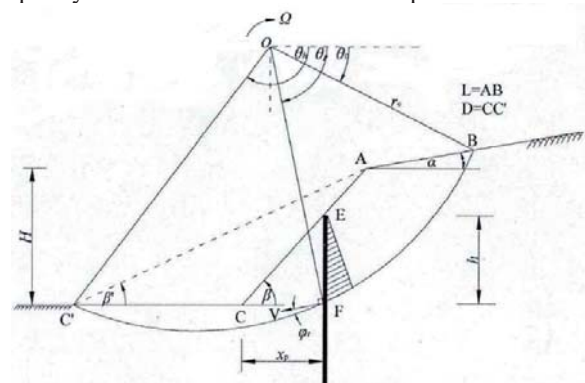


Figure 1. The left is the destruction mechanism of slope stability



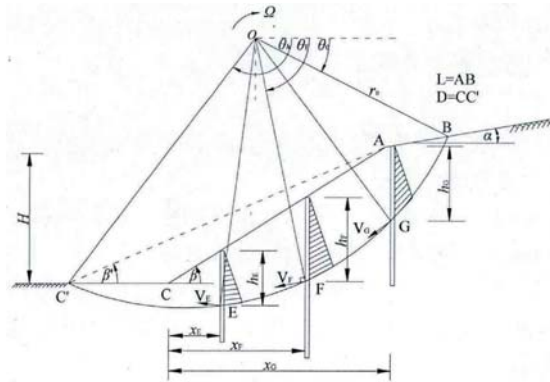


Figure 2. The right is the destruction mechanism of reinforced slope stability analysis by rows of micropiles

The results show that the micropile reinforcement can effectively improve the anti-deformation ability and overall stability of the embankment; Micropile has large deformation in loaded segment, little deformation in fixed end, and each row of micropiles bear the force and deformation simultaneously; bending moments, shear and deformation are basically equal among each pile; potential failure modes of micropile reinforcement subgrade slope are the combination damage of shear and bending; lateral force micropile group, when the pile spacing parallel to the direction of the load is under one time pile diameter and the pile spacing perpendicular to the direction of the load is under several times pitch, there will appear pile group effect.

Sun Shuwei [15] made a systematic research on the force mechanism of the micropiles and the consolidated slopes through engineering precedents, site investigation, theoretical analysis and numerical simulation or other methods. He explored how the constraint situation on the pile bodies and on the top of the piles would affect the safety coefficient of the slopes, and did numerical simulation on the force mechanism of the piles of different rows. By doing indoor experiment, he compared the force mechanism of the micropiles with normal anti-slide piles. He also

$$K = \frac{\sum_{i=1}^n [cL + (W + Q) \cos \alpha \tan \phi] + \sum_{i=1}^m \frac{T}{S_h} (\sin \beta \tan \phi + \cos \beta) + \sum_{i=1}^m \frac{T_c}{S_h} (\sin \beta - \cos \beta \tan \phi)}{\sum_{i=1}^n (W + Q) \sin \alpha} \quad (2)$$

Where,  $c$ ,  $\phi$  are the soil cohesion and internal friction angle at the bottom of the soil strip;  $W$ ,  $Q$  are the weight of the soil and the overload the top of the soil strip suffered (kN);  $T$ ,  $T_c$  are tension and shear of the soil nail on the sliding surface (kN), and  $T_c$  is known by the formula (1);  $L$  is the arc length of the soil strip (m);  $\alpha$  is the angle between the tangent of sliding surface and the horizontal line ( $^\circ$ );  $\beta$  is the angle between the tangent of sliding surface and the soil nail ( $^\circ$ );  $S_h$  is the horizontal spacing between near soil nails (m);  $n$ ,  $m$  are the number of soil nails and the of soil nails' layers.

studied the force mechanism of micropiles under the thrust force of the slopes, and the feasibility of micropiles as an alternative for traditional anti-slide piles.

Results from the modeling experiments showed that an array of micropiles can effectively support the soil and block landslide. Judging from the horizontal displacement of piles, the bearing capacity of micropiles is slightly smaller than normal anti-slide piles. They can be an alternative for normal anti-slide piles under certain conditions.

Nie Zhenjun [16] and else studied on the shear and bending deformation of soil nails, the layers of soil, and the shear capacity of the micropiles. They explored the analysis method for the stability of leading Micropile-soil nail composite, and proposed the formula to calculate the safety coefficient of the internal stability of the composite. We can study plastic analysis method in Fig.3.

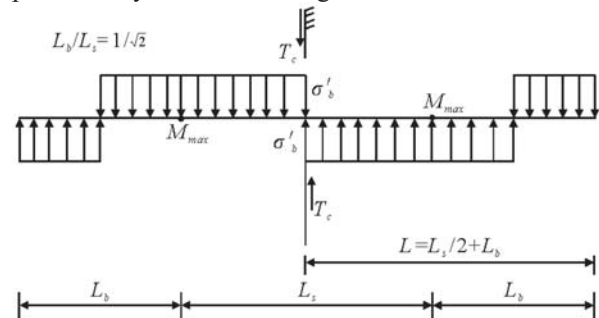


Figure 3. Bending and shear plastic analysis diagram  
By derivation, soil nail with a circular cross section suffered its biggest shear:

$$T_c = \frac{8D(T_p - T)}{3\pi L_s} \quad (1)$$

Where,  $T$  is the lever pull force;  $T_p$  is the lever by the critical tension;  $D$  is the diameter of the rod.

By derivation, in consideration of tension and shear [18], general soil nailing global safety coefficient can be calculated as follows:

Results showed that the safety coefficient is insensitive to the shear capacity of soil nails, the impact degree is within 5%. That is to say, the axial force capacity of soil nails is the main factor when doing stability analysis.

Lai Penghui [17] and else proposed another idea of composite system. It is a combination of micropiles and reinforced retaining walls. A couple of vertical micropiles and a couple of inclined micropiles stick through the reinforced backfill soil on the ground and are anchored in the foundation. Later on the bearing platforms and the foundation beams are poured on the

top of the piles. Other fabrics are used to make the guardrails on the highways, the foundation beams and the micro beams a complete constitution.

The numerical analysis of the stress and strain of retaining walls, compared with different fabrics of the retaining walls, showed that this composite system can effectively diminish displacement.

Compared with non-pile walls, single vertical pile walls, walls equipped with vertical piles and inclined anchors, and walls equipped with vertical piles and horizontal anchors, the displacement of the composite of micropiles and reinforced retaining walls is declined respectively by 46.9%, 34.6%, 33.3% and 22.7%. The bending deformation of vertical micropiles, compared with single vertical pile walls, walls equipped with vertical piles and inclined anchors, and walls equipped with vertical piles and horizontal anchors, is declined respectively by 72.7%, 72% and 47.7%. Hence the advantage of micropiles on deformation situation is validated.

The micropiles makes up the defects of reinforced soil retaining ramp wall--backfill area prone to the overall downward trend along the slope, so that the differential settlement of the pavement significantly reduce, and the enlarged pressure is effectively weakened.

To some extent, it reduce requirements about the retaining wall structure, making retaining wall easier to maintain stable in mountainous. Inclined reinforcing member use micropiles that have more bending and shearing capability in micropile--reinforced soil retaining wall, and it not only coordinates the force, also provides direct skid torque for the downward trend to backfill area. Calculation results also show that, in fact, inclined micropiles play a more important role in backfill area for inhibition of decline, so it is necessary to employ micropiles that have high bending and shearing resistance strength in the inclined direction.

## 5. PROBLEM AND SUGGESTIONS

As a supporting and retaining structure, micro anti-slide piles find a wide application in slope treatment, deep landslide repair and deep foundation pit support projects. In recent years, with the constant engineering practice that micropiles control landslide ongoing, new forms of anti-slide structures that micropiles combine with other slope treatments appears constantly. There exist some problems in dire need of deep researches and discusses of the masses of scientific researchers, including the following aspects.

(1) Experimental study of new forms of anti-slide structures that piles combine with other slope treatments is not complete. To solve this problem, model test researches specifically for the new structure forms are needed, so that elements which affect performances of micro anti-slide piles can be analyzed systematically and comprehensively.

(2) Working characteristics of micro anti-slide piles,

such as the overall mechanical properties of composite structures, load transfer and failure mode effects need further research, and especially working performances under different combinations need to be further studied and compared to find the best form of combinations under specific working conditions.

(3) Theoretical studies on new forms of anti-slide structures that piles combine with other slope treatments need to be further optimized and proposed reference models, give full consideration to the pile-soil interaction, to meet the needs of practical engineering and make the results more economical and safe.

(4) For the independent micro anti-slide pile and the composite micro anti-slide pile, engineering designs of micropiles need to establish suitable calculation model and put forward clear, reasonable calculation method. The working principle, bearing model, design and calculation theory of new composite anti-slide structures require further discuss at the same time, on the other hand, the mechanism of new structure needs to be fully understood, either. After that it is possible to design more economical and rational structures of micro anti-slide piles in engineering practice under the case of security, then maximize its effectiveness and serve production better.

In this paper, we explore the current engineering application, experiment breakthrough and theoretical breakthrough about micropiles. And aiming at present problems, we put forward reasonable suggestions. Micropiles will play more and more important roles, so the study should also follow the trend, to adapt to engineering applications. Theory serves practice, while practice can provide new ideas for the theoretical research. Micropiles will certainly play a greater role in the future.

## ACKNOWLEDGMENT

This work was supported in part by a grant from Institute of Civil Engineering of Chongqing University. We are very grateful for the comments from the anonymous reviewers. The author would like to thank my teacher Yuntian Wu for offering great support and help in the whole process of this study and thank one anonymous referee for his (her) helpful comments and suggestion, which improved the content and composition substantially.

## REFERENCES

- [1] Shi Shigang. "Working mechanism of micro anti-slide piles in loess landslide" [D]. Shaanxi: Xi'an University of Architecture and Technology, 2015.
- [2] "Micro Pile Design and Construction Guidelines" [M]. 2000, FHWA, USA.
- [3] Shi Peidong, He Kaisheng. Origin, "Application and Development of Small Pile" (I) [J]. Geotechnical Engineering, 2005, 8 (8): 18-19.
- [4] Xiao Chunjin. "Micro Steel Tube Pile for Slope Treatment and Theoretical Analysis" [J]. Roadbed Construction, 2010, 4 (151).

- [5]Zhou Lei, Wang Huanlong. "Application of micropile in red beds accumulation body slope" [J]. Roadbed Construction, 2010,4 (151).
- [6]Zhang Dongdong. "Field Test Study of Force Characters of micropiles in a Slope Treatment" [D]. Shanxi: Xi'an University of Architecture and Technology, 2015.
- [7]Gao Peng. "Application of micropile in Waste Dump Mountain Landslide Treatment" [J]. Shanxi Architecture, 2014,05 (40).
- [8]Lin Shiquan. "Analysis of Bearing Capacity of Pile Foundation Retaining Walls of Micro Still Tube Bored Pile" [J] Chinese Journal of Underground Space and Engineering, 2008,4 (2): 341-379.
- [9]Ding Guangwen, Wangxin. "Application of Micropile Composite Structure in Slope Treatment" [J]. Geotechnical Engineering and Technology, 2004,18 (1): 47-50.
- [10]Zhao Wei. "Application of Bending Resistance Micropile in Slope Treatment" [J]. Engineering Technology, 2009,37-38.
- [11]Wu Wenping. "Model Test and Calculation Discussion of Micropile structure in Slope Reinforcement" [J]. Roadbed Construction, 2009,3 (144).
- [12]Yan Jinkai. "Large Scaled Model Test Research of Micropile in Slope Treatment Technology" [D]. Shanxi: Chang'An University, 2010.
- [13]Shi Minsong. "Model Test and Surpporting Design Research of Micropile Composite Soil Nailing Wall" [D]. Jiangxi: Nanchang University, 2015.
- [14]Yang Xucheng. "Reinforcement Design and Application Research of Micropile of Existing Railway Embankment Slope" [D] .Hunan: Central South University, 2012.
- [15]Sun Shuwei. "Force Mechanism and Design Calculation Theory Research of Slope Reinforced by Micropile Structure" [D]. China Academy of Railway Science, 2009.
- [16]Nie Zhenjun, Li Haishen. "Discussion of Internal Stability of Micropile and Soil Nailing Composite Supporting" [J]. Geotechnical Foundation, 2009 (23).
- [17]Lai Penghui, Huang Rufa. "Micropile-- Analysis of Stress Deformation and Strengthening Mechanism of Reinforced Earth Retaining Wall" [J]. Fujian Construction Science 2016, No. 1.
- [18]Griffiths D.V. and Li C.O. "Analysis of Delayed Failure in Sloping Excavation" [J] .Geotech. Eng rg., ASCE, 1993, 119(9)

# Risk Analysis of Public Hospitals Medical Technology Innovation

Chen Ran<sup>1,2</sup> YangLin<sup>3</sup>

<sup>1</sup> The International Emergency Medical Committee (TEMC), Beijing, 100044, China

<sup>2</sup> The Ministry of health personnel exchange service center, Beijing, 100044, China

<sup>3</sup> STATE GRID PUYANG POWER SUPPLY COMPANY, PUYANG, 457000, China

**Abstract:** This paper relies on Chinese public hospitals medical technology innovation system research. Starting from the background of public hospitals, it elaborates connotation and innovation path of hospital medical technology innovation, and identifies medical technology innovation risk, then using risk matrix to analysis risk management of medical technology innovation, and promote the development of medical technology innovation.

**Keywords:** public hospitals; medical technology innovation; risk matrix analysis

## 1. INTRODUCTION

With the development of medical services and the promotion of health system orderly pushing, the internal and external environment of public hospitals changing profoundly and increasingly higher requirements of medical technology, public hospitals medical technology innovation has become the mainstream direction. Meanwhile, the combined effects of changes in society, population, economics, technology, etc. have been changing the pattern of medical technology range. These changes inevitably lead to the risk, and with the deeply reform of hospital medical technology innovation, the risk of public hospitals is also developing toward diversity and complexity. Risk factors gradually emerge, which focus on scientific research, bio-medicine, hospital management, and medical equipment, etc.. How to analysis and control medical technology innovation path has become an important issue in the field of medical technology innovation, also the basic guarantee of normal development of health care reform system.

Lu Yang believes the goal of medical research performance evaluation is through scientifically and rationally allocating research resources to achieve the maximum benefit of research output, and it is an important form of medical research management.[1] Ding Xueming mentioned technology innovation of biomedical industry fraught with great risk, managers must take all possible measures to control risk.[2] From three major aspects of the hospital management system innovation, hospital management operation innovation and hospital management technology innovation, Chen Xiaoyang has researched the modern hospital management innovation.[3] It weekly studied about

the public hospital medical . So the paper uses he relevant theory literature of generalized technology innovation risk control to elaborate medical technology innovation path and path characteristics, and it will achieve the medical technology innovation risk factors set, then using risk control model to analysis and control in order to provide protection mechanism for the public hospital medical technology innovation.

## 2. THE DEFINITION AND CHARACTERISTICS OF MEDICAL TECHNOLOGY INNOVATION

### (1) the meaning of medical technology innovation

Our medical technology innovation has mainly showed in the following aspects: science research results actively transform, the technical transformation of medical field, advanced diagnostic technology introduction and digestion, and technology breakthroughs of equipment checks. It is because of these efforts, public hospital reform can proceed smoothly. ZhouYa et al pointed out that medical innovation include three aspects: the invention of new practical technologies, migration and integration between different areas of present technology, innovation of medical technology path.[4] Yang Guobin et al, who pointed out that the connotation of medical technology innovation should include medical theory innovation and improvement and treatment technology research and development. For treatment technology, the focus of innovation should include the following two aspects: First, the research and development of clinical diagnosis, treatment technology and methods. Second, the research, development and application of new drugs, new medical devices, medical materials.[5] Chen Fei et al, who believed that medical technology innovation is the process of introducing, modifying or creating existing medical theory or technology, and putting into medical technology activities in order to enhance the quality of medical care.[6] This study defines the connotation of medical technology innovation is that clinical applications, innovation and development of medical theory and research and improvement of treatment technology, wherein, the medical technology innovation focus on clinical diagnosis, research and development of treatment technology and methods.

### (2) medical technology innovation characteristics

Technology innovation has general characteristics,



which are non-exclusive of innovation income, uncertainty of innovation, marketing of innovation and systematicness of innovation. Due to the special nature of the public hospital, therefore, except these basic features, there are other features led by the special nature of the industry.

① The special nature of the service objects. Public hospital provides services to people with a certain degree of particularity. It requires public hospitals to aim at different disease groups during medical technology innovation, and to put people's lives in the first.

② High risk. Medical technology innovation is not only to meet their own needs in public hospitals, but be careful and rigorous in order to reduce the innovation risk in the maximum possible, and reduce the risk of personal injury, avoiding bringing hospitals and social problems.

③ Large interdisciplinary. Medical innovation is not just about medical pathology knowledge, and in the field of biology, chemistry, mechanical engineering, management and other requirements are also high.

Distinctive characteristic of public service. Our health is the social welfare, which implemented by government with some welfare policies. Public hospitals is the subject of health service system, when maintaining the public nature of public medical and health institutions as the core, and gradually establishing the external conditions of a standardized, scientific, efficient and orderly public hospitals operation mechanism, it is particularly necessary to strengthen the construction of public welfare using hospital culture as the carrier in the hospitals, in order to stimulate social responsibility of public medical institutions and medical person, and establish the concept of commonweal, and maintain commonweal of public hospitals.

Large requirements of Innovation. At this stage, while people's living standards improving, physical fitness is fall. Such as cancer and other diseases cannot be drastically treated by medical technology. So under the changes of disease spectrum in the health care market, the demand for medical technology innovation is still very great. The new features of public services in public hospitals determine the social benefits of medical technology innovation outcomes apply to saving lives much more.

### 3. THE ANALYSIS OF MEDICAL TECHNOLOGY INNOVATION RISK

#### (1) Medical Technology Innovation path and characteristics

Selecting medical technology innovation path depends on the advantages, innovation capacity and opportunity for the possibility of development of the hospital, which accumulated in the development process of hospital. In the process of hospital medical technology innovation with the principles of sustainability and feasibility and driven by the

internal and external power of technology innovation environment, medical technology innovation has its own characteristics. The group have developed some questionnaires, which are related to public hospitals medical technology innovation path. Issuing 134 questionnaires to director level and above and returning 122 copies, include 104 valid questionnaires. Questionnaires recovery is 91.04%, valid questionnaires rate is 85.25%. By hospital visits, expert seminars and other ways, the group have summarized the innovation paths of public hospital medical technology innovation process, which include following aspects: First, model innovation, which independently innovated by hospital and individual. Second, content innovation. Theoretical innovation regard medical research as core. Third, equipment innovation. Technology innovation, which is based on medical technology and equipment introduction. Fourth, subject innovation. Talent team innovation, which is oriented by technology innovation team. Through the deep analysis of the hospital medical technology innovation path to get its associated characteristics: First, intellectual property protection is not in place, and prone to innovation dilemma. Second, scale of self-innovation is small, and low conversion rate of innovation. Third, it is lack of cooperation awareness and innovation platform.

#### (2) identification of medical technology innovation risk

Medical technology innovation is a high risk activity. Medical technology innovation risk identification is the key prerequisite for success of innovation.[7]

##### ①Contents of Risk identification

Risk identification is a medical project throughout the whole process of risk management. It is not a one-time behavior, and there should be regularly throughout the innovation process, and its main contents include the following aspects:

##### 1) identifying potential risks of medical technology innovation

Only determine what risks you may encounter, can it analyze the nature and consequences of these innovative projects further. Therefore, in work of medical innovation risk identification, the first is to comprehensively analyze the various factors, and to find out all kinds of possible risks, and aggregate into the list of risks.

##### 2) identifying the main source of risk

Only clearly identifying the main factors of risk for each of the innovation process, can grasp the law of risk developing changes and measure the size of the risk and the possibility of consequences, which is possible to cope with risks and control risks.

##### 3)predicting possible consequences caused by risks

The fundamental purpose of risk identification is to refine and cancel the adverse consequences brought by medical technology innovation risk. After identifying the main sources of medical technology



innovation risk and the risk of medical technology innovation. It must be a comprehensively analyze the possible consequences leaded by risks and the

severity of the consequences. Of course, the identification and analysis of this phase is mainly qualitative analysis.

Table 1. Medical technology innovation risks and measures

| Risk Factors    |   | Strategies   |
|-----------------|---|--|
| Technology Risk | lack of hospital medical technology capacity                | Tackle key technology, introduce technical talents, cooperative innovation, train and improve the enterprise science and technology person |
|                 | Alternative technology appearance                           | If r&d technology take the lead, it can continue to innovate. If not, stop innovating  |
| Market Risk     | unstable market demand                                      | Strengthen the publicity to guide the consumer preferences; Take the portfolio strategy to disperse demand changing risks                  |
|                 | unfair competition  | Apply for a patent, register trademark or use anti-fake measures in advance to prevent; Resort to law                                      |
| Account Risk    | the large funds needed by innovation projects               | Change the technical route to reduce the total cost; strengthen the cost control   |
|                 | difficulties of credit funds                                | Introduce foreign capital; Adopt share-holding system  |
| Management Risk | Top managers do not take the                                | Keep communication with senior managers  |
|                 | the lack of effective coordination among departments        | Increase collaboration opportunities, information flow and sharing among departments   |
|                 | the low management level                                    | Train the project directors  |
| Policy Risk     | Macroeconomic situation changes                             | Know the national policies and related economic and technical policies; Analyze the economic cycle and the macroeconomic aggregate changes |
|                 | the protection restrictions of intellectual property rights | If the development of technology innovation violated the patents of others, it should be given up or stop in time                          |
| Culture Risk    | weak hospital cohesion                                      | Increase the communication among employees, promote the generation of cohesion   |
|                 | Health care workers fear changes                            | Increase innovation propaganda, making employees believe that innovation can bring benefits to them  |

### (3) characteristics of medical technology innovation risk

Medical technology innovation is an economic activity, which is full of exploratory and creativity. During medical technology innovation, it is inevitable to encounter a variety of risks. China's medical market increasingly competing, medical technology innovation risks have become one of the most important factors that hinder hospital medical technological innovation.[8]

① Medical technology innovation risk is speculative risk, which is manageable.

Speculative risk is the risk, which has the opportunity to loss or profit. There are three possible consequences: profit, loss, and break even. Hospitals hope to obtain the desired benefits through successful medical technology innovation. But ultimately, under the influence of external factors and internal factors, there are three possible medical technology innovation outcomes: Firstly, successful innovation, which has achieved the desired objectives. Secondly, unsuccessfully innovation, which fails to achieve the

desired goals, even not returns the early recovery investment funds. Thirdly, technology innovation cannot achieve the desired results, which just makes the revenue be equal to the investment. So in the type of risks, the risk of medical technology innovation belongs to speculative risk.[9]

② Medical technology innovation risk is a dynamic risk, and has its own complexity. That is, due to changes of external factors or internal factors of technology innovation system, such as changes in economic, society, technology, policy, and market, and research and development, marketing research, clinical trials and other aspects management don't arrive, it may also lead to the risk.

③ In some extent medical technology innovation risk can be prevented and controlled. Medical technology innovation is a purposeful, organized innovation activity. Through organizational management of medical technology innovation system, in particular to establish risk awareness, and improve risk management, it is possible to prevent and control the risk of loss in a certain extent, which makes the

controlled technology innovation activities toward the expected targets.[10]

Medical technology innovation risk is a risk, which is in the rational process. In the process of technology innovation, it will be influenced by many variables and inestimable uncertainties. These factors make the results of innovation be uncertain. However, the hospital medical technology innovation process is leaded by rational behavior, and not what people think or believe that is a strong uncertainty random process. Because in the hospital medical technology innovation, all works are purposeful and organized. Each stage includes analysis, evaluation, decision-making and implementation, which are rational behaviors accorded with the logic. During the hospital medical technology innovation, each stage possibly exists technology risk, financial risk, market risk, management risk, decision risk, policy risk, or the risks of different characteristics, such as technology, market, management, decision-making, etc. It has different distributions at different stages. There is a significant difference in the law of changes.[11]

Hospitals need to make before and inwards analysis for possible risk factors. On the one hand, they can take risk management measures, so that the risk is set in monitored status, reducing the loss caused by risks. On the other hand, they can improve technology innovation management, such as marketing research, and carry out clinical trials and evaluation on innovative ideas, and effectively innovate medical technology in accordance with the requirements of patients population and the needs of the hospital development strategies. Making and implementing effective technology innovation strategies in order to make medical technology innovation achieve its objectives.[12]

Therefore, this paper uses risk matrix to analyze the comprehensive consideration of risk factors and risk strategies to predict and assess medical technology innovation risk.

#### 4. Medical Technology Innovation Risk Management Model

Risk Matrix Analysis(MARA) is a method used to guide the innovation risk prevention based on the risk factor analysis and risk countermeasure analysis. It can identify the most critical risk factor, which impacts medical technology innovation and can enhance the relationship between technology innovation and risk analysis. It is also the direct method of innovating and assessing risks during medical technology life-cycle process.[13]

Set  $F = \{f_1, f_2, \dots\}$  is the hospital medical technology innovation risk factors set, and  $P = \{p_1, p_2, \dots\}$  is the hospital medical technology innovation risk strategy set, then the risk matrix analysis method is mainly to provide the basis for the hospital medical technology innovation risk

prevention by analyzing the impact relationship between  $F$  and  $P$ . The steps are as follows:

(1) establishing set of risk factors and set of key risk factors

Firstly, establishing risk factors set  $F$ , in general, element  $f_i$  in  $F$  mainly include: lack of hospital medical technology capacity; unstable market demand; unfair competition; the large funds needed by innovation projects; difficulties of credit funds; the low hospital management level; the lack of effective coordination among departments; the protection restrictions of intellectual property rights; weak hospital cohesion; improper hospital organizational structure and management; errors of medical technology solutions or technology loopholes; long innovation cycle; requires a lot of new equipment; poor technology adaptability and so on. Then choosing key factors from the above factors, these factors constitute the focus factor set  $F'$ , and  $F' < F$ . Selecting key factors evaluation index is:

$$S_i = R_i C_i L_i, i = 1, 2, \dots (1)$$

In the formula  $S_i$  is the evaluation index,  $R_i$  is an occurrence probability of factor,  $C_i$  is uncontrollable degree,  $L_i$  is the expected loss degree of.  $R_i, C_i, L_i \in [0, 1]$ , using fuzzifying mathematics and experts evaluation to assign value.[13]

(2) establishing of risk prevention strategy set and viable strategy set

Firstly, establishing a risk prevention strategy set (referred as strategy set)  $P$ , its main element  $p_i$  include: Strengthening information research; organizing tackle key technology problems; strengthening feasibility demonstration; establishing medical programs decision-making responsibility system; establishing project implementation responsibility system; quality management of medical technology innovation process; early warning systems; introducing medical technology or buying patents; hospital joint development or technical tender; grouping medical items; training medical personnel; applying patents protection in time; strengthening cost control; understanding national policies cohesion; advertising hospital culture to increase cohesion and so on. In practice, the hospital should refine the strategy set based on the actual situation of hospital and the specific circumstances of project. Then, building viable strategy set  $P' \in P$ , which means a collection of those hospitals have the ability to use these strategies. Hospitals should fully assess its own capacity and level, and then to build a viable strategy set  $P'$ .

(3) establishing risk matrix and selecting strategy combination

Matrix of hospital medical technology innovation risk prevention as follows:

$$A = \begin{matrix} & f'_1 & f'_2 & \cdots & f'_n \\ \begin{matrix} P'_1 \\ P'_2 \\ M \\ P'_m \end{matrix} & \begin{bmatrix} a_{11} & a_{12} & \Lambda & a_{1n} \\ a_{21} & a_{22} & \Lambda & a_{2n} \\ M & M & M & M \\ a_{m1} & a_{m2} & \Lambda & a_{mn} \end{bmatrix} \end{matrix} \quad (2)$$

Where  $a_{ij}$ ,  $i=1,2,\dots,m$ ;  $j=1,2,\dots,n$ , represents the validity of strategy  $P'_i$  for risk factor  $f'_j$ , and it can also be assigned by experts grading.

Validity of strategy  $P'_i$  can be defined as:

$$U_i = \sum_{j=1}^n a_{ij} S_j = \sum_{j=1}^n a_{ij} R_i C_i L_i \quad (3)$$

The objective function of the hospital technology innovation risk prevention strategy combination selection is:

$$\max J = \sum_{i=1}^m U_i X_i \quad (4)$$

In the formula,  $J$  is the total validity of strategy combination,  $X_i=1$  indicates adopting strategy

$P'_i$ ,  $X_i=0$  indicates abandoning strategy  $P'_i$ .

Hospital will pay a certain amount of manpower, money and time to use technology innovation risk prevention strategies, thus need to establish the relevant constraints, for example, funding constraints as follows:

$$\sum_{i=1}^m b_i X_i \leq b \quad (5)$$

In the formula,  $b_i$  is the required funds of implementing strategy  $i$ ,  $b$  is financial constraints. Similarly, it can also build constraints related to manpower and time.

There are some strategies must be used in the hospital medical technology innovation risk prevention. If there are two strategies  $p'_k$  and  $p'_l$  that only one appears, it need to add constraints:

$$p'_k - p'_l = 0 \quad (6)$$

It is well to select one of some strategies, such as the hospital joint development strategy and technology bidding strategy, it is more than those who choose a relationship between technology introduction strategy. If there are two strategies  $p'_u$  and  $p'_v$  that only one appears, it need to add constraints:

$$p'_u - p'_v \leq 1 \quad (7)$$

Combining objective functions and constraints above to constitute an integer programming problem. It will achieve the best strategy combination of hospital medical technology innovation risk prevention by

solving this problem.

## 5. Conclusion

This paper initially discusses the connotation and characteristics of public hospital medical technology innovation risk, through analysis of public hospitals and medical technology innovation path to identify medical technology innovation risk. Construction of public hospitals, medical technology innovation risk matrix analysis model has guiding significance for public hospitals identifying, evaluating, early warning and monitoring medical technology innovation risk and taking appropriate measures. During the process of medical technology innovation, public hospitals should be combined with the special nature of the external environment of the hospital, to build a medical technology innovation risk analysis system with strongly operability and pertinence to ensure smoothly carry out medical technology innovation.

## ACKNOWLEDGEMENTS

This paper is some result of project "Research on the system of medical technology innovation in public hospital" of Special topics of the Ministry of health and medical science and technology development and research center of Ministry of health in 2012, No. 28-13-3.

## REFERENCES

- [1] Lu Yang, Research of construction and results of medical research performance evaluation system, Hebei United University, 2011: 17-22.
- [2] Ding Xueming, Risk control of biomedical industry technology innovation, Central South University, 2002.
- [3] Chen Xiaoyang, Zeng Xiaobo, Study of ethics value of hospital implementing limit price of single disease, Medicine and Philosophy, 2008, 29(1): 49-50.
- [4] Zhou Ya, Ma Wenfeng, Geng Renwen, Zhou Zenghuan, Exploration of "Special Medical Technology" concept, People's Liberation Army Hospital Administration Journal, 2006, (2): 169.
- [5] Yang Guobin, Li Yongchang, Yi Xueming, Using technology innovation to drive healthservice quality new leap, Chinese Hospital Management, 2011, (10): 23-24.
- [6] Chen Fei, Yang Guobin, Action on medical quality brought by medical technology innovation theory and practice, Southeast National Defense Medical, 2011, 9(5): 467-468.
- [7] Yang Guobin, Li Yongchang, Yi Xueming, Using technology innovation to drive healthservice quality new leap, Chinese Hospital Management, 2011, (10): 23-24.
- [8] Hu Zhengdong, Research of High-Tech Enterprise Technology Innovation Risk Management, Changsha: Hunan University, 2003: 45-46.
- [9] Li Xiaofeng, Study of Enterprise Technology Innovation Risk Measurement and Decision and

Pre-control, Chengdu: Sichuan University, 2005: 228-230.

[10]Qu Haiyan, Ye Changqing, etc., The thinking and practice of strengthening medical quality control, South China Military Medical Journal, 2013, 5.

[11]Chen Yuhe, three-dimensional model of technology innovation risk analysis, Chinese Soft

Science, 2007, 5.

[12]Chen Dehua, Technology Innovation Risk analysis and prevention, Business Management, 2003.

[13]Zhang Youxu, MARA of Enterprise Technology innovation risk prevention, Modern Intelligence, 2005, 3.

# Study on the Virus Resistance of ChIFN- $\alpha$ Transgenic Tobacco

Jiahang Miao

China Anhui Wuhu Tobacco Industry Corporation, Anhui Wuhu 241000

**Abstract:** To explore the virus resistance of ChIFN- $\alpha$  Transgenic Tobacco. **Method:** Use TMV to analyze the infective characterization and post-infective gene expression of ChIFN- $\alpha$  Transgenic Tobacco. **Result:** The incidence of wild-type plants is up to 60% on the 10th day of virus treatment. Leaf veins become gradually clear and conspicuous until the 13th day, on which the vein clearing covers in all leaves. The onset of symptoms of non-transgenic plants is 100% on the 16th day. ChIFN- $\alpha$ -transferred tobacco appears minor vein clearing after 13 days of infection, and leaves become uneven on the 16th day and appear mild mosaic symptoms on the 19th day. The expression quantity of ChIFN- $\alpha$  Transgenic Tobacco is 284 times higher than non-transgenic tobacco PR-1a on the 6th day of viral infection and 178 times higher on the 15th day; the expression quantity of ChIFN- $\alpha$  Transgenic Tobacco is 547 times higher than non-transgenic tobacco MAPK on the 6th day of viral infection and 369 times higher on the 15th day. ChIFN- $\alpha$  Transgenic Tobacco is equipped with strong antiviral capabilities.

**Key words:** ChIFN- $\alpha$  Transgenic Tobacco; antiviral; transgenic

## 1. INTRODUCTION

Mainly distributed in southern tobacco-growing areas, TMV (tobacco mosaic virus) is the virus that can bring tobacco mosaic disease to tobacco, tomato, pepper, potato and other crops, which belongs to the positive single-stranded RNA virus. It usually causes very serious degradation of crop characters and decline in the quality of agricultural products, thus posing a significant threat to the agricultural development of the country. Strong viral infection ability, high pathogenicity and poor control effect of plants have always been the problems that must be solved in the agricultural development. With the continuous development of biological science, transgenic technology has been proven to be effective to improve the antiviral capabilities of crops. And the excavation of antiviral genes contained in animals, plants and micro-organisms has also declared that TMV of plants will no longer pose a threat to crops. It is of great significance for virus prevention of crops to transfer exogenous antiviral gene into the plant genome by means of molecular biology, so as to obtain crops with antiviral characters and then cultivate excellently shaped antiviral species.

Found in chick chorioallantoic membrane in 1957,

Interferon (IFN) has a variety of biological activities, whose components are proteins. As a kind of effective and inclusive antiviral substances, it is believed to play an important role in animal defense system after studying it. By combination with intracellular interferon receptors, it can induce antiviral gene transcription and translation to help the body resist foreign invasion of the virus. Chicken interferon is divided into two categories, the first one is the type I interferon, type II interferon is the second. And type I interferon can be divided into IFN- $\alpha$  and IFN- $\beta$ , both of which have a high homology in the nucleotide sequence and amino acid composition. According to the relevant research, antiviral capability of IFN- $\alpha$  is significantly higher than the other two, and two kinds of exogenous interferon can not only significantly enhance the antiviral ability of plants, but also inhibit the TMV and PVX amplification. In 1980, people began to study interferon, but few of them involved in the study of resistance to plant virus. Currently, most plant viruses are RNA viruses. Therefore, transferring interferon into plants may get more antiviral characters.

ChIFN- $\alpha$  (Chicken interference alpha) is cloned from virus-induced chick-embryo cell. The interferon gene is composed of 10 subtypes of multi-copy genes and introns are not contained in genomes. Many scholars have found that cloned ChIFN- $\alpha$  has a strong sequence conservation.

In reference to the reported ChIFN- $\alpha$  gene sequences and plant codon preference, this paper synthesizes the ChIFN- $\alpha$  gene and connects it with the plant expression vector pSMONH by means of double digestion, then uses Agrobacterium-mediated method to transform the vector into *nicotiana tabacum*, and finally conducts a molecular identification for the transgenic tobacco obtained. The identification results show that transgenic tobacco plants have a resistance to TMV.

## 2. MATERIALS AND METHODS

### 2.1 Materials

ChIFN- $\alpha$  Transgenic Tobacco (multiplied and kept by the Company), TMV virus (provided by the Guizhou Academy of Tobacco Science)

### 2.2 Methods

In the experiment, PBS of appropriate concentration is used to dilute the TMV virus, which is then inoculated in the well-growing transplantation group of the tobacco greenhouse for tissue culture seeding.



The size of tobacco is controlled within 1-4 leaves, and laboratory temperature and humidity are in accordance with the tobacco industry-standard management. Tobacco disease situation is observed and recorded in accordance with standard diseases grading method in the tobacco industry. The experiment is repeated three times.

#### 1.3 Tobacco mosaic virus inoculation

8 leaf-stage  $T_0$  nicotiana tabacum and transgenic tobacco in the same batch of propagation are selected for inoculation experiment, and each tobacco is inoculated with the leaves in four different positions. First of all, tobacco leaves are thoroughly cleaned with tap water for inoculation half an hour later, and then the tobacco are placed in the greenhouse for cultivation in a certain temperature and humidity. Finally, the experiment makes a disease statistics on the tobacco inoculated with 10d referring to the tobacco grading method in China.

#### 1.4 Gene expression examination

Before and after virus infection, several plants of tobacco tissue culture seeding are randomly selected for total RNA extraction. Due to poor RNA stability, the RNA is reversely transcribed into cDNA. With the cDNA as a template and Actin gene as the reference gene, real-time quantitative PCR is used to detect gene expression by designing primers. Differential display comparison is made between virus resistance gene PR-la (associated with the duration of plants) and gene MAPK (used to promote cell division). Two-step method PR is adopted in the experiment for amplification, and gene level is calculated according to the average value of three holes in the three-hole repeated experiment.

### 3. RESULTS AND ANALYSIS

#### 3.1 Leaf characterization

In 26 days, the transgenic tobacco showed the ability of resistance to TMV in the early TMV infection. It has more significant differences from non-transgenic tobacco in the phenotype of the virus infection, and its average time of onset of symptoms is 3-6 days longer than non-transgenic tobacco, the incidence is lower as well. The incidence of wild-type plants is up to 60% in the 10<sup>th</sup> days of virus treatment. Afterwards, leaf veins become gradually clear and conspicuous until the 13<sup>th</sup> day, on which the vein clearing covers in all leaves. The onset of symptoms of non-transgenic plants is 100% on the 16<sup>th</sup> day. ChiFN- $\alpha$ -transferred tobacco appears minor vein clearing after 13 days of infection, and leaves become uneven on the 16<sup>th</sup> day and appear mild mosaic symptoms on the 19<sup>th</sup> day.

#### 3.2 PCR Results

PCR results show that after the tobacco is infected with TMV, the transcription of PR-la gene and MAPK gene in plant cells is generally rising, and the gene expression quantity of transgenic tobacco is higher than that of non-transgenic plants. The expression quantity of ChiFN- $\alpha$  Transgenic Tobacco

is 284 times higher than non-transgenic tobacco PR-la on the 6<sup>th</sup> day of viral infection and 178 times higher on the 15<sup>th</sup> day; the expression quantity of ChiFN- $\alpha$  Transgenic Tobacco is 547 times higher than non-transgenic tobacco MAPK on the 6<sup>th</sup> day of viral infection and 369 times higher on the 15<sup>th</sup> day.

### 4. DISCUSSION

Tobacco is characterized by long onset time, mild state of illness and so on after it is ChiFN- $\alpha$  gene-transferred and infected with TMV. Thus, the study has demonstrated that Chi-TFN Transgenic Tobacco can be remarkably resistant to TMV infection and can inhibit the amplification of plant virus TMV. During the experiment, in order to obtain more obvious incidence of transgenic infected virus TMV, we have increased the concentration of virus inoculation with the use of tissue culture tobacco. After adjusting the experimental conditions, it is found that the incidences of both transgenic tobacco and nicotiana tabacum are very clear with fast onset and more severe symptoms. Due to higher inoculum concentrations, the regulatory mechanism of Chi-IFN $\alpha$  induction may not catch up with the expression of interferon, so it is unable to clearly show the difference between the transgenic tobacco and the tobacco in control groups. Furthermore, according to reports, changes in the exogenous gene's insertion site and regulation mechanism of translation expression can affect the protein expression and resistance.

Without appearing interferon in the long-term evolution, plants do not contain interferon receptor consequently. Exogenous interferon gene expression of interferon in plants may cause a competitive effect between interferon and other types of proteins, so the lack of interferon receptor in transgenic tobacco may cause ChiFN- $\alpha$  antiviral activity decreased.

The study first proposes interferon also has antiviral capabilities in plants. The results show that exogenous interferon gene expression is gradually increasing with the development process of viral infection, which has enriched people's understanding of interferon and will be helpful to further elucidate the mechanism of action of interferon in the body of plants. It is believed that with the in-depth study of interferon in animals and plants, the use of animal-derived interferon genes in plant protection has broad prospects for development.

### REFERENCES

- [1] Yang Fan, Li Fengxia, Sun Yuhe, Wang Lu, Yang Aiguo, Su Zhengang, Li Yuanyuan, Zhao Baiying, Liu Hui, Wang Yuanying. Construction of RNAi Expression Vector of Antiviral Tobacco-related R Gene [J]. Chinese Tobacco Science, 2012, 01: 23 -26.
- [2] Yang Jun, Zhou Hanping, Song Jizhen, Yin Qisheng. Post-transcriptional Gene Silencing (PTGS) and Antiviral Tobacco Breeding [J]. Acta Tabacaria Sinica, 2006, 06: 38-43.

- [3]Li Li, Zhou Xuezhong, Li Min, Wang Yujiong. Construction and Expression of ASP-ChIFN- $\alpha$  fusion gene [J]. Journal of Ningxia University (Natural Science), 2008, 02: 157-160.
- [4]Wan Duorong, Yin Xian, Jiang Yixi, Chen Xiaobo, Zhang Haiyan, Xiao Zunan. Preliminary Study on the Pap Gene Expression and Antiviral Physiology of Transgenic Tobacco [J]. Journal of Beijing Normal University (Natural Science), 2008, 04: 411-416.
- [5]Bai Qinrong, Zhu Junhua, Liu Xiaoling, Zhu Changxiang, Song Yunzhi, Wen Fujiang. RNA-mediated Transgenic Tobacco Resistant to Two Viruses [J]. Journal of Plant Pathology, 2005, 02: 148-154.
- [6]Li Peng, Song Yunzhi, Liu Xiaoling, Zhu Changxiang, Wen Fujiang. A Study on the Disease Resistance of Potato Virus Y CP Gene 5' and 3' Ends Mediated by Inverted Repeats [J]. Journal of Plant Pathology, 2007, 01: 69- 76.
- [7]Song Li, Zhao Degang, Tian Xiaoe, Wu Yongjun. ChIFN- $\alpha$  Gene Expression in Tobacco and Transgenic Tobacco's Resistance to TMV [J]. Journal of Agricultural Science and Technology, 2010, 01: 118-122.
- [8]Chen Shuai, Liu Guanshan, Zhou Jia, Yang Aiguo, Wang Yuanying, Sun Yuhe. Clone and Analysis of PVY-induced tobacco aspartic protease gene Ntasp [J]. Chinese Agricultural Sciences, 2010, 16: 3331-3339.
- [9]Wang Xinduo, Li Li, Wang Xifeng. Application and Safety of Antiviral Transgenic Crops based on RNA Interference Principle [J]. Plant Protection, 2011, 06: 48-54.
- [10]Tao Shengli, Qiu Yinsheng, Zhang Yanping, Zhu Jiang jiang, Xiang Zhiwei, Zhu Huiling. Effects of Mixed-drinking Low-dose ChIFN- $\alpha$  on Healthy Broilers' Immune Function and Production Performance [J]. China Animal Husbandry and Veterinary Medicine, 2009, 05: 49- 52.
- [11]Tao Shengli, Qiu Yinsheng, Zhu Jiangjiang, Zhang Yanping, Xiang Zhiwei. Effects of Mixed-drinking Low-dose ChIFN- $\alpha$  on Broilers' Cellular Immune Function and Cytokine Levels [J]. Chinese Journal of Preventive Veterinary Medicine, 2009, 08: 637- 641.

# The 3D Cube16 Based on ARM

Qiu Gang

Signal and Information Processing Key Lab, Chongqing Three Gorges University, Chongqing, China

**Abstract:** People improve the quality of life requirements, an increasing number of people are not satisfied with the material enjoyment, beginning to pursue spiritual enjoyment. With the development of the electronics industry, LED put our life more colorful. The theme of the 3D cube LED monitor, designed to redefine our vision. 3D cube can be displayed in English characters, gorgeous three-dimensional animation, music spectrum, the clock display, besides, the 3D cube monitor is equipped with entertainment features, of course, all thanks to a strong HT32F1765 SCM, 3D cube monitor will be a revolution of the application of the LED.

**Keywords:** 3D, ARM, Monitor, FFT

## I. INTRODUCTION

The design based on a single-chip HT32F1765 as the core of detecting and controlling, in order to achieve the button, automatic control, automatic recording, check out the recording data and other functions.

Just thinking, could an LED display products, not only accomplish the usual dot matrix LED's function, but also lead us to the 3D visual world? which is the kind of effect? A complicated 3D LED monitor can display the music spectrum, Chinese characters, English, some brilliant animation, the clock, and also recollect the memory of classic games among the 80s, such as Snake, Super Mario.

Based on the above reasons, our team decided to make the "wall cube dancer" which based on Holtek HT32F1765 chip. Actually, it was a 3D cube monitor.

## II. WORKING PRINCIPLE

The design uses Holtek HOLTEK MCU as the master chip, and rocker modules, audio capture module and 3D cube display, make up our Cube Dancer.

### A. Works' working principle

The series of the Holtek MCU HT32F1755/1765/2755 are based on ARM® CortexTM-M3 processor core, it is the MCU which has 32-bit, high-performance, low-power. CortexTM-M3 tightly bound the Nested Vectored Interrupt Controller (NVIC), the system tick timer (SysTick Timer) and advanced debugging support in a new generation of processor cores. In this product, CortexTM-M3 as a main control unit and analog signal acquisition, providing clock signals.

Audio capture module input the signals into the MCU port PA, obtained the value of AD through the AD conversion, then through the fast Fourier the value of AD transformed into frequency spectral values. Finally, Spectral values are sent to the 3D cube monitor.

3D cube monitor uses a unique algorithm, it stored dozen movies in the internal MCU, such as a rotating surface, cube transformation, the plane goes, falling raindrops and other animation. Furthermore, it can show three-dimensional characters, English letters and numbers. The display stores some characters of the English alphabet, of course, in later time, the word can be displayed directly through PC, you can change the effect at any time if you like.

Not only that, our team also made use of Holtek MCU RTC real time clock function, display the time.

Rocker module sent data to HOLTEK MCU, after processing of the MCU, the data is transmitted to the cube monitor, in order to achieve the effect of "Super Mario". Of course, other types of games can be also achieved by using this similar methods.

3D cube monitor provides interactive interface, every 0.014 seconds scanning 4096, all controlling amount and the results of the keyboard are displayed on the LCD, intuitively and generously.

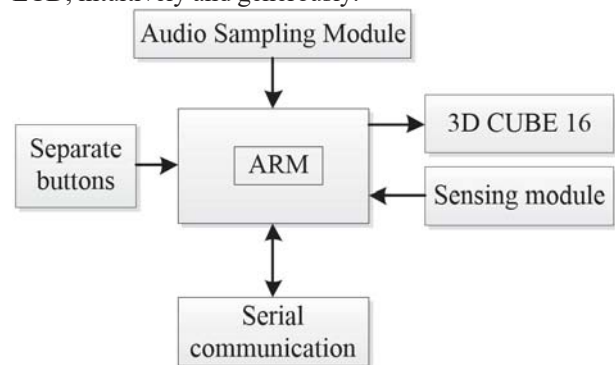


Figure 1. Overall system block diagram

### B. Basic function

In the "spectrum display mode", Holtek MCU's PA port will be assigned to a AFIO clock, as the standard of ADC, while the AD conversion mode is set to continuous mode, open external interrupts, after AD 128 times, it will get 128 values and stored inside of the input array FFT(that is, sampling 128 points), through fast Fourier transform, obtaining 128 spectral values, processing the spectral values and then made the spectral values scattered high and low, displaying with the sense of rhythm, with a various modes, the amount of the energy column is continued to increase, of course, with the rhythm of music, it will bring the same shock to you are not.

Our team stored a dozen movies in the Holtek MCU, firstly, removing some simple mold. Applying algorithm to realize the multiple apply, shift, substitute, etc., using the pointer transfer the data to display subroutine. The system distribute the clock port to

PB, PC, designated IO port as the status of inputting and outputting status. PC0, PC1, PC2, PC3 of the MCU are represented as the input port SDI of the MBI5026, CLK, LE, OE. PB0, PB1, PB2, PB3 as a decoder A0, A1, A2, A3. When all the data is transmitted to the decoder and MBI5026, opening OE, every 0.0147 seconds MCU will be dynamic scanning 4096 LED status, obtaining brilliant animation.

Holtek MCU with integrated real-time clock function, 3.3V power supply to ensure the normal operation of the clock. Firstly, open the RTC interrupt, via serial communication to set the time, after complete setting, store the value of RTC interrupt into the the array of the monitor every time, following the same steps of the animation.

### 3. SOME OF HARDWARE CIRCUIT

The "Wall Cube Dancer" hardware portion consists of four major parts: First, the power supply circuit; second, a display layer selection circuit, one of 74HC154 decoder, a 74HC245 signal power amplifier, six separate buttons, 8 of APM4953 power tube; third, the display column selection circuit, 16 of MBI5026 constant current LED driver; Fourth, the signal power amplifier circuit, one of 74HC245; fifth, 3D cube display, composed by 4096 of LED; Sixth, including the master : one of HT32F1765 MCU, 8M crystal, button batteries.

#### A. Column selection circuit

Column selection circuit mainly composed by 16 of MBI5026 16-bit Constant Current Driver, socket1 and socket2 two communication ports, connecting respectively the front and rear stage level, cascading a total of 16. The last one does not cascade, The first of the last level connect the IO port of the master. Thereby obtaining data.

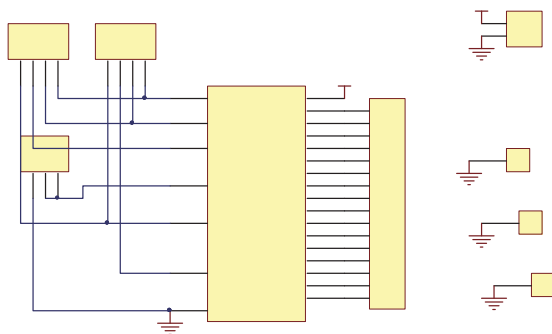


Figure 2. Column selection circuit

MBI5026 is a 16-bit constant current LED driver. Apply the advanced technology CMOS to product, its current value can be adjusted by an external resistor .MBI5026 contain 16-bit shift register, 16 latches, 1.2V reference, and 16 high-precision constant current drive, etc. modules.

#### B. Layer selected circuit

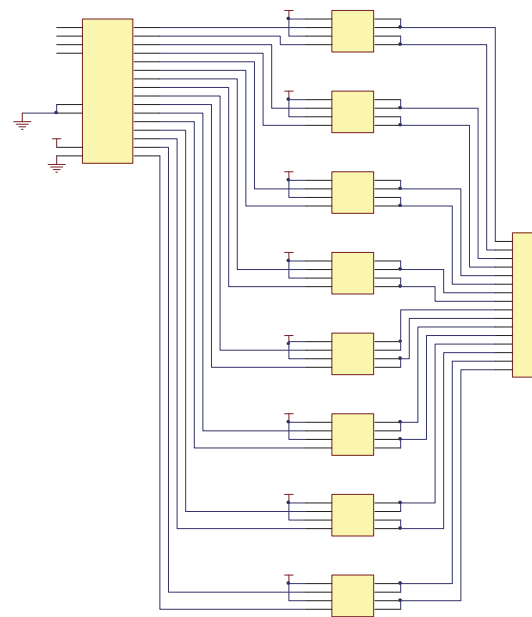


Figure 3. Layer selected circuit

Layer selected circuit mainly composed by one of the 74HC154 decoder, 8 of APM4953 power amplifier tube. When the decoder output low, it works, APM4953 only input low, the output to be high. In this way, that is to say, every scanning, there is only one high, the other is low.

#### C. Signal power amplifier circuit

Signal from the power amplifying circuit is mainly composed of two of 74HC245, one signal is used for the transport layer, one is used for surface of the column.

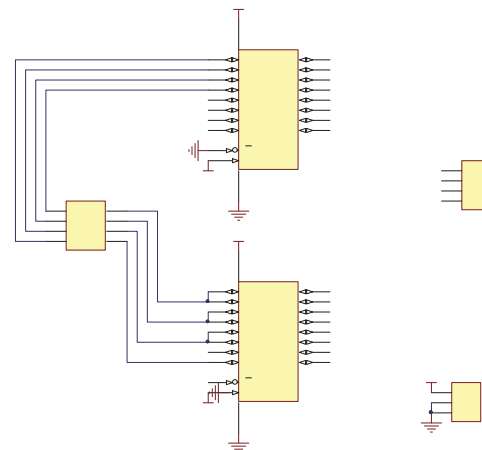


Figure 4. Signal power amplifier circuit

### IV. SOFTWARE

The design software using C language. The approximate flow chart is as follows:

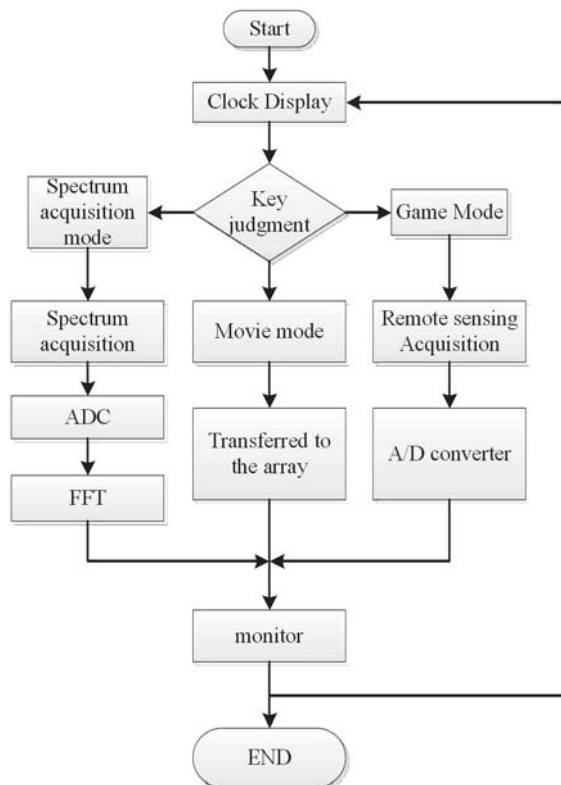


Figure 5. Overall system flow chart

3D cube monitor is switched into the time display mode, through three buttons entering different modes, namely the spectrum display mode, movie mode, game mode, spectrum mode requires access to audio capture module, the game mode requires access rocker module. The program of the 3D cube monitor basically done in the interrupt, such as AD conversion interrupt after 128 times into the FFT, another example the clock display, once every second access register, this display mode, made the control conveniently.

## 5. CONCLUSION

3D Cube16 Based on ARM The 3 system hardware and software design method is reliable, through the engineering test, the system works normally, achieves the expected design goal.

## REFERENCES

[1]T. Yasue et al, "A 1.7-in,33-Mpixel,120-frames/s CMOS Image Sensor With Depletion-Mode MOS Capacitor-Based 14-b Two-Stage Cyclic A/D Converters,"IEEE Trans. Electron. Devices, vol. 63, no. 1,pp.153-161, Jan. 2016.  
 [2]Ali Shagerdmootaab and Mehrdad Moallem, "A Double-Loop Primary-Side Control Structure for HB-LED Power Regulation,"IEEE Trans. Power Electron, vol. 31, no. 3, pp. 2476-2484, Mar. 2016.  
 [3]Hsin-Fu Luo, Yi-Jun Liu, and Ming-Der Shieh, "Efficient Memory-Addressing Algorithms for FFT Processor Design,"IEEE Trans. Very Large Scale Integr. (VLSI) Syst, vol. 23,no. 10, pp.2162–2172, Oct. 2015.  
 [4]Zhuosheng Lin, Simin Yu, Jinhu Lü, Shuting Cai, and Guanrong Chen, "Design and ARM-Embedded

Implementation of a Chaotic Map-Based Real-Time Secure Video Communication System,"IEEE Trans. Circuits Syst. Video Technol.,vol. 25, no. 7, pp.1203-1216, Jul. 2015.

[5]M. Perenzoni et al, "A 160 × 120 Pixel Analog-Counting Single-Photon Imager With Time-Gating and Self-Referenced Column-Parallel A/D Conversion for Fluorescence Lifetime Imaging,"IEEE J. Solid-State Circuits, vol. 51, no. 1, pp.155-167,Jan. 2016.

[6]Rafael Adaime Pinto, J. Marcos Alonso, Marina S. Perdigão, Marcelo F. da Silva, and Ricardo N. do Prado, "A New Technique to Equalize Branch Currents in Multiarray LED Lamps Based on Variable Inductors,"IEEE Trans. Ind. Appl., vol. 52, no. 1, pp. 521-530,Jan./Feb. 2016.

[7]Cheng Ma, Qian Zhou, Jie Qin, Weilin Xie, Yi Dong, and Weisheng Hu, "Fast Spectrum Analysis for an OFDR Using the FFT and SCZT Combination Approach,"IEEE Photon. Technol. Lett.,vol.28,no.6,pp.657-660,Mar.2016.

[8]Edson Luiz Padoin, Laércio Lima Pilla, Márcio Castro, Francieli Z. Boito, Philippe Olivier Alexandre Navaux, Jean-François Méhaut, "Performance/energy trade-off in scientific computing:the case of ARM big.LITTLE and Intel Sandy Bridge,"IET Comput. Digit. Tech., vol. 9, Iss. 1, pp. 27-35,2015.

[9]Han Yu, Guo Tinghang, LI Meng, "Design of Data Transfer Module Based on STM32 in Monitoring System of Cold Chain Transportation,"in Conf. Rec. 2015 Fifth International Conference on Instrumentation and Measurement, Computer, Communication and Control,pp.77-80,2015.

[10]Yuxiao Xu, Tao Jin, Hao Chi, Shilie Zheng, Xiaofeng Jin, and Xianmin Zhang, "Time-Frequency Uncertainty in the Photonic A/D Converters Based on Spectral Encoding,"IEEE Photon. Technol. Lett,vol.28,no.8,pp.841-844,Apr.2016.

[11]C. S. Wong,K. H. Loo,Y. M. Lai,Martin H. L. Chow, and Chi K. Tse, "An Alternative Approach to LED Driver Design Based on High-Voltage Driving,"IEEE Trans. Power Electron.,vol.31,no.3,pp. 2465-2475, Mar. 2016.

[12]Albert T. L. Lee, Huanting Chen, Siew-Chong Tan, and S. Y. (Ron) Hui, "Precise Dimming and Color Control of LED Systems Based on Color Mixing,"IEEE Trans. Power Electron.,vol.31,no.1,pp.65-80, Jan. 2016.

[13]Wei Gao, Sam Kwong and Hongshi Sang, "Low-cost memory data scheduling method for reconfigurable FFT bit-reversal circuits,"Electron. Lett.,vol.51,no.3, pp.217-219, Feb.2015.

[14]James Myers, Anand Savanth, Rohan Gaddh, David Howard, Pranay Prabhat, and David Flynn, "A Subthreshold ARM Cortex-M0+ Subsystem in 65 nm CMOS for WSN Applications with 14 Power Domains, 10T SRAM, and Integrated Voltage Regulator,"IEEE J. Solid-State Circuits, vol. 51, no. 1, pp. 31-44, Jan. 2016.



- [15] Weihua Liu, and Jianxiong Dai, "Design of Attitude Sensor Acquisition System Based On STM32," in Conf. Rec. 2015 Fifth International Conference on Instrumentation and Measurement, Computer, Communication and Control, pp.1851-1853, 2015.

# The Prediction of Photovoltaic Power Output based on the Extreme Learning Machine Algorithm of Particle Swarm Optimization

Wang manshang<sup>1, 2</sup>

<sup>1</sup>School of electrical and information engineering, Jiangsu University, Zhenjiang 212000;

<sup>2</sup> State Grid Zhenjiang power supply company, Zhenjiang 212000)

**Abstract:** With the large-scale application of photovoltaic power generation system, the output power prediction technology can effectively alleviate the negative impact of this type of random energy on power system. In this paper, a short-term forecasting model of photovoltaic power generation system based on the extreme learning machine of the particle swarm optimization(PSOELM) is proposed, and the output power of the output power is predicted directly by the meteorological data, and the output power is predicted directly by the meteorological data. Through the analysis of the factors affecting the output power, the theoretical basis for the selection of the input variables of the prediction model is obtained. In this paper, we do a comparative analysis of the extreme learning machine(ELM) model, and get the results that the PSOELM can achieve higher prediction accuracy with fewer hidden layer nodes. A feasible solution is provided for the prediction of the output power of photovoltaic power generation.

**Key words:** PSOELM; photovoltaic output power; ELM; Hidden layer node

## 1. INTRODUCTION

In recent years, photovoltaic power generation has been developed rapidly because of the characteristics of clean energy. However, due to the influence of solar radiation intensity and weather factor, the output power of the photovoltaic power generation system is fluctuating and intermittent. The grid connected operation of large scale photovoltaic power generation system will affect the security, stability and economic operation of power system. The accurate prediction of the output power of photovoltaic power generation system is advantageous to the dispatching department of power system, so as to effectively reduce the adverse impact of photovoltaic power generation system access to the grid. The research method of photovoltaic power generation system is generally divided into the following two methods. One is based on physical methods, for example, the establishment of the simulation model, the solar photovoltaic strength to predict the simulation, the conversion efficiency of solar cells to establish a mathematical model, the simulation of the output of the statistical analysis. The other is based on the statistical method. Based on

the meteorological data, the intelligent control algorithm is used to predict the output power. For example, in the literature [1], the author established a PV system output model based on improved BP neural network algorithm. In the literature [2], the authors propose a distributed short term photovoltaic power generation output forecasting model based on nuclear extreme learning machines. In the literature [3], the author put forward an output power prediction model based on entropy weight method.

With the development of intelligent algorithm, the output power of the photovoltaic power generation system prediction method has made great progress. In this paper, based on the PSOELM, the power prediction model of photovoltaic system based on particle swarm optimization algorithm is established. In this paper, based on the improved particle swarm optimization algorithm, the power prediction model of photovoltaic system based on particle swarm optimization algorithm is established.

## 2. ANALYSIS OF INFLUENCING FACTORS OF OUTPUT POWER

There are many factors that affect the output power of photovoltaic power generation. In general, the influence of meteorological factors on the output power of photovoltaic system is the biggest. For example, the intensity of solar radiation, temperature, relative to the wind, wind speed and rainfall, etc. If each influencing factor is used as the input of the forecast model, the complexity of the model will be increased. And increasing the input variables will also increase the difficulty for the collection of historical data of the photovoltaic power generation system. Therefore, it is directly related to the availability and accuracy of the prediction model to analyze the factors associated with the output power and to be used as input.

For a fixed solar system, the maximum output power can be determined by the following formula:

$$Q_s = \eta SK [1 - 0.005(T_0 + 25)] \quad (1)$$

In the above formula, the  $\eta$  is the conversion efficiency of the photovoltaic system; The  $S$  is the total area of the PV array solar panel; the  $I$  is a photovoltaic array received with respect to the solar radiation intensity(  $KW / m^2$  ), The  $T_0$  is solar

panels work temperature ( $^{\circ}\text{C}$ ).

In this paper, the output power and the corresponding meteorological data information of a small photovoltaic power generation system which is located in a certain area of Australia is selected as an example. The system array rating is 1.98kw, and the solar cell panel is  $15.1\text{ m}^2$ , and Solar energy plate for 12.

The following figure 1 is the curve of the system output power and related meteorological data in January 27, 2016. The sampling interval of the data is no interval of 5 minutes. From the graph, it can be found that the solar radiation intensity is proportional to the output power of the photovoltaic system, and the trend of the change curve is basically the same. And, the output power and the temperature was positively correlated. Ambient temperature increases, the output power increases, but when the temperature exceeds a certain value, the increase of the temperature will affect the conversion efficiency of the system, so that the output power of the system has decreased. The appropriate wind speed can clean the dust on the solar panel and improve the conversion efficiency of the solar energy, but when the wind speed is too large, it is easy to cause the fixed angle of the solar panel to be offset. So wind speed over the assembly to reduce the output power of photovoltaic system.

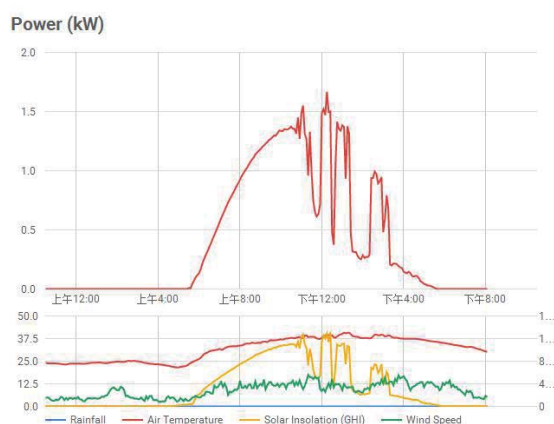


Figure 1. The curve relationship between output power and meteorological factors

### 3. PREDICTION MODEL

#### A. Extreme learning machine (ELM)

The ELM is a neural network algorithm proposed by Huang Guangbin. Compared to the traditional neural network, it has the advantages of fast learning speed and good performance.

Figure 2 is the output power forecast model structure of the photovoltaic power generation system, which is composed of input layer, hidden layer and output layer.

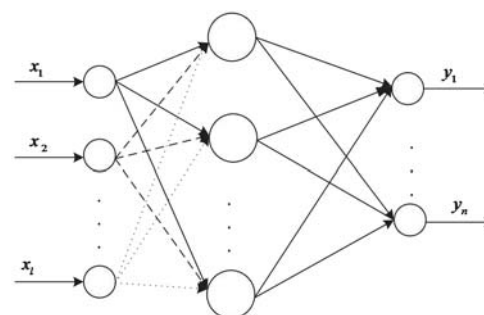


Figure 2. The Structure of prediction model

#### B. Input layer

From the previous analysis, the input variables of the model are many meteorological factors. For example, the solar radiation intensity, air temperature, relative humidity, wind speed, etc..

#### C. Output layer

The prediction samples of this paper are the predicted value of the output power of the photovoltaic power generation system. The predictive value of the sampling time every 5 minutes. Prediction time period is 7:00-18:00 and the prediction time period is 7:00-18:00.

#### D. Hidden layer

Improved extreme learning machine accuracy can be by increasing the hidden layer node number method to achieve. In the structure implementation, it is more simple than the number of the hidden layer, so the output power prediction model of photovoltaic power generation system uses a single hidden layer structure. The selection of the number of hidden layer neurons is directly related to the scale and precision of the neural network. In this paper, we use the method of repeated experiments to determine the optimal number of hidden layer nodes in the model.

#### E. Normalization processing

The output power prediction model of the photovoltaic power generation system is different from the input variable unit, and the quantity level difference is bigger, and the output of the neuron is usually restricted to a certain range. In this paper, the prediction model is designed using a single ended S type excitation function, the output is limited to 0 ~ 1, so the original data need to be normalized, in order to avoid the neuron over saturation. The normalization formula is shown as follows.

$$X^* = \frac{X - \min}{\max - \min} \quad (2)$$

### 4. THE EXTREME LEARNING MACHINE OF THE PARTICLE SWARM (PSOELM)

The PSOELM is a new single hidden layer neural network algorithm proposed by the authors in the literature [4]. It can achieve higher accuracy with fewer hidden layer nodes, and has better generalization performance than the ELM, and can effectively reduce the over fitting of the extreme learning machine. In this paper, the output power prediction model of photovoltaic power generation

system based on the PSOELM is proposed. The flow chart of the algorithm of particle swarm optimization is given.

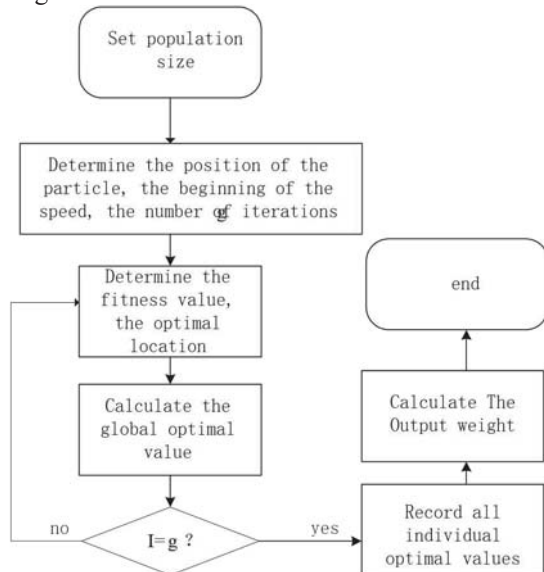


Figure 3. The flow chart of the PSOELM

## 5. THE FORECAST RESULT ANALYSIS

In this paper, the output power prediction model of photovoltaic power generation system based on the ELM and the output power prediction model of photovoltaic power generation based on the PSOELM are established. Select the same number of days of training samples for training, and the same day of the PV output power forecast.

In order to make an accurate assessment of the prediction model, a certain evaluation index is needed. The most commonly used indicators of evaluation and prediction are the mean absolute percentage error (Absolute Percentage Error MAPE, Mean), as shown in the formula (6). The lower the MAPE value is, the higher the predictive accuracy of the model is.

$$MAPE = \frac{100}{N} \sum_{i=1}^N \left| \frac{P_F^i - P_Z^i}{P_Z^i} \right| \% \quad (3)$$

The RMSE is also used as the evaluation criterion of system model prediction accuracy. Its basic formula is as follows:

$$X_{RMS} = \sqrt{\frac{\sum_{i=1}^N X_i^2}{N}} \quad (4)$$

Figure 4 and figure 5 are the PV output power prediction curve of ELM and PSOELM. In Figure 4, the number of hidden layer nodes is 100, and the number of hidden layer nodes is 50 in figure 5. In Figure 4 the RMSE is 0.4020, the latter of the RMSE is 0.203.

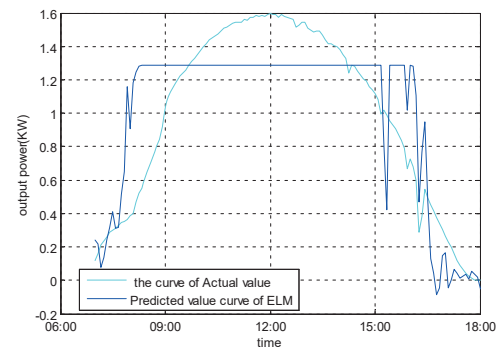


Figure 4 The curves between the predictive value and the actual value of the model of the ELM

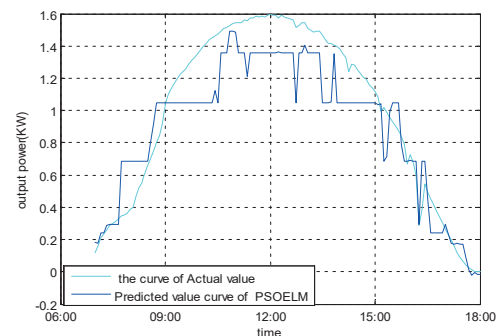


Figure 5 .The curves between the predictive value and the actual value of the model of the PSOELM

## 5. CONCLUSION:

In this paper, a photovoltaic power generation system based on PSOELM is established. The model can predict the output power directly, avoiding the complex modeling and simplifying the prediction process. By analyzing the factors that affect the output of photovoltaic power generation system, the relevant meteorological information is selected as the input of the forecast model, which can effectively improve the prediction speed and accuracy; Finally, the comparison of the model with the model of ELM is analyzed, and the feasibility of the model of PSOELM to predict the PV output power is verified.

## REFERENCE

- [1]Zhang Liying "Output power prediction of photovoltaic power station based on double layer BP neural network" Electrical Measurement & Instrumentation, vol. A 11, June,2012.
- [2]Liu Nian, "Distributed photovoltaic short term power prediction based on kernel function limit learning machine," Transactions of the Chinese Society of Agricultural Engineering, vol. A 30February 2014
- [3]Yang Xiyun, "Combined forecasting model of photovoltaic output power based on entropy weight method", Acta Energiæ Solaris Sinica, vol 35, May,2014.
- [4]WANG jie, BI HAO YANG. "A New Extreme Learning Machine Optimized By PSO"J.Zheng zhou Univ.(Nat.Sci.Ed).vol.45,Mar.2013

# The Research on Automatic Assembly Device Design Method of Threaded Connections Bath Product Based on TRIZ

Zhiwei Luo<sup>1,\*</sup>, Yulong Yang<sup>1</sup>, Yingying Luo<sup>1</sup>, Wenguang Lin<sup>1</sup>, and Zhihong Li<sup>1</sup>

<sup>1</sup> School of Mechanical and Automotive Engineering, Xiamen University of Technology, Xiamen, 361024, China

**Abstract:** TRIZ is a highly abstract theory system of innovation design. In order to verify the theoretical efficiency in guiding the specific product design, according to the problems faced in automatic assembly device design of bath product of threaded connections. The paper uses comprehensively tools providing by TRIZ theory, including problem analysis, standardization and problem solving, to obtain the corresponding solution of innovative principle, separation solution and the standard solution, and process experiment of 3D model construction simulation and physical sample. The result proves the feasibility of the solution obtained, in the same time design risks have also been reduced.

**Keywords:** TRIZ; Design method; Automatic assembly device; Threaded connection; Bath product

## 1. INTRODUCTION

Threaded connections, with firm connection, easy disassembly, good sealing, and low processing cost, are widely used in modern defend bath products<sup>[1-2]</sup>. Due to the fact that defend bath design process often use plastic or iron materials to reduce costs, thread automatic assembly process needed accurate positioning, moderate pretightening force and stable feeding, once appearing deviation, it will cause irreparable damage or even result in stopping production, greatly influences the efficiency of assembly<sup>[3]</sup>. Without changing the inherent product design and production cost, that how to ensure the assembly efficiency and stability of threaded connection defend bath products is problem that urgently needed solving in enterprise.

TRIZ(Teorijz Rezhnija Izobretatel' Skitch Zadach), put forward by the former Soviet union inventor archie schuler which are on the basis of summarizing a lot of achievements in research and patent, is a world-class innovation methods to address the design conflict, which has good maneuverability, systematicness and practicability and has wide application in the field of design<sup>[4]</sup>. In this paper, by means of the theory of solving development problems of complex curved surface of sprinkler assembly equipment, this products automates assembly become possible.

## 2. DESCRIPTION OF ASSEMBLY PROBLEM

Product design process need closely embracing the problems needed to be solved, it is vital that how to accurately define these problems<sup>[5]</sup>. So, problem definition is the basis of product design, it provides general research direction for designers. Accurate description can reduce the irrelevant research work and lower the cost of research and development. Screw thread bath product assembly process mainly exist the following questions:

(1) Due to the small size of bath product and relatively compact space being available for component connection, in order to improve the reliability of the whole structure, between the components, we general use fine thread to connect. Bath product materials are mostly using polymer materials at the same time, the thread strength and hardness is generally low. The demand of fitting precision of fine thread is higher, assembly is so fast that often appearing screwing in deviation and result in thread failure, even the waste of entire product, as shown in Fig.1a.

(2) In order to maintain the sealing of bath product, rubber seal is placed between some components. Because the rubber sealing ring has a degree of elasticity that will produce deformation by manipulator clamping, which will lead to seal fall off and affect the product assembly efficiency, as shown in Fig.1b.

(3) In screw tread assembly, if the pre-tightening force is too large, it will cause the clamp surface and element surface slid and wear, more over lead to serious deformation of components and even damage of screw thread. If the pre-tightening force is too small, would cause component relaxed and even fall off, result that products can't normal use, as shown in Fig.1c.

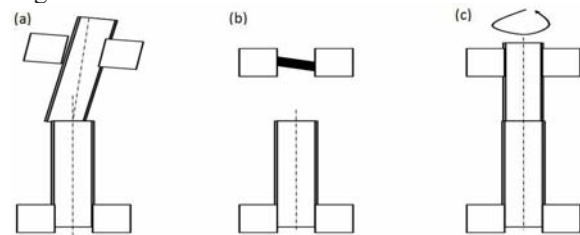


Figure 1. Three typical threaded connections problems of bath product assembly process (a)docking deviation (b)deformation of Sealing ring (c)imprecision of pre-tightening force



### 3. ASSEMBLY PROBLEM SOLVING BASED ON TRIZ

TRIZ theory, perfected after years of development, has become a set of complete and systematic system

of design problem analysis, standardization and solving process, as shown in Fig. 2<sup>[6]</sup>.

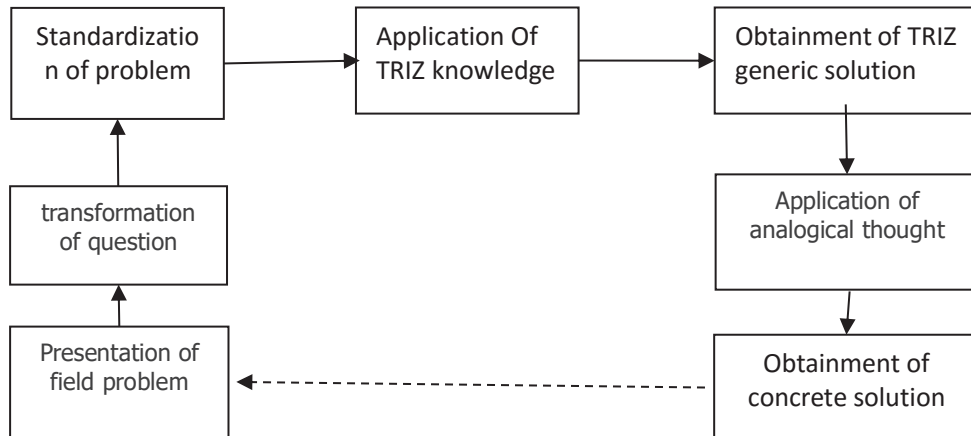


Figure 2. Solving process of TRIZ theory

#### 2.1 Problem standardization

TRIZ is a highly abstract theory, in using process, need standardization for problems in specific field<sup>[7]</sup>, in order to choose corresponding tools. According to the existing several problems of the threaded connection bath product assembly, this paper standardize this problem one by one.

(1) In the process of screwing of threaded connection work piece, designers don't want to adjust component alone to make assembly adapt to a certain deviation of components to improve the adaptability and generality of assembly body. But it will reduce the reliability of the assembly process. The adaptability and reliability is a technical contradiction.

(2) Using manipulator to clamp, mobile and placement rubber sealing ring, because the jig is rigid, once using too much force, it will cause deformation, however the force is necessary, such problems in the system is a structured problem. It is difficult to use physical or technical contradictions to define, but suit to use Su-field analysis method. The model is shown in Fig. 3.

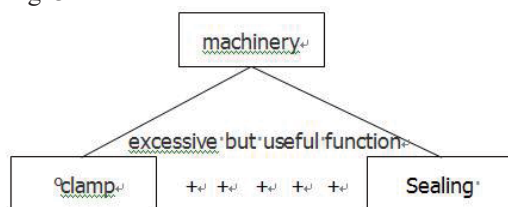


Figure 3. Sealing ring clamping field model

(3) According to the definition of TRIZ physical conflict, that is when a technical system to the same element with mutually exclusive (opposite or different) requirements, physical contradiction arises. In threaded connection, the pre-tightening force whether too large or too small will have an effect to products, therefore increase or reduce of prestressing force is a physical conflict.

#### 2.2 Obtainment of general solution

According to the technical and physical contradictions and Su-field model, TRIZ respectively provides tools of standard solution obtainment, such as contradiction matrix, 40 innovation theory, 4 separation method and 76 general solution. According to the results of the problem standardization of 2.1 provided, this paper using these tools respectively gives the corresponding solutions.

(1) Technical contradictions need integrating contradiction matrix and innovation theory to solve, because the adaptability and reliability of engineering parameter is number 35 and 27, finding out that corresponding solution through technical contradiction matrix theory number that is 8, 13, 24 and 35, specific content as is shown in Tab. 1. Through further analysis, we can find that the number 13 reverse action can solve such problem, that is to adapt and adjust to each other through a reverse rotation between the thread to reduce the angular deviation, at the same time to avoid damaging to the threads.

Table 1. Four kinds of innovation principle and its evaluation results

| number | content             | Whether have a specific solution or not |
|--------|---------------------|---|
| 08     | Weight compensation | no                                      |
| 13     | Reverse function    | yes                                     |

|    |  |    |
|----|--|----|
| 24 | With the help of mediation                 | no |
| 35 | Parameters change of physics and chemistry | no |

(2) According to the standard problem 2, TRIZ theory through 76 standard solution system gives the solution of number 2.2.1, that is a transition to Su-field that is controllable field, through steady controllable field to replace the existing mechanical field. In the existing field, in addition to the mechanical field, there are gravity field, magnetic field, the aura, radiation field and so on. As rubber material is no magnetic material, lighter weight, and

no radiation, thus preliminary consideration is use aura to holding.

(3) In view of the physical conflict, TRIZ provides four separation principle solution, including space separation, separation time, conditions and structure separating. In this paper, these four kinds of solution are evaluated specifically, choosing solutions to apply to both products threaded assembly process. The solution and evaluation results is shown in Tab. 2.

Table 2. Four separation principle and its evaluation results

|                       | Description of detail  | Whether have a specific solution or not |
|-----------------------|--|---|
| space separation      | Separating the contradiction on the two sides in the different space | yes                                     |
| separation time       | Separating the contradiction on both sides in different times        | no                                      |
| conditions separating | Separating the contradiction both sides under different conditions   | no                                      |
| Structure separating  | Separating the contradiction both sides at different level           | no                                      |

### 2.3 The obtainment of specific solution

According to the standard solutions provided by the preceding section and the evaluation results, this paper gives the corresponding specific solution and its concepts scheme.

(1) According to the inaccurate position of thread, through the concretization of reverse mechanism solution, we can obtain reverse direction against the thread screwing by using manipulator clamping device, on the one hand, making two for assembling components in the same axial alignment, on the other hand, two component thread won't bite each other, which is used to avoid the wrong connection. Stopping the reverse rotation and instead of positive normal rotation to realize threaded connections when the two components be on the same axis aligned. The principle and realization process is shown in Fig.4.

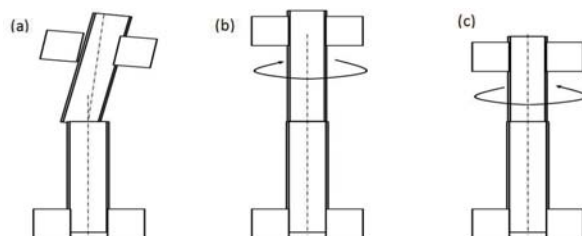


Figure 4. Principle of threaded connection principle and its implementation process based on the reaction theory (a) docking deviation (b) reverse adjustment (c) positive screwing (2) In view of the deformation problem of the rubber sealing ring in the process of clamping, through of number of 2.2.1 solution given by 76 standard solution system, we can come to the conclusion that using the vacuum adsorption can produce an aura. Sealing ring can be

tightly adsorbed on the clamp, at the same time not causing the deformation of seal ring. It do not affect movement and placement because the weight of sealing ring and the force of adsorption is smaller, the pressure and the deformation is smaller due to the larger of the seal positive area.

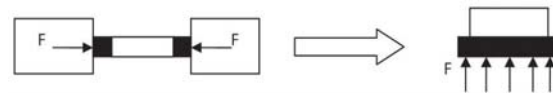


Figure 5. Vacuum adsorption principle

(3) According to Physical contradiction produced by pre-tightening force of screw thread, through concretization based on Spatial separation method, its implementation principle is that there are rubber bearings between manipulator clamp and work piece. When two work piece are tightened, the pre-tightening force exceeds the frictional force between rubber bearings and work piece, this will causes relative sliding between them, realizes over loading protect. Thus, screw threads and surface of work piece will not be damaged.

### 3. DETERMINATION AND VALIDATION OF DESIGN SCHEMES

In order to further verify the above analysis and results, this paper chooses defend bath that is typical for is screw tread with cover of sprinkler as assembly object. According to its own characteristics and requirements of the enterprise, we are design a corresponding assembly structure, as shown in Fig.6. The actual prototype and its assembly process is shown in Fig.7, the whole machine running well, the assembly efficiency and product quality meets the requirements.

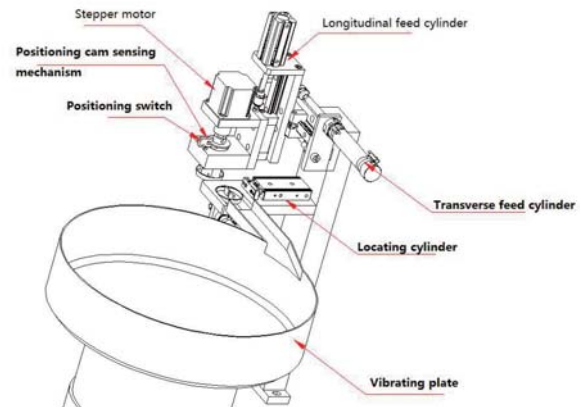
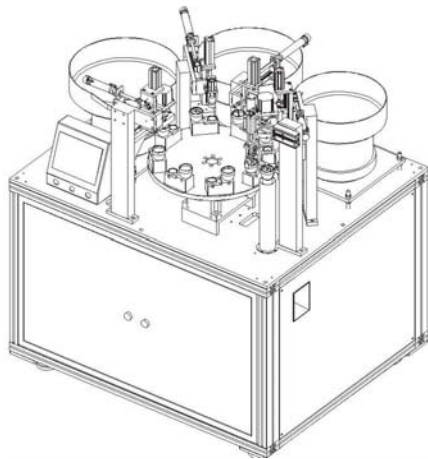


Figure 6. 3D-model of assembly institution with the cover of sprinkler

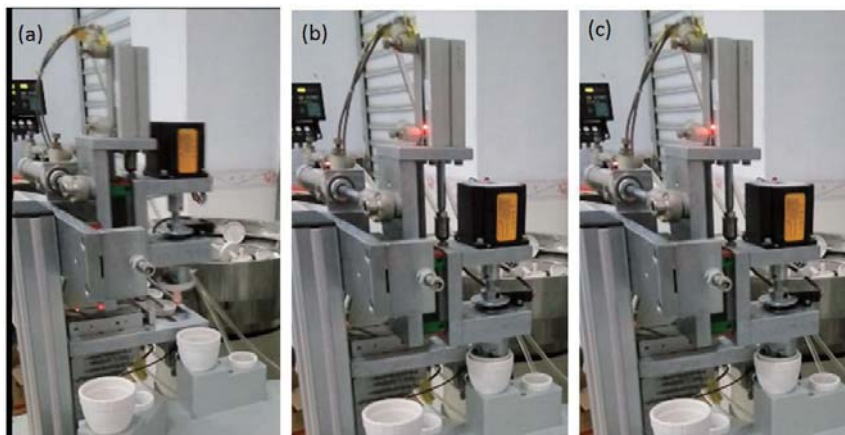


Figure 7. The process of actual assembly(a)clamping of work piece(b)thread screwing(c)adsorption of sealing ring

#### 4. CONCLUSION

TRIZ theory is a set of mature methods of innovation, which can use to guide the design personnel for scientific and efficient product exploitation. This paper comprehensively uses triz theory, including innovative principle, separation principle and su-field models, to solve conflicts and issues that exists in the assembly process that the screw thread connections defend bath product and obtain a reasonable solution. This solution were verified in a 3-D simulation and prototype experiment. The success development of the assembly device will improve the assembly efficiency of the defend bath industry product and the market competitiveness of related businesses.

#### ACKNOWLEDGEMENTS

This work was financially Supported by Natural Science Foundation of Fujian Province of China (2015J01227), Xiamen Science and Technology Plan Projects(3502Z20153028) , Fujian Educational Committee Foundation (JA13237)

#### REFERENCES

- [1]Liu Jianwen. Threaded connection and tightening technology [J]. Automotive technology and materials, 1999 (07), 5-7.
- [2]He Cheng, Chen Baoxue. Optimization of automatic tightening speed of screw [J]. Mechanical design and manufacture, 2015 (5): 100-102.
- [3]Jiang Wenjun, Jin Xiangnan, Du Juncheng. Study on reliability of screw joint in precision assembly [J]. Mechanical engineer, 2014 (3): 213-215.
- [4]R ANTANEN K, DOMB E. Simplified TRIZ: New problem solving applications for engineers and manufacturing professionals [M] . New York: Auerbach Publishing, 2008
- [5]Pahl G, Beitz W, Feldhusen J, et al. Engineering design: A systematic approach[J]. Nasa Sti/recon Technical Report A, 2007
- [6]EMILY M S. From Russia with TRIZ[J]. Mechanical Engineering, 2003, 125:18-20.
- [7]Zhao Min. TRIZ entry and practice [M]. Science Press, 2009

# Analysis on Single Arch Rib Ultimate Bearing Capacity and Stability of Concrete-Filled Steel Tubes Arch Bridge

ZHAO Guo<sup>1,\*</sup>, JIAO Yufeng<sup>1</sup>, Yi Jianlong<sup>2</sup>

<sup>1</sup> School of Civil Engineering, Henan University of Science and Technology, Luoyang, Henan, 471023, China

<sup>2</sup> Zhejiang Hangxiao Steel Structure Co., Ltd., Hangzhou, Zhejiang, 310000, China

**Abstract:** The present paper is research on ultimate bearing capacity and stability of concrete-filled steel tubes arch bridge. Aimed at existing drawbacks of finite element modeling of concrete-filled steel tubes arch bridge, a more refined calculation model is proposed in this paper, which calculates in-plane ultimate bearing capacity and out-of-plane stability of single arch rib of concrete-filled steel tubes arch bridge. Results reveal that in-plane deflection calculation result is consistent with actual measurement result. In addition, arch instability configuration and in-plane and out-of-plane instability sequence of arch rib with lateral horizontal wind load is analyzed, offering theoretical foundation for engineering practice.

**Key words:** concrete-filled steel tubes arch bridge, stability, nonlinearity, finite element analysis

## 1. INTRODUCTION

Concrete-filled steel tubes arch bridge, as a relatively new bridge type, has been developed rapidly in China in recent two decades for its high bearing capacity, good plasticity and toughness, constructing convenience, and excellent economic effect. [1]

As a bridge type that adopts new material, the theoretical research on concrete-filled steel tubes arch bridge at present is still insufficient. [2] Recently many scholars have conducted a series of correlation researches on it. Hu Jiaping[3] took a deck type concrete-filled steel tubes arch bridge as research object, and built its spatial finite element model, conducted nonlinearity stability analysis on this bridge, to discuss the impact of symmetrical eccentricity and dissymmetrical eccentricity on stability coefficient. Wang Wei et al [4] took a through concrete-filled steel tubes arch bridge whose span was 2×125 m as an example to discuss the impact of structure parameters such as main arch ring steel ration, sectional area and arrangement of wind bracing, arch rib in-plane initial deflection, deck width and rise-span ratio on bridge dynamic properties. Zeng Derong et al [5] built up constitutive relation of bond between steel tube and concrete. Results show the impact of bond degree between steel tube and concrete on the overall buckling load and security and stability coefficient of concrete-filled steel tubes arch bridge. However,

generally research on concrete-filled steel tubes arch bridge is relatively insufficient.

For arch bridge with large span, due to its large span and small width-span ratio, it has smaller rigidity. Therefore, study on stability of this kind of structure is of great significance. [6] In the present paper, with a concrete-filled steel tubes arch bridge as example, a more refined finite element analyses model of concrete-filled steel tubes arch bridge is built, and Total Lagrange method (T.L method) is employed to derive tangent rigidity matrix of 8-node solid element and 4-node flat shell element. Based on this foundation, in-plane ultimate bearing capacity and out-of-plane stability of single arch rib of concrete-filled steel tubes arch bridge are calculated. With comparison between in-plane deflection calculation result and real measuring result, rules of its property and ultimate bearing capacity in the whole loading progress are obtained. Example calculation reveals that finite element calculation model in the present paper not only can simulate concrete-filled steel tube arch rib of any section shape, with any boundary condition and load, but also obtain more accurate arch rib in-plane and out-of-plane instability form and ultimate bearing capacity when compared to single beam element that adopted united theory, offering theoretical foundation for engineering practice.

## 2 INTRODUCTION TO PROJECT

A concrete-filled steel tubes arch bridge, which adopts through double-rib concrete-filled steel tubes arch bridge structure with parabolic arch axis, is as shown in Fig. 1. There are two concrete-filled steel tubes arch ribs in the whole bridge, 19 hangers in total for each arch rib with interval of 4m, as shown by the dashed line of figure 1. Bridge load is designed as: car-20, trailer-100 grade, crowd 3.5kN/m<sup>2</sup>. The arch bridge span is 80m, rise is 16m, rise-span ratio 1:5, deck width 20.4m, in which running lane width 18.4m.

Steel tube adopts A3, whose thickness is 12mm, yield strength  $f_{y1}=307.67$  MPa, ultimate tensile strength  $f_s=467$ MPa, elasticity modulus  $E_{s1}=2.06\times10^5$ MPa; arch rib concrete was C50, whose  $f_{ck}=32.4$  N/mm<sup>2</sup>,  $f_{tk}=2.64$ N/mm<sup>2</sup>,  $E_c=3.45 \times 10^4$ MPa. For structural requirement, reinforcing steel bar is added in concrete-filled steel tube. Due to its large proportion,



its contribution to concrete-filled steel tube strength cannot be neglected. Reinforcing steel bar includes longitudinal carrying steel and horizontal stirrup, whose diameter is both 18mm, grade is HPB300, tensile strength standard value  $f_{y2}=235\text{N/mm}^2$ , elasticity modulus  $E_{s2}=2.1\times 10^5\text{MPa}$ .

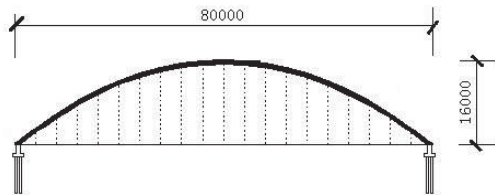


Figure. 1 Bridge General Layout Diagram

### 3 ARCH BRIDGE FINITE ELEMENT METHOD

#### 3.1 arch bridge finite element modeling

The key of arch bridge calculation model simulation is simulation of structural rigidity, quality and boundary condition. Here structural rigidity simulation refers simulation of axial rigidity, bending rigidity, shear rigidity and torsional rigidity of arch rib structure. Sometimes, it also includes simulation of warping rigidity and connection rigidity of different materials; structural quality simulation primarily refers quality simulation of bar at translation and rotation motion; simulation of boundary condition should agree with structural support condition. [7]

According to practical condition, there is some rational simplification in the calculation model of concrete-filled steel tubes arch bridge. Mapping method is adopted in modeling process to divide gridding. According to this concrete-filled steel tubes arch bridge type and its loading features, three

element models of ANSYS are adopted in total in this modeling process: LINK8, SOLID65 and SHELL element. In which, LINK8 element stimulates reinforcing bar in concrete-filled steel tube, SOLID65 element for concrete, and SHELL181 as steel tube.

#### 3.2 load condition and major calculation

Bridge load test is a kind of test method for direct test of bridge structure working condition. The major purpose of bridge structure static test is to test bridge structural quality and estimate structural security and reliability. Therefore, it is generally non-destructive load test. [8] In this load test, nine vehicles weighing 30 ton are arranged according to maximum midspan displacement, whose arrangement diagram on deck is as shown in Fig.2. Finite element analysis and experimental study of this model were carried out respectively for the analysis on this bridge.

The arch rib calculated in the present paper is arch rib at bridge advanced position. And vehicle load was transferred to this arch rib. In calculation self-weight of arch rib and bridge were neglected. In calculating process, the test load was added as first load step. Then load of same proportion was added on each vehicle step by step until there was singular value in arch rib rigidity matrix. The load at the moment was the ultimate load of this arch rib. If load was added on this basis, load will reduce gradually while displacement on arch rib top will increase rapidly.

In calculating process double nonlinearity of geometry and material should be taken into account. Loading coefficient of arch bridge was obtained as well as relation curve between section displacement and strain. Validity and effectiveness of calculation procedure and its model were verified by comparison between that and experimental result.

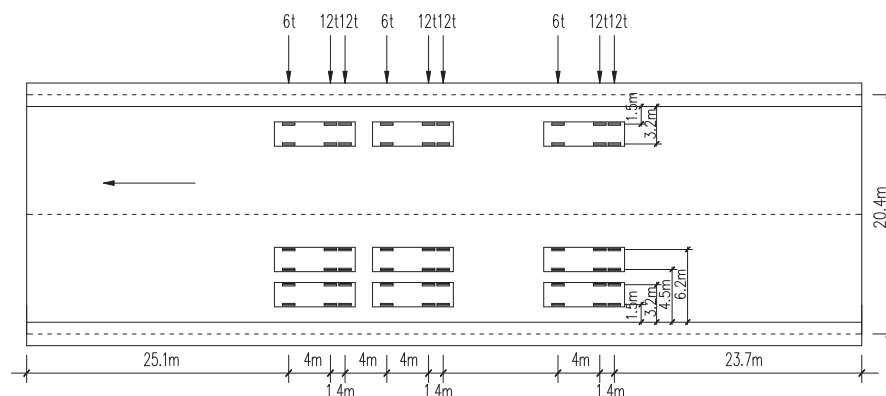


Figure. 2 Arrangement Diagram of Vehicle under Test Load on Deck

### 4. CALCULATION RESULTS AND ANALYSIS

As shown in Fig. 3 and Fig.4, relation curves of load coefficient, section displacement and strain are calculated according to the nonlinear finite element calculation method. The calculation result of the midway deflection is 7.739mm, the actual test value is 6.97mm, and the error is 11.03% in the loading tests, the calculated value is smaller than the test value, the condition of single arch is considered in the calculation process, makes the actual load equal to

the arch rib structure without the consideration of the combined action of the double arch rib and the bridge deck, which actually increases the overall rigidity of the arch bridge, and causes the actual deflection of the bridge smaller than the calculated value, that is the reason for the smaller value through preliminary analysis.



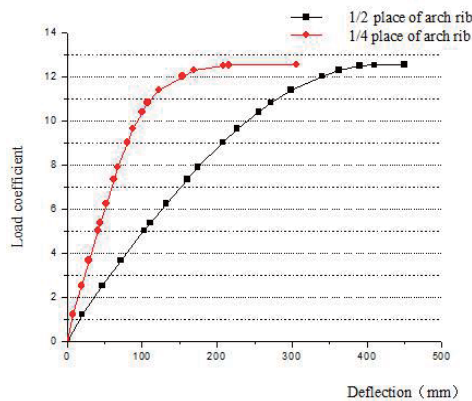


Figure3. Load-Displacement Curves under the Action of Equivalent Load

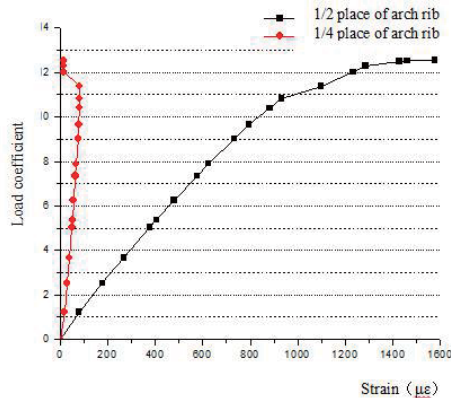


Figure4. Load- Strain Curves under the Action of Equivalent Load

It can be seen from figure 3 that destruction strength limit of the arch rib structure rises when load coefficient reaches 12.55, which is the ideal state, and the weight of each car reaches  $12.55 \times 30T$  as shown in figure 2, displacement value, either in the 1/2 place of arch or in the 1/4 place of arch dramatically increases, maximum displacement in the 1/2 place of arch up to 450mm, strain at the top of the arch rib is as high as  $1577\mu\epsilon$  when in the limit state, the steel has entered the stage of plastic-flow, and the structure has been destroyed. The concrete-filled steel tubes arch bridge is not allowed to appear such large deformation in practical engineering applications since the bridge deck is formed by concrete pouring, concrete is a brittle material, which has poor ductility, when there is a large deformation, the concrete will occur brittle failure; In addition, such a large deformation is also not allowed from the perspective of comfort. The weight of each car is 30T in actual tests, that is, the load coefficient is 1, and the test displacement at the top of the arch rib is 6.97mm, while the calculated result is 7.739, the error is 11.03%, so the calculation results are acceptable.

#### 5. STABILITY ANALYSIS OF ARCH BRIDGE

The in-plane rigidity is often large for concrete-filled steel tubes arch bridge with long span, but the out-of-plane rigidity is often too small, in general, the external rigidity is reduced with the reduction of the ratio of width and span of the concrete-filled steel

tubes arch bridge, thus, the stability out of plane of concrete filled steel tube arch rib cannot be ignored.

When using numerical method to analyze the nonlinear stability, the buckling deformation out of plane will not occur if the load on the structure is completely in the plane, that is, when only with membrane force or axial force, and the analysis carried out cannot obtain results of stability analysis of the real structure. A very small disturbance force out of plane is applied to the arch bridge to stimulate the external buckling response in this paper in order to overcome this problem. The loading conditions are shown in Fig. 5. The relatively small arch rib lateral disturbance load  $F_z$  is added to stimulate the buckling of arch rib out of plane in the solving process. As shown in Fig. 5, the interference force  $F_z$  is used to simulate the wind load. Then double nonlinear external stability analysis of geometry and material of this bridge is carried out. The following wind load here is calculated according to the formula of *General Code for Design of Highway Bridges and Culverts* (JTJ201-89) : [10]

$$w = k_1 k_2 k_3 k_4 w_0 \quad (1)$$

In which:  $k_1=1.0$ , important coefficient;  $k_2=1.1$ , body coefficient;  $k_3=1.3$ , height coefficient;  $k_4=1.4$ , geographical condition;  $w_0=550Pa$ , reference wind pressure, obtained according to the *General Code for Design of Highway Bridges and Culverts*.

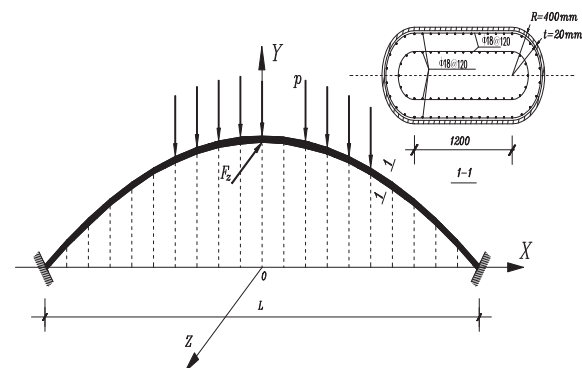


Figure. 5 Arch Bridge Load Layout Diagram

Assuming that put all wind pressure to the top of the arch rib, concentration force  $F_z$  on the top is 59.46kN, lateral force  $F_z$  in actual calculation process is 60kN, which is 2.35 time of the wind pressure. Then first analyze the stability characteristic value of the arch rib.

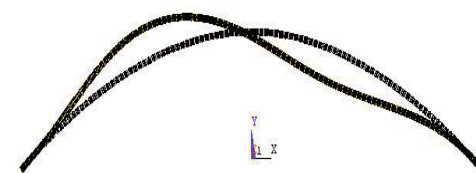


Figure. 6 Arch Rib First-Order Instability In-Plane Elevation Chart

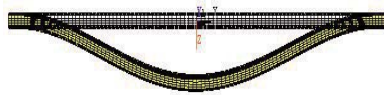


Figure. 7a Arch Rib Second-Order Instability out-of-Plane Elevation Chart

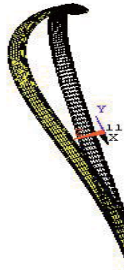


Figure. 7b Arch Rib Second-Order Instability out-of-Plane Elevation Chart



Figure. 7c Arch Rib Second-Order Instability out-of-Plane Elevation Chart

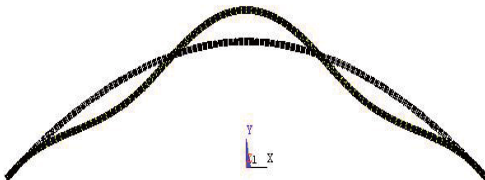


Figure. 8 Arch Rib Third-Order Instability in-Plane Elevation Chart

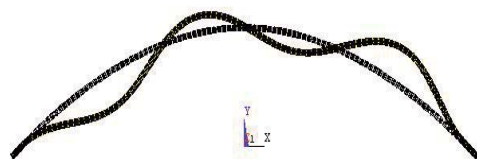


Figure. 9 Arch Rib Forth-Order Instability in-Plane Elevation Chart

It can be found through the analysis of the characteristic values of the arch rib that the first-order instability of this arch rib is in plane, the second-order instability is out of plane, and the third and the fourth order instabilities are both in plane, the shapes of the instability mode are shown in Fig. 6 to Fig.9. The out-of-plane rigidity of the arch rib is larger than that in plane base on analysis, the in-plane instability appears first without the influence of interference forces.

In order to reflect the instability sequence of the arch

rib in plane and out of plane, the relationship curves of vertical load and in-plane displacement ( $y$  direction) and displacement out of plane ( $z$  direction) when lateral force  $F_z$  is 60 kN is shown in Figure 10. It can be seen from the Fig.10 that when the vertical load coefficient reaches 12, in case of small increasing load coefficient, the vertical displacement increases sharply, while the change of lateral displacement is very small, which show that limit destruction of this arch rib still belongs to in-plane instability damage.

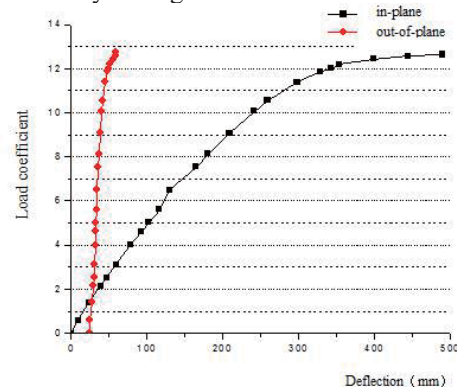


Figure. 10 Arch Rib Load-Displacement Curve in the out-of-Plane Stability Analysis

## 6 CONCLUSIONS

The present paper is research on ultimate bearing capacity and lateral stability in plane of concrete-filled steel tubes arch bridge, compare the analysis results with the experimental results and find they are in good agreement. Indicate that the calculation results can reflect the actual stress characteristics and deformation process of the concrete-filled steel tube arch rib, especially with higher accuracy in the elastic stage, and is feasible to the stability analysis of concrete filled steel tube arch rib. The following conclusions are drawn through calculation, comparison and analysis:

(1) First-order instability of the symmetric concrete filled steel tube arch rib either is anti-symmetric instability form in plane or symmetric instability form out of plane, which is decided by the relative in-plane or out-of-plane rigidity.

(2) It is feasible to calculate the rolling (out-of-plane) instability ultimate load of the arch structure by applying a small lateral (out-of-plane) interference force in numerical analysis. The results show that the ability of resisting lateral deformation of arch rib is also different under the influence of different lateral disturbing forces. The ability of resisting lateral deformation of arch rib reduces with the increasing of the disturbing forces, the stability out of plane becomes poor and the vertical ultimate bearing capacity decreases; while the ultimate bearing capacity of instability out of plane maintains same when the disturbing forces are in the small range of change, and can be considered that is corresponding to the same instability form.

(3)The numerical simulation and the load-displacement curves obtained from tests show that the concrete filled steel tube has good ductility, which is determined by the internal working mechanism of the concrete filled steel tube material: on the one hand, the steel tube itself has good plastic deformation ability, and the ability to resist local buckling is improved through function of the core concrete; restraint effect of steel tube to the concrete, on the other hand, let the concrete in a complicated three direction compression state, its bearing capacity and plastic property performance has been improved. Combination of steel tube and concrete not only enable concrete filled steel tube to have a very high bearing capacity but also with a good ductility to avoid brittle failure of the structure.

#### REFERENCE

- [1]Ceng Y, Ma R J, Tan H M. Dynamic Properties Large Span Deck-Type Concrete-Filled Steel Tubular Arch Bridge. *Journal of China & Foreign Highway*,2014, 34(4):113-117.
- [2]Kang H G, Zhang J, Yu D S. Reliability Analysis of Concrete-filled Steel Tubular Arch Bridge. *Journal of Dalian University of Technology*, 2011, 51(2):226-228.
- [3]Huang X W, Wang H, Li A Q, et al. Analysis on Dynamic Characteristics of Half-through Special-shaped CFST bridge. *Journal of architecture and civil engineering*, 2012, 29 (1):87-93.
- [4]Wang W, Ma Q S. Effect of Structural Parameters on Parameters on Dynamic Characteristics of Through Concrete-filled Steel Tube Arch Bridge. *Bridge Construction*, 2011, (2):34-38.
- [5]Zeng D R, Li J. Stability Analysis of Large Span Concrete-Filled Steel Tube Arch Bridge Based on Slips Theory. *Highway*,2010,(2):34-38.
- [6]Xiao Y G, Jing W F. Elastic Stability Analysis of Long-Span Arch Bridge of Concrete-Filled Steel Tubes. *Journal of China & Foreign Highway*, 2014,34(2):129-132.
- [7]Jiao Y F, Yi J L, Chen S F. Nonlinearity Finite Element Analysis of Concrete-filled Steel Tubular Arch Bridge. *Journal of Henan University of Science and Technology (Natural Science)*, 2008, 29(2):75-78.
- [8]Yang C X, Yang W J, Zhang J R. An Analysis of Failure Risk of the Bridge Load Test Based on Proof Load Method. *Journal of Changsha Communications University*, 2004, 20 (2):25-29.

# An Index Page Replacement Policy for KNN Algorithm

Jiaoling Liu<sup>1,\*</sup>, Dexian Zhang<sup>1</sup>, Lin Yang<sup>2</sup>

<sup>1</sup>School of Information Science and Engineering, Henan University of Technology, Zhengzhou, 450000, China

<sup>2</sup>State Grid Puyang Power Supply Company, Puyang, 457000, China

**Abstract:** A disadvantage of k-nearest neighbor(KNN) algorithm is the large amount of calculation. The tree index structure can reduce the amount of calculation but it will generate an index page buffer management problem in the case of the main memory capacity is limited. The traditional page replacement policy is not aimed at a tree-based high-dimensional indexing structure design features, so the page buffer hit ratio is lower. Therefore, we analyzed the characteristics of tree index structure and then designed a replacement policy based access probability distribution, the experimental results show that the replacement policy is effective.

**Keywords:** KNN algorithm, index page, replacement policy, access probability

## 1. INTRODUCTION

KNN algorithm is a mature classification algorithm in theory, this method is based on the sample in the feature space K nearest sample belongs to category for determining the sample category, for sample set for points overlaps between more conditions have more advantages than other methods.[1] But the disadvantage of this method is its large amount of calculation, such as the linear sweep method, with the growth of data set size and the performance will become unbearable. For KNN algorithm, a series of high-dimensional indexing technique based on the tree one after another was introduced, including the tree of R-tree,[2] R+-tree,[3] SS-tree,[4]  $\Delta$ -tree[5] etc, these index structures are based on triangle inequality and pruned to reduce the computational cost during the process of KNN algorithm implementation.

However, with the growth in size of the dataset, the index file formed by these indexes structure will then expend. For the scenarios, which main memory capacity is limited, part of the index page had to be buffer in main memory, then resulted the issues of replacement of the buffer index page. The traditional page of oriented operating system or database system designed replacement policy[6] is not aimed at a tree-based high-dimensional indexing structure design features, so there is a problem of lower page buffer hit ratio. For this reason, we proposed replacement policy based access probability distribution by analyzing, discussed the relationship between the level of index pages and the access probability and gave the corresponding experimental comparison.

## 2. THE ANALYSIS OF THE TRADITIONAL REPLACEMENT STRATEGY

There are many page buffer replacement strategies proposed formerly, typical example FIFO, LRU, etc. We will analysis these strategies applicability to evaluate whether they are suitable for the index page buffer replacement. Let's assume that indexes contain N index pages, KNN query accesses M index pages every time averagely and buffer has m index page frames. Now we will investigate the FIFO and LRU taking the root node which has the highest accessed frequency as an example.

Let's start with FIFO. For KNN query, the root node is to be accessed firstly, and as it continues to access the M-th node, the root node will be taken out based on the rules of FIFO. Obviously FIFO is not the suitable replacement strategy for the index frame buffer. Because the firstly entered page is likely to be the frequently accessed page, the FIFO is not suitable for this situation.

LRU is to select the longest unused page in a period of time as the eliminated object. So it has the judgment of accessing probability. But for KNN query, the LRU judgment of accessing probability is difficult to take effect for the limitation of the frame buffer size when  $m < M$ . For KNN query, the first accessed node is the root node, and as it continues to access to the  $m+1$  node, the root node will be eliminated based on the rules of the LRU. Thus the LRU has the same poor effect under the condition of  $m < M$ .

Furthermore, let's test the probability of the establishment of  $m < M$ . Based on the understanding of the higher dimensional space, we know that with the increase of space dimension, the phenomenon of page domains overlap resulted by the node split will be more and more serious. The direct result is M that the number of the pages accessed in the process of KNN querying rises sharply, which means with the increase of the dimension, the ratio of M and N will decrease rapidly. And with the expansion of the data scale, the number of pages that index needs rises also. It makes M rising accordingly. Relative to character, the probability of the establishment of  $m < M$  increases accordingly.

## 3. TKL REPLACEMENT POLICY

According to what we have analyzed about traditional replacement policy FIFO and LRU from last chapter, we consider that the main reason why



these methods are not effective is that it's not able to analyze and make use of the unique distribution feature of KNN query against the node access. So in this chapter we are going to analyze the probability distribution of KNN query against the node access first, then come up with a relative replacement policy accordingly to achieve a better result.

To make it easy, we start with Perfect K-ary Tree as a analytic target to evaluate the probability distribution of nodes. According to the nature of Perfect K-ary Tree, we can easily get the number of index page of different layer  $PageCount(i) = k^{i-1}$ ,  $i$  is the number of layer. Due to the pruning effect of KNN query, we can just access to part of its subpage to access to any index page, which makes the ratio of the number of adjacent layers less than  $k$ , namely:

$$\frac{AccessPageCount(i)}{AccessPageCount(i+1)} = \frac{1}{k_i}, k_i < k. \quad (1)$$

We can further calculate the ratio of the access probability of adjacent layers:

$$\begin{aligned} & \frac{AccessRatio(i)}{AccessRatio(i+1)} \\ &= \frac{AccessPageCount(i)/PageCount(i)}{AccessPageCount(i+1)/PageCount(i+1)} \\ &= \frac{AccessPageCount(i)}{AccessPageCount(i+1)} \cdot \frac{PageCount(i+1)}{PageCount(i)} = \frac{k}{k_i}. \end{aligned} \quad (2)$$

Due to  $k_i < k$ , we can get the smaller the number of layer of index page, the bigger the probability of access. Suppose  $\alpha_i = \frac{k_i}{k}$ , we can get

$AccessRatio(i+1) = AccessRatio(i) \cdot \alpha_i$ . Because the index page will be accessed, we will have  $AccessRatio(1) = 1$ . Substituting that, we can get the access probability of every layer.

Until now, we know that the access probability of any index page depends on the product of  $\alpha_i$  of its previous pages.  $\alpha_i$  means the efficiency of pruning. Because the biggest reason that influences the efficiency of pruning is the overlapping of page regions, we can get access probability of every layer is due to the degree of overlapping of its previous index pages. Let's further analyze the relationship between the degree of overlapping and the number of layer. Suppose two index pages doesn't overlap on the  $m$ -th layer, then their sub-index pages won't overlap on the  $n$ -th layer ( $n > m$ ), but false on the contrary. Just as Fig. 1, even though the sub-index pages in  $R1$  and  $R2$  don't overlap, its corresponding index pages in the lower layer obviously overlap. So we can get the degree of overlapping of index pages is inversely proportional to the number of layers.

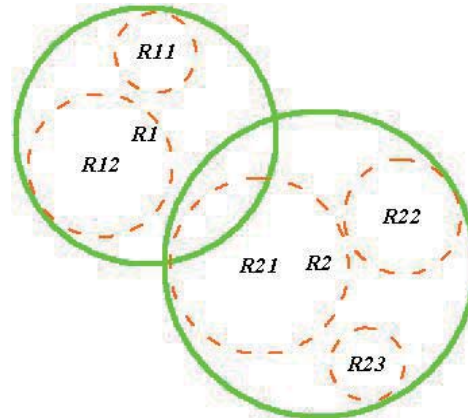


Figure 1. Relationship between the degree of overlapping and the number of layers

Because the degree of overlapping mainly influences the efficiency of pruning, we can get  $\forall i, j (i < j \rightarrow \alpha_i > \alpha_j)$ . Combining the formula of access probability of index pages in every layer that we got before, we can get the assumption that access probability of index pages will decrease faster and faster as its layer increases. The basis is shown in the following formula:

$$\forall i, k \left( i < k \rightarrow \frac{AccessRatio(i+1)/AccessRatio(i)}{AccessRatio(k+1)/AccessRatio(k)} = \frac{\alpha_i}{\alpha_k} > 1 \right). \quad (3)$$

Based on the above analysis, we know the probability of being accessed in each layer index page and its trend along with the number of layers changing. Next, we will observe the access probability distribution of the KNN query through experiments. Experiments based on SS-tree,  $k=10$ , the scale of data set for 160 thousand and the dimensions of the feature vector for 182. The formation of index file is 216 MB. We have count the average probability of the nodes in the query processing of 10-NN queries for 1000 times. As shown in Fig. 2.

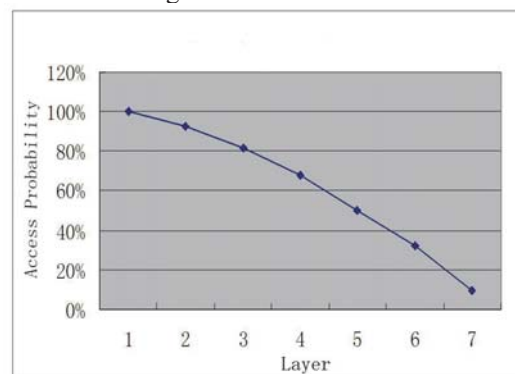


Figure 2. Probability variation trend of index structure in each layer based on KNN search

As can be seen, along with the number of layers increases the probability of the index page has been significantly reduced access probability. First layers smaller probability are accessed much higher than the largest number of layers. Moreover, with the number of layers increases the probability of the index page has been accessed more quickly the rate of decline. This is consistent with the conclusions obtained by



theoretical analysis. Further, we observe the space requirements of each layer of the index structure. Experiments in space requirements for data layers measured as shown in Tab. 1. It can see the front

layers of a smaller number of layers required to store a small space. Therefore, It be loaded into the main memory formed by the storage pressure with respect to the entire index to be much lower.

Table 1.Space requirement index structure in each layer

| Layers | the layers of pages/ total pages | space requirements (MB) |
|--------|----------------------------------|-------------------------|
| 1      | 0.001%                           | 0.001314765             |
| 2      | 0.004%                           | 0.007888589             |
| 3      | 0.027%                           | 0.059164417             |
| 4      | 0.205%                           | 0.443733126             |
| 5      | 1.541%                           | 3.327998442             |
| 6      | 11.556%                          | 24.95998831             |
| 7      | 86.667%                          | 187.1999123             |

Comprehensive the above analysis, we think the page buffer management process should be paid to the layer number of small index pages more resident in main memory of opportunity. For several levels of the highest access probability, the index page may be "fixed" in the buffer. Based on the guidance of this idea, we give a replacement strategy TKL(Top-K Level), specific as follows. Setting index page  $h$  layers, if the fore  $k$  layers could be fully loaded, the fore  $k$  layers would be loaded into the buffer and no longer be part of the subsequent replacement, the rest of the space based on LRU management, would be used to buffer  $K+1$  layer to  $h$  layer index page.

#### 4. THE EXPERIMENTAL ANALYSIS AND DISCUSSION

In order to give an assessment about the effect of TKL, we make a contrastive experiment between TKL and LRU. In this experiment, the size of data set is 160 thousand, the vector dimension is 182, index file is 216 MB, then inquire 10-NN for 1000 times, get the average page hit number and the non- hit number in this two kinds of replacement policy.

In the beginning, we make a text in the situation where the main memory page buffer pool is 10MB, the index page accommodate is about 5%, and get the findings as follow:

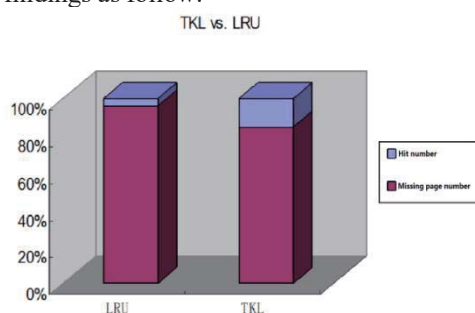


Figure 3. Comparison of page hit rate between TKL and LRU

By analyzing the Fig. 3, we see that TKL is quite better than LRU. Next we get the proportion of index pages can be put into main memory rise to 50% from 5%. Repeat the above experiment, the test results are

shown in Fig. 4.

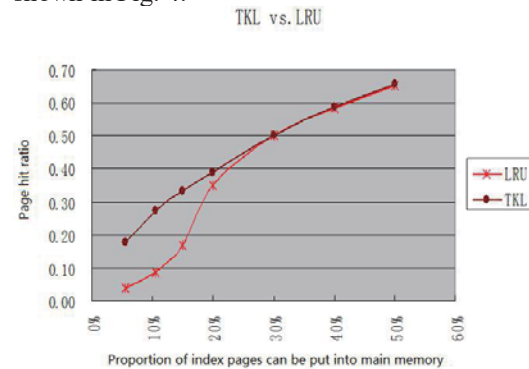


Figure 4. With the proportion of index page in memory increasing,the comparison of hit rate between TKL and LRU

We find that TKL is much better than LRU when the proportion between the page buffer pool space and index file is lower than 20%. While LRU turns better when the proportion is higher than 15%, LRU and TKL become coincide when the proportion is above 30%.

By analyzing LRU in previous section, we think the reason cause the above phenomena as follows: As the space of page buffer pool is small, the condition of  $m > M$  can't be established, then the effect of LRU is difficult to play, and TKL make the several most welcomed layer fixed in the buffer, all these cause the proportion of page hit is higher than LRU. But with the increase of the space of page buffer pool, the condition of  $m > M$  can be established, the effect of LRU is easy to play, and at this time, most space of TKL is commanded by LRU, so there is not so much difference.

Then we can see, the effect of TKL is quite better than LRU when the proportion is small, while there is not so much difference between TKL and LRU when the space of main memory is big enough. All in all, TKL make up the defect of LRU when the space of buffer pool is small. As it can be applied in a broader space, it is a better choice.

#### 5. CONCLUSIONS

Aimed at the index page replacement strategy which based on tree index structure in the limited memory capacity of KNN algorithm, we introduce the correlation analysis between the index page level and access probability, then according the analysis put forward a replacement strategy TKL in view of distribution the access probability. The method integrates of the traditional LRU replacement policy further under full account of tree high-dimensional indexing structure, thus significantly improving the index buffer page hit rate while the KNN algorithm executes, enhance the overall performance of the algorithm.

#### REFERENCES

[1]Gregory Shakhnarovich, Trevor Darrell, Piotr Indyk. Nearest-Neighbor Methods in Learning and Vision [M]. Cambridge, MA: The MIT Press, 2005, 64-72.  
 [2]Antonin Guttman. R-trees: A Dynamic Index Structure for Spatial Searching [C]// Proceedings of the 1984 ACM SIGMOD International Conference on

Management of Data. Boston, Massachusetts: ACM Press, 1984, 47-57.

[3]Timos K. Sellis, Nick Roussopoulos, Christos Faloutsos. The R+-Tree: A Dynamic Index for Multi-Dimensional Objects [C]//The 13th International Conference on Very Large Data Bases. Brighton, England: Morgan Kaufmann Press, 1987, 507-518.

[4]White D.A., Jain R. Similarity indexing with the SS-tree [C]//Proceedings of the Twelfth International Conference on Data Engineering. New Orleans, Louisiana: IEEE Computer Society, 1996, 516-523.

[5]Bin Cui, Beng Chin Ooi, Jianwen Su, Kian-Lee Tan. Contorting high dimensional data for efficient main memory KNN processing [C]// Proceedings of the 2003 ACM SIGMOD International Conference on Management of Data. San Jose, California: ACM Press, 2003,479-490.

[6]Andrew S. Tanenbaum. Modern Operating Systems [M]. Upper Saddle River, New Jersey: Prentice Hall, 2001,214-227.

# The Key Research on Recognition of the Parts Orientation Based on Template Matching

Yangyang Li, Teng Li, Wencheng Guo

Tianjin Polytechnic University, Tianjin, 300387, China

**Abstract:** Machine vision has promising future in modern industry. The recognition of parts based on the machine vision becomes the hot spot in automation manufacture field. But the recognizing the parts orientation based on the template matching has seldom been studied. Through the article, the recognition system for the parts orientation is designed. The system can be divided into two parts, image capturing sub-system, and image processing sub-system. A camera with high accuracy is used in the capture sub-system. And the image processing sub-system adopts the appropriate template matching algorithm to realize the identification, rapidly and correctly. According to the actual experiments, the desired results can be achieved.

**Keywords:** machine vision, template match ,image capture,image process

## 1. INTRODUCTION

Eliminate and sort the defective parts is done by the amounts of workers in traditional industrial field, because of the low efficiency and workers' non-proficiency, the quality of the products after the examination is not ideal, causing huge losses for the entrepreneurs. In the present day, when the competition is serious, factory owners like to use the automatic devices to conduct products activities instead of the common workers. And the key parts of these devices are image processing system and mechanical device. Since the middle of the 20<sup>th</sup> century, [1] thanks to the development of image processing, machine vision starts to step into the field of automatic production. But the image processing is mainly based on the basic shapes like angle and perimeter, height and width. In the end of the 20<sup>th</sup> century, the booming of 3d reconstruction technique, as well as the perfect combination of robot technology and machine vision, makes the machine vision get a promising application in parts recognition and sort. [2] Recently, machine vision has already got a series of breakthrough, realizing the similar functions of common human eyes. Various robot technologies and image processing algorithms for different functions are enhanced. More and more image processing systems are applying to all kinds of situations. Modern industry gradually is heading to unmanned and intelligent direction. The automatic recognition of parts becomes the practical desire. In essence, the robot system introduces the machine vision that offers the 3D information, realizing the

recognition and sort of the parts. [3]Some developed countries have obtained the huge achievements in machine vision, our country's independent researches on robot-vision technology fill the many vacuums, and still many technological problems remain to be solved. The robots work in the complex context, easily affected by the light and dust, the limitation of the industrial camera causes the uncompleted image capture, making the decline of the algorithm and the timeliness. Fig.1 below shows the rough idea of the structure of the system.

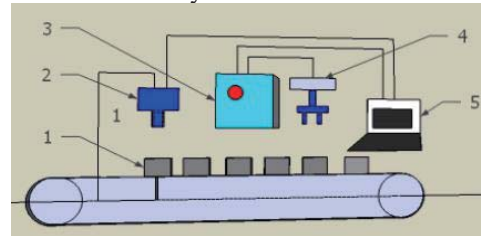


Figure 1. Image of structure of the system

The recognition and the sort of the parts are accomplished through the combination of the corner detection and template match. The whole system consists of two parts, one is image capture image sub-system, and the industrial camera mainly capture the image, another one is used to processing the image, the actual 3D information can be obtained. At last, according to the relevant results of the processing image, execution module carries out the corresponding action. The figure below is needed to illustrate the main idea of the system. And the number 1 means the actual part in assembly line, the number 2 presents the camera device, the number 3 stand for the electrical equipment for the robot arm, and the number 4 expresses the robot arm, and the PC is shown by number 5.

## 2. CAMERA CALIBRATION

### 2.1 camera coordinate system

The basic task of machine vision is to deduce the geometrical information of the objects in three-dimensional space through the image captured by the camera, reconstructing and recognizing the objects for further understand of the real world. [4] Simply put, the purpose of camera calibration is to build the corresponding relationship between the world coordinate system and the planar reference frame. The mathematical model of the camera decides the mutual relation between the spot in the image and the real location of the spot of the surface of the object in the space. Fig.2 shows the camera coordinate system. Camera calibration is to obtain the

intrinsic and extrinsic parameters of camera and the correction matrix. The precision of the camera calibration determines the final result of the machine vision, and prompting the precision of the camera calibration is of great significance for the development of machine vision, and the main job for the researchers is to enhance the precision of the camera calibration.

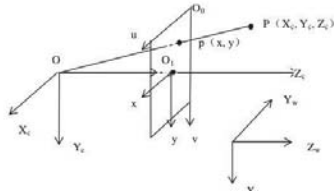


Figure 2. Image of camera coordinate system

## 2.2. calibration process

Calibration target and the Halcon software are needed for the process; the Halcon provides the target with the description file. After choosing the proper calibration target, the description file is generated by using the corresponding functions. [4] And the calibration target can be printed by the Gsview software. And the calibration process is done by posting the target on the bearing surface. Camera Calibration starts after the work of making calibration target is done; the flow chart1 well illustrates the process.

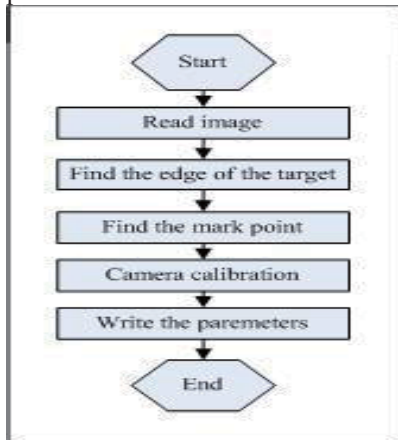


Chart 1. Camera calibration

This calibration aims to figure out all the external and internal parameters, and those parameters remain stable if the camera and the parts keep the fixed location.

## 3. IMAGE PROCESS

### 3.1. corner detection

The image processing sub-system firstly obtains the image of specific part from the camera, and then extracts the angular point data from the image using the certain algorithm. Those data is used to get the template image of the part. Finally the template image will compare those template images stored in the objects library, and the most similar one will be chosen, the mark of the template image will sent to the execution module.[4] Corner detection based on the gray level image, namely the combination of gradient and template, is adopted in the image

processing sub-system. Convolution operation for every point of the gray level image is needed. Those mathematical formulas are used to get the gradient of the centre point.

$$dx = \begin{bmatrix} -1 & 0 & 1 \\ -1 & 0 & 1 \\ -1 & 0 & 1 \end{bmatrix}, dy = \begin{bmatrix} -1 & -1 & -1 \\ 0 & 0 & 0 \\ 1 & 1 & 1 \end{bmatrix} \quad (1)$$

And the first derivatives in x-direction ( $I_x$ ) and y-direction ( $I_y$ ) and the product ( $I_{xy}$ ) of  $I_x$  and

$I_y$  can easily be obtained.

The matrix M is built:

$$M = mbys \otimes \begin{bmatrix} I_x^2 & I_{xy} \\ I_{xy} & I_y^2 \end{bmatrix} = \begin{bmatrix} \langle I_x^2 \rangle & \langle I_{xy} \rangle \\ \langle I_{xy} \rangle & \langle I_y^2 \rangle \end{bmatrix} \quad (2)$$

$$mbys = e^{(x^2+y^2)/\sigma^2} \quad (3)$$

$$\langle I_x^2 \rangle = mbys, \langle I_y^2 \rangle = mbys \otimes I_y^2 \quad (4)$$

$$\langle I_{xy} \rangle = mbys \otimes I_{xy} \quad (5)$$

$\lambda_1$  and  $\lambda_2$  are the characteristic value of matrix M, and the corner response function is defined below.

$$CRF(x, y) = \det(M) - k(\text{trace}(M))^2 \quad (6)$$

$$\det(M) = \lambda_1 \lambda_2 = I_x^2 * I_y^2 - I_{xy} * I_{xy} \quad (7)$$

$$\text{trace}(M) = \lambda_1 + \lambda_2 = I_x^2 + I_y^2 \quad (8)$$

When the value of the CRF is small, the detection point lies in the area where gray lever has not much change. And the value is bigger than the given value of *thresh*; the detection is the corner point.

### 3.2 template matching

The match method based on the gray level is the common algorithm. [5] All the data is recorded in the gray image, thus, the matching process can make full use of the gray information without getting images' characteristics, enhancing the match precision. This method generally uses the gray information of the whole image to build similarity measurement between two images, and a certain search method is adopted to find out the biggest or the smallest parameter value of the transnational model.

$$D(i, j) = \sum_{m=1}^M \sum_{n=1}^N [S^{i+j}(m, n) - T(m, n)]^2 \quad (9)$$

[6]This system uses the absolute balance search (ABS) method to determine the correlation between the template image and matching image. Supposing the template image is presented by  $T(m, n)$ , and the matching image is presented by  $S(w, h)$ , namely the scale of template image is  $m * n$ , and the scale of matching image is  $w * h$ . And the total number of

matching points is  $(W - m + 1) * (H - n + 1)$ . The formula (9) well illustrates the algorithm. The combination of  $i$  and  $j$  shows these points coordinate. According to the actual comparison between the experimental result and given threshold value, the matching degree can be easily obtained.

#### 4. EXPERIMENT RESULT

##### 4.1. template library

This template library stores 12 kinds of template images, those images are shown in Tab.1. and one kind of matching picture is shown in Fig3. After the accomplishment of the template matching, the Figure 3. Matching image


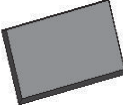



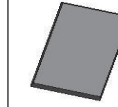

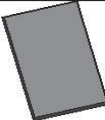
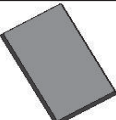
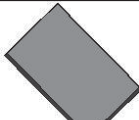
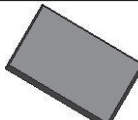
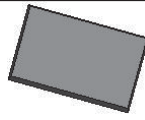
|          |   |   |   |   |  |   |
|----------|---|---|---|---|--|---|
| NUM      | 1( $0^\circ$ )  | 2( $15^\circ$ )   | 3( $30^\circ$ )   | 4( $45^\circ$ )   | 5( $60^\circ$ )  | 6( $75^\circ$ )   |
| Template |  |  |  |  |  |  |
| NUM      | 7( $90^\circ$ )   | 8( $105^\circ$ )  | 9( $120^\circ$ )  | 10( $135^\circ$ )   | 11( $150^\circ$ )  | 12( $165^\circ$ )   |
| Template |  |  |  |  |  |  |

Table 1. Template images

During the whole experiment, DDC 8mm is provide as the camera, and the light device is ring illuminator. Three kinds of different parts were chosen as the object, the experiment result is shown in Tab.2. And these data indicates the design based on machine vision is workable.

Table 2. Experimental result

| Serial number | Num: Samples | Num: matching | Precision/% | Process time/s |
|---------------|--------------|---------------|-------------|----------------|
| Part 1        | 50           | 50            | 100         | 1.370          |
| Part 2        | 50           | 49            | 98          | 1.534          |
| Part 3        | 50           | 47            | 94          | 1.826          |

#### 4. CONCLUSION

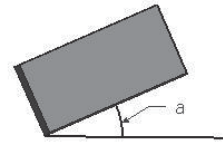
In the industrial scene, the parts of the automatic assembly line have many kinds of orientation. [1] And sometime orientation consistency is needed for enhancing the efficiency of collecting and assembling parts. In this paper, the key technology of parts orientation recognition is studied. Many groups image are tested by the actual algorithm, and the experimental results show this algorithm indeed realizes the automatic recognition of parts orientation. However, paper just proposes a method in theory to identify the parts orientation. For the further study, the template matching algorithm should be adopted in the actual industrial scene. And this is the next direction of the research.

#### ACKNOWLEDGMENT

I want to express my deep gratitude to my supervisor. During the whole research, my supervisor supply me with amounts of technological guidance, especially he encourages me to offer different ideas about how to deal with the gray degree level, and give me practical advice of building template library. In addition, the accomplishment of the experiment is under the help of the seniors in the lab, they give me confidence, especially when I am stuck.

execute module will start the corresponding movement. There are so many possibilities of part orientation, and the  $a$  ( $0^\circ \leq a < 180^\circ$ ) means the offset angle compared the template image 0, to simplify things, rule is made below.

$$(a \pm 7.5^\circ) = a \quad (10)$$



#### REFERENCES

- [1]Wuyi Zhang, Qiangsong Zhao and Dongyun Wang, Actualities and Developing Trend Of Machine Vision, journal of Zhongyuan University of technology. Zhen Zhou, 2008, 19(1): 9-15.
- [2]Jing Tang, Qing Li, The Design of Visual Identity system, Journal of computer Application, Chang Sha, 2010, 30(6): 1559-1662.
- [3]ZhongAn Zhang, A new method of calibration camera, Journal of Digital Technology and Application, Shandong, 2013, 6(1): 134-136.
- [4]Jing Tang, Qing Li, The application of Harris corner detector in machine visual, Journal of computer Application, Chang Sha, 2010, 30(6): 1559-1662.
- [5]Zhang Z, Aflexible newtechnique for camera calibration. IEEE Transactions on Pattern Analysis and Machine Intelligence, American, August 2000.
- [6] M. Fiala. Designing highly reliable fiducially markers. IEEE Transactions on Pattern Analysis and Machine Intelligence, 2010.



# Research of Wireless Relay Monitoring Networks Status

Yubo Ning, Chuansheng Wu

University of Science and Technology Liaoning, Anshan, P. R. China

**Abstract:** Directed to a communicating between a series of medical devices and remote monitoring devices, and more particularly, to a wireless relay module for receiving communications from and transmitting communications to medical devices via one or more wireless relay networks, for transferring the communications received from the remote monitoring devices via one or more internet-accessible wireless communications networks, and for monitoring the status of the networks.

**Key words:** monitoring networks; monitoring; wireless; relay

## 1. INTRODUCTION

In critical care and home care health service centers including hospitals, clinics, assisted living centers and the like, care giver-patient interaction time is at a premium. Moreover, response times by care givers to significant health conditions and events can be critical. Systems of centralized monitoring have been developed to better manage care giver time and patient interaction. In such systems, physiological data from each patient is transmitted to a centralized location. At this centralized location, a single or small number of technicians monitor all of this patient information to determine patient status[1,2]. Information indicating a patient alarm condition will cause the technicians and/or system to communicate with local care givers to provide immediate patient attention, for example via wireless pagers and/or cell phones, and/or by making a facility-wide audio page[3,4].

Implementing such centralized monitoring systems using wireless networks may present a number of difficulties. In order to effectively monitor patient status using information provided by a variety of medical devices that may be dynamically assigned to patients in a variety of rooms and on a variety of floors in a facility, it would be desirable to establish communications between the medical devices and the centralized location by means of a local area network such as, for example, a "WiFi" network based on IEEE 802.11 standards. However, as such networks are typically already in place in facilities to support a variety of other functions (for example, physician access to electronic medical records (EMRs), facility administrative systems and other functions), it is often undesirable to secure sufficient local area network access for the purpose of providing centralized monitoring. Moreover, when a patient is

located remotely from a critical care health service center (for example, at home), access to traditional local area network facilities such as a WiFi network may be unavailable or not sufficiently reliable to support critical care monitoring applications[5].

## 2. EXEMPLARY MEDICAL DEVICE NETWORK ARCHITECTURE

A diagram of an exemplary architecture 0 for a system for monitoring medical devices in accordance with the present invention is illustrated in Fig. 1. One or more medical devices are provided at a patient facility for monitoring the medical condition and/or administering medical treatment to one or more patients. Patient facility may comprise a critical care health service center (for example, including hospitals, clinics, assisted living centers and the like) servicing a number of patients, a home facility for servicing one or more patients, or a personal enclosure (for example, a backpack) that may be attached to or worn by an ambulatory patient[5,6,7].

Associated with each medical device is an interface circuit that includes one or more of a transmitter and/or a receiver in the form of, for example, a transceiver, for respectively transmitting and receiving signals in a facility-oriented wireless network such as, for example, a Low-Rate Wireless Personal Area Networks or "LR-WPAN," ZIGBEE network or another low-power personal area network such as a low power BLUETOOTH network, existing or presently under development or consideration. See, e.g., Houda Labiod et al., Wi-Fi, Bluetooth, Zigbee and WiMax, Springer, which is incorporated by reference herein in its entirety. It should be understood that interface circuit may be contained within or disposed external to medical device in accordance with the present invention. Also provided within the patient facility are one or more relay modules, a.

Each of the relay modules, a includes at least one transceiver configured to communicate with other relay modules, a in the wireless relay network. Relay modules a further include at least a second transceiver for communicating over the WWAN with the access point. As further described in greater detail with regard to Fig. 3, each module a includes a first transceiver having a respective receiver and transmitter for receiving signals from and transmitting signals to the interface circuits in one or more of the facility-oriented wireless networks. Each relay module a, further includes a second transceiver

having a respective receiver and transmitter for wirelessly transmitting signals to and receiving signals from an access point via a wireless wide-area network or "WWAN".

Suitable WWANs for use with the present invention include, for example, networks based on a Global System for Mobile Communications (GSM) or Code Division Multiple Access (CDMA) cellular network or associated with the 2G, 3G, 3G Long Term Evolution, 4G, WiMAX cellular wireless standards of the International Telecommunication Union Radiocommunication Sector (ITU-R). See, e.g., Vijay Garg, *Wireless Communications & Networking*, Morgan Kaufmann 07, which is incorporated by reference herein in its entirety. Additional suitable exemplary WWANs include metropolitan area networks (MANs), campus area networks (CANs), local area networks (LANs), home area networks (HANs), personal area networks (PANs) and body area networks (BANs).

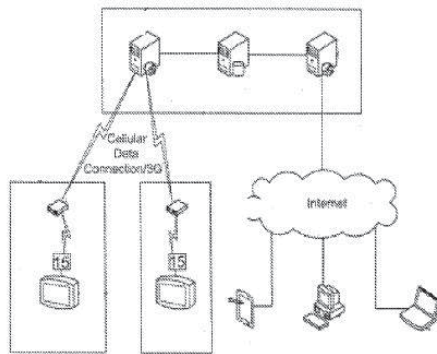


Figure 1. Presents a block diagram of an exemplary medical device network architecture that incorporates a wireless relay module

For compliance with HIPAA regulations, communications over each of the facility-oriented wireless network and WWAN are preferably conducted securely using encryption based upon, for example, any of a Secure Sockets Layer (SSL) protocol and a Transport Layer Security (TLS) protocol.

As illustrated in Fig. 1, a suitable access point useable with the present invention may include an inbound web server 41 that incorporates or otherwise has access to a transceiver (not shown) for communicating with the relay modules a over a particular WWAN. Medical device data received by the inbound web server 41 over the WWAN is forwarded to a secure data storage server, which is configured for example to log the received data in association with identification information of the associated medical devices. "Medical device data" as generally used herein means data from or about the medical device including, for example, medical device identification, medical device software, medical device settings or status information (including alarm information and/or alarm priority),

patient identification information, patient personal identification number(s) "PIN(s)", patient prescriptions, and/or patient medical and/or physiological data as is collected, produced and/or generated by at least one of the medical device and patient identification device; as well as wireless relay network information such as location or status information.

Referring once more to Fig. 1, an outbound web server is configured, for example, to receive and qualify data retrieval requests submitted by one or more of remote monitoring devices, and over a broad-band network 50 (for example, over the Internet), to request associated medical device data to be retrieved from the secure data storage server, and to format and transmit the retrieved data or portion thereof to the one or more remote monitoring devices, and for display on associated device displays. It should be understood that any architecture for the access point that enables the receipt, storage and retrieval of medical device data on a device display of the one or more remote monitoring devices, and is suitable for use in conjunction with the present invention. Variations of the exemplary architecture may involve utilizing a web server integrated with a data storage server[8,9].

Illustrating exemplary wireless network components of the architecture

Fig. 2 presents a block diagram that further illustrates exemplary components of the inventive architecture that are located within or otherwise associated with the patient facility. In Fig.2, a number of interface circuits and relay modules, a are arranged in a single wireless relay network within the patient facility for illustration purposes only. It should be understood that other interface circuits and relay modules, a may communicate over other wireless relay networks similar to network in the patient facility. In Fig.2, the interface circuits and relay modules, a are configured to communicate with one another via associated wireless links. In a preferred embodiment of the present invention represented in Fig.2, the network is a self-configurable mesh network and can also be a self-healing mesh network such as a ZIGBEE compliant-mesh network based on the IEEE 802.4 standard. However, the wireless relay network or additional wireless relay networks in the patient facility may be organized according to a variety of other wireless local area network (WLAN) or WPAN formats including, for example, WiFi WLANs based on the IEEE 802.11 standard and BLUETOOTH WPANs based on the IEEE 802.15.1 standard.

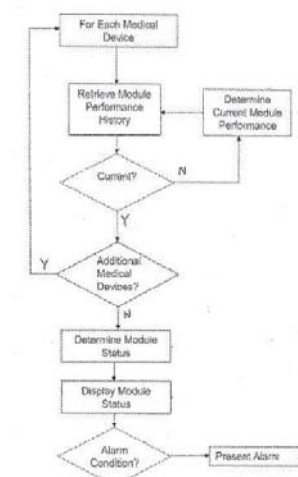


Figure 2. Presents a block diagram further illustrating exemplary wireless network components

In the illustrated wireless relay network, each of the interface circuits includes a communications interface such as, for example, a wired communications interface, to an associated medical device. As previously stated, each of the relay modules, a includes at least one transceiver configured to communicate with other relay modules, a in the wireless relay network. Relay modules a further include at least a second transceiver for communicating over the WWAN with the access point.

The use of a ZIGBEE mesh network for network provides the advantages of being self-configurable when one or more interface circuits and/or relay modules, a are added to the network, and self-healing when one or more interface circuits and/or relay modules, a are removed from or otherwise disabled in the network. Sub- groupings of the interface circuits and relay modules, a may be provided in a defined geographic space (for example, on an individual floor or within a region of a floor in a multi- floor home or care facility).

Illustrates an exemplary control panel for the wireless relay module

Fig. 3 provides a block diagram illustrating exemplary components of relay module a. The relay module a of Fig. 3 includes a first transceiver for wirelessly communicating with interface circuits and other relay modules, a in the WLAN or WPAN network of Fig. 2 via an antenna a. The relay module a further includes a second transceiver for wirelessly communicating with the access point over the WWAN via an antenna a. Each of the transceivers, is in communication with a data processing circuit, which is configured to operate under the control of a controller, e.g., processor, to accept data received by the transceivers, and store the received data in a memory such as buffer element. In addition, the data processing circuit is further configured to retrieve data from the buffer element under the direction of

the processor and provide the retrieved data to a selected one of the transceiver or transceiver for transmission. In order to make a selection, the processor is configured to communicate with respective status modules b, b of the transceivers, in order to determine a communications status of each of the transceivers,. One or more of the data processing circuit and/or controller may also preferably include commercially available encryption circuitry for encrypting data to be sent by the transceivers, and to decrypt data received by the transceivers,. in accordance for example with HIPAA requirements.

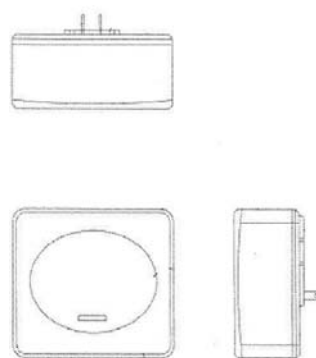


Figure 3. Illustrates an exemplary control panel for the wireless relay module according

The processor is also preferably in communication with a memory for storing an operating program of the processor and/or data stored by and/or retrieved by the processor. The processor is also in communication with an input/output circuit, which provides signals to one or more display elements of the relay module a, for example, for indicating a start-up or current status of the relay module a, including communication or connection status with the WLAN or WPAN network and WWAN. Input/output circuit may also be configured to provide signals to indicate an A/C power loss, and or to be responsive to signals provided by one or more input devices provided in proximity to the one or more display elements.

Relay module a may preferably be provided as a small physical enclosure with an integral power plug and power supply circuit, such that the relay module a may be directly plugged into and supported by a conventional wall outlet providing commercial alternating current AC power. Relay module a may also preferably include a subsystem battery back-up circuit (not shown) to provide uninterrupted power in the event of external power outage of short duration. Battery back-up may also be advantageous, for example, for using the relay module a in an ambulatory mode that enables the patient to move within and potentially at a distance from the facility. In this configuration of facility, for example, any of the medical device, the interface circuit and relay module a may be conveniently carried in a mobile

platform such as any patient-wearable backpack, vehicle or other transport vessel.

It is possible for the relay module to have a substantially similar configuration as the relay module a but excluding the transceiver for communicating over the WWAN with the access point.

Figs. 3 respectively illustrate top, front and side views of an exemplary module configuration for the relay module a. Configuration includes a housing, which is shown in configured essentially as a rectangular box or prism. It should however be noted that the housing may alternatively be configured in any of a variety of three-dimensional shapes having a sufficient interior volume for housing the associated circuits, having a sufficient area on a front panel of the housing for locating a control panel (as further illustrated in Fig.3), and having a sufficient area on a rear panel for providing a receptacle support and power plug for supportably plugging the module configuration into a conventional power outlet or socket. The power plug may also be provided in a modular and replaceable removable configuration enabling power plugs to be configured according to a variety of national or international standards.

configuration that may constitute a portion of the one or more display elements. The exemplary control panel preferably includes, for example, a power switch for powering and/or de-powering the module configuration after it has been connected to a power supply, e.g., plugged into the conventional wall outlet or equipped with a charged battery back-up subsystem. In addition, the control panel preferably includes an alarm switch which allows a user to mute and/or de-mute an audible alarm (for example, a conventional buzzer, bell or audible sound generator and associated loudspeaker, not shown) which is coupled to an alarm circuit (not shown) that is configured to issue an alarm, when, for example, external AC power to the module configuration has been interrupted. The control panel also includes one or more power indicators which may preferably be provided as one or more light-emitting diode (LED) indicator segments which are activated when external power has been provided to the module configuration. Optionally, the indicator may be intermittently or periodically activated when AC power is lost (for example, by means of back-up battery power) to signal the loss of AC power.

The exemplary control panel of Fig.3 also includes a battery indicator to indicate a status of the subsystem battery back-up circuit. For example, and as illustrated in Fig. 3, the battery indicator may preferably include indicator segments which may be selectively activated to indicate a capacity of the back-up battery. Indicator segments may also be preferably provided as LED segments, or as one or more multicolor LEDs for which color is indicative of capacity. If implemented as individual segments,

the segments may, for example, be activated to indicate that the back-up battery is fully charged, and ones of the segments may be progressively deactivated (for example, proceeding downwardly from an uppermost one of the segments ) as battery power is drawn down. In the event that remaining battery power is insufficient to operate the module configuration, each of the segments may be deactivated. Alternatively, the indicator segments may be provided as one or more multicolor LED segments (for example, red, yellow and green). In operation, it is possible for all LED segments to be illuminated as green indicated a full backup battery charge and then progressively, sequentially deactivated as battery charge levels are reduced to a first low power threshold. Then, the LED segments may progressively, sequentially illuminated red as power is further diminished so that all LED segments are illuminated red when battery power is no longer sufficient to power the module configuration :

As further illustrated in Fig. 3, the control panel may further include a relay module network indicator to indicate a status of the portion of the WLAN or WPAN network used to provide communications between the relay module a and its associated interface circuits and medical devices. This relay module network status indicator is preferably backlit with one or more multi-color LEDs to indicate a relative "health" of the associated portion of the network (for example, using "green" to indicate a healthy(e.g., level of accessibility) network, "yellow" to indicate a network having one or more issues but still operable, and "red" to indicate a network that is inoperative and indicating an alarm condition). Optionally, the indicator element may be intermittently or periodically activated when the portion of the WLAN or WPAN network that provides communications between the relay module a and its associated interface circuits and medical devices has relatively poor communications between these devices, or is unavailable to support such communications. In addition, an audible alarm (for example, a conventional buzzer, bell or audible sound generator and associated loudspeaker, not shown) may be initiated under such conditions.

Indicator elements may also be provided, for example, in an array to indicate the status of individual communications with medical devices and or other relay modules, a. For example, the indicator elements may preferably be provided with multicolor LEDs capable, for example, of illuminating a green segment for a healthy a communications path, a yellow segment for operative communication path with issues, and a red segment to indicate a communications path that is inoperative. Alternatively, individual red, yellow and green LEDs may be used in place of the multi-color LEDs. A WWAN indicator may preferably be provided to indicate a status of access to the WWAN network (using



"green" to indicate a healthy network, "yellow" to indicate a network having one or more issues but still operable, and "red" to indicate a network that is inoperative and indicating an alarm condition). As depicted in Fig. 3, the indicator may preferably be backlit with one or more multicolor LEDs. Optionally, the indicator element ) may be intermittently or periodically activated, for example, when a signal strength of the WWAN network available to the module configuration is too low to support communications, or is unavailable to support such communications. In addition, the audible alarm may be initiated under such conditions.

Finally, the control panel may include a WLAN/WPAN indicator to indicate an overall health of the entire WLAN/WPAN (or at least of the portion available to provide an alternate path for the relay module a to the WWAN network). The WLAN/WPAN indicator may preferably indicate an overall status of the WLAN/WPAN (using "green" to indicate a healthy network, "yellow" to indicate a network having one or more issues but still operable, and "red" to indicate a network that is inoperative and indicating an alarm condition). As depicted in Fig. 3, the indicator may preferably be backlit with one or more multicolor LEDs. Optionally, the indicator element may be intermittently or periodically activated when the signal strength of the WLAN network available to the module configuration is too low or insufficient to support communications. In addition, the audible alarm may be initiated under such conditions. As previously indicated, the alarm switch may be configured to allow a user to mute and/or un-mute one or more of the audible alarms entirely, or for a specified time period (similarly to a conventional clock alarm "snooze function") indicators of the module configuration such as indicators - may preferably be electrically connected to the input- output circuit depicted in Fig. 3.

In addition, it is possible for the wireless relay module a to employ, for example, hardware or software to implement an International Telecommunication.

### 3. CONCLUSIONS AND IMPLICATIONS

Information indicative of a status of network communications of at least one of the wireless relay network and the internet-accessible wireless communications network can be transmitted to at least one of the medical devices and/or to a device in communication with one of the internet- accessible wireless communication networks. The wireless relay module may include a display having an indicator of status of network communications. The display may further include an indicator of the status of accessibility of communications over the internet-accessible wireless communications network and/or an indicator representative of a status of the wireless relay network.

### REFERENCES

- [1] SU Nina, JIN Zhenkui, SONG Fan Faculty of Natural Resource and Information Technology, China University of Petroleum, Beijing 102249, China. Distribution and genesis of secondary pores in Paleogene clastic reservoirs of Beidagang structural belt in the Huanghua depression[J]. Mining Science and Technology. 2014(01).
- [2] WANG Jianpeng, GAO Jingxiang, LIU Chao, WANG Jian School of Environment and Spatial Informatics, China University of Mining & Technology, Xuzhou 221008, China. High precision slope deformation monitoring model based on the GPS/Pseudolites technology in open-pit mine[J]. Mining Science and Technology. 2013(01).
- [3] DENG Cunbao<sup>1</sup>, WANG Jiren<sup>1</sup>, WANG Xuefeng<sup>1</sup>, DENG Hanzhong<sup>2</sup> <sup>1</sup>College of Safety Science and Engineering, Liaoning Technical University, Fuxin 123000, China <sup>2</sup>College of Materials Science and Engineering, Liaoning Technical University, Fuxin 123000, China. Spontaneous coal combustion producing carbon dioxide and water[J]. Mining Science and Technology. 2014(01).
- [4] WEI Jiuchuan<sup>1</sup>, LI Zhongjian<sup>1</sup>, SHI Longqing<sup>1</sup>, GUAN Yuanzhang<sup>2</sup>, YIN Huiyong<sup>1</sup> <sup>1</sup>College of Geology Science and Engineering, Shandong University of Science and Technology, Qingdao 266510, China <sup>2</sup>Yanzhou Mining Co., Ltd., Jining 272100, China. Comprehensive evaluation of water-inrush risk from coal floors[J]. Mining Science and Technology. 2015(01).
- [5] GU Qinghua<sup>1</sup>, LU Caiwu<sup>1</sup>, GUO Jinping<sup>1</sup>, JING Shigun<sup>2</sup> <sup>1</sup>School of Management, Xi'an University of Architecture & Technology, Xi'an 710055, China <sup>2</sup>Luoyang Luanchuan Molybdenum Industry Group Inc., Luoyang 471500, China. Dynamic management system of ore blending in an open pit mine based on GIS/GPS/GPRS[J]. Mining Science and Technology. 2013(01).
- [6] NIETO Antonio. GPS and Google Earth based 3D assisted driving system for trucks in surface mines[J]. Mining Science and Technology. 2015(01).
- [7] MA Fengying~(1,2,\*) <sup>1</sup> College of Electronic Information and Control Engineering, Shandong Institute of Light Industry, Jinan 250100, China <sup>2</sup> State Key Laboratory of Coal Resources and Safe Mining, China University of Mining & Technology, Beijing 100083, China. EFT/B interference transmission model and method of anti-interference in a coal mine monitoring substation[J]. Mining Science and Technology. 2013(03).
- [8] LIAO Taiping<sup>1,\*</sup>, HU Jingjing<sup>2</sup>, ZHANG Furong<sup>1</sup>, LIU Lijing<sup>3</sup> <sup>1</sup>Chongqing University of Science and Technology, Chongqing 401331, China <sup>2</sup>Research Institute of Petroleum Exploration and Development, PetroChina, Beijing 100083, China <sup>3</sup>Institute of Geology and Geophysics, Chinese



Academy of Sciences, Beijing 100029, China.  
Reconsideration of the sediment characteristics of the second member of the Triassic Xujiahe Formation in Sanhuiba, Huaying Mountain[J]. Mining Science and Technology. 2010(04).

[9] ZHANG Fan\*, LI Ming State Key Laboratory of

Coal Resources and Safe Mining, China University of Mining & Technology, Beijing 100083, China.  
Wavelet analysis method of harmonics and electromagnetic interference in coal mines[J]. Mining Science and Technology. 2014(04).

# A Certainty-based Active Learning Framework of Meeting Speech Summarization

Dan Meng

University of Science and Technology Liaoning, Anshan, P. R. China

**Abstract:** This paper proposes using a certainty-based active learning framework for extractive meeting speech summarization in order to reduce human effort in generating reference summaries. Active learning chooses a selective set of samples to be labeled by annotators. A combination of informativeness and representativeness criteria for sample selection is proposed. The results of summarizing parliamentary meeting speech, show that the amount of labeled data needed for a given summarization accuracy can be reduced by more than 40% compared to random sampling. The certainty-based active learning framework can be effectively reduced the need of labeling samples for training. Furthermore, compared with lecture speech summarization task, the experiments show that the proposed active learning method of meeting speech summarization is obviously more affected by choice of different kinds of classifiers.

**Index Terms:** Sample Selection, Certainty-based Active Learning, Spontaneous Speech Summarization

## 1. INTRODUCTION

The need for the summarization of spontaneous speech, such as: classroom lectures, conference speeches, parliamentary speeches, is ever increasing with the advent of remote learning, distributed collaboration and electronic archiving. Short abstracts cannot sufficiently meet these user needs. State-of-the-art summarization systems are built by the extractive summarization method in a passive supervised learning framework, which compiles a summary from sentences or segments chosen from the transcribed document using some saliency criteria [1-3]. However, these supervised learning extractive summarization systems require a large amount of training data of reference summaries[4-6]. There is no clear guideline for compiling stable and reproducible reference summaries. To minimize the human annotation efforts yet still producing the same level of performance as a supervised learning approach, we study how to apply active learning approach for training extractive speech summarizer. We then propose three criteria and strategies in our certainty-based active learning framework of meeting speech summarization.

Being the first piece of work on active learning for

lecture speech summarization task, we produced stable and reproducible reference summary and minimized the need for human annotation efforts, yet still producing the same level of performance as a supervised learning approach [7]. In this article, we further describe our certainty-based active learning framework in detail and verify its effectiveness on different genres of spontaneous speech.

The rest of this article is organized as follows: section 2 describes our certainty-based active learning framework, the criteria and the strategies for selecting samples. Section 3 first describes the parliamentary meeting speech corpus, for our experiments, and then outlines the acoustic/prosodic and lexical feature sets for representing each sentence of the transcriptions, and then briefly depicts the probabilistic SVM classifier and naive Bayesian classifier as our extractive summarizers. Our experimental setup and the evaluation results are described in Section 4. Our conclusion follows in the end of this article.

## 2. ACTIVE LEARNING FRAMEWORK AND SAMPLE SELECTION STRATEGIES

### A. Active Learning Algorithm

Human annotators label a small set of training data with summary labels. The training data is used to learn the initial model of the classifier. Then the classifier is used to predict labels for the sentences belonging to all transcribed documents from an unlabeled pool. Because human annotators usually annotate sentences of each document with summary labels by taking the context of the document into account, at each iteration they choose several unlabeled transcribed documents from the pool according to some sample selection strategies. Next the chosen transcribed documents are labeled by human annotators. These annotated transcribed documents are then added for retraining the classifier. This approach is described as follows.

#### Initialization

For an unlabeled data set:  $U_{all}$ ,  $i = 0$

(1) Randomly choose a small set of data  $X_{\{i\}}$  from  $U_{all}$ ;  $U_{\{i\}} = U_{all} - X_{\{i\}}$

(2) Label each sentence in  $X_{\{i\}}$  as summary or non-summary using the RDTW-based semi-automatic annotation procedure proposed by Zhang et al. [5],

and save these sentences and their labels in  $L_{\{i\}}$

Active Learning Process

- (3)  $X\{i\} = \text{null}$
- (4) Train the classifier  $M\{i\}$  using  $L\{i\}$
- (5) Test  $U\{i\}$  by  $M\{i\}$  and select the most useful documents from  $U_{\text{fig}}$  based on informative-ness/representativeness strategies described in Section 1.2.3
- (6) Save selected documents into  $X\{i\}$
- (7) Label each sentence in  $X\{i\}$  as summary or non-summary using the RDTW-based semi-automatic annotation procedure
- (8)  $L\{i+1\} = L\{i\} + X\{i\}$ ,  $U\{i+1\} = U\{i\} - X\{i\}$
- (9) Evaluate  $M\{i\}$  on the testing set  $E$
- (10)  $i = i + 1$ , and repeat from (3) until  $U\{i\}$  is empty or  $M\{i\}$  obtains expected performance
- (11)  $M\{i\}$  is produced and the process ends

We propose the following two criteria for choosing the most useful samples  $X$  from the unlabeled data  $U$  for annotation.

### B. Sampling Criteria

#### Criterion 1: Informative-ness

All active learning scenarios involve evaluating the informative-ness of unlabeled samples. The simplest and most commonly used query framework is uncertainty sampling [8]. The basic idea of informative-ness criterion is that samples that the current model is most uncertain about are selected for annotation. This criterion is often straightforward for probabilistic learning models. When we use a probabilistic model for binary classification as the summarizer, an informative-ness based uncertainty sampling simply selects the samples whose posterior probability of being summary sentences (positive examples) are close to the classification hyper plane. This intuition is justified by D. Lewis and J. Catlett[9], and G. Schohn and D. Cohn[10] based on a version space analysis. They claim that labeling a sample that lies on or close to the hyper plane is guaranteed to have an effect on the model construction.

We measure the informative-ness score of unlabeled transcribed document  $D = \{s_1, s_2, \dots, s_n, \dots, s_N\}$  by  $\text{Score}_{\text{inf}}(D) = (1/N) \sum \text{informative}(s_n)$ , which indicates the ratio of the number of informative sentences to that of all sentences in the document  $D$ .

If the sentence  $s_n$  satisfies the informative-ness criterion:

$P(c(s_n) = 1|D) \geq [(1 - P)^T, (1 + P)^T]$ , where  $c(s_n) = 1$  means the

sentence  $s_n$  is a summary sentence, then  $\text{Informative}(s_n)$  is equal to 1; if not,  $\text{Informative}(s_n)$  is equal to 0.

We denote  $T = P(c(s_n) = 1)$  as the prior probability of the sentence  $s_n$  which is a summary sentence without considering any information on document  $D$ . We

have tried different values for  $T$  when we evaluate our method on the development set. We found  $T$  as

0.12 is suitable empirically for meeting compression tasks.  $p$  is tuned by evaluating the development set sentences to optimize the active learning algorithm. Sentences that satisfy the informative-ness criterion are close to the classification hyper plane. Misclassification implies that the model is most uncertain about the samples.

#### Criterion 2: Representativeness

Another general active learning criterion [11] is to query the sample that would impart the greatest change to the current model if we knew its label. This criterion has also been applied to probabilistic sequence models like Conditional Random Fields (CRFs) [11]. The intuition behind this criterion is that it prefers samples that are likely to most influence the model regardless of the resulting query label. This criterion has been shown to work well in empirical studies though it will be computationally expensive if both the feature space and set of labels are very large[11].

We consider that the model will become more robust if it can be re-trained by the samples selected by this representativeness criterion. The basic idea of representativeness criterion is that samples that are most generalized and are likely to be margin points are selected.

We measure the representativeness score of unlabeled transcribed document  $D = \{s_1, s_2, \dots, s_n, \dots, s_N\}$  by  $\text{Score}_{\text{repre}}(D) = (1/N) \sum \text{representative}(s_j)$ , which indicates the ratio of the number of representative sentences to that of all sentences in the document  $D$ .

If the sentence  $s_n$  satisfies the representativeness criterion:

$P(c(s_n) = 1|D) \geq [0, p^T] \cup [(1 - p)^T, 1]$ , then  $\text{representative}(s_n)$  is equal to 1; if not,  $\text{representative}(s_n)$  is equal to 0.

Sentences with classification scores in the range  $[0, p^T]$  are believed to be most likely a non-summary sentences. Sentences with scores in the range  $[(1 - p)^T, 1]$  are believed to belongs most likely to the summary -sentence class. It means that if  $P(c(s_n) = 1|D)$  is close to 1, the sentence  $s_n$  is most likely summary sentence. If the samples from the above range are misclassified, those samples would impart the greatest change to the current model. Adding those samples to the training data set for labelling will improve the robustness of the model.

### C. Sample Selection Strategies

We apply the following Sample Selection strategies based on the above criteria for selecting the most useful unlabeled examples from the unlabeled pool at each active learning iteration.

**Random Selection Baseline:** A baseline sample selection strategy is to randomly choose  $K$  documents from  $U\{i\}$  to  $X\{i\}$ .

**Length Selection Baseline:** A baseline sample selection strategy is to choose  $K$  documents from  $U\{i\}$  to  $X\{i\}$  according to the average length of a

sentence. The documents with larger average length of a sentence are chosen first.

Sample Selection Strategy 1 (Informative-ness): We choose K documents with the highest value of Scoreinfo(D) from  $U\{i\}$  to  $X\{i\}$  for annotation.

Sample Selection Strategy 2(Robustness): We choose K documents with the highest value of Scorerepr(D) from  $U\{i\}$  to  $X\{i\}$  for annotation.

Sample Selection Strategy 3(Hybrid): We build a hybrid strategy by considering Criterion 1 and Criterion 2 together for striking a proper balance between the informative-ness and representativeness criteria to reach the maximum effectiveness on speech summarization. We choose K documents with the highest value of Score(D), defined as  $\text{Score}(D) = \text{Scoreinfo}(D) * [\text{Scorerepr}(D)]$  if from  $U\{i\}$  to  $X\{i\}$  for annotation, where X (0 K 1) is tuned by evaluating the development set Sentences to optimize the active learning algorithm.

### 3. MEETING CORPUS, FEATURES, AND SUMMARIZERS

Our parliamentary meeting speech corpus contains meeting audio files, the Hansard transcriptions, and the meeting minutes from the Hong Kong Legislative Council. For our experiments, we use all 70 Ordinary Session meeting data from the year 2008 and the year 2009, including audio files, Hansards, and minutes.

We represent each sentence by a feature vector which consists of acoustic features and linguistic features as follows.

Similar to text summarization, the linguistic information can help us predict the summary sentences. We extract eight linguistic features from transcribed documents: Len I (the number of words in the sentence), Len II /Len III (the previous/next sentence's Len I value), TFIDF(the summation of the  $\text{tf} * \text{idf}$  value of each word in the sentence) and Cosine(cosine similarity measure between two sentence vectors).

We extract all linguistic features from the manual and ASR transcribed documents respectively. We segment Chinese words of these transcribed documents for calculating length features. We use an off-the-shelf Chinese lexical analysis system, the open source HIT IR Lab Chinese Word Segmenter [5] to process our corpora.

We had a detailed study of linguistic features based on the word segmentation result. We find that the errors produced by the word segmentation process have little effect on the summarization process. We also find the number of words as a feature is better than the number of characters because word can convey more unambiguous information.

Acoustic/prosodic features in speech summarization system are usually extracted from audio data. Researchers commonly use acoustic/prosodic variation -changes in pitch,

intensity, speaking rate - and duration of pause for tagging the important contents of their speeches. We also investigate these features for their efficiency in predicting summary sentences of presentation speech and meeting speech.

Our acoustic feature set contains twelve features: Duration I (time duration of the sentence), SpeakingRate(average syllable duration), F0 (I-V)(F0 min, max, mean, slope, range), and E (I-V)(Energy min, max, mean, slope, range).

We calculate Duration I from the annotated manual transcriptions that align the audio documents. We then obtain SpeakingRate by phonetic forced alignment by HTK [7]. Next, we extract F0 features and energy features from audio data by using the Praat tool [7].

We then build a discriminative model—Support Vector Machine (SVM) classifier as our summarizer based on these sentence feature vectors.

We apply a generative model—Naive Bayesian classifier implemented by ourselves for the summarizer to investigate whether our active learning method is affected by choice of different machine learning methods.

### 4. EXPERIMENTAL RESULTS AND EVALUATION

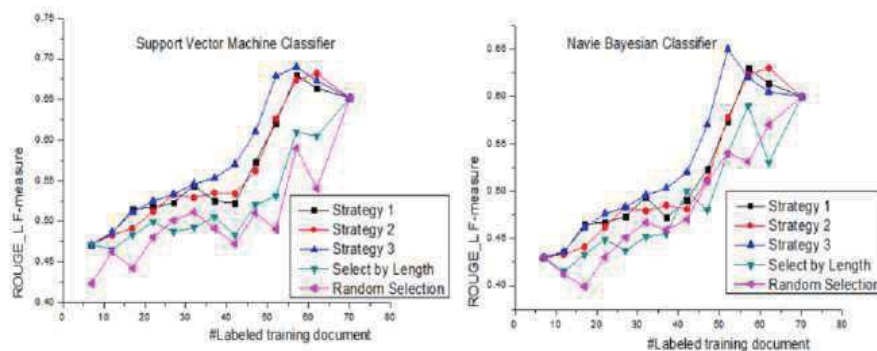
We perform 10-fold cross validation experiments on manual transcriptions, one group for lecture speeches and another one for meeting speeches. First, we divide the 70 meeting speeches into ten subsets. Each subset has seven ones. We use nine subsets as the unlabeled data pool and use the remaining one for test.

We start our experiments by randomly choosing seven speeches from the unlabeled data pool as seeds for manual labeling. We then train the initial classifier using the seeds. We gradually increase the training data pool by choosing five more speeches from the unlabeled data pool each time for annotation. We separately carry out ten sets of experiments for each genre of speech for comparison according to the above three strategies. For each sample selection step, we also choose the unlabeled documents by random selection baseline strategy and length selection baseline strategy. In each group of experiment, we repeat the process of randomly choosing seven speeches as seeds, six times. We evaluate the summarizer by ROUGE-L (summary-level Longest Common Subsequence) F-measure [5]. We calculate the mean value of ROUGE-L F-measure of each active learning step as the final performance of this step. For meeting speeches, all the evaluation results of the three active learning strategies and the two baseline strategies using the SVM classifier and the Naive Bayesian classifier is respectively shown in Fig. 1. We train the classifiers by using a combination of linguistic features and acoustic features.

We consider the extractive summarization problem as a binary classification problem. From Fig.1, we find that, for classification performance, random sample selection strategy is always consistently and significantly outperformed by the active learning methods using our proposed sample selection strategies. By using only 37 documents for training, the performance of the SVM classifier achieved by Strategy 3 which combines the informative-ness criterion and representativeness criterion for selecting samples is better than that of the SVM classifier trained by random sample selection using all 70 presentations (ROUGE- L F-measure of 0.512 vs. that of 0.502). This shows that our active learning approach requires 40% less training data. We also find that using Strategy 3 our active learning approach requires less training data to obtain the same level of summarization performance compared to that using Strategy 1. In other words, Strategy 3 is better than Strategy 1. When we apply Naive Bayesian classifier as our summarizer, we obtain the same finding as that shown in Fig. 1. Besides, we find that the length sample selection method produces worse

performance than our active learning sample selection strategies. This indicates that the performance gains of the active learning methods are due to their ability to choose the unlabeled transcribed documents which contain more informative and representative samples which help find more accurate classification hyper-plane and improve the summarization performance. However, the random sample selection strategy and the length sample selection strategy cannot guarantee selecting those documents with more informative and representative samples.

We compare a discriminative model—SVM classifier with a generative model—Naive Bayesian classifier as shown in Fig. 1 to investigate the effectiveness of active learning using different kinds of machine learning methods. We find that our active learning method of meeting speech summarization is obviously affected by choice of different classifiers. For meeting speech corpus, the best performance of SVM classifier is absolute a 4% higher than that of the Naive Bayesian classifier (0.69 vs 0.65).



**Fig. 1** Average performance of the SVM classifier and the Naive Bayesian classifier trained by using the combination of acoustic features and linguistic features on parliamentary meeting speech corpus

## 5. Conclusion

This paper described an approach of active learning to reduce the need for human annotation for summarizing parliamentary meeting speech. We chose the unlabeled examples according to a combination of informative-ness criterion and representativeness criterion. The summarization results showed an increasing learning curve, consistently higher than that by using randomly chosen training samples. Furthermore, the experiments showed that the proposed active learning method of meeting speech summarization was obviously affected by choice of different classifiers.

## REFERENCES

[1]Y. Fujii, K. Yamamoto, N. Kitaoka and S. Nakagawa. Class Lecture Summarization Taking into Account Consecutiveness of Important Sentences. In Proceedings of Interspeech, IEEE. pp,

2438-2441(2013).

[2]C. Hori and S. Furui. Advances in automatic speech summarization, In Proceedings of Eurospeech2001. Pp, 1771-1774(2015).

[3]J. Mrozinski, E. Whittaker, P. Chatain, and S. Furui. Automatic sentence segmentation of speech for automatic summarization, in Proceedings of ICASSP. 1(5), 12(2015).

[4]T. Kawahara, H. Nanjo, and S. Furui. Automatic transcription of spontaneous lecture speech, in Proc. IEEE Workshop on Automatic Speech Recognition and Understanding, IEEE. pp, 186-189(2015).

[5]J. Zhang, S. Huang, and P. Fung. RSHMM++ for Extractive Lecture Speech Summarization, In Proceedings of 2008 IEEE Workshop on Spoken Language Technology, IEEE. pp,161-164(2014).

[6]X. Zhu and G. Penn. Evaluation of sentence selection for speech summarization, in Workshop of Crossing Barriers in Text Summarization, RANLP2005, Bulgaria, Citeseer(2015).



- [7]J. Zhang and P. FUNG. Active learning of extractive reference summaries for lecture speech summarization, in Proceedings of the 2nd Workshop on Building and Using Comparable Corpora (BUCC), Association for Computational Linguistics. pp,23-26(2013).
- [8]D. Lewis and J. Catlett. Heterogeneous uncertainty sampling for supervised learning, in Proceedings of the Eleventh International Conference on Machine Learning. Morgan Kaufmann. pp,148-156(2014).
- [9]G. Schohn and D. Cohn. Less is more: Active learning with support vector machines, in Machine Learning-International Workshop THEN Conference-. pp,839-846(2013).
- [10]S. Tong and D. Koller. Support vector machine active learning with applications to text classification. The Journal of Machine Learning Research. 2(1), 45-66(2015).
- [11]B. Settles. Active learning literature survey, University of Wisconsin-Madison. Computer Sciences Technical Report. pp, 1648-1715(2015).

# Algorithm for Three Associated Continued Fractions Newton Blending Rational Interpolant

Le Zou

Department of Computer Science and Technology, Hefei University, Hefei, China

**Abstract:** Interpolation has widely application in image processing, Computer Aided Geometric Design(CAGD) and electrochemistry. As we know, Newton's polynomial interpolation may be the favorite linear interpolation, three associated continued fractions interpolation is a new type nonlinear rational interpolation. We use three associated continued fractions interpolation and Newton's polynomial interpolation to construct a new type of bivariate blending rational interpolants. We also present the interpolation theorem, interpolation algorithm and discuss the dual interpolants and vector case and matrix case. Multivariate case and some new interpolation as its generalization are given in remarks. Numerical example is given to show the effectiveness of the results.

**Index Terms:** Three Associated Continued Fractions Interpolation; Blending Rational Interpolants; Image Processing

## 1. INTRODUCTION

Newton interpolation and associated continued fraction interpolation may be the favoured linear interpolation and nonlinear interpolation[1-2]. Rational interpolation is an important method of nonlinear approximation. One common method for constructing the rational interpolation is based on continued fractions. The advantage of the continued fractions lies in simple structure and convenient calculation; we don't have to solve linear equations as constructing the general rational interpolation function, but only calculate the corresponding differences based on the scheme of interpolation, Siemaszko studied bivariate Thiele-type rational interpolation, Kuchmins'ka and Vozna constructed the Newton-Thiele-like interpolation scheme. Tan constructed Newton-Thiele and Thiele-Newton type bivariate blending rational interpolation[1,3]. This method just needed to calculate the Newton-Thiele type or Thiele-Newton type blending differences, and then one could construct the interpolation formula. Tan constructed vector valued rational interpolation by using Thiele-type branched continued fractions and Samelson inverses[1]. Bivariate blending rational interpolation by combine associated to Newton and Thiele continued fractions are treated in the papers by some of the authors[4,5].

In this age of ever-increasing digitization in the storage, processing, analysis, and communication of

information, it is not difficult to find examples of applications where this problem occurs. Some scholars has been studying their application in image processing, curves/surface[6-13]. Our contribution in this paper is to construct a new bivariate blending rational interpolation. The organization of the paper is as follows. We obtain the interpolation algorithm and interpolant theorem in section II. Matrix algorithm is discussed in section III. Numerical example is given in section IV to show the effectiveness of the results. Section V presents some remarks.

Given a set of real points

$$X_n = \{x_0, x_1, \dots, x_{3[n/3]+2}\} \subset [a, b] \subset \mathbb{R} \quad (1)$$

and a function  $f(x) \in C^{3[n/3]+3}[a, b]$ .

It is well known that  $f(x)$  can be expanded into the following Newton's polynomial interpolation with remainder[2]

$$f(x) = \sum_{i=0}^{3[n/3]} f[x_0, x_1, \dots, x_i] \omega_i(x) + \omega_{3[n/3]+2}(x) f[x_0, x_1, \dots, x_{3[n/3]+2}; x]. \quad (2)$$

where  $\omega_0(x) = 1$ ,  $\omega_i(x) = (x - x_0)(x - x_1) \cdots (x - x_{i-1})$ ,  $i = 1, 2, \dots, 3[n/3] + 2$ .

and  $f[x_0, x_1, \dots, x_i]$  denotes the divided difference of  $f(x)$  at points  $x_0, x_1, \dots, x_i$  defined by

$$f[x_p] = f(x_p), \quad p = 0, 1, \dots, 3[n/3] + 2. \quad (3)$$

$$f[x_0, x_1, \dots, x_i] = \frac{f[x_0, x_1, \dots, x_{i-2}, x_i] - f[x_0, x_1, \dots, x_{i-2}, x_{i-1}]}{x_i - x_{i-1}}.$$

Let

$$P_{3[n/3]+2}(x) = \sum_{i=0}^{3[n/3]+2} f[x_0, x_1, \dots, x_i] \omega_i(x) \quad (4)$$

then  $P_{3[n/3]+2}(x)$  is a polynomial of degree  $3[n/3] + 2$  satisfying

$$P_{3[n/3]+2}(x_i) = f(x_i), \quad i = 0, 1, \dots, 3[n/3] + 2. \quad (5)$$

and

$$f(x) - P_{3[n/3]+2}(x) = f[x_0, x_1, \dots, x_{3[n/3]+2}; x] \omega_{3[n/3]+3}(x) \quad (6)$$

$$= \frac{f^{(3[n/3]+3)}(\xi)}{(3[n/3] + 3)!} \omega_{3[n/3]+3}(x)$$

with  $\xi$  located among  $x_0, x_1, \dots, x_{3[n/3]+2}, x$ .

Another approximation to  $f(x)$  is the following three associated continued fraction expansion[3,15].

$$r_{3[n/3]+2}(x) = \omega_0[x_0] + \omega_1[x_1](x-x_0) + \omega_2[x_2](x-x_0)(x-x_1) + \frac{(x-x_0)(x-x_1)(x-x_2)}{\omega_3[x_3] + \omega_4[x_4](x-x_3) + \omega_5[x_5](x-x_3)(x-x_4)} + \dots + \frac{x-x_{3[\frac{n}{3}]-3})(x-x_{3[\frac{n}{3}]-2})(x-x_{3[\frac{n}{3}]-1})}{\omega_{3[\frac{n}{3}]}[x_{3[\frac{n}{3}}] + \omega_{3[\frac{n}{3}]+1}[x_{3[\frac{n}{3}]+1}](x-x_{3[\frac{n}{3}}]) + \omega_{3[\frac{n}{3}]+2}[x_{3[\frac{n}{3}]+2}](x-x_{3[\frac{n}{3}})(x-x_{3[\frac{n}{3}]+1})} \quad (7)$$

where

$$\omega_0[x_i] = f(x_i) \quad \forall x \in X_n, \quad \omega_{3k}[x_{3k}] = \omega_{3k}[x_0, \dots, x_{3k-1}, x_{3k}] = \frac{x_{3k} - x_{3k-1}}{\omega_{3k+1}[x_0, \dots, x_{3k-2}, x_{3k}] - \omega_{3k-1}[x_0, \dots, x_{3k-2}, x_{3k-1}]}, \quad (8)$$

$$\omega_{3k+1}[x_{3k+1}] = \omega_{3k+1}[x_0, \dots, x_{3k}, x_{3k+1}] = \frac{\omega_{3k}[x_0, \dots, x_{3k-1}, x_{3k+1}] - \omega_{3k}[x_0, \dots, x_{3k-1}, x_{3k}]}{x_{3k+1} - x_{3k}}, \quad (9)$$

$$\omega_{3k+2}[x_{3k+2}] = \omega_{3k+2}[x_0, \dots, x_{3k+1}, x_{3k+2}] = \frac{\omega_{3k+1}[x_0, \dots, x_{3k}, x_{3k+2}] - \omega_{3k+1}[x_0, \dots, x_{3k}, x_{3k+1}]}{x_{3k+2} - x_{3k+1}}, \quad (10)$$

where  $k = 0, 1, \dots, [n/3]$ ,  $[\mu]$  is entire function.

Let

$$R_{3[n/3]+2}(x) = \frac{A_{3[n/3]+2}(x)}{B_{3[n/3]+2}(x)} = \omega_0[x_0] + \omega_1[x_1](x-x_0) + \omega_2[x_2](x-x_0)(x-x_1) + \frac{(x-x_0)(x-x_1)(x-x_2)}{\omega_3[x_3] + \omega_4[x_4](x-x_3) + \omega_5[x_5](x-x_3)(x-x_4)} + \dots + \frac{x-x_{3[\frac{n}{3}]-3})(x-x_{3[\frac{n}{3}]-2})(x-x_{3[\frac{n}{3}]-1})}{\omega_{3[\frac{n}{3}]}[x_{3[\frac{n}{3}}] + \omega_{3[\frac{n}{3}]+1}[x_{3[\frac{n}{3}]+1}](x-x_{3[\frac{n}{3}}]) + \omega_{3[\frac{n}{3}]+2}[x_{3[\frac{n}{3}]+2}](x-x_{3[\frac{n}{3}})(x-x_{3[\frac{n}{3}]+1})} \quad (11)$$

then  $R_{3[n/3]+2}(x)$  is a rational function and which satisfying

$$R_{3[n/3]+2}(x_i) = f(x_i), i = 0, 1, \dots, 3[n/3] + 2.$$

## 2. NEW APPROACH TO BIVARIATE BLENDING RATIONAL INTERPOLATION

From the univariate case, we find that the divided differences and inverse differences play important roles in constructing linear and nonlinear interpolants respectively. We expect to obtain a new bivariate rational interpolants by defining a kind of blending differences.

To this end, we set

$$X_{3[n/3]+2} = \{x_0, x_1, \dots, x_{3[n/3]+2}\} \subset [a, b] \subset R$$

$$Y_{3[m/3]+2} = \{y_0, y_1, \dots, y_{3[m/3]+2}\} \subset [c, d] \subset R$$

$$\Pi_{x,y}^{n,m} = X_{3[n/3]+2} \times Y_{3[m/3]+2}$$

and let a bivariate function  $f(x, y)$  be defined on

$$D = [a, b] \times [c, d].$$

**Definition 1** Let

$$\phi[x_i, y_j] = f(x_i, y_j), \quad (12)$$

$$i = 0, 1, \dots, 3[n/3] + 2, j = 0, 1, \dots, 3[m/3] + 2.$$

$$\phi[x_0, x_1, \dots, x_i; y_j] =$$

$$\frac{\phi[x_0, \dots, x_{i-2}, x_i; y_j] - \phi[x_0, \dots, x_{i-2}, x_{i-1}; y_j]}{x_i - x_{i-1}} \quad (13)$$

$$\phi[x_0, \dots, x_i; y_0, \dots, y_{3j-1}, y_{3j}] = \frac{y_{3j} - y_{3j-1}}{\phi[x_0, \dots, x_i; y_0, \dots, y_{3j-2}, y_{3j}] - \phi[x_0, \dots, x_i; y_0, \dots, y_{3j-2}, y_{3j-1}]} \quad (14)$$

$$\phi[x_0, \dots, x_i; y_0, \dots, y_{3j-1}, y_{3j}, y_{3j+1}] = \frac{\phi[x_0, \dots, x_i; y_0, \dots, y_{3j-1}, y_{3j+1}] - \phi[x_0, \dots, x_i; y_0, \dots, y_{3j-1}, y_{3j}]}{y_{3j+1} - y_{3j}} \quad (15)$$

$$\phi[x_0, \dots, x_i; y_0, \dots, y_{3j}, y_{3j+1}, y_{3j+2}] = \frac{\phi[x_0, \dots, x_i; y_0, \dots, y_{3j}, y_{3j+2}] - \phi[x_0, \dots, x_i; y_0, \dots, y_{3j}, y_{3j+1}]}{y_{3j+2} - y_{3j+1}} \quad (16)$$

$$\phi[x_0, \dots, x_i; y_0, \dots, y_j] = \frac{\phi[x_0, \dots, x_{i-2}, x_i; y_0, \dots, y_j] - \phi[x_0, \dots, x_{i-2}, x_{i-1}; y_0, \dots, y_j]}{x_i - x_{i-1}} \quad (17)$$

We call  $\phi[x_0, x_1, \dots, x_i; y_0, y_1, \dots, y_j]$  defined by (12)-(17) as the blending difference of  $f(x, y)$  at the set of points  $\{x_0, x_1, \dots, x_i\} \times \{y_0, y_1, \dots, y_j\}$ .

We construct a two-dimension rational interpolation function

$$R(x, y) = K_0(y) + K_1(y)(x-x_0) + K_2(y)(x-x_0)(x-x_1) + L + \frac{K_{3[n/3]+2}(y)(x-x_0)(x-x_1)L - (x-x_{3[n/3]+1})}{Q(x, y)} \quad (18)$$

with

$$\begin{aligned} K_i(y) &= \phi[x_0, \dots, x_i; y_0] + \phi[x_0, \dots, x_i; y_0, y_1](y-y_0) + \\ &\phi[x_0, \dots, x_i; y_0, \dots, y_2](y-y_0)(y-y_1) + \\ &(y-y_0)(y-y_1)(y-y_2) / ((\phi[x_0, \dots, x_i; y_0, \dots, y_3] + \\ &\phi[x_0, \dots, x_i; y_0, \dots, y_4](y-y_3) + \\ &\phi[x_0, \dots, x_i; y_0, \dots, y_5](y-y_3)(y-y_4)) + \dots + \\ &(y-y_{3[\frac{m}{3}]-3})(y-y_{3[\frac{m}{3}]-2})(y-y_{3[\frac{m}{3}]-1}) / \\ &(\phi[x_0, \dots, x_i; y_0, \dots, y_{3[\frac{m}{3}]}] + \phi[x_0, \dots, x_i; y_0, \dots, y_{3[\frac{m}{3}]+1}](y-y_{3[\frac{m}{3}]}) \\ &+ \phi[x_0, \dots, x_i; y_0, \dots, y_{3[\frac{m}{3}]+2}](y-y_{3[\frac{m}{3}]})(y-y_{3[\frac{m}{3}]+1}))), \\ i &= 0, 1, \dots, 3[m/3] + 2. \end{aligned} \quad (19)$$

We call the interpolation defined by (18) and (19) is three associated continued fraction Newton blending rational interpolation. Then we can get the theorem:

**Theorem 1:** Let  $\phi[x_0, x_1, \dots, x_i; y_0, y_1, \dots, y_j]$  be given by formulas (12)-(17). Then relation (18) and (19) is an interpolation formula, i.e,

$$R(x_i, y_j) = f(x_i, y_j), \quad \forall (x_i, y_j) \in \Pi_{x,y}^{3[n/3]+2, 3[m/3]+2} \quad (20)$$

Provided that every blending difference  $\phi[x_0, x_1, \dots, x_i; y_0, y_1, \dots, y_j]$  exists.

**Proof:** we can proof  $K_i(y_j) = \phi[x_0, x_1, \dots, x_{i-1}, x_i; y_j]$  with the method similar to one variable[1]

Therefore by (13), (14) and (17), we get

$$\begin{aligned} R(x_i, y_j) &= K_0(y_j) + K_1(y_j)(x_i - x_0) \\ &+ K_2(y_j)(x_i - x_0)(x_i - x_1) + \dots + \\ &K_i(y_j)(x_i - x_0)(x_i - x_1) \dots (x_i - x_{i-1}) \\ &= \varphi[x_0; y_j] + \varphi[x_0, x_1; y_j](x_i - x_0) + \dots + \\ &(x_i - x_0)(x_i - x_1) \dots (x_i - x_{i-1}) \\ &\varphi[x_0, \dots, x_{i-2}, x_i; y_j] - \varphi[x_0, \dots, x_{i-2}, x_{i-1}; y_j] \\ &\frac{x_i - x_{i-1}}{x_i - x_{i-1}} \\ &= \varphi[x_0; y_j] + \varphi[x_0, x_1; y_j](x_i - x_0) + \dots + \\ &(x_i - x_0)(x_i - x_1) \dots (x_i - x_{i-2}) \varphi[x_0, x_1, \dots, x_{i-2}, x_i; y_j] \\ &= \dots = \varphi[x_i; y_j] = f(x_i, y_j) \end{aligned}$$

as asserted.

### 3. MATRIX algorithm

In this section, we give the matrix algorithm of general interpolation formula of block based bivariate interpolation.

Step1: Initialize

$$f_{i,j}^{(0,0)} = f(x_i, y_j), i = 0, 1, L, 3[n/3] + 2; j = 0, 1, L, 3[m/3] + 2. \quad (21)$$

Definity the follow information matrix

$$M = \begin{bmatrix} f_{0,0}^{(0,0)} & f_{1,0}^{(0,0)} & \dots & f_{3[n/3]+2,0}^{(0,0)} \\ f_{0,1}^{(0,0)} & f_{1,1}^{(0,0)} & \dots & f_{3[n/3]+2,1}^{(0,0)} \\ \vdots & \vdots & \ddots & \vdots \\ f_{0,3[m/3]+2}^{(0,0)} & f_{1,3[m/3]+2}^{(0,0)} & \dots & f_{3[n/3]+2,3[m/3]+2}^{(0,0)} \end{bmatrix} \quad (22)$$

Step2: for

$$j = 0, 1, \dots, 3[m/3] + 2; p = 1, 2, \dots, 3[n/3] + 2;$$

$$i = p, p+1, \dots, 3[n/3] + 2$$

Let

$$f_{i,j}^{(p,0)} = \frac{f_{i,j}^{(p-1,0)} - f_{p-1,j}^{(p-1,0)}}{x_i - x_{p-1}} \quad (23)$$

The initial information matrix  $M$  by recursion will changed into (column conversion)

$$M_1 = \begin{bmatrix} f_{0,0}^{(0,0)} & f_{1,0}^{(1,0)} & \dots & f_{3[n/3]+2,0}^{(3[n/3]+2,0)} \\ f_{0,1}^{(0,0)} & f_{1,1}^{(1,0)} & \dots & f_{3[n/3]+2,1}^{(3[n/3]+2,0)} \\ \vdots & \vdots & \ddots & \vdots \\ f_{0,3[m/3]+2}^{(0,0)} & f_{1,3[m/3]+2}^{(1,0)} & \dots & f_{3[n/3]+2,3[m/3]+2}^{(3[n/3]+2,0)} \end{bmatrix} \quad (24)$$

Step3:for

$$i = 0, 1, \dots, k-1, k+1, \dots, 3[n/3] + 2; q = 1, 2, 4, 5, \dots, 3[m/3] + 1, 3[m/3] + 2; j = q, q+1, \dots, 3[m/3] + 2$$

let

$$f_{i,j}^{(i,q)} = \frac{f_{i,j}^{(i,q-1)} - f_{i,q-1}^{(i,q-1)}}{y_j - y_{q-1}} \quad (25)$$

For

$$i = 0, 1, L, k-1, k+1, L, 3[n/3] + 2; q = 3, 3, L, 3[m/3];$$

$$j = q, q+1, L, 3[m/3] + 2$$

,

let

$$f_{i,j}^{(i,q)} = \frac{y_j - y_{q-1}}{f_{i,j}^{(i,q-1)} - f_{i,q-1}^{(i,q-1)}} \quad (26)$$

from recursion the column  $0, 1, \dots, k-1, k+1, \dots, 3[n/3] + 2$  of the information matrix  $M_1$  will changed into (row conversion)

$$M_2 = \begin{bmatrix} f_{0,0}^{(0,0)} & f_{1,0}^{(1,0)} & \dots & f_{k-1,0}^{(k-1,0)} & f_{k+1,0}^{(k+1,0)} & \dots & f_{3[n/3]+2,0}^{(3[n/3]+2,0)} \\ f_{0,1}^{(0,1)} & f_{1,1}^{(1,1)} & \dots & f_{k-1,1}^{(k-1,1)} & f_{k+1,1}^{(k+1,1)} & \dots & f_{3[n/3]+2,1}^{(3[n/3]+2,1)} \\ \vdots & \vdots & \ddots & \vdots & \vdots & \ddots & \vdots \\ f_{0,n}^{(0,n)} & f_{1,n}^{(1,n)} & \dots & f_{k-1,n}^{(k-1,n)} & f_{k+1,n}^{(k+1,n)} & \dots & f_{3[n/3]+2,n}^{(3[n/3]+2,n)} \end{bmatrix} \quad (27)$$

Step4: using the  $i+1$  column of the matrix  $M_2$ , one can construct associated continued fractions rational interpolation

$$\begin{aligned} K_i(y) &= \varphi[x_0, \dots, x_i; y_0] + \varphi[x_0, \dots, x_i; y_0, y_1](y - y_0) + \\ &\varphi[x_0, \dots, x_i; y_0, \dots, y_2](y - y_0)(y - y_1) + \\ &(y - y_0)(y - y_1)(y - y_2) / ((\varphi[x_0, \dots, x_i; y_0, \dots, y_3] + \\ &\varphi[x_0, \dots, x_i; y_0, \dots, y_4](y - y_3) + \\ &\varphi[x_0, \dots, x_i; y_0, \dots, y_5](y - y_3)(y - y_4)) + \dots + \\ &(y - y_{3[\frac{m}{3}]-3})(y - y_{3[\frac{m}{3}]-2})(y - y_{3[\frac{m}{3}]-1}) / \\ &(\varphi[x_0, \dots, x_i; y_0, \dots, y_{3[\frac{m}{3}]}] + \varphi[x_0, \dots, x_i; y_0, \dots, y_{3[\frac{m}{3}]+1}](y - y_{3[\frac{m}{3}]}) \\ &+ \varphi[x_0, \dots, x_i; y_0, \dots, y_{3[\frac{m}{3}]+2}](y - y_{3[\frac{m}{3}]})(y - y_{3[\frac{m}{3}]+1}))), \\ &i = 0, 1, \dots, 3[m/3] + 2. \end{aligned}$$

Step5: let

$$\begin{aligned} R(x, y) &= K_0(y) + K_1(y)(x - x_0) + K_2(y)(x - x_0)(x - x_1) + L + \\ &K_{3[n/3]+2}(y)(x - x_0)(x - x_1)L (x - x_{3[n/3]+1}) \end{aligned} \quad (28)$$

Then  $R(x, y)$  is three associated continued fractions Newton bivariate blending rational interpolation.

### 4. NUMERICAL EXAMPLE

In this section, we take a simple example to show how flexible our method are.

Example Let  $(x_i, y_j)$  and  $f(x_i, y_j)$  be given in the table.

Table 1. interpolation data

|           | $y_0 = 0$ | $y_1 = 1$ | $y_2 = 2$ | $y_3 = 3$ | $y_4 = 4$ |
|-----------|-----------|-----------|-----------|-----------|-----------|
| $x_0 = 0$ | 1         | 0         | -1/3      | -2        | -2        |
| $x_1 = 1$ | 2         | 1/2       | 8/3       | 17/2      | 99/5      |
| $x_2 = 2$ | 4         | 0         | 14/3      | 24        | 281/5     |

Using the method in the paper, we can construct associate continued fractions Newton blending rational interpolation:

$$\begin{aligned} R(x, y) &= 1 - y + \frac{y(y-1)}{3} + \frac{y(y-1)(y-2)}{-3-5(y-3)} \\ &(1 - \frac{y}{2} + \frac{y(y-1)}{2/3} + \frac{y(y-1)(y-2)}{3+2(y-3)})x + \\ &(\frac{1}{2} - y + \frac{y(y-1)}{2} + \frac{y(y-1)(y-2)}{3+2(y-3)})x(x-1) \end{aligned}$$

It is easy to verify that

$$R(x, y) = f(x_i, y_j), i = 0, 1, 2; j = 0, 1, 2, 3.$$

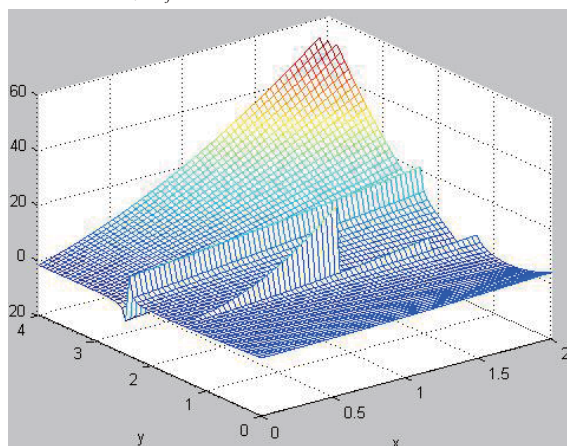


Fig1. image of interpolation function

### 5. REMARKS

Remark 1 Similar to blending rational interpolation given in (18) and (19), we can construct the dual interpolant function of the three associated continued fractions Newton blending rational interpolant as follows:

$$R_1(x, y) = K_0(x) + K_1(x)(y - y_0) + K_2(x)(y - y_0)(y - y_1) + \dots + K_{3[m/3]+2}(x)(y - y_0)(y - y_1) \dots (y - y_{3[m/3]+1}) \quad (29)$$

With

$$K_i(x) = \omega_0[x_0; y_0, \dots, y_i] + \omega_1[x_1; y_0, \dots, y_i](x - x_0) + \omega_2[x_2; y_0, \dots, y_i](x - x_0)(x - x_1) + (x - x_0)(x - x_1)(x - x_2) / ((\omega_3[x_3; y_0, \dots, y_i] + \omega_4[x_4; y_0, \dots, y_i](x - x_3) + \omega_5[x_5; y_0, \dots, y_i](x - x_3)(x - x_4)) + \dots + (x - x_{3[\frac{m}{3}]-3})(x - x_{3[\frac{m}{3}]-2})(x - x_{3[\frac{m}{3}]-1}) / (\omega_{3[\frac{m}{3}]}[x_{3[\frac{m}{3}}; y_0, \dots, y_i] + \omega_{3[\frac{m}{3}+1]}[x_{3[\frac{m}{3}+1}; y_0, \dots, y_i](x - x_{3[\frac{m}{3}}]) + \omega_{3[\frac{m}{3}+2]}[x_{3[\frac{m}{3}+2}; y_0, \dots, y_i](x - x_{3[\frac{m}{3}})(x - x_{3[\frac{m}{3}+1}]))), \quad (30)$$

$$i = 0, 1, \dots, 3[m/3] + 2.$$

and  $\phi[x_0, x_1, \dots, x_i; y_0, y_1, \dots, y_j]$ , also called blending difference, are recursively computed according to the following formulas

$$\phi[x_i, y_j] = f(x_i, y_j), i = 0, 1, L, 3[n/3] + 2, j = 0, 1, L, 3[m/3] + 2. \quad (31)$$

$$\phi[x_i; y_0, \dots, y_j] = \frac{\phi[x_i; y_0, \dots, y_{j-2}, y_j] - \phi[x_i; y_0, \dots, y_{j-2}, y_{j-1}]}{y_j - y_{j-1}} \quad (32)$$

$$\phi[x_0, \dots, x_{3i-1}, x_{3i}; y_0, \dots, y_j] = \frac{x_{3i} - x_{3i-1}}{\phi[x_0, \dots, x_{3i-2}, x_{3i}; y_0, \dots, y_j] - \phi[x_0, \dots, x_{3i-2}, x_{3i-1}; y_0, \dots, y_j]} \quad (33)$$

$$\phi[x_0, \dots, x_{3i-1}, x_{3i}, x_{3i+1}; y_0, \dots, y_j] = \frac{\phi[x_0, \dots, x_{3i-1}, x_{3i+1}; y_0, \dots, y_j] - \phi[x_0, \dots, x_{3i-1}, x_{3i}; y_0, \dots, y_j]}{x_{3i+1} - x_{3i}} \quad (34)$$

$$\phi[x_0, \dots, x_{3i-1}, x_{3i+1}, x_{3i+2}; y_0, \dots, y_j] = \frac{\phi[x_0, \dots, x_{3i+1}, x_{3i+2}; y_0, \dots, y_j] - \phi[x_0, \dots, x_{3i+1}, x_{3i+1}; y_0, \dots, y_j]}{x_{3i+2} - x_{3i+1}} \quad (35)$$

$$\phi[x_0, x_1, \dots, x_i; y_0, y_1, \dots, y_j] = \frac{\phi[x_0, \dots, x_i; y_0, \dots, y_{j-2}, y_j] - \phi[x_0, \dots, x_i; y_0, \dots, y_{j-2}, y_{j-1}]}{y_j - y_{j-1}} \quad (36)$$

36)

It is not difficult to show

$$R_1(x_i, y_j) = f(x_i, y_j), i = 0, 1, L, 3[n/3] + 2; j = 0, 1, L, 3[m/3] + 2.$$

and the error estimation similar to theorem 2 can be established.

Remark 2 Similar to blending rational interpolation given in (18) and (19), we can also get Newton three associated continued fractions blending rational interpolant as follows:

$$R_2(x, y) = b_0(x) + b_1(x)(y - y_0) + b_2(x)(y - y_0)(y - y_1) + \sum_{k=0}^{3[m/3]-2} \frac{(y - y_{3k})(y - y_{3k+1})(y - y_{3k+2})}{b_{3k+3}(x) + b_{3k+4}(x)(y - y_{3k+3})} \quad (37)$$

with

$$b_j(x) = \tau[x_0; y_0, L, y_j] + \tau[x_0, x_1; y_0, L, y_j](x - x_0) + L + \tau[x_0, L, x_{3[n/3]+2}; y_0, L, y_j](x - x_0)(x - x_1) \dots (x - x_{3[n/3]+1}), \quad (38)$$

$$j = 0, 1, L, 3[m/3] + 2.$$

and  $\tau[x_0, x_1, \dots, x_i; y_0, y_1, \dots, y_j]$ , also called blending difference, are recursively computed as in definition 1.

It is not difficult to show

$$R_2(x_i, y_j) = f(x_i, y_j), \quad (39)$$

$$i = 0, 1, L, 3[n/3] + 2, j = 0, 1, L, 3[m/3] + 2.$$

and we can also estimate the error of above formula.

Remark 3 Instead of defining  $R(x, y)$  respect to  $x$  be the Newton interpolant polynomial, one defines it to be the associated continued fraction interpolation,

$$R_3(x, y) = b_0(x) + b_1(x)(y - y_0) + b_2(x)(y - y_0)(y - y_1) + \sum_{k=0}^{3[m/3]-2} \frac{(y - y_{3k})(y - y_{3k+1})(y - y_{3k+2})}{b_{3k+3}(x) + b_{3k+4}(x)(y - y_{3k+3})} \quad (40)$$

With  $K_i(y)$  is defined as (19).

Then  $R_3(x, y)$  turns out to be a new bivariate blending rational interpolants.

Remark 4 One can also construct news kind of bivariate blending rational interpolants via combining any two interpolation of Thiele-type interpolant continued fraction, associated continued fractions interpolation[6,13-16], three associated continued fractions interpolation and their block based case, parameterized continued fraction fitting method[17], Lagrange interpolation, barycentric rational interpolation, symmetry blending rational interpolation and their dual interpolation.

### 6. Conclusions CONFLICT OF INTEREST ACKNOWLEDGMENT

This paper presents a three associated continued fractions Newton blending rational interpolant which is constructed by Newton's polynomial interpolation and three associated continued fractions interpolation. Clearly our method provides us with a new choice for bivariate blending rational interpolation function. We give a brief discussion of the blending rational



interpolation algorithm, its dual interpolants and error estimation. We also give some new blending interpolation formulae which was constructed by three associated continued fraction, Thiele continued fractions, Newton polynomial interpolation, barycentric interpolation, symmetry interpolation, Lagrange interpolation, parameterized continued fraction fitting method and their dual interpolation. We conclude this paper by pointing out that one can extend the method in the paper to multivariate case, vector-valued case and matrix-valued case[2,18].

#### CONFLICT OF INTEREST

The authors confirm that this article content has no conflicts of interest.

#### ACKNOWLEDGMENT

The authors would like to express their thanks to the referees for their valuable suggestions. This work was partly supported by the grant of Anhui Provincial Natural Science Foundation, China (No.1508085QF116), the grant of Support Key Project for Excellent Young Talent in College of Anhui Province, China (No.gxyqZD2016269), the Scientific Research major Foundation of Education Department of Anhui Province, China (Nos.KJ2013B232, KJ2016A603, KJ2015A206), Key Constructive Discipline of Hefei University, China (No.2014xk08), Training Object for Academic Leader of Hefei University China (No. 2014dtr08). The construction plan of the college students' Innovation quality engineering project of Anhui Province, China (No.2015ckjh061), Comprehensive reform pilot project of quality engineering project of Anhui Province, China (No.2015zy054).

#### REFERENCES

- [1]Wang RH. Numerical Approximation[M]. Beijing:Higher Education Press,1999(in Chinese)
- [2] Tan JQ. Theory of Continued Fractions and its Applications[M]. Beijing:Science Publishers, 2007(in Chinese)
- [3]Zou L, Xie J, Li CW. A New Approach to Trivariate Blending Rational Interpolation, Advanced Materials Research, 2012: Vols. 546-547, 570-575.
- [4]Wang RH, Qian J. On branched continued fractions rational interpolation over pyramid-typed grids, Numer Algor, 2010:54(1): 47-72.
- [5]Jiang P,Tan JQ. A Neville-like method via continued fractions,J Comput Appl Math, 2004:163, 219-232.
- [6]Bai T, Tan JQ, Hu M. A novel algorithm for removal of salt and pepper noise using continued fractions interpolation, Signal Processing,2014; 102:247-255.
- [7]Bai T, Tan JQ, Hu M, Wang Y. Compression and reconstruction of time series data based on vector valued continued fraction, Journal of Information & Computational Science,2014;11(8):2459-2466.
- [8]Ghadami R, Rahebi J, Yayli Y.A fast method based on DeMoivre for spherical linear interpolation in Minkowski space.Energy Educ Sci Technol Part A 2012;30: 549-552.
- [9]Gensane T. Interpolation on the Hypersphere with Thiele type rational interpolants. Numer Algor 2012;60:523-529.
- [10]Zhang YF, Bao FX, Zhang CM, Duan Q. A weighted bivariate blending rational interpolation function and visualization control, J Comput Anal Appl, 2012;14(7):1303-1320.
- [11] Frank GL. Thiele rational interpolation for the numerical computation of the reversible Randles-Sevcik function in electrochemistry. J Sci Comput 1999; 14: 259-274
- [12]Huo X, Tan JQ, He L, Hu M. An automatic video scratch removal based on Thiele type continued fraction. Multimed Tool Appl 2014;71:451-467.
- [13] Dyn N, Floater M S. Multivariate polynomial interpolation on lower sets, J Approx Theory,2014;177:34-42.
- [14]Zhang YG, Zou L. Associated Continued Fractions-Barycentric Blending Rational Interpolation and Its Application in Image Processing, Fourth International Conference on Computational and Information Sciences, 2012: Vol 2, pp612-615
- [15]Zou L, Tang S. A new approach to general interpolation formulae for bivariate interpolation.Abstract and Applied Analysis 2014, Article ID 421635, 11 pages, 2014. doi:10.1155/2014/421635.
- [16] Zou L, Tang S. General Structures of Block Based Interpolation Function, Comm. Math. Res., 2012;28(3), 193-208.
- [17] Zhan TS. Study on parameterized continued fraction fitting method and its application, Mathematics in Practice and Theory, 2012;42(22):156-159.
- [18]Zhu GQ, Tan JQ. A note on matrix-valued rational interpolants, J Comput Appl Math, 1999:110(1):129-140.

# Research of Constant Temperature and Energy Saving Bath Cycle of Bathtub

Caiquan Gu<sup>1</sup>, Leijie Shen<sup>1</sup>, Zhitong Guo<sup>1</sup>, Liya Wang<sup>2\*</sup>

<sup>1</sup> Yisheng College, North China University of Science and Technology, Tangshan, 063000, China

<sup>2</sup> College of Science, North China University of Science and Technology, Tangshan, 063000, China

**Abstract:** According to the heat conduction law and the differential equation of the water temperature in the process of bathing, designed a constant flow intermittent injection and constant temperature control scheme in this paper, and the temperature change of the bath at different stages of the equation to calculate. Research indicates, in this paper, the establishment of the water injection, drainage cycle model is not only applicable to the bath, but also can be extended to the swimming pool, hot springs and other aspects, with a wide range of applicability and rationality.

**Key words:** bathtub; constant temperature control; injection and drainage cycle

## 1. INTRODUCTION

With the development of economy and the level of science and technology and the change of the way of life, traditional bathtub has been unable to meet the needs of people in urgent need of more intelligent, more energy-efficient bath to improve people's lives. To achieve the purpose of intelligent and energy saving, firstly, the need to maintain a constant temperature in the bath. Secondly, if water injection time is determined, and then determine the energy-saving thermostatic bath tub period, it will have far-reaching implications for Intelligence Research bathtub.

Scholars all over the world have done a number of researches on making thermostatic water bath. Om Prakash Verma<sup>[1]</sup> has solved the problem of controlling water temperature and making thermostatic water bath system on the basis of Fuzzy Logic (FL) and Adaptive-Network-based Fuzzy Inference System (ANFIS). His researches are of great significance to the development of thermostatic water bath. Sam Howison<sup>[2]</sup> (2004) succeeded to control the temperature of the bathtub water based on the heat conduction theory and Newton's law of cooling. J.Ottesen<sup>[3]</sup> (2014) achieved the purposes of thermostatic water bath and water saving on account of limit and the law of conservation. Despite the various researches on bathtubs, there are few on thermostatic water bath and water saving. The existed studies in this field are not systematic, most of which are complicated to calculate. The above methods do solve problems on some extent, but they are not easy to be spread and applied in practical applications. Based on this, by designing constant flow intermittent

injection, drainage mode of constant temperature control scheme, obtains the periodic model of water injection and water discharge, and the calculation formula and process are given in detail.

## 2. CONSTANT TEMPERATURE CONTROL SCHEME DESIGN

According to law of heat conduction and its differential equation, the heat transfer equation among water, cylinder wall and outside air is determined. The function relationship between the temperature in bathtub and time is then determined<sup>[4]</sup>.

$$\begin{cases} c \cdot m \cdot \frac{dT}{dt} = \Delta E_1 + \Delta E_2 + \Delta E_3 + \Delta E_4 \\ T_{(t=0)} = T_0 \end{cases} \quad (1)$$

In the formula, when the water temperature is reduced to a certain extent, the first drain after injection. Hot thermal energy released into the bath  $\Delta E_1$ , the heat loss caused by the heat conduction in the wall of the bathtub and the outside world  $\Delta E_2$ , heat energy carried by cold water  $\Delta E_3$ , the heat loss caused by the upper surface of the water in the bathtub and the convection of the outside  $\Delta E_4$ .

The requirements are both the keeping of constant temperature in the bathtub and the least consumption of water. According to this, an injected and drained product cycle model is necessary to be built up, to balance the temperature control and water saving, and accomplish an optimal strategy.

Suppose that this capacity can satisfy the demand of most people, denoted as  $V_0 \pm \Delta V$ . The initial temperature of the water in the bathtub is the optimum temperature for human body, considering the temperature within  $T_0 \pm \Delta T$  is the eligibility.

The time of water filling and discharge  $t_{in}$  and  $t_{out}$  should be determined according to flow rate of injected water, outlet water and the volume of injected water and outlet water. Before draining away water, the time from the initial temperature  $t_0$  should be determined during which the water temperature reduces from its initial temperature  $T_0$  to  $T_{min}$ . The processing steps of the above mentioned problem:

STEP1. Solution to  $t_0$

The water temperature in the bathtub reduces from initial temperature  $T_0$  to  $T_{\min}$ , when there is no injection of draining away of water. According to still bathtub model, the relation between temperature and time can be deduced as following:

$$cm \frac{dT}{dt} = \Delta E_1 + \Delta E_2 + \Delta E_3 + \Delta E_4 \quad (2)$$

The formula shows that the water in the bathtub from the temperature  $T_0$  drops to the temperature  $T_{\min}$ , with the time for  $t_1$ .

STEP2. Solution of  $t_{out}$

The flow rate of the outlet of the bathtub is  $S_{out}$ , the cross sectional area of the water outlet is  $L_{out}$ , the volume of the draining away water is  $\Delta V$ , then

$$t_{out} = \frac{\Delta V}{S_{out} L_{out}} \quad (3)$$

The flow rate of the outlet is  $S_{out}$ , according to Bernoulli principle, the flow rate of the liquid is in relationship with the intensity of the pressure it undertakes. Let the outside atmospheric pressure is  $P_0$ , the pressure at the outlet of the bathtub is  $P_1$ , the height of the liquid is  $h'$  under the condition of that the volume of the bathtub is  $V_0$ . According to this, Bernoulli's equation is established:

$$\frac{1}{2} \rho S_{out1}^2 + P_1 = \rho gh + P_0 \quad \text{and} \quad \frac{1}{2} \rho S_{out2}^2 + P_1 = \rho gh' + P_0 \quad (4)$$

In the two equations,  $\rho$  represents the density of water,  $g$  represents the acceleration of gravity. During the process of water draining, because the change of the height of water, the pressure at the outlet of water will also change, therefore, select the average value of the flow rate at highest level and lowest level of the liquid, namely,

$$S_{out} = \frac{1}{2} (S_{out1} + S_{out2}) \quad (5)$$

Therefore the solution of time of the water draining  $t_{out}$ :

$$t_{out} = \frac{\Delta V}{S_{out} L_{out}} = \frac{\Delta V}{\frac{1}{2} \left( \sqrt{\frac{2(\rho gh + P_0 - P_1)}{\rho}} + \sqrt{\frac{2(\rho gh' + P_0 - P_1)}{\rho}} \right) L_{out}} \quad (6)$$

STEP3. Solution to  $t_{in}$

Similarly, water injecting time  $t_{in}$  is equal to  $V_{in}$

dividing its displacement  $S_{in} L_{in}$ . The flow rate is a determined value when injecting hot water, the key is to figure out the solution of  $V_{in}$ . Under the condition of ensuring the state of temperature, reduce the times of injecting water and draining water, lengthening the time when the water reaches its optimum temperature. The change of the water volume should be satisfied with the following conditions:

$$V_0 - \Delta V + V_{in} = V_0 + \Delta V \quad (7)$$

$V_0 - \Delta V$  is the left water volume in the bathtub after water draining;  $V_{in}$  is the volume of injected water in the bathtub;  $V_0 + \Delta V$  is the maximum value of the capacity of bathtub. According to calculating formula of quantity of heat, the outlet quantity of the water is

$$E_{out} = c \rho (V_0 - \Delta V) (T_0 - T_{\min}) \quad (8)$$

The injected temperature of the hot water is already denoted as  $T_{in}$ . According to the fundamental law of heat conduction, the released heat of the injected hot water in the bathtub can be

$$E_{in} = S_{in} \rho c T_{in} \quad (9)$$

After adding hot water, when it reaches to  $T_{\max}$ , the final energy in bathtub is

$$E_{end} = c \rho (V_0 - \Delta V + V_{in}) (T_{\max} - T_0) \quad (10)$$

According to the relationship of conservative of energy,  $E_{end} - E_{start} = E_{in} + E_{out}$ , then can be obtained

$$V_{in} = \frac{(V_0 - \Delta V) (T_0 - T_{\min}) + S_{in} T_{in}}{T_{\max} - T_0} + \Delta V - V_0 \quad (11)$$

the final value of entering into water can be obtained

$$t_{in} = \frac{V_{in}}{S_{in} L_{in}} = \frac{(V_0 - \Delta V) (T_0 - T_{\min}) + S_{in} T_{in}}{(T_{\max} - T_0) S_{in} L_{in}} + \frac{\Delta V - V_0}{S_{in} L_{in}} \quad (12)$$

According to three period, calculate the value of  $t_0$ ,  $t_{in}$ ,  $t_{out}$  respectively, the time cycle of water injecting, water draining can be figured out, and then the discrete relationship model between the water injecting, water draining and the time can be determined. The water injecting and water draining cycle can be drawn up as the follows:

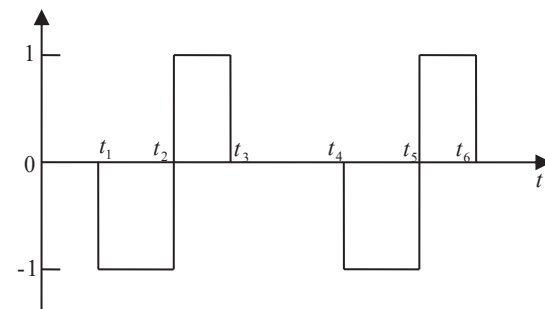


Fig1. Water injection drainage cycle diagram

Where, 1 denotes the injected hot water, -1 the drained cool water.  $(0, t_1)$  represents the time consumed from  $T_0$  to  $T_{\min}$ ;  $(t_1, t_2)$  and  $(t_4, t_5)$  represent the time discharging cool water;  $(t_2, t_3)$  and  $(t_5, t_6)$  are time of injection hot water;  $(t_3, t_4)$  is the time when temperature drops from  $T_{\max}$  to  $T_{\min}$ .

### 3. CONCLUSION

Based on the principle of heat conduction and heat conduction differential equation, studied the three factors between water and air, the bathtub wall, construction of the temperature - time model, determine the note, drain cycle of the bathtub. Under the premise of satisfying the least waste water, keeping the water temperature within the suitable water temperature range of the human body,

coordinate the balance between temperature control and water saving, in this paper, the establishment of the water injection, drainage cycle model is not only applicable to the bath, but also can be extended to the swimming pool, hot springs and other aspects, with a wide range of applicability and superiority.

### REFERENCE

- [1]Om Prakash Verma.Intelligent temperature controller for Water-Bath System [J]. International scholarly and science research & innovation,2012,6(9)
- [2]J.Ottesen.Compartment models [J]. 2014,1(7)
- [3]Sam Howison. Practical applied mathematics,approximation[J]. Mathematical Institute Oxford Unversing,2004
- [4]S.K.Upadhyay. Bayesian modeling of bathtub shaped hazard rate using various Weibull extensions and related issues of model selection [J]. Sankhya B, 2012, Vol.74 (1), pp.15-43.

# Based on the Finite Element Analysis of Steel Structure Fire Resistance Research

En Hui SUN, Ying Hui MA, Xing Guo WANG

A College of Architecture Engineering

North China University of Science And Technology, Tang Shan, 063000, China

**Abstract:** The steel structure is a kind of building material with good structural performance, which has the advantages of light weight, good flexibility, high space and high strength, and has a wide application range. However, when the material is in a fire, with the increase of temperature refractory performance particularly fast.

In this paper, the nonlinear finite element analysis of steel materials is carried out. Using the curve of SO-834 in *ABAQUS* to simulate fire conditions, Using three-dimensional thermal coupling mechanics analysis was carried out on the material, through the fire simulation analysis are conducted on the single double span steel frames of different units, different fire unit under the stress contours are obtained. Finally, the calculation of the fire response of a single beam and a steel frame is compared.

Through finite element of *ABAQUS* analysis, we can draw the conclusion: a single member in case of fire, the fire resistance is much lower than the fire resistance of the whole steel frame structure. Through the analysis, we hope to contribute a bit to the future research of fire resistance.

**Keywords:** nonlinear finite element analysis fire resistance research steel frame

## 1. INTRODUCTION

Since the 21st century, the world trend of the development of construction industry, has been largely to the steel market, more and more building started using steel structure, steel structure at the same time also created a lot of achievements and civilization, be familiar with New York's world trade center, China's bird's nest is a steel frame structure, etc.

There are many advantages of steel structure, lighter weight, high strength, good seismic behavior, ductility and shorter construction period, etc., is a kind of green building materials. The steel structure has many advantages, but 9.11 event occurred, in the fire resistance of steel structure has caused the great attention of people from all walks of life. In the steel structure is more and more vigorous today, more and more high-level structure in large span vitality now, steel structure in fire resistance has a ineffable importance.

With the development of the society, in the application of new materials, we need to do a lot of efforts in the application of new materials, so that the construction industry more healthy development.

## 2. STEEL MATERIAL PHYSICAL PROPERTIES ANALYSIS

### 2.1 Thermal expansion coefficient of structural steel at high temperature

From the perspective of structural stress analysis:

(1) static structure, the temperature will only make the structure produce displacement does not produce internal force.

(2) the statically indeterminate structure, external force does not make the structure deformation, the temperature will make the structure internal force will cause deformation.

When the fire structure frame, each fire face temperature distribution is different, it will cause the internal force and deformation of structure deformation, thermal expansion of the considered as follows.

In this paper, through *mathmatic* to draw a figure that several countries use more number of thermal expansion of the express at present, through drawing can be found that when the temperature is below 600 °C, the expansion coefficient of material as the change of temperature, as shown below:

(1) America's *AISC* thermal expansion coefficient formula is:

$$\delta_s = \frac{\Delta l}{l} = 6.2 \times 10^{-9} T_s + 1.10 \times 10^{-5}$$

(2) The thermal expansion coefficient formula of Japan is:

$$\delta_s = \frac{\Delta l}{l} = 5.57 \times 10^{-9} T_s + 1.10 \times 10^{-5}$$

(3) The thermal expansion coefficient formula of Australia *AS4100* is:

$$\delta_s = \frac{\Delta l}{l} = 1.0 \times 10^{-8} T_s + 1.10 \times 10^{-5}$$

(4) The thermal expansion coefficient formula of Tongji university, Dr. Formula is:

$$\delta_s = \frac{\Delta l}{l} = 3.0 \times 10^{-8} T_s + 1.10 \times 10^{-6}$$

(5) The thermal expansion coefficient of *ECCS* advice:

$$\delta_s = \frac{\Delta l}{l} = 1.40 \times 10^{-5}$$



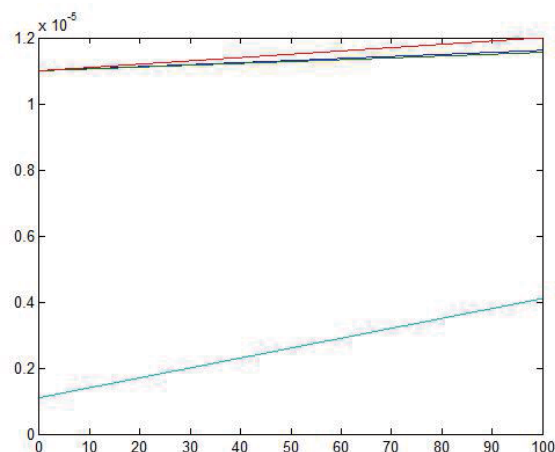


Fig. 1 Comparison of the coefficient of expansion in various countries

$$\Phi_E = \frac{E_T}{E} = \begin{cases} -17.2 \times 10^{-12} T_s^4 + 11.8 \times 10^{-9} T_s^3 - 34.5 \times 10^{-7} T_s^2 + 15.9 \times 10^{-5} T_s + 1.0 & 0^\circ C \leq T_s \leq 600^\circ C \\ 8.66 \times 10^{-4} (800 - T_s) & 600^\circ C \leq T_s \leq 1000^\circ C \end{cases}$$

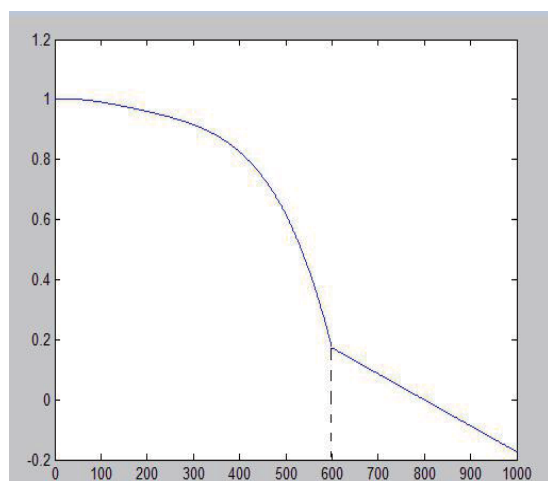


Fig. 2 initial modulus of steel structure

### 2.3 Poisson's ratio

In the steel structure of the Poisson's ratio change very small and negligible when temperature changes, so that the temperature changes under the steel structure of the Poisson's ratio is constant, that is:

$$\mu_s = 0.3$$

### 3 The fire resistance analysis

In the case of fire, due to the performance of various materials will change, so here to establish a nonlinear parabolic partial differential equations, in order to simplify the problem, make the following assumptions:

- (1) The temperature field in the column, beam component is a two-dimensional problem, namely the length direction unchanged;
- (2) Within the component does not consider water evaporation and flow, no heat is generated;
- (3) Do not consider the influence of internal stress between field and temperature field;

It can be found that, in addition to small values in the United States, adopted by the national expansion coefficient values changed little. Through the comparative analysis, Compared with *ECCS*, other national average of roughly the same, in order to simplify the calculation, this paper take *ECCS* expansion coefficient calculation.

### 2.2 Calculation formula of initial elastic modulus of steel at high temperature

As with the expansion coefficient, the elastic modulus of the steel structure will be changed when the temperature changes. Because of the change of temperature, the structure of the structure is more and more accurate. In order to make the calculation more accurate, this paper uses *ECCS* to calculate the elastic modulus of the structure. As shown below:

- (4) Do not consider the influence of residual stress and residual strain.

### 4 Analysis of fire resistance of steel frame under different cross sections

#### 4.1 Comparison of stress field analysis

Use the transient thermal analysis methods to analyze the section temperature field of steel framework structure, according to the international of the beam and column of steel frame structure. Frame beam at the bottom beam subjected to fire load, the inside of the frame column and column under fire load, the effect of both side frame column in column is full of fire load. The fire load of energy through the air heat transfer to the surface of the frame beam and column, and then within the frame structure has been spread to the other side of the heat transfer. Frame structure

in this paper for the initial temperature  $20^\circ C$  of frame structure, the heat transfer in a standard way of heating temperature, the physical properties of the frame structure change as described earlier. With software finally calculate the temperature change way of frame structure components, as well as the cross section stress field distribution, In this article, through the form of cloud and observe the stress distribution of intuitive and convenient.

By the fire in the left side of the rectangular frame column under the condition of stress nephogram is as follows:

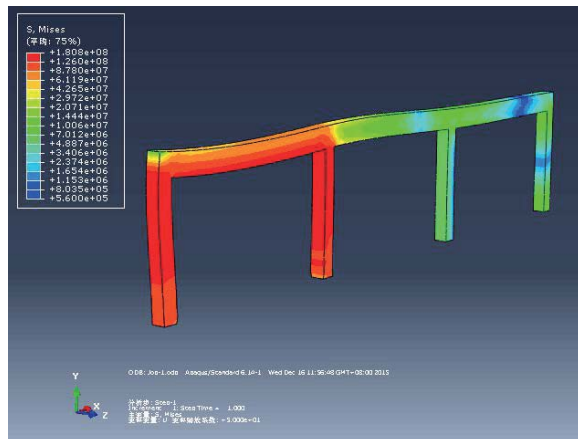


Figure 3 rectangular column on the left side of the frame under fire

In the case of a fire in the middle, the stress cloud of the rectangular frame column is as follows:

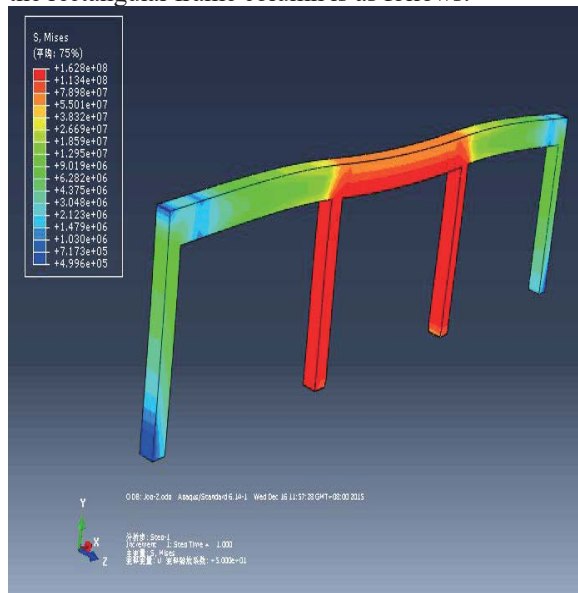


Fig. 4 the fire in the middle frame of the rectangular column

The stress cloud images of a rectangular frame column are as follows in the case of three cross fire:

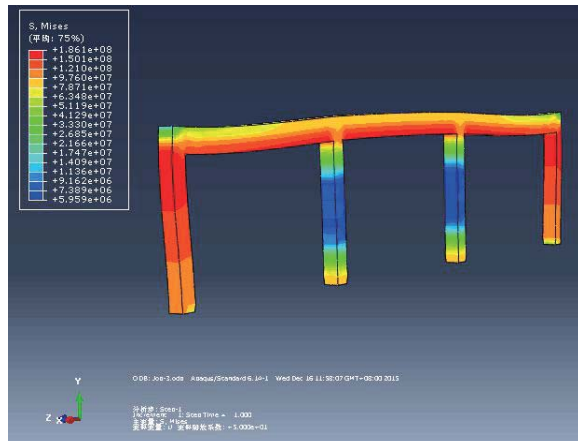


Figure 5 The three span of the rectangular column is subjected to fire within the frame.

In the case of the left side of the fire, the stress cloud of the frame column is as follows:

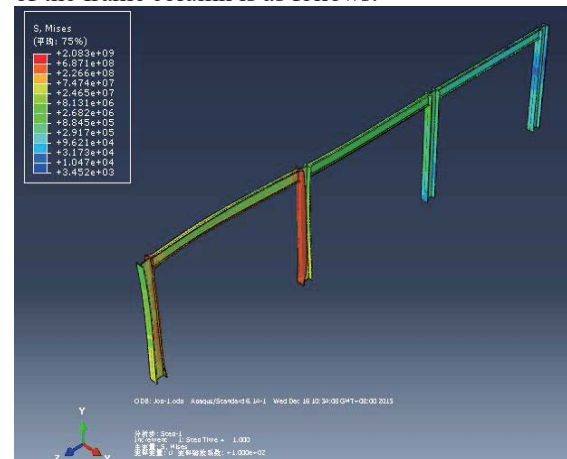


Figure 6 the left side of the frame column by the fire stress cloud

In the middle of the case of fire, the stress cloud of the frame column is as follows:

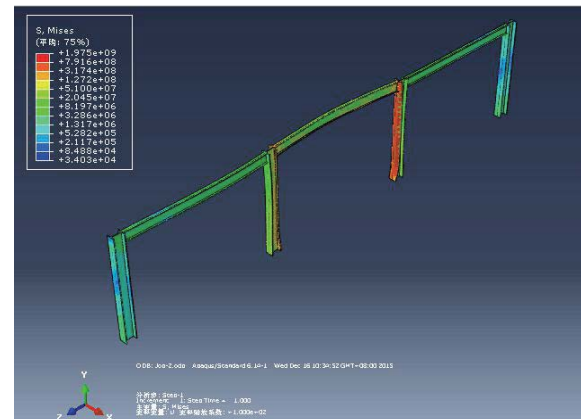


Fig. 7 the stress cloud of the fire in the middle frame of the frame column

At the same time, the stress cloud of the frame column with the three span and the same time is as follows:

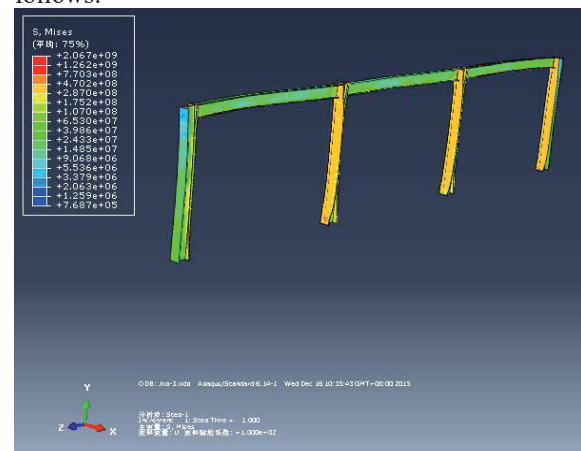


Figure 8 I-shaped frame column three span under fire stress nephogram

Fig. 9 the stress cloud image of single beam:

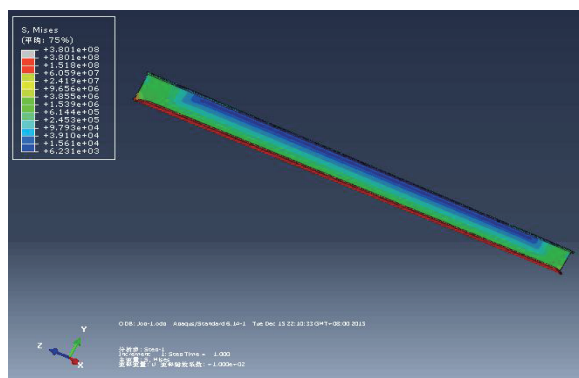


Fig. 9 analysis of the stress of the beam under fire  
By the stress image of the frame column and the column, it is obvious that the surface stress which is affected by the fire is the biggest in the whole frame structure. After the standard heating process, showing the stress difference.

4. 2 When the fire broke out, the analysis of fire resistance is not the same as the room

Eight nodes using solide70 three-dimensional body unit, coefficient of thermal conductivity, specific heat,

Table 1 the location of fire and the analysis of fire under different column cross

| Location of fire   | Critical low stress ( °C ) | Critical high stress ( °C ) |
|--|----------------------------|-----------------------------|
| Rectangular column on the left side of the frame is heated | $5.6 \times 10^5$          | $1.808 \times 10^8$         |
| Heated rectangular column                                  | $4.996 \times 10^5$        | $1.628 \times 10^8$         |
| Rectangular column three span frame heat                   | $5.959 \times 10^6$        | $1.861 \times 10^8$         |
| The left frame is heated.                                  | $3.452 \times 10^3$        | $2.083 \times 10^9$         |
| The middle frame of the intermediate frame is heated.      | $3.403 \times 10^4$        | $1.975 \times 10^9$         |
| Rectangular column three span frame heat                   | $7.687 \times 10^5$        | $2.067 \times 10^9$         |
| Single beam heating  | $6.231 \times 10^3$        | $3.801 \times 10^8$         |

Through the table, we can see: steel frame structure in this paper in three spans without fire prevention measures and effects in different standard width of a room by the fire, stress distribution is quite different. It can be seen from the stress that when the fire occurs, the steel structure is the most disadvantage. This conclusion is the same as the real life. When the fire occurred in the bottom layer, the load is very large, the first to lose the stability of the fire will cause the building to collapse. If the fire occurred in the span of the structure under the constraints of both sides and the horizontal displacement is relatively small. But the vertical displacement of the span increases rapidly. The vertical displacement of the whole structure is the first to reach the limit state. But the overall structure of the fire in the room is better than Dan Genliang's fire resistance. Thus, the overall

density and so on material properties; Calculating the section size of steel framework, so as to establish a steel frame model, and then to the role of fire surface heat convection and radiation. Steel frame of the initial temperature of 20, 30 second step for a long time, and then carried out in accordance with the standard temperature curve of steel framework structure temperature and calculate the stress distribution of each point in steel frame cross-section. Load and constraints. Set column bottom of steel framework to fixed support, add level support at steel frame the right end of beam and column node and a plane bearing. Take the lead in the static analysis, and then set time range, the input of temperature distribution in the above, each step of the stipulated time, instantaneous analysis frame stress distribution is obtained.

Through the analysis of the corresponding to comparison can get the fire position and different columns under fire stress data, as shown in the following table:

structure of the steel frame is better than the single frame of the anti fire performance is much better.

This article through to the rising process of temperature at different cross section of frame beam and column is an accurate analysis of the temperature changes of different components. You can see that the stress of the rectangular column received smaller than h column, in comparison, the rectangular column refractory performance is better, that is consistent with actual also, because the rectangular column temperature the slower, smaller fire stress.

4.3 Effect of column section size and strength on the fire resistance of structures

In the case of steel frame beam with the same section size and load, only the section size of frame column and the change of the strength of the column is increased from HK400b to HK600b, and the size of the concrete is as follows:

Table 2 Comparison of column dimensions

| Column section | height (mm) | width (mm) | The thickness of the web (mm) | The thickness of the flange (mm) |
|----------------|-------------|------------|-------------------------------|----------------------------------|
|                | 400         | 300        | 13.5                          | 24.0                             |

|        |     |     |      |      |
|--------|-----|-----|------|------|
| HK600b | 600 | 300 | 15.5 | 30.0 |
|--------|-----|-----|------|------|

In accordance with the above similar analysis method, it can be obtained, increasing the section size, can make the structure of the fire resistance performance is enhanced, the resulting stress is relatively reduced.

#### 5. Conclusion

In conclusion, the steel frame structure in fire calculation is very difficult and complex, is very difficult and high level of nonlinear problems, due to the limited time and level and a lot of problems need systematical research on a higher level. For example, when a fire occurs, the strength of the bearing capacity of the node is very important to the stability of the structure, the structure should be analyzed and studied at high temperature. Fire resistance analysis of the whole structure. In addition to the steel structure under high temperature, there are still many problems to be solved, such as: the stability of the overall structure, strength and local buckling and so on. Under high temperature, the research and calculation of the steel frame structure is too large, in the error limit, we can take a part of the calculation, thus greatly reducing the amount of calculation.

#### References

The design and fire protection of structural steel. Steel structure, 2002.

Li Guoqiang, Jiang Shouchao, Lin Guixiang. Fire resistance calculation and design of steel structure. Beijing: China Architectural Industry Press, 1999

Dong Xinming on fire fire and fire resistance design of steel structure building by the typical fire. Fire science and technology, 2002 .

hole Xiangqian. Application of finite element method in heat transfer in (Third Edition). Beijing: Science Press, 1997

ECCS. European Recommendations for the Fire Safety of Steel Structures, 1983

Ding Jun, Li Guoqiang, Jiang Shouchao, temperature analysis of steel structural members under fire, steel structure, 2002.

Jin Wenyan, the fire [Master degree thesis of Shandong University] resistance of steel frame structure, 2006.

Yang Xina, steel structure fire resistance research [Master's degree thesis of Xi'an University of Science And Technology, 2006.

# Energy-saving Thermostat Bath Tub Model Based on Heat Conduction Principle

Meilin Ding<sup>1</sup>, Tianlong Li<sup>1</sup>, Di Zhang<sup>1</sup>, Yan Li<sup>2\*</sup>, Xiaoqiang Guo

<sup>1</sup> North China University of Science and Technology, Tangshan, 063000, China

<sup>2</sup> College of Science, North China University of Science and Technology, Tangshan, 063000, China

**Abstract:** people in the process of bath, the bath comfort level, water temperature and water has a certain demand for energy saving and emission reduction and meet the comfort degree, of bath of constant temperature energy-saving optimization research is very necessary. In this paper, based on the principle of heat conduction, a constant temperature and energy saving model is put forward under the premise of not using the circulation injection system and the steam cycle. Given the bath water temperature changes under the form of static model, the heat dissipation of the bath water temperature. Constant temperature water saving target, construct a solution of the bathing process, optimal row, water cycle model, the model can be under the premise of constant flow rate and water temperature, water use and water conservation capacity of to measure, so that the constant temperature water system has been adjusted and optimized. In order to achieve the purpose of environmental protection and water saving, this paper further discusses the optimal design of the bathtub, and gets the model of constant temperature and water saving bathtub.

**Key words:** heat conduction principle ; optimal drainage cycle; temperature and energy saving

## 1. INTRODUCTION

With the sustainable development of economy and technology, humanization and intelligence are highly focused by people. But, there is usually no reheating system in a household bathtub. During the shower, the temperature of the water gradually goes down, and it is difficult to keep it thermostatic by pouring in warm water.

Scholars all over the world have done a number of researches on making thermostatic water bath. J.Ottesen<sup>[3]</sup> (2014) achieved the purposes of thermostatic water bath and water saving on account of limit and the law of conservation. William J. Roesch<sup>[5]</sup> (2012) focused on the curve of the bathtubs and studied their mass and reliability. Despite the various researches on bathtubs, there are few on thermostatic water bath and water saving. The existed

studies in this field are not systematic, most of which are complicated to calculate. What's worse, they are not easy to be spread and applied in practical applications.

Therefore, the following four issues will be resolved in this paper:

1) A bathtub with a special shape will be designed to save water as well as to satisfy the demands of the bathers.

2) A mathematic model will be made to adjust water temperature over time for an empty bathtub, and a scheme of making thermostatic water and saving water will be provided.

## 2. THE OPTIMAL SHAPE OF THE BATH

Set three dimensional space coordinate system, the center of bathtub bottom as the origin of coordinate.

Let semi major axis of ellipsoid be  $x$ , semi minor axis be  $y$ , so diameter of ball is  $2y$ .  $z_1(x, y)$  is ellipsoid equation;  $z_2(x, y)$  is sphere equation, and the following conditions should be met between  $x$  and  $y$ :

$$\begin{aligned} \text{Min} \quad & \iint z_1(x, y) dx dy + \iint z_2(x, y) dx dy \\ \text{s.t.} \quad & \begin{cases} x + y \leq 1700 \\ x \leq 1200 \\ y \leq 700 \\ x > y \end{cases} \end{aligned}$$

Obviously, ellipsoidal bottom of bathtub is not suitable for bathing. Assume that we use smooth surface satisfying functional equation  $S(x, y)$  to cut lower surface of composite body. The surface we cut satisfy the characteristic which is narrow in the front and wide in the back. Under the condition of satisfying the ellipsoid condition, solve integral function, and analyze the results. We know that when the bathtub is connected by  $\frac{1}{4}$  ellipsoid and

$\frac{1}{4}$  ball, the shape of bathtub is optimized water saving tragedy. Simple structure of it is shown in Fig 1.



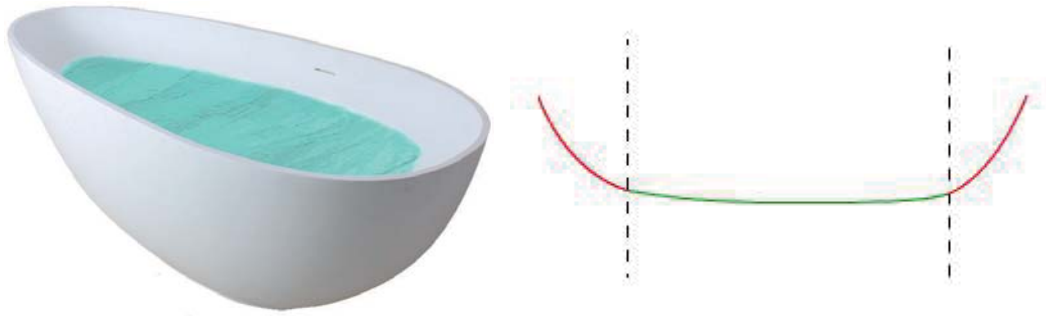


Fig 1. Sketch map of typical energy saving bathtub

### 3. SETTING WATER TEMPERATURE CHANGE MODEL BASES ON PRINCIPLES OF HEAT TRANSFER

When no one is in the bathtub and water volume in it is  $V_0$ , there exist heat conduction, heat convection and heat radiation between water and bathtub wall. Only heat convection with air and only heat conduction between bathtub wall and outside. So the heat loss on this time is: the heat loss  $\Delta E_2$  because of heat conduction between bathtub wall and outside, the heat loss  $\Delta E_4$  because of heat convection on upper surface of water in the bathtub, which is:

$$\Delta E_2 = -\frac{S_1 \lambda (T - T_1)}{d} \quad \text{and} \quad \Delta E_4 = H_2 S_2 (T - T_3) \quad (1)$$

According to the heat balance relationship, differential equation model of water temperature change in bathtub is as formula 6.2 shows:

$$\begin{cases} cm \frac{dT}{dt} = \Delta E_2 + \Delta E_4 \\ T_{(t=0)} = T_0 \end{cases} \quad (2)$$

When water temperature falls to a certain extent, first drainage and injection after. The releasing heat energy when hot water is injected in the bathtub  $\Delta E'_1$ , the heat loss  $\Delta E'_2$  because of heat conduction between bathtub wall and outside, heat energy discharged from cold water  $\Delta E'_3$ , the heat loss  $\Delta E'_4$  because of heat convection on upper surface of water in the bathtub, which is:

$$\Delta E'_1 = f_1 \rho c (T_1 - T) ; \quad \Delta E'_2 = -\frac{S_1 \lambda (T - T_1)}{d} ;$$

$$\Delta E'_3 = -f_2 \rho c (T_0 - \Delta T) ;$$

$$\Delta E'_4 = -H_2 S_2 (T - T_2).$$

Therefore, differential equation model of water temperature when time changes in all condition is as formula 6.3 shows:

$$\begin{cases} c \cdot m \cdot \frac{dT}{dt} = \Delta E'_1 + \Delta E'_2 + \Delta E'_3 + \Delta E'_4 \\ T_{(t=0)} = T_0 \end{cases} \quad (3)$$

### 4. THE DESIGN OF CONSTANT TEMPERATURE SCHEME

Suppose that this capacity can satisfy the demand of most people, denoted as  $V_0 \pm \Delta V$ . The initial temperature of the water in the bathtub is the optimum temperature for human body, considering the temperature within  $T_0 \pm \Delta T$  is the eligibility.

The time of water filling and discharge  $t_{in}$  and  $t_{out}$  should be determined according to flow rate of injected water, outlet water and the volume of injected water and outlet water. Before draining away water, the time from the initial temperature  $t_0$  should be determined during which the water temperature reduces from its initial temperature  $T_0$  to  $T_{min}$ . The processing steps of the above mentioned problem:

#### STEP1. Solution to $t_0$

The water temperature in the bathtub reduces from initial temperature  $T_0$  to  $T_{min}$ , when there is no injection of draining away of water. According to still bathtub model, the relation between temperature and time can be deducted as following:

$$cm \frac{dT}{dt} = \Delta E'_1 + \Delta E'_2 + \Delta E'_3 + \Delta E'_4 \quad (4)$$

The formula (6.4) shows that the water in the bathtub from the temperature  $T_0$  drops to the temperature  $T_{min}$ , with the time for  $t_1$ .

#### STEP2. Solution of $t_{out}$

The flow rate of the outlet of the bathtub is  $S_{out}$ , the cross sectional area of the water outlet is  $L_{out}$ , the volume of the draining away water is  $\Delta V$ , then

$$t_{out} = \frac{\Delta V}{S_{out} L_{out}} \quad (5)$$

In 6.5, the flow rate of the outlet is  $S_{out}$ , according to Bernoulli principle, the flow rate of the liquid is in relationship with the intensity of the pressure it undertakes. Let the outside atmospheric pressure is  $P_0$ , the pressure at the outlet of the bathtub is  $P_1$ , the height of the liquid is  $h'$  under the condition of that the volume of the bathtub is  $V_0$ . According to this, Bernoulli's equation is established:

$$\frac{1}{2} \rho S_{out1}^2 + P_1 = \rho gh + P_0 \quad \text{and}$$

$$\frac{1}{2} \rho S_{out2}^2 + P_1 = \rho gh' + P_0$$

In the two equations,  $\rho$  represents the density of water,  $g$  represents the acceleration of gravity. During the process of water draining, because the change of the height of water, the pressure at the outlet of water will also change, therefore, select the average value of the flow rate at highest level and lowest level of the liquid, namely,

$$S_{out} = \frac{1}{2} (S_{out1} + S_{out2}) \quad (6)$$

Therefore the solution of time of the water draining  $t_{out}$ :

$$t_{out} = \frac{\Delta V}{S_{out} L_{out}} = \frac{\Delta V}{\frac{1}{2} \left( \sqrt{\frac{2(\rho gh + P_0 - P_1)}{\rho}} + \sqrt{\frac{2(\rho gh')}{\rho}} \right)}$$

STEP3. Solution to  $t_{in}$

Similarly, water injecting time  $t_{in}$  is equal to  $V_{in}$  dividing its displacement  $S_{in} L_{in}$ . The flow rate is a determined value when injecting hot water, the key is to figure out the solution of  $V_{in}$ . Under the condition of ensuring the stale of temperature, reduce the times of injecting water and draining water, lengthening the time when the water reaches its optimum temperature. The change of the water volume should be satisfied with the following conditions:

$$V_0 - \Delta V + V_{in} = V_0 + \Delta V \quad (7)$$

$V_0 - \Delta V$  is the left water volume in the bathtub after water draining;  $V_{in}$  is the volume of injected water in the bathtub;  $V_0 + \Delta V$  is the maximum value of the capacity of bathtub. According to calculating formula of quantity of heat, the outlet quantity of the water is

$$E_{out} = c\rho(V_0 - \Delta V)(T_0 - T_{min}) \quad (8)$$

The injected temperature of the hot water is already denoted as  $T_{in}$ . According to the fundamental law of heat conduction, the released heat of the injected hot water in the bathtub can be

$$E_{in} = S_{in} \rho c T_{in} \quad (9)$$

After adding hot water, when it reaches to  $T_{max}$ , the final energy in bathtub is

$$E_{end} = c\rho(V_0 - \Delta V + V_{in})(T_{max} - T_0) \quad (10)$$

According to the relationship of conservative of energy,  $E_{end} - E_{start} = E_{in} + E_{out}$ , then can be obtained

$$V_{in} = \frac{(V_0 - \Delta V)(T_0 - T_{min}) + S_{in} T_{in} + \Delta V - V_0}{T_{max} - T_0} \quad (11)$$

the final value of entering into water can be obtained

$$t_{in} = \frac{V_{in}}{S_{in} L_{in}} = \frac{(V_0 - \Delta V)(T_0 - T_{min}) + S_{in} T_{in} + \Delta V - V_0}{(T_{max} - T_0) S_{in} L_{in}} + \frac{\Delta V - V_0}{S_{in} L_{in}} \quad (12)$$

According to three period, calculate the value of  $t_0$ ,  $t_{in}$ ,  $t_{out}$  respectively, the time cycle of water injecting, water draining can be figured out, and then the discrete relationship model between the water injecting, water draining and the time can be determined. The water injecting and water draining cycle can be drawn up as the follows:

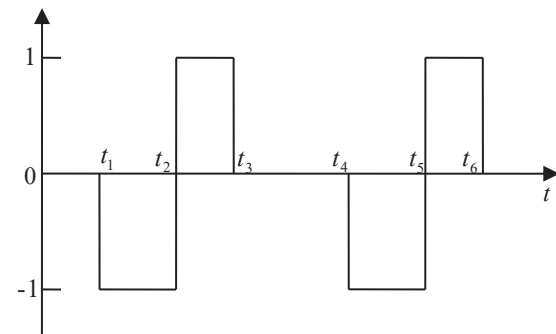


Fig 6. Water injection drainage cycle diagram

Where, 1 denotes the injected hot water, -1 the drained cool water.  $(0, t_1)$  represents the time consumed from  $T_0$  to  $T_{min}$ ;  $(t_1, t_2)$  and  $(t_4, t_5)$  represent the time discharging cool water;  $(t_2, t_3)$  and  $(t_5, t_6)$  are time of injection hot water;  $(t_3, t_4)$  is the time when temperature drops from  $T_{max}$  to  $T_{min}$ .

## 5. NUMERICAL SIMULATION OF WATER INJECTION AND DRAINAGE MODEL

In order to facilitate the solution of water injection and drainage model, set conditions as follows:

Initial temperature  $T_0 = 40^\circ\text{C}$ ;  $\Delta T = 5^\circ\text{C}$ ; initial water volume in the bathtub is  $V_0$ ; water injection

velocity is  $S_{in} = 0.21L/s$ ; caliber of water filling nozzle  $L_{in} = 20mm$ ; caliber of water drainage  $L_{out} = 32mm$ ; set initial height of liquid level  $h$ ; external atmospheric pressure is  $1.01 \times 10^5 Pa$ ; density of water is  $1 \times 10^3 kg/m^3$ , from Bernoulli

equation  $\frac{1}{2} \rho S_{out1}^2 + P_1 = \rho gh + P_0$ , we get  $S_{out} = 0.55L/s$ . Under the goal of constant temperature and energy saving, we work out the time water injection and drainage under the following four models, as shown in the following table 2:

Table 2 Numerical simulation of water injection and drainage time

| Cycle | I    |          |           |      | II       |           |      | III      |           |      |
|-------|------|----------|-----------|------|----------|-----------|------|----------|-----------|------|
| Model | Wait | Drainage | Injection | Wait | Drainage | Injection | Wait | Drainage | Injection | Wait |
| 1     | 300  | 120      | 460       | 450  | 130      | 450       | 480  | 135      | 490       | 500  |
| 2     | 260  | 125      | 455       | 420  | 115      | 430       | 450  | 110      | 450       | 450  |
| 3     | 230  | 120      | 450       | 400  | 100      | 410       | 430  | 120      | 430       | 420  |
| 4     | 200  | 120      | 445       | 370  | 120      | 470       | 390  | 115      | 460       | 380  |

## 5. CONCLUSION

Advantage of model:

- 1) Based on the same surface area and same capacity, we have comparison and analysis. Then we conclude that the optimal bathtub shape is combined with ellipsoid and sphere.
- 2) By using the Law of Conservation of Energy, we make periodization for the process of heat dissipation/water injection and drainage and establish injection/ drainage-time model, which is to minimize the water volume, connect each variable closely and obtain a clear result and strong system.

Disadvantage of Model

This model does not take the different temperature under different water layer into consideration, which may have some influence on the accuracy of the result and the control of the injection and drainage time.

## REFERENCES

- [1]Sam Howison. Pratical applied mathematics,approximtion[J]. Mathematical Insitute Oxford Unversting,2004
- [2]William J. Roesch. Using a new bathtub curve to correlate quality and reliability [J]. Microelectronics Reliability,2012Vol.52 (12) Pages 2864–2869

# Research of Constant Temperature and Energy Conservation Bath on the Basis of Dynamic Programming Mode

Leijie Shen<sup>1</sup>, Caiquan Gu<sup>1</sup>, Zhitong Guo<sup>1</sup>, Aimin Yang<sup>2\*</sup>

<sup>1</sup> Yisheng College, North China University of Science and Technology, Tangshan, 063000, China

<sup>2</sup> College of Science, North China University of Science and Technology, Tangshan, 063000, China

**Abstract:** For bathing process, the demand for water temperature and water supply volume, combined with the concept of energy conservation. On the premise of the bath tub shape optimization, the optimization model of the bath constant temperature and energy saving was calculated, and the constant flow rate and the constant flow rate of the water drainage were obtained under different conditions, and the calculation results are compared with the actual situation. The results show that the dynamic temperature control model has excellent energy saving effect, which verifies the validity and superiority of the model.

**Key words:** dynamic programming; the shape optimal; injection and drainage; control scheme; constant temperature and energy saving

## 1. INTRODUCTION

With the sustainable development of economy and technology, humanization and intelligence are highly focused by people. But, there is usually no reheating system in a household bathtub. During the shower, the temperature of the water gradually goes down, and it is difficult to keep it thermostatic by pouring in warm water. Scholars all over the world have done a number of researches on making thermostatic water bath. Om Prakash Verma<sup>[1]</sup> has solved the problem of controlling water temperature and making thermostatic water bath system on the basis of Fuzzy Logic (FL) and Adaptive-Network-based Fuzzy Inference System (ANFIS). His researches are of great significance to the development of thermostatic water bath. Sam Howison<sup>[2]</sup> (2004) succeeded to control the temperature of the bathtub water based on the heat conduction theory and Newton's law of cooling. J.Ottesen<sup>[3]</sup> (2014) achieved the purposes of thermostatic water bath and water saving on account of limit and the law of conservation. Despite the various researches on bathtubs, there are few on thermostatic water bath and water saving. The existed studies in this field are not systematic, most of which are complicated to calculate. The above methods do solve problems on some extent, but they are not easy to be spread and applied in practical applications. Based on this, the following studies are carried out in this paper :One: A mathematic model will be made to adjust water temperature over time for an empty

bathtub, and a scheme of making thermostatic water and saving water will be provided. Two: To promote the model, for someone in the bathtub, human movement and use of bubble bath like the specific case to analysis, optimization.

## 2. DYNAMIC CONSTANT TEMPERATURE AND ENERGY SAVING BATH MODEL UNDER DIFFERENT CONDITIONS OF BATH

### 2.1 Water temperature change model based on the principle of heat transfer

The heat loss because of heat conduction between

bathtub wall and outside  $\Delta E_1 = -\frac{S_1 \lambda (T - T_1)}{d}$ ,

the heat loss because of heat convection on upper surface of water in the bathtub  $\Delta E_2 = H_2 S_2 (T - T_3)$ . According to the heat balance relationship, differential equation model of water temperature change in bathtub

$$\text{is } \begin{cases} cm \frac{dT}{dt} = \Delta E_1 + \Delta E_2 \\ T_{(t-0)} = T_0 \end{cases}, \text{ among them, } S_1 \text{ for the}$$

surface area of the bathtub wall,  $S_2$  for the upper surface area of the water in the bathtub,  $H_1$  for the heat dissipation coefficient of the bathtub wall,  $H_2$  for the water heat dissipation coefficient,  $d$  for the thickness of the wall of the bathtub.  $T_1$  for hot water to enter the temperature,  $T_0$  for the initial temperature of the water bath,  $T_2$  for the external environment temperature,  $T_3$  for the surface temperature of the bathtub.

When the water temperature is lower than a certain degree, the first drainage, after the water injection. Hot thermal energy released into the bath  $\Delta E'_1 = f_1 \rho c (T_1 - T)$ , bathtub wall with the outside world due to heat loss caused by the heat conduction  $\Delta E'_2 = -\frac{S_1 \lambda (T - T_1)}{d}$ , discharging

cold water carried heat  $\Delta E'_3 = -f_2 \rho c (T_0 - \Delta T)$  on the surface of water in the bathtub due to heat loss

and external convection  $\Delta E'_4 = -H_2 S_2 (T - T_2)$ , among them,  $\rho$  the ratio of the density of the water,  $f_1$  the amount of hot water is injected into the tub,  $f_2$  the water flowing out of the bathtub,  $m$  the bathtub when the initial mass of water,  $c$  the specific heat of water. At this time, model of water temperature when time changes in all condition is as formula (1) shows:

$$\begin{cases} cm \frac{dT}{dt} = \Delta E'_1 + \Delta E'_2 + \Delta E'_3 + \Delta E'_4 \\ T_{(t=0)} = T_0 \end{cases} \quad (1)$$

## 2.2 Climate control design

Given the volume of water in the bathtub, and assume that the capacity can meet the requirements of most people, as  $V_0 \pm \Delta V$ . Given the initial temperature of the water in the bathtub, recorded as  $T_0 \pm \Delta T$ . In order to determine the injection and drainage period, the need to determine the time of filling  $t_{in}$  and drainage time  $t_{out}$ . Before draining away water, the time from the initial temperature  $t_0$  should be determined during which the water temperature reduces from its initial temperature  $T_0$  to  $T_{min}$ . The processing steps of the above mentioned problem:

STEP1. Solution to  $t_0$ : The water temperature in the bathtub reduces from initial temperature  $T_0$  to  $T_{min}$ , when there is no injection of draining away of water. According to still bathtub model, the relation between temperature and time can be deducted as following:

$$cm \frac{dT}{d} = \Delta E'_1 + \Delta E'_2 + \Delta E'_3 + \Delta E'_4 \quad (2)$$

The formula (2) shows that the water in the bathtub from the temperature  $T_0$  drops to the temperature  $T_{min}$  with the time for  $t_0$ .

STEP2. Solution of  $t_{out}$ : The flow rate of the outlet of the bathtub is  $S_{out}$  the cross sectional area of the water outlet is  $L_{out}$  the volume of the draining away water is  $\Delta V$ , according to Bernoulli principle, the flow rate of the liquid is in relationship with the intensity of the pressure it undertakes. Let the outside atmospheric pressure is  $P_0$ , the pressure at the outlet of the bathtub is  $P_1$  the height of the liquid is  $h$  under the condition of that the volume of the bathtub is  $V_0$ . According to this, Bernoulli's equation is established:

$$\frac{1}{2} \rho S_{out1}^2 + P_1 = \rho gh + P_0 \text{ and}$$

$$\frac{1}{2} \rho S_{out2}^2 + P_1 + P_0 \quad (3)$$

In the two equations,  $\rho$  represents the density of water,  $g$  represents the acceleration of gravity. During the process of water draining, because the change of the height of water, the pressure at the outlet of water will also change, therefore, select the average value of the flow rate at highest level and lowest level of the liquid, namely  $S_{out} = \frac{1}{2}(S_{out1} + S_{out2})$ ,

Therefore the solution of time of the water draining: (4)

$$t_{out} = \frac{\Delta V}{S_{out} L_{out}} = \frac{\Delta V}{\frac{1}{2} \left( \sqrt{\frac{2(\rho gh + P_0 - P_1)}{\rho}} + \sqrt{\frac{2(\rho gh') + P_0 - P_1}{\rho}} \right) L_{out}}$$

STEP3. Solution to  $t_{in}$ : Water injecting time  $t_{in}$  is equal to  $V_{in}$  dividing its displacement  $S_{in} L_{in}$ . Under the condition of ensuring the stale of temperature, The change of the water volume should be satisfied with the following conditions:  $V_0 - \Delta V + V_{in} = V_0 + \Delta V$ ,  $V_0 - \Delta V$  is the left water volume in the bathtub after water draining;  $V_{in}$  is the volume of injected water in the bathtub;  $V_0 + \Delta V$  is the maximum value of the capacity of bathtub. the outlet quantity of the water is  $E_{out} = c\rho(V_0 - \Delta V)(T_0 - T_{min})$ , The injected temperature of the hot water is already denoted as  $T_{in}$  the released heat of the injected hot water in the bathtub can be  $E_{in} = S_{in} \rho c T_{in}$ . After adding hot water, when it reaches to  $T_{max}$ , the final energy in bathtub is  $E_{end} = c\rho(V_0 - \Delta V + V_{in})(T_{max} - T_0)$ . According to the relationship of conservative of energy,  $E_{end} - E_{start} = E_{in} + E_{out}$ , then can be obtained

$$V_{in} = \frac{(V_0 - \Delta V)(T_0 - T_{min}) + S_{in} T_{in}}{T_{max} - T_0} + \Delta V - V_0 \quad (5)$$

the final value of entering into water can be obtained

$$t_{in} = \frac{V_{in}}{S_{in} L_{in}} = \frac{(V_0 - \Delta V)(T_0 - T_{min}) + S_{in} T_{in}}{(T_{max} - T_0) S_{in} L_{in}} + \frac{\Delta V - V_0}{S_{in} L_{in}} \quad (6)$$

water draining cycle can be drawn up as the follows:



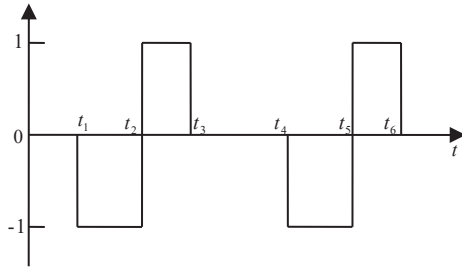


Fig 1. Water injection drainage cycle diagram  
Where, 1 denotes the injected hot water, -1 the drained cool water.  $(0, t_1)$  represents the time consumed from  $T_0$  to  $T_{\min}$ ,  $(t_1, t_2)$  and  $(t_4, t_5)$  represent the time discharging cool water;  $(t_2, t_3)$  and  $(t_5, t_6)$  are time of injection hot water;  $(t_3, t_4)$  is the time when temperature drops from  $T_{\max}$  to  $T_{\min}$ .

### 2.3 Optimization Model of Constant Temperature and Energy-Saving Bath Based on Dynamic Programming

When people enter the bathtub, the men's movement would speed up the tub water heat emission. Meanwhile, in the bubble bathing, foam floating on the liquid surface will affect the water's heat dissipation. The problem shows that, constant temperature and energy-saving is the most important goal. We need a dynamic programming problem. Based on this analysis, based on the dynamic goal planning, optimization and energy saving bath thermostatic model is established. Types are as follows:

- 1) The optimization model of constant temperature and energy saving when people are still in the bathtub.
- 2) Constant temperature and energy saving optimization model for the movement of people in bathtub.
- 3) The thermostat and energy saving optimization model of using the bath bubble additive.

On the basis of constant temperature model, people's total water consumption shall meet minimum energy efficiency. The total water consumption is  $Z$ ; average time taken to a bath is  $C$ . The design of constant temperature control shows total times of

$$\text{filling water during bathing are } n = \frac{C - t_0}{t_1 + t_2 + t_0}.$$

Based on the above analysis, this paper established the objective function,  $Z = V_0 + \sum_{i=1}^n V_i(in)$  and solve the objective function.

$$s.t. \begin{cases} T_0 - \Delta T \leq T(t) \leq T_0 + \Delta T \\ V_0 - \Delta V \leq V(t) \leq V_0 + \Delta V \\ V_0 - \Delta V + V_{in} = V_0 + \Delta V \\ E_{out} = c\rho(V_0 - \Delta V)(T_0 - T_{\min}) \\ E_{in} = S_{in}\rho c T_{in} \\ E_{end} = c\rho(V_0 - \Delta V + V_{in})(T_{\max} - T_0) \\ E_{end} - E_{start} = E_{in} - E_{out} \\ cm \frac{dT}{dt} = \Delta E'_1 + \Delta E'_2 + \Delta E'_3 + \Delta E' \end{cases} \quad (7)$$

Seeking solution to the above problem, the minimum water consumption  $Z_{\min}$  can be obtained with the normal range of bath time.

#### 2.3.1 The Optimization Model of Constant Temperature and Energy Saving When People Still in the Bath

Let the surface area of the human body  $S_3$  the volume  $V_1$  assuming that the person's temperature is constant at  $T_4$ , and  $H_3$  is the person's heat dissipation coefficient. The heat loss caused by convection of the water in the bathtub between the people is  $Q_1 = -H_3 S_3 (T - T_4)$ . The heat energy of the human body through the radiation loss is  $Q_2 = -\varepsilon \sigma S_3 (T_4^4 - T_4^3)$ . The human body into the bath will make the water temperature decrease fast, and make bath process of total water consumption increases. Under the premise of constant velocity, water injection time  $t_{in}$  and drainage time  $t_{out}$  will increase, and the water and drainage time interval will be shorten.

#### 1.3.2 Constant Temperature and Energy Saving Optimization Model for the Movement of People in Bathtub

When people move in the process of bathing, it will increase the water flow rate, and thus will accelerate the heat radiation of water in the bathtub. Then the bath water temperature and time relationship will not be  $T(t)$ . It also needs to consider the influence of the people motion state, denoted as  $\varepsilon(t)$ . The bathtub water temperature is  $T = T(t) + \varepsilon(t)$ . Take it as the constraint conditions of the objective function, to solve it, we obtain the total amount of water increases.  $t_{in}$  and  $t_{out}$  will be more than people still in the bathtub, and the relative water injection drainage time interval will be shortened.

#### 1.3.3 The Thermostat and Energy Saving Optimization Model of Using the Bath Bubble Additive

After using bath bubble additive, the foam will float at the surface of water which reduces the contact with

air. Suppose that impact of foam on the bathtub water is  $\mu(t)$ . Based on the thermostatic and energy saving optimization model while bathing, bathtub water temperature is  $T' = T(t) + \varepsilon(t) + \mu(t)$ . Analyze it as the objective function. When people use bubble additive, the total amount of used water,  $t_{in}$  and  $t_{out}$  are smaller than not using bubble agent and the intervals will become longer.

3. NUMERICAL SIMULATION IS CARRIED OUT  
According to the objective function

$\min Z = V_0 + \sum_{i=1}^n V_{i(in)}$  respectively calculate the total water consumption of the four models

$Z_{use} = V_0 + S_{in} \sum_{i=1}^n t_i, i = 1, 2, \dots, n$ , and

calculate the percentage of water-saving

$P = \frac{Z_N - Z_{use}}{Z_N} \times 100\%$  According to the

non-water-saving bathtub's water consumption  $Z_N$  then check the accuracy of the model, as shown in figure 1.

Table 1. Percentage of water saving

|                                 | $Z_{use}(L)$ | $Z_N(L)$ | Percentage of water saving |
|---------------------------------|--------------|----------|----------------------------|
| When no one is in the bath      | 604          | 890      | 32.0%                      |
| People are still in the bathtub | 590          | 820      | 28.0%                      |
| Movement in the bathtub         | 580          | 820      | 29.0%                      |
| Use shower gel                  | 598          | 870      | 31.0%                      |

The bathtub's water saving performance is best in case of the confidence coefficient  $\alpha = 0.05$ . When it meets the inequality<sup>[4]</sup>,

$$28\% \leq \frac{Z_N - Z_{use}}{Z_N} \leq 34\%$$

,the bathtub's water saving performance is good. On the basis of the numerical simulation and test results,  $Z_{use}$  is in the scope, which explains the rationality of the model.

#### 4. Conclusion

Based thought multiobjective programming and dynamic programming, the establishment of a temperature - time model, under the condition that the waste water is satisfied, the water temperature is maintained in the suitable water temperature range of the human body. According to the human body with a shape, size, movement and whether factors like bubbles, the model continuously optimized to make the results more authenticity and universality. Using the energy conservation, the heat dissipation, water injection and drainage are periodic, and the water injection and drainage time model is established, each variable will work closely together, results clear, systematic; However, this does not take into account the different layers of different temperature, to control the accuracy of the results and model of injection and drainage time, have a certain influence.

#### REFERENCE

- [1]Om Prakash Verma.Intelligent temperature controller for Water-Bath System [J]. International scholarly and science research & innovation,2012,6(9)
- [2]J.Ottesen.Compartment models [J]. 2014,1(7)
- [3]Sam Howison. Pracial applied mathematics,approximtion[J]. Mathematical Insitute Oxford Unversting,2004
- [4]Luonade feishe.Statistical Methods and Scientific Inference: Oxford University Press (1990-1963).

# Terahertz's Development and Utilization Prospect

Li Yanting<sup>1,a</sup>, Li Bin<sup>2,b</sup> and Zhu Yanyu<sup>3,c</sup>

<sup>1</sup>College of Biological and Chemical Sciences and Engineering, University of Jiaying, Jiaying, Zhejiang, P. R. China

<sup>2</sup>College of Biological and Chemical Sciences and Engineering, University of Jiaying, Jiaying, Zhejiang, P. R. China

<sup>3</sup>Zhejiang Wanxu Terahertz Technology Company, Jiaying, Zhejiang, P. R. China

**Abstract:** Terahertz science and technology is developing rapidly as a new cross-disciplinary area in recent decades. In the electromagnetic spectrum band, Terahertz is defined as some waves' frequency located between millimeter waves and infrared, its coverage scope is generally from 0.1 THz to 10THz. Main characteristics of terahertz include the following five aspects: high penetration, ps level pulse magnitude, fingerprint spectrality, low-energy property and dispersion property. Terahertz would play an important role in the field of environment-protection and energy-saving, medical diagnostic and military.

**Keywords:** terahertz, time-domain spectroscopy, trench waste cooking oil.

## 1. INTRODUCTION

Terahertz (THz) science and technology is developing rapidly as a new cross-disciplinary area in recent decades. In the electromagnetic spectrum band, Terahertz is defined as some waves' frequency located between millimeter waves and infrared, its coverage scope is generally from 0.1 THz to 10 THz, corresponding wavelength range is from 30 $\mu$ m to 3mm. In the electromagnetic spectrum, light period of oscillation corresponding to radiation frequencies of one THz is one-trillionth ( $10^{-12}$ ) second, namely Picosecond (ps), corresponding wavelength is 300 $\mu$ m, corresponding wave number is 33cm<sup>-1</sup>, corresponding photon energy is 4.1meV, and corresponding blackbody radiation temperature is 476K [1].

Currently, Terahertz applications are still in the progress of continuous development and research, and its vast scientific outlook has been recognized in the world. Academic value and practical application value for terahertz is quite important due to its electromagnetic wave position of characteristic spectrum. Furthermore, some technologies related with terahertz have been put to practical use, academic community and industrial community of various countries in the world pay close attention to terahertz. In the last decade, a highly efficient, compact, low-cost pulse terahertz light source was driven and developed due to femtosecond laser technology, causing a terahertz science and

technology research boom. In just a few years, a large number of terahertz technologies with great value and better prospect has been developed, such as terahertz time-domain spectroscopy, terahertz non-destructive imaging and security inspection screening technology and terahertz communication technology.

Terahertz band is a field of electromagnetic radiation with great scientific value and broad application prospects in information and communications, imaging, biochemistry and other research fields, but terahertz technology is not yet fully developed [2]. Before 1980, scientist's terahertz knowledge was quite limited, even scientific community call this phenomenon as "terahertz gap" [3]. From the point of view of energy radiation, terahertz's size is between electron and photon. While from the point of view of the electromagnetic spectrum, terahertz wave band is located between millimeter wave and infrared ray, belongs to far-infrared band. Technology for far-infrared, mid-infrared and microwave on both sides of Terahertz wave band has been developed quite maturely, but terahertz wave technology is still far from perfect [4].

## 2. MAIN CHARACTERISTICS OF TERAHERTZ

Main characteristics of terahertz include the following five aspects: high penetration, ps level pulse magnitude, fingerprint spectrality, low-energy property and dispersion property.

Terahertz wave radiation could penetrate substances such as plastic and fabric, etc. Therefore, terahertz could be used to detect low concentration gas due to its weak attenuation properties, applying to control indoor air pollution. Terahertz wave radiation could also penetrate walls and ceramic almost lossless, so that it can play a role in certain specific fields [5].

Terahertz could be used to analyze various materials due to its typical wave pulse width of ps level and time-resolved property. Furthermore, some novel terahertz sampling and measuring technology could be developed, to restrain background interference of liquids, biological samples, semiconductors, superconductors quick conveniently, effectively and stably. Currently, Signal Noise Ratio (SNR) of terahertz radiation intensity measured could be greater than  $10^{10}$ , far higher than that of Fourier Transform Infrared Spectroscopy technology.

Terahertz contains a wealth of physical and chemical information, vibration and rotation energy level transition of most polar molecules and biological macromolecules is in the terahertz band. Terahertz spectrum of a substance contains a wealth of physical and chemical information, making emission, reflection and transmission of terahertz has a unique characteristic similar to fingerprint. Thus according to the corresponding fingerprint spectrum, terahertz spectral imaging technology could distinguish shape and component identification of an object, providing theoretical basis and detection technology for counter-narcotics, counter-terrorism and explosive ordnance disposal [6].

Terahertz photon with lower energy is even weaker than X-ray photons, not causing damage and bringing side-effect due to ionization to biological tissue. Terahertz photon energy is one-fortieth of that of visible light, energy efficiency is much higher making terahertz wave as information carrier instead of visible and near-infrared light [7].

From gigahertz (GHz) to Terahertz band, many organic molecules exhibit strong absorption and dispersion characteristics due to molecular's vibration and rotation energy level transition. Molecular's rotational and vibrational spectra from 10 GHz to 10 THz is described by real and imaginary parts of dielectric function of terahertz spectrum [8].

### 3. TERAHERTZ GENERATION METHOD

Currently, accelerated electron generation is a frequently-used method to generate terahertz. There are three main methods for accelerated electron to generate terahertz, namely relativity theory, the free electron laser and backward wave oscillator. And another frequently-used photonic methods are mainly concerned with ultrashort laser pulse, including optical rectification method generating broadband subpicosecond terahertz radiation, photoconductive method and nonlinear optical frequency difference method. In addition, research on high-energy accelerator with thermal radiation to produce terahertz is also developing. Terahertz radiation power generated by accelerated electron is the highest in all emission sources.

Main principle of relativistic electrons to generate terahertz radiation is as followings. When laser irradiation gets close to GaAs, a bunch of free electrons could be produced, and then linear accelerator accelerated the free electrons to a relativistic speed, at this moment electrons enter a transverse magnetic field, gaining normal acceleration, thereby terahertz wave radiation is generated.

Terahertz radiation could be also generated by free-electron laser, and free electron is the best source of electromagnetic wave radiation. When a beam of ultrashort electron flow close to light speed with an adjustable energy enters through a strong magnetic field, it will spontaneously radiate electromagnetic

waves, turning electron kinetic energy into light energy, obtaining radiation from X-ray to far infrared. Jefferson Laboratory in the United States successfully built a free electron laser (FEL) device with 20W of terahertz band power, and its peak power is up to 2.7kW in 2002. In addition, average power of FEL in Novosibirsk of Russia from 120Lm to 180Lm reached 200W, and its maximum peak power reached 0.6MW. However, FEL device is bulky and expensive, not suitable for general trials and commercial use.

Principle for backward wave oscillator is similar to FEL. When heated cathode tube radiates electrons, electrons are focused in a magnetic field, rocking to positive electrode, emitting electromagnetic radiation in the reverse applying process. By changing voltage on the positive and negative electrode, radiation frequency can be adjusted. It is another efficient terahertz radiation source.

In addition to speeding electrons, there are other methods to generate terahertz, such as by a semiconductor instantaneous currents, optical rectification, heat radiation and high-energy accelerator. Photoconductive terahertz is of high-gain, and we believe that it would have better development prospect after a further improvement of its transmitting antenna geometry. Nonlinear difference frequency technology will become the most potential method due to its simple equipment, harmonization terahertz generated having no threshold. Research will focus on finding organic nonlinear optical crystal with minimal absorption coefficients to improve its conversion rate.

### 4. TERAHERTZ APPLYING FIELDS

Terahertz would play an important role in the field of environment-protection and energy-saving, and so on. Terahertz could apply in explosive and trench waste cooking oil detection.

Many explosives are aromatic compounds containing nitro. Rotational and vibrational spectra of a variety of explosive molecules is located within terahertz wave band. Terahertz Time-domain Spectroscopy (THz-TDS) technology can help to obtain such spectra and structure information of these sampling substances as refractive index and absorption coefficient. Compared to Fourier Transform Infrared Spectroscopy (FTIR), THz-TDS has a higher SNR without cryogenic bolometer, carrying out lossless non-ionizing spectral measurement of explosives with high sensitivity [9]. For example, Hexogon, namely RDX, aroused interest of many researchers due to its high energy, excellent thermostability and versatility, etc. Some groups use transmission-type THz-TDS technology study RDX. However, because that RDX has a strong absorption coefficient, it is suitable for reflective use in practical applications. Test results using transmission-type THz-TDS technology show that, a considerable number of explosives including RDX have corresponding



characteristic spectrums in terahertz band spectrum. Therefore, not only low frequency motion of substance and molecular collective vibration mode could be analyzed, and corresponding explosives could be identified and detected based on these features.

Currently, due to lack of effective detection technology, trench waste cooking oil frequently appears in people's dining-table, bring great harm to people's health. Therefore, looking for quick and accurate detection method is an effective way to reduce people's trench waste cooking oil consumption. In recent years, THz- TDS method has been applied to study properties and structure of trench waste cooking oil analysis as a fast non-destructive detection method. Its superiority is to get a sample's amplitude and phase information, measuring dipolar vibrational and rotational energy transitions of intermolecular weak interactions such as hydrogen bonding and van der Waals forces, etc., obtaining molecular collective vibration information such as low-frequency vibration in the lattice of crystal [10-11].

Trench waste cooking oil samples with different compositions and contents result in different absorption coefficients in corresponding terahertz bands. This indicates molecular persad's different absorption properties of unsaturated fatty acids, saturated fatty acids, trans fatty acids, peroxide. According to terahertz properties, transmitted spectrum will show absorption property in an organic molecule's energy level resonance position. This resonance absorption is generally due to molecular rotation and vibration, intermolecular weak interactions or molecular persad's overall vibration mode. Therefore, according to this terahertz spectral information, molecular persad of trench waste cooking oil can be analyzed and measured.

## 5. SUMMARY

Terahertz science and technology is developing rapidly as a new cross-disciplinary area in recent decades. Terahertz band locates between millimeter wave and infrared, associated with microwave, far infrared, mid-infrared, nano and micro-nano. Main characteristics of terahertz include the following five aspects, namely high penetration, typical ps level pulse magnitude, fingerprinting spectrality, low-energy property, dispersion property. There are three main methods to generate terahertz by accelerated electrons, namely relativity theory, FEL and backward wave oscillator. Terahertz main application fields include explosives and trench waste cooking oil detection around our life, etc. We believe that along with scientist's continuing in-depth study and exploration of various types of physical and

chemical properties of terahertz material, nanosized material and terahertz technology would be evaluated rationally and would bring a new industrial revolution boom.

## ACKNOWLEDGEMENT

Supported by the following project grants from Student Innovative Ability Training Project in Jiaxing University, Humanities and Social Sciences Planning Fund under Ministry of Education (Grand No. 14YJAZH030), Jiaxing Environmental Protection Bureau (Grand No. 00512086), Zhejiang Province for Key Innovation Team Project of Circular Economy and Development of Transformation & Upgrading (Zhe-Wei-Ban, [2012]68), South China Institute of Technology for program of International S&T Cooperation (Subproject, Grand No. 2011DFA60290), Chongqing University for National Social Science Fund of China (Subproject, Grand No. 12&ZD209), Philosophy Social Sciences Foundation in Zhejiang province (Grand No. 14NDJC005Z), Zhejiang Federation of Humanities and Social Sciences Circles (Grand No. 2013N101).

## REFERENCE

- [1]N. Liu, K.J. Xu, J.P. Zhou, J.L. Ma and B.B. Jin: Prog. Pharm. Sci. Vol. 32(9) (2008), p. 398-406 (in Chinese).
- [2]X.J. Ma, H.W. Zhao, B. Dai and M. Ge: J. Spectrosc. Spectral Anal. Vol. 28(10) (2008), p. 2237-2242 (in Chinese).
- [3]Y.F. Wang, W.C. Yu, F.J. Zhou and Z.H. Xue: Prog. Biochem. Biophys. Vol. 37(5) (2010), p. 484-489 (in Chinese).
- [4]X.M. Wang, X.L. Xu and F.L. Li: J. Capital Normal University (Nat. Sci. Edition) Vol. 24(3) (2003), p. 17-25 (in Chinese).
- [5]S.G. Liu: China Basic Sci. Vol. 8(1) (2006), p. 7-12 (in Chinese).
- [6]K.J. Mu, Z.W. Zhang, C.L. Zhang: J. China Academy Electron. Inf. Technol. Vol. 4(3) (2009), p. 221-237 (in Chinese).
- [7] C.Y. Xie and M.H. Yuan: Laser J. Vol. 31(1) (2010), p. 7-9 (in Chinese)
- [8]J.Q. Yao, Y. Lu, B.G. Zhang and P. Wang: J. Optoelectronics•Laser Vol. 16(4) (2005), p. 503-510 (in Chinese).
- [9]G.F. Liu, H.W. Zhao, M. Ge and W.F. Wang: J. Spectrosc. Spectral Anal. Vol. 28(5) (2008), p. 966-969 (in Chinese).
- [10]R.M. Bao, K. Zhao, X.M. Teng, J. Li, X.Y. Lu and J. Ma: China Oil and Fats Vol. 38(4) (2013), p. 61-65 (in Chinese).
- [11]Y. Zhang, and Z. Han: Sci. Rep. Vol.5, (2015), p. 18606-18613.



# Research on Application of Active Head Restraint of Automobile Seat

Wu sheng Tang

College of mechanical and vehicle engineering, Scientific Research Administrative Department, Changchun University, Changchun City of Jilin Province, China 130022

**Abstract:** The paper proposes the necessity of equipping the automobile seats with active head restraints based on the fact that drivers and passengers often suffer from head or neck whiplash in the crashes; elaborates the operating principle and protective effects of the head restraints; makes an analysis of the active head restraints of several popular automobile brands available on the current market and then points out the crucial significance of equipping the seats with active head restraints.

**Key words:** whiplash injury, automobile seat, active, head restraint

## 1. INTRODUCTION TO ACTIVE HEAD RESTRAINT

According to the statistics of traffic accidents, the drivers and passengers in the front of the vehicle are inclined to have whiplash injury in rear-end collision, which is a very common accident. Whiplash injury, not as lethal as injuries to head or chest, will be difficult to cure and the injurers are likely to have after-effects, for which they are obliged to suffer a long term and bear high cost of treatment. An active head restraint just came into being in order to lower the risk of injury to the neck for the drivers and passengers in the front. It is a protective buffer device designed for the most common head and neck injuries caused by speedy back inclining of the head when an automobile is knocked by another one in the back. According to statistics of Insurance IIHS (Institute of Highway Safety) in 1999, 26% of the injured suffered from neck twist in the crash and the claim incurred accounted for 66% of all the injuries, amounting to as much as over 7 billion \$ insurance claim every year. The head restraint will be attached to the neck of the drivers or passengers and reduce injuries. The test proves that the active head restraint, as an extremely effective security configuration, will effectively protect the drivers or the passengers' head and neck in the rear-end accidents[1].

## 2. OPERATING PRINCIPLE OF ACTIVE HEAD RESTRAINT

The active head restraint will automatically adjust the distance between the head restraint and the head of the passengers in rear-end collision. The sensing of the head restraint functions in two ways: the protective device will be activated on the seat by the weight of the passengers, with the head restraint automatically moving forward and upward; the

sensors installed in the bumper or within the car will monitor a rear-end and send the instruction for the head restraint to move forward and upward. What is worth mentioning is that the active head restraints in some cases will function well without any maintenance, which is an utterly convenient safety equipment for the car owners.

Most active head restraints are designed as a mechanical system, with a pressure board linked by the connecting rod to the seat back as the pad above the seat. Moreover, one starter is devised within the head restraint. The body of the passengers will collide with the seat back and push back the pressure board under the impact of crash, compelling the linking rod to rise and head restraint to move forward, so that the head restraint will be against the head of the passengers when the head moves backward rapidly, so as to buffer, prevent or lower the risk of head and neck injuries. After the collide, the active head restraint will return to the normal position and can be reused next time without any maintenance[2].

## 3. ANALYSIS OF APPLICATION OF ACTIVE HEAD RESTRAINT

Active head restraint is a safety equipment as crucial as safety belt and airbag. With the drivers' increasing demand for safety performance in recent years, the manufacturers begin to attach higher attention to the equipment of active head restraints, resulting in increasing rate of configuration in various models. The active head restraint was originally invented by SAAB Automobile Corporation of Sweden and thereafter Volvo, Benz and Toyota began to launch their active head restraints respectively.

(1) The application of active head restraint in BMW series. Many advanced technique and equipment have been applied to BMW- 6 series, with active head restraint as a highlight on safety configuration. In case of rear-end collision, the active head restraint will move forward instantly within 20ms and gently hold the head of the driver during the process of rebound so as to reduce injury to the greatest extent.

(2) The application of active head restraint in Toyota series. Toyota is one of the manufacturers which originate the research of active head restraint. Toyota has played a vital position in active security configuration from "collision-proof smart head restraint", seat with the concept of WIL (Whiplash Injury Lessening) to active head restraint for lessening whiplash injury. Moreover, Toyota is one of

the few manufacturers which equip each model of all the vehicles with active head restraint including Crown, Reiz, Carola, Vios of FAW Toyota and Camry, Yaris of GAC Toyota, which definitely improves security of Toyota for passengers in case of rear-end collision.

(3) The application of active head restraint in Benz series. Benz has long been regarded as the symbol of dignity and coziness, while it has been considerate on security for the drivers as well. Benz devised the Neck-pro--- responsive neck protective device in the front seats, and made it standard configuration for Benz Class C and Class E. In case of rear-end collision, the design will effectively lower the risk of injury from excessive flexion and extension of cervical spine. When the sensing system detects the preset collision strength at the rear of the vehicle, the pre-loaded spring will be released and the neck restraint will rapidly move approximately 40mm forward and 30mm upward so that the driver and the passenger in the front will be protected in advance. After the neck restraint is activated, the driver can release it and return it to its original state by means of the on-board kit and reuse it again next time[3].

(4) The application of active head restraint in Volvo series. Volvo--- a well-known Swedish automobile manufacturer has been acknowledged for its focus on security, and it has its distinctive features in active head restraint by launching its unique WHIPS (Whiplash Protection System), which has been applied in S40, S60 and S80. In the rear-end, people's back will collapse in the seat back. The system will move seat back and head restraint 50 mm backward horizontally and then incline 15° backward by the fine construction of the seat, resulting in gentle and balanced support and protection for the upper body and head. Compared with seats without WHIPS, those with WHIPS will impair 40% - 60% of impact force on neck, and avoid lifelong or lethal injury to vulnerable neck. According to the statistics, the technique will lower over 90% risk on the necks of driver and passengers in the front during the rear-end collision.

(5) The application of active head restraint in Volkswagen series. Shanghai Volkswagen Tiguan, an SUV model, is equipped with advanced configuration that other SUVs of the same class haven't. Taking security for example, Tiguan is not only equipped with multiple active security configuration such as ABS, ESP, MSR, but also the latest active head restraint of Volkswagen. In the rear-end accident, the head restraint will respond quickly and eject forward so as to reduce the shaking extent of head towards

backward and minimize the neck injury.

(6) The application of active head restraint in Berk series. The originator of active head restraint SAAB has been affiliated to GM (General Motors) for a long term and GM has every reason to apply its security technique to other models of SAAB. As the main models of Shanghai GM, Buick LaCrosse and Regal have been equipped with new four-way active head restraints. In the event of rear-end collision, the vehicle will automatically adjust the position of the head restraint 45 mm forward so as to support the head and reduce the neck injury of the driver and passengers in the front at the early stage of the collision[4].

#### 4. CONCLUSION

Besides the above mentioned models, there are also other models equipped with active head restraints, mainly for middle-class and high-class models. In the head-on collision, the restraint system such as safety belt and airbag will reduce the injury to passengers' head or chest; in the side collision, the airbag and side curtain airbag may also protect the passengers from being injured. While in the rear-end accident, it is only the head restraint that will protect the vulnerable neck. Compared with safety belt and airbag, it is relatively less popularized. Nowadays, active head restraints have been regarded as a crucial standard for configuration of the automobiles in some countries of Europe and America. It is believed that with consumers and manufacturers' more attention on rear-end collision, active head restraint will be equipped in more and more models and will play an essential role in protecting the drivers and passengers' head and neck in the rear-end accidents.

#### ACKNOWLEDGEMENT

This research work was sponsored by the project of Changchun City funded science and technology project (NO:2013319)

#### REFERENCES

- [1] Michiel van Ratingen, James Ellway, Matthew Avery, et al. The Euro NCAP Whiplash Test. 21st ECV Paper. No. 09-0231.
- [2] Liu de wei Study on the anti whiplash seat headrest, Light vehicle technology 2014 (8) P36-39.
- [3] Watanabe Y, Ichikawa H, Kayama O, et al. Influence of Seat Characteristics on Occupant Motion in Low-speed Rear Impacts[J]. Accident Analysis and Prevention, 2000, 32(3): 243-250.
- [4] Anders Kullgren, Anders Lie, Claes Tingvall. The Effect of Whiplash Protection Systems in Real-Life Crashes and Their Correlation to Consumer Crash Test Programmes [C]. Paper No: 07-0468.

# Research on Aerial Spare Parts Joint Support Methods

Yadong Wang<sup>1</sup>, Xiaobin Wei<sup>1</sup>, Shenyang Liu<sup>1</sup>

Department of Aviation Four Stations, Air Force Logistics College, Xuzhou 221000, China

**Abstract:** Through making a analysis of the aerial spare parts joint support system that consists of two supply departments, this paper has established proportion between support degree and expense models of spare parts joint support. The arithmetic of spare parts joint support storage based on proportion between support degree and expense is presented. Then optimal method of aerial spare parts joint support is determined. Applicability of the method is given by way of a numerical example.

**Keywords:** Cost-effectiveness, Joint Support, Aerial Spare Parts Storage, Spare Parts Supply

## 1. INTRODUCTION

One spare-parts joint guarantee system consists of supplier 1, supplier 2 and several clients. The density function of annual demand amount produced by clients is known. When a client has parts shortage, each supplier can supply the parts with only 1 piece every time, and the client could only choose one of the supplier.

When determining the storage volume, either supplier 1 or supplier 2 should consider the following factors: the average purchasing price of single spare-parts, the average inventory cost of spare-parts, the average backloging cost of spare-parts, the average shortage cost of spare-parts, the delivery distance between storage location and the location of client, the average time per km when delivering the parts from supplier to client, the average time for urgently producing a single part when supplier has a stock-out, etc. the annual demand amount of the each client guaranteed by the two suppliers depend on the equipment amount of client, the amount of unit in single equipment, the annual maintenance amount of single equipment unit and the specific guarantee model.

Determining the optimal plan of joint guarantee from the perspective of cost-effectiveness, is to get the storage amount for supplier 1 and supplier 2 respectively, and which clients they will guarantee separately, in this way to maximize the annual expectation of total guarantee degree.

Based on the above analysis, determining the optimal plan of guarantee model of client, storage amount for supplier 1 and supplier 2 which realizes the maximum cost-effectiveness.

## 2. CODE DESCRIPTION AND FUNDAMENTAL ASSUMPTION

### 2.1. Code description

$P$  ——— purchasing price of single part;

$\alpha_1$  ——— the average inventory cost of spare-part stored by supplier 1;

$\beta_1$  ——— the average backloging cost of spare-part stored by supplier 1;

$\gamma_1$  ——— the average shortage cost of spare-part stored by supplier 1;

$\alpha_2$  ——— the average inventory cost of spare-part stored by supplier 2;

$\beta_2$  ——— the average backloging cost of spare-part stored by supplier 2;

$\gamma_2$  ——— the average shortage cost of spare-part stored by supplier 2;

$f_{01}(r_{01})$  -the density function of total annual demand amount guaranteed by supplier1;

$f_{02}(r_{02})$  -the density function of total annual demand amount guaranteed by supplier2;

$D_{1k}$  -the distance between supplier 1 and the client  $k$ ;

$D_{2k}$  -the distance between supplier 2 and the client  $k$ ;

$k_0$  -the average time per km when delivering the parts from supplier to client;

$X_k$  -the annual demand amount of the client  $k$ , which is random variable;

$N_k$  -the equipment amount of client  $k$ ;

$t_1$  - the average time for supplier 1 to urgently produce a single part when supplier has a stock-out;

$t_2$  - the average time for supplier 2 to urgently produce a single part when supplier has a stock-out;

$X_{01}$  -storage amount for supplier 1;

$X_{02}$  -storage amount for supplier 2;

$\lambda_k$  -the parameter to determine which supplier to guarantee the client  $k$ ; if client  $k$  is guaranteed by supplier 1,  $\lambda_k = 1$ ; if client  $k$  is guaranteed by supplier 2,  $\lambda_k = 0$ .

The paper submitted to the conference should be 6-18 pages.

### 2.2. Fundamental assumption

(1) Ignore the transportation expenses in the process of spare parts supply;

(2) Solely considers getting the optimal plan in the case of spare-part replacement after equipment failure.

## 3. MODELING

### 3.1. Cost model

The guarantee expenditure of supplier 1 is mainly

consisted of the average purchasing price and the average inventory cost of spare-parts.

$$C_1(X_{01}) = pX_{01} + \alpha_1 X_{01} + \beta_1 \int_0^{X_{01}} (X_{01} - r_{01}) f_{01}(r_{01}) dr_{01} + \gamma_1 \int_{X_{01}}^{+\infty} (r_{01} - X_{01}) f_{01}(r_{01}) dr_{01} \quad (1)$$

The guarantee expenditure of supplier 2

$$C_2(X_{02}) = pX_{02} + \alpha_2 X_{02} + \beta_2 \int_0^{X_{02}} (X_{02} - r_{02}) f_{02}(r_{02}) dr_{02} + \gamma_2 \int_{X_{02}}^{+\infty} (r_{02} - X_{02}) f_{02}(r_{02}) dr_{02} \quad (2)$$

The total expenditure of supplier 1 and supplier 2

$$C(X_{01}, X_{02}) = C_1(X_{01}) + C_2(X_{02}) \quad (3)$$

### 3.2. Guarantee degree model

It is known that the equipment amount guaranteed by supplier 1 is  $\sum_{k=1}^n \lambda_k N_k > 0$ , then within the given

time  $t_0$ , the average downtime of single equipment caused by lack of the part:

$$\bar{T}_{01} = \frac{T_{01}}{\sum_{k=1}^n \lambda_k N_k} = \frac{k_0 \sum_{k=1}^n \lambda_k D_k E(X_k) + t_1 \int_{X_{01}}^{+\infty} r_{01} f(r_{01}) dr_{01}}{\sum_{k=1}^n \lambda_k N_k} \quad (4)$$

Similarly, within the given time  $t_0$ , the average downtime of single equipment caused by lack of the part of supplier 2:

$$\bar{T}_{02} = \frac{T_{02}}{\sum_{k=1}^n (1-\lambda_k) N_k} = \frac{k_0 \sum_{k=1}^n (1-\lambda_k) D_k E(X_k) + t_2 \int_{X_{02}}^{+\infty} r_{02} f(r_{02}) dr_{02}}{\sum_{k=1}^n (1-\lambda_k) N_k} \quad (5)$$

For every single client's demand for guarantee in one year, the guarantee will be conducted by either supplier 1 or supplier 2, without guaranteed by them together. Thus, the average downtime of single equipment caused by lack of the spare part will be"

$$T = \lambda_k \bar{T}_{01} + (1-\lambda_k) \bar{T}_{02} \quad (6)$$

It's given that the total equipment amount of joint guarantee is  $\sum_{k=1}^n N_k$ , then within given time  $t_0$ , the average guarantee degree of single equipment will be:

$$A(X_{01}, X_{02}) = 1 - \frac{T}{t_0} = 1 - \frac{\lambda_k \bar{T}_{01} + (1-\lambda_k) \bar{T}_{02}}{t_0} \quad (7)$$

Substitute formula(4) and formula(5) into formula(7) to get:

$$A(X_{01}, X_{02}) = 1 - \lambda_k \frac{k_0 \sum_{k=1}^n \lambda_k D_k E(X_k) + t_1 \int_{X_{01}}^{+\infty} r_{01} f(r_{01}) dr_{01}}{t_0 \sum_{k=1}^n \lambda_k N_k} - (1-\lambda_k) \frac{k_0 \sum_{k=1}^n (1-\lambda_k) D_k E(X_k) + t_2 \int_{X_{02}}^{+\infty} r_{02} f(r_{02}) dr_{02}}{t_0 \sum_{k=1}^n (1-\lambda_k) N_k} \quad (8)$$

### 3.3. Cost-effectiveness model

The guarantee degree is closely related to the budget of spare-parts joint guarantee. To maximize the cost-effectiveness is a more reasonable and ideal goal.

The cost-effectiveness is the ratio of the guarantee degree to the budget of spare-parts joint guarantee. And then

$$F(X_{01}, X_{02}) = \frac{A(X_{01}, X_{02})}{C(X_{01}, X_{02})} \quad (9)$$

Get the storage amount for supplier 1 and supplier 2 respectively, and which clients they will guarantee separately, in this way to maximize the cost-effectiveness.

### 4. MODELING SOLUTION

When the  $\lambda_k$  is given, for solving optimal solution of the formula(9), given that  $\frac{\partial F(X_{01}, X_{02})}{\partial X_{01}} = 0$ ,  $\frac{\partial F(X_{01}, X_{02})}{\partial X_{02}} = 0$ , get the extremum of  $F(X_{01}, X_{02})$ . Then

$$\begin{cases} \frac{\frac{\partial A(X_{01}, X_{02})}{\partial X_{01}} C(X_{01}, X_{02}) - A(X_{01}, X_{02}) \frac{\partial C(X_{01}, X_{02})}{\partial X_{01}}}{C^2(X_{01}, X_{02})} = 0 \\ \frac{\frac{\partial A(X_{01}, X_{02})}{\partial X_{02}} C(X_{01}, X_{02}) - A(X_{01}, X_{02}) \frac{\partial C(X_{01}, X_{02})}{\partial X_{02}}}{C^2(X_{01}, X_{02})} = 0 \end{cases} \Rightarrow \begin{cases} \frac{\frac{\partial A(X_{01}, X_{02})}{\partial X_{01}} C(X_{01}, X_{02})}{\frac{\partial A(X_{01}, X_{02})}{\partial X_{01}} C(X_{01}, X_{02})} = \frac{\frac{\partial C(X_{01}, X_{02})}{\partial X_{01}}}{\frac{\partial C(X_{01}, X_{02})}{\partial X_{01}}} \\ \frac{\frac{\partial A(X_{01}, X_{02})}{\partial X_{02}} C(X_{01}, X_{02})}{\frac{\partial A(X_{01}, X_{02})}{\partial X_{02}} C(X_{01}, X_{02})} = \frac{\frac{\partial C(X_{01}, X_{02})}{\partial X_{02}}}{\frac{\partial C(X_{01}, X_{02})}{\partial X_{02}}} \end{cases} \quad (10)$$

The formula(10) is nonlinear equation, which should be solved by program. Get that  $X_{01} = \hat{X}_{01}$ ,  $X_{02} = \hat{X}_{02}$ .

When the  $\hat{X}_{01}$ ,  $\hat{X}_{02}$  are not integers, should round down or up on them to get the optimal solution, which realizes the maximum  $F(X_{01}, X_{02})$  will be the optimal one.

Solve  $\lambda_k$  by enumeration method because of  $\lambda_k$  is discrete variable. Compare the value of  $F(X_{01}, X_{02})$ , and chose the larger one as the optimal plan.

### 5. EXAMPLE ANALYZING

The guarantee system consists of supplier 1, supplier 2 and client 1, client 2, client 3. Each client can be guaranteed by either supplier 1 or supplier 2. The equipment amount of client 1, client 2, client 3 is 1, 2, 3 respectively. One equipment needs 2 parts, price is 100 CNY, the annual amount of demands for the parts is  $N(2,1)$ . The average inventory cost of spare-part stored by supplier 1 and supplier 2 respectively are 40 and 100 CNY, the average backlogging cost of spare-part stored by supplier 1 and supplier 2 respectively are 160 and 240 CNY, the average shortage cost of spare-part stored by supplier 1 and supplier 2 respectively are 2900 and 3200 CNY; With the above, please get the storage amount for supplier 1 and supplier 2 respectively, and which clients they will guarantee separately, in this way to maximize the annual expectation of total guarantee degree.

There are 8 plans for as shown in figure 1:

Table 1. plans for supplier 1 and supplier 2 to guarantee the clients

| plans | Client 1 | Client 2 | Client 3 |
|-------|----------|----------|----------|
|-------|----------|----------|----------|

|   |            |            |            |
|---|------------|------------|------------|
| 1 | supplier 1 | supplier 1 | supplier 1 |
| 2 | supplier 1 | supplier 2 | supplier 1 |
| 3 | supplier 1 | supplier 1 | supplier 2 |
| 4 | supplier 1 | supplier 2 | supplier 2 |
| 5 | supplier 2 | supplier 2 | supplier 2 |
| 6 | supplier 2 | supplier 2 | supplier 1 |

|   |            |            |            |
|---|------------|------------|------------|
| 7 | supplier 2 | supplier 1 | supplier 1 |
| 8 | supplier 2 | supplier 1 | supplier 2 |

For on the 8 plans, normalize these plans and divide by the maximum cost 59764 , use formula (9) get the result of joint guarantee amount based on cost-effectiveness , as shown in figure 2:

Table 2.result of joint guarantee amount based on cost-effectiveness

| plans | guarantee degree | guarantee cost (yuan) | cost-effectiveness | storage amount |            |
|-------|------------------|-----------------------|--------------------|----------------|------------|
|       |                  |                       |                    | supplier 1     | supplier 2 |
| 1     | 0.9054           | 56154                 | 0.9636             | 25             | 0          |
| 2     | 0.9113           | 58804                 | 0.9262             | 15             | 12         |
| 3     | 0.9129           | 57049                 | 0.9563             | 12             | 13         |
| 4     | 0.9321           | 59524                 | 0.9359             | 5              | 21         |
| 5     | 0.9624           | 59764                 | 0.9624             | 0              | 25         |
| 6     | 0.9554           | 55454                 | 1.0297             | 13             | 12         |
| 7     | 0.9102           | 58754                 | 0.9258             | 18             | 7          |
| 8     | 0.9553           | 58750                 | 0.9718             | 7              | 19         |

The optimal plan is plan 6: the cost-effectiveness is 1.0297, the supplier 1 guarantees client 3, the supplier 2 guarantees client 1 and client 2, the storage amount of supplier 1 is 13, the storage amount of supplier 2 is 12.

#### VI. Conclusion

Adopting probabilistic and mathematic statistics method, this essay establishes the guarantee model of spare parts joint guarantee, gives the solution calculation method of storage amount based on cost-effectiveness, and determines the optimal plan which realizes the maximum cost-effectiveness, through analysis and problem simplification on the joint guarantee system with 2 suppliers. This given method provides a theoretical basis for determining the optimal spare parts storage amount for guarantee system with several suppliers.

#### REFERENCES

- [1]Qi Gao, Ordnance Maintenance Materiel Equipment Management, Beijing: National Defense Industry, 2011.
- [2]Tiening Wang, Hongwei Wang, Yu Cao, et al. "Research on material supply chain of joint inventory management strategy "J. China Logistics & Purchasing, no.13,pp. 56~57,2009
- [3]Craig C. Sherbrooke, Model of Equipment Spare Parts Optimum Inventory——Multi-stage Technology ( Second Edition ),Beijing: Electronic Industry Press, 2008.K. Elissa, "Title of paper if known," unpublished.
- [4]Min Ren, Quanqing Chen, Zhen Shen, Aircraft-spares Supply, Beijing: National Defense Industry, 2013.